Studies on the role of the *Arabidopsis thaliana* *LATERAL ORGAN BOUNDARY DOMAIN* (*LBD*) gene family

Inaugural-Dissertation

zur Erlangung des Doktorgrades
der Mathematisch-Naturwissenschaftlichen Fakultät
der Heinrich-Heine-Universität Düsseldorf

vorgelegt von

Madlen I. Rast

aus Freiberg

Düsseldorf, Juli 2011

aus dem Institut für Genetik

der Heinrich-Heine Universität Düsseldorf

Gedruckt mit der Genehmigung der
Mathematisch-Naturwissenschaftlichen Fakultät der
Heinrich-Heine-Universität Düsseldorf

Referent: Professor Dr. R. Simon

Koreferent: Dr. D. Schubert

Tag der mündlichen Prüfung:

CHAPTER I

INTRODUCTION

The introduction presented in this chapter is in part published in:

Rast, M.I., and Simon, R. (2008). The meristem-to-organ boundary: more than an extremity of anything. Curr Opin Genet Dev **18,** 287-294.

1. INTRODUCTION

1.1. Embryonic pattern formation

Plant development proceeds in a different manner to that of animals, as plant organogenesis occurs postembryonically through the activity of the shoot apical meristem (SAM) and the root meristem (RM). All above ground tissues such as leaves, flowers and shoot branches ultimately derive from the SAM. The root system, consisting of primary and secondary roots, derives from the RM. Nevertheless, establishment of the two apical meristems, formation of the apical-basal and radial axis, as well as determination of the basic plant body requires a precise order of cell divisions during plant embryogenesis. This process, termed embryonic pattern formation, is therefore fundamental for further postembryonic growth and development.

Embryonic pattern formation starts with an asymmetric division of the zygote that produces a smaller apical (ac) and a larger basal cell (bc) (Fig. 1.1). The apical daughter cell undergoes several stereotypical cell divisions to give rise to the proembryo. The basal daughter cell divides to generate the suspensor which serves as a connection between the developing embryo and maternal tissue. Only the uppermost suspensor cell, the hypophysis (hy), adopts an embryonic fate. At globular stage this cell undergoes a sequence of reproducible divisions to give rise to the quiescent centre (QC), the future organizer of the RM (Scheres et al., 1994). Further refinement of the embryonic pattern occurs during succeeding developmental stages. Finally, the mature embryo consists of four distinct structures: cotyledons, SAM, hypocotyl and root harboring the RM (Fig. 1.1; reviewed in Moller et al., 2009)

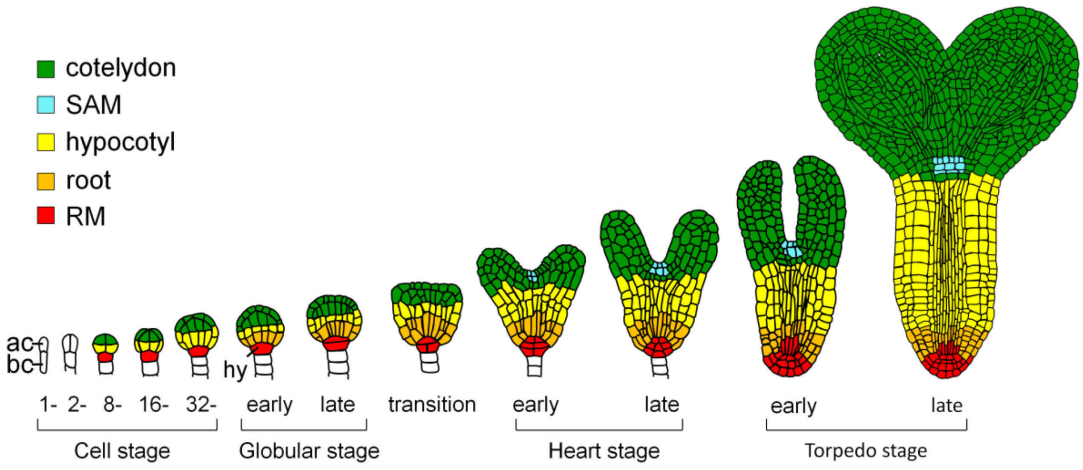

Fig. 1.1: Stages of embryo development. The zygote divides asymmetrically to produce a smaller apical (ac) and a larger basal cell (bc). Descendants of the apical daughter cell undergo a sequence of reproducible cell divisions to give rise to the proembryo. The basal daughter cell divides transversally to produce the extra-embryonic suspensor. At globular stage the uppermost suspensor cell becomes specified as hypophysis (hy) and contributes to the embryonic RM. Colors identify origins of the five structures of mature embryos.

1.2. Organization of the Shoot Apical Meristem (SAM)

The dome shaped SAM can be subdivided into different zones and layers on the basis of cell division rate and orientation, cell origin and morphology (Fig 1.2). The central zone (CZ) contains slowly dividing pluripotent stem cells. Their daughter cells are displaced to the surrounding peripheral zone (PZ). Cells in the PZ divide more rapidly and can join each other to found new organs and enter the pathway towards differentiation (Steeves et al., 1989). To separate organ founder cells and stem cell descendants in the PZ, morphological boundaries, consisting of distinct, mitotically nearly inactive cells, are formed (Kwiatkowska, 2006; Breuil-Broyer et al., 2004; Aida et al., 2006). The rib meristem beneath the CZ and PZ gives rise to the plants corpus and vasculature.

In a longitudinal section, the SAM is composed of three clonally distinct cell layers (L1-L3; Fig. 1.2B). Cells in the L1 and L2 preferentially divide anticlinal; thus, their daughter cells remain in their layer of origin. The L1 layer consists of epidermal progenitors, while cells in the L2 will give rise to sub-epidermal tissues and the gametes. The multilayered L3 shows anti- and periclinal cell divisions and produces the majority of the plants ground tissue and vasculature (Vaughn, 1952; Steeves, 1989). As stem cells are located in the upper 4-5 cell layers of the CZ, they contain cells of all three clonal layers. The organizing centre (OC), a group of cells with a low division rate beneath the CZ, is required for the initiation of stem cells during embryogenesis and later for their maintenance (reviewed in Bleckmann et al., 2009).

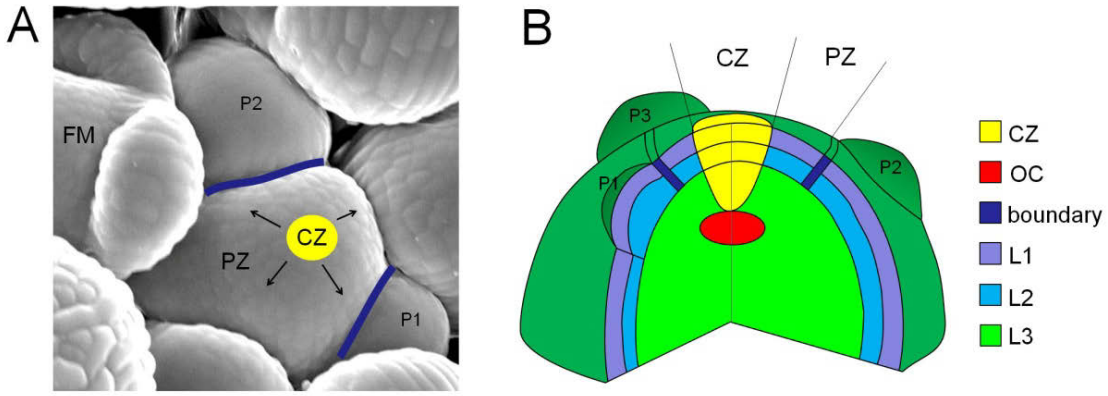

Fig. 1.2: SAM organization. (A) Scanning Electron Micrograph (SEM) of an *Arabidopsis* SAM. The central zone (CZ; yellow) at the summit of the meristem contains slowly dividing stem cells; stem cell descendants are shifted (arrows) to the peripheral zone (PZ) where they form new organ primordia (P1; P2) or contribute to the boundary formation (dark blue). After floral transition, determinate floral meristems (FM) are initiated at the SAM flanks. (B) The SAM consists of three clonally distinct cell layers (L1, L2 and L3). In the L1 and L2 layer cell divisions are preferentiallly anticlinal, cell divisions in the L3 occur in all planes. The stem cell population in the CZ (yellow) contains cells of all three layers. The organizing centre (OZ, red) is required for stem cell maintenance. Modified from Bleckmann et al., 2009.

During the vegetative stage, the SAM produces only rosette leaves. After floral transition, new, specialized meristems, that will produce shoots (axillary meristem (AXM)) or flowers (floral meristem (FM)), are initiated in the PZ. Each FM establishes floral organs in four concentric whorls: 4 sepals, 4 petals, 6 stamen and 2 carpels. The FM, in contrary to the SAM, is determinate: it arrests after it produced the full range of floral organs.

1.2.1. SAM homeostasis and lateral organ formation

Genetic mosaics and laser ablation experiments showed that a cells position within the SAM and not its clonal origin determines its fate (Poethig, 1989, Irish, 1991, Reinhardt et al., 2003). Indeterminate shoot growth therefore requires a balance between stem cell division and daughter cell differentiation to maintain the domain specific SAM organization (Fig. 1.2).

Within the past years, genetic analyses have identified a number of transcriptional regulators required to control meristem homeostasis and organ development. The analyses of mutant phenotypes and expression studies of the corresponding genes have shown that a mutual downregulation between meristem specific and organ specific genes is essential for normal development. Moreover, several studies highlighted the role of boundary establishment between the meristem and organ primordia. It was shown that cells within these boundaries play dual roles.

A number of transcriptional regulators encoded by boundary specific genes act to repress cell division and growth, resulting in the separation of organs from the meristem (M-O boundaries) or in a separation of adjacent organs (O-O boundaries) (Breuil-Broyer et al., 2004; Aida et al., 2006; Kwiatkowska, 2006). Beside this function, boundary specific genes participate in various regulatory networks to define and maintain indeterminate and determinate cell fates in the SAM (reviewed in Aida et al., 2006). More detailed information about the regulatory networks, involving meristem, organ and boundary specific genes, are provided in the enclosed review (Rast et al., 2008).

1.2.2. The meristem-to-organ boundary: more than an extremity of anything

The review: “The meristem-to-organ boundary: more than an extremity of anything” (Rast et al., 2008) was published in *Current Opinon in Genetics and Development* (impact factor: 9.3). The manuscript was written by me and overworked by Prof. Dr. R. Simon.

Available online at www.sciencedirect.com
ScienceDirect
Current Opinion in Genetics & Development

The meristem-to-organ boundary: more than an extremity of anything

Madlen I Rast and Rüdiger Simon

In plant shoot meristems, cells with indeterminate fate are separated from determinate organ founder cells by morphological boundaries. Organ founder cells are selected at sites of auxin accumulation. Auxin is channeled between cells via efflux carrier proteins, but influx carriers are needed to concentrate auxin in the outer meristem layer. The genetic programmes executed by organs and meristems are established by mutual repression of transcription factors, involving the sequestration of enhancer elements into DNA loops. Boundary cells play a dual role in separating and maintaining meristem and organ domains, and express unique genes that reduce cell division and auxin efflux carrier activity, but activate meristematic gene expression. Boundary positions depend on signals emitted from indeterminate cells at the meristem center.

Address
Institute of Genetics, Heinrich Heine University, D-40225 Düsseldorf, Germany

Corresponding author: Rast, Madlen I. (madlen.rast@uni-duesseldorf.de) and Simon, Rüdiger (ruediger.simon@uni-duesseldorf.de)

Current Opinion in Genetics & Development 2008, **18**:287–294

This review comes from a themed issue on
Pattern formation and developmental mechanisms
Edited by Ottoline Leyser and Olivier Pourquié

Available online 14th July 2008

0959-437X/$ – see front matter

DOI 10.1016/j.gde.2008.05.005

Introduction

Most higher plants maintain the unique ability to produce new organs throughout their entire lifetime. This is possible owing to collections of pluripotent cells called the shoot apical meristem (SAM) that reside at the shoot tip. The dome-shaped SAM carries non-differentiating stem cells at its top region, which divide slowly to generate more cells as the building material for lateral organs. When stem cells divide, daughter cells are shifted outwards to the periphery, where they can join others to found a new organ, or differentiate after further division rounds. Cell fate is therefore connected to a cell's location within the meristematic dome. Between meristematic cells and the young organ, a boundary is generated which is not only '. . . that which is an extremity of anything. . .', as Euclid defined it; instead, it consists of specialized cells with distinct gene expression programs and behavior. In this review, we will first discuss how sites of organ formation are selected, which gene expression programs are involved, and then concentrate on the functions and interactions of genes that are expressed specifically in the meristem-to-organ boundary.

Where organs are made: a primer on phyllotaxis

In most plants, organs are initiated at regular angles to each other. The groundlaying mechanism for generating such phyllotactic patterns involves the transport and local accumulation of the phytohormone auxin. Owing to a lower extracellular pH, auxin is uncharged when entering the cell, but becomes deprotonated inside and requires the help of membrane resident auxin export carriers to leave the cell again. A key molecule is PIN1 [1], an auxin efflux carrier that is predicted to be oriented in cell walls towards the higher auxin concentration, thereby pumping auxin against a concentration gradient [2••]. Using reporter genes that are sensitive to auxin signaling, it has been shown that auxin accumulates at sites of future organ initiation, and is simultaneously depleted from cells in the vicinity [3,4] (Figure 1). Within the developing leaf primordium, auxin is then channeled towards the stem tissue below. Where auxin levels are artificially raised at the flank of a meristem, a new organ will be generated [5]. By following a set of simple rules governing auxin diffusion and the activity and orientation of auxin efflux carriers, virtual meristem models can be generated that allow *in silico* reproduction of the phyllotactic patterns observed in nature [4,6]. In these simulations, only auxin distribution in the outer meristem layers is considered to control patterning.

However, extracellular (apoplastic) auxin could get lost from this patterning engine by diffusion, and it has been proposed that also auxin influx carriers of the AUX1/LAX1 family are redundantly required to maintain high auxin concentrations in the outermost layer of the meristem [7••]. Eliminating all auxin influx carrier activity in quadruple mutant combinations severely disturbs phyllotaxis, causing the formation of primordia at irregular angles, or even primordia cluster, because sharp auxin peaks cannot be maintained. But in contrast to *pin1* mutants that also show organ fusions and alterations in organ size, the inter-organ boundaries are still established, which becomes evident from the formation of separate organs. Once initiated, a primordium could generate an inhibitory field that prevents the formation of further primordia in the immediate vicinity. Because *pin1*

Figure 1

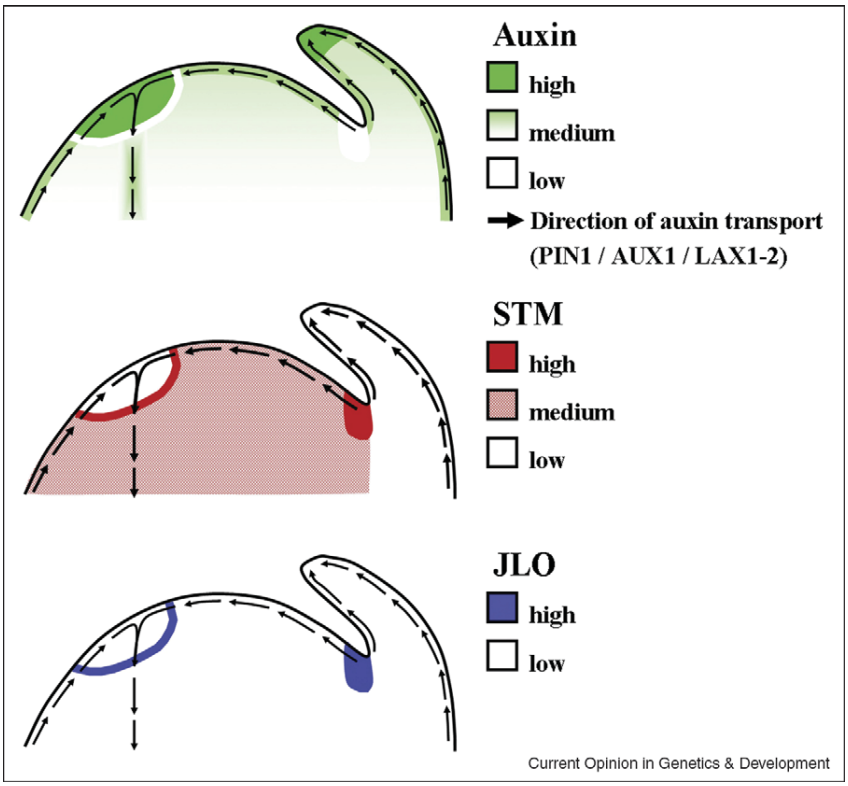

Comparison of local auxin concentrations (green) in the *Arabidopsis* SAM with the expression patterns of *STM* (class I KNOX; red) and *JLO* (LBD family; blue). Arrows indicate the direction of auxin transport via the auxin efflux carrier PIN1. Auxin influx carriers of the AUX1/LAX1 family counteract auxin diffusion into underlying tissues and maintain high auxin concentrations in the L1 layer [7••]. Cycles of auxin build-up in future primordia followed by decrease results in initiation of lateral organ primordia and phyllotactic patterning of the shoot. *STM* is expressed in a complementary pattern to auxin accumulation. Expression is visible throughout the whole meristem with a maximum in the boundary region, and downregulated in organ primordia [2••]. *JLO* expression is boundary-specific [21•] and promotes expression of class I KNOX genes, while repressing PIN1 expression.

mutants generate naked inflorescences or fused organs, *PIN1* dependent accumulation of auxin in primordia is a prerequisite for the establishment of the boundary surrounding the organ.

Positioning the meristem-to-organ boundary: a role for the stem cell domain?

Organ formation and the growth of stem tissue require a continuous supply of new cells. Both shoot and floral meristems can provide these owing to the activity of stem cells that reside in a central zone at the meristem tip. Primordia initiation occurs at a distance from the stem cell zone, in the surrounding peripheral zone. The size of this non-differentiating cell pool is controlled from a group of cells that reside underneath the stem cells and express the homeodomain transcription factor WUSCHEL (WUS) [8]. One way that WUS affects the stem cell pool is by downregulating the expression of several ARR proteins, which are negative regulators of cytokinin signaling [9•]. However, cytokinin alone is probably not sufficient to induce stem cell fate, and increased cytokinin signaling in WUS expressing cells alone cannot explain the very local induction of stem cell fate only at the meristem tip. This suggests that other target genes regulated by WUS and regional factors contribute to the determination of stem cell fate. Stem cells signal back to restrict *WUS* expression via the *CLV* pathways, consisting of the signaling molecule CLV3 that is secreted from stem cells, and two receptor systems that act to restrict *WUS* expression upon CLV3 release from stem cells [10•]. Improvements in the toolbox that allow meristem imaging have stimulated research into the dynamics of signaling between stem cells and the remainder of the meristem. One study used inducible RNAi to downregulate *CLV3* expression during development, which resulted in a rapid upregulation of *WUS*, and fate reversion of cells from the peripheral zone that reacquired stem cell identity [11••]. The converse experiment, that is induced upregulation of *CLV3* signaling, and thereby downregulation of *WUS* during development, led to a continuous reduction of the central zone [12•]. Primordia were initiated close to the meristem centre, apparently 'consuming' the cells of the central

Figure 2

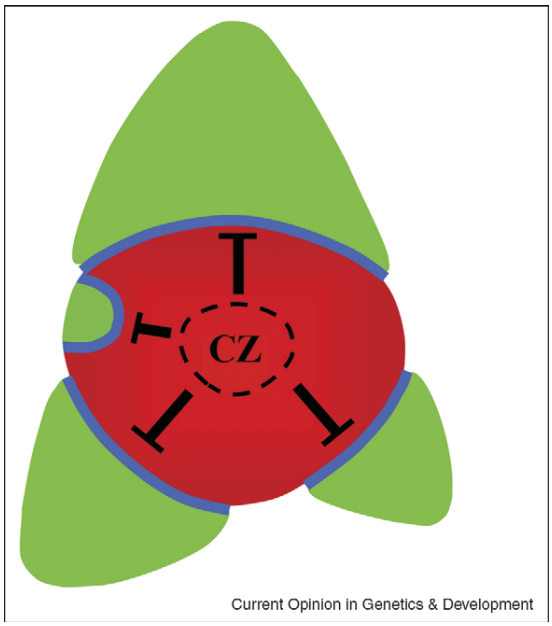

Schematic representation of a shoot apical meristem (top view). A signal from the central zone (CZ) is required to restrict organ formation to the periphery (red: meristematic region; blue: boundary domain; green: primordia; dotted lines indicate the stem cell domain).

zone. An obvious interpretation of this phenomenon is that a signal from the stem cell domain is required to inhibit organ formation in the vicinity (Figure 2). Thus, one factor positioning the meristem-to-organ boundary is the presence and activity of the stem cell domain.

Antagonistic regulation of gene expression in meristem and organ

The gene expression programs of organ primordia at lateral positions and the remainder of the meristem differ drastically (Table 1). Maintenance of meristematic fate requires expression of homeodomain transcription factors of the class1 *Knotted-like homeobox* family (*KNOX*), such as *SHOOTMERISTEMLESS* (*STM*) [13] (Figures 2 and 3). In primordia, *KNOX* gene expression is downregulated owing to the activity of MYB-domain transcription factors that belong to the ARP (Asymmetric leaves 1/Rough sheath 2/Phantastica) family (Figure 3). The ARP protein AS1 was shown to act together with the LATERAL ORGAN BOUNDARY (LOB) domain (LBD) protein ASYMMETRIC LEAVES2 (AS2) and the chromatin remodeling factor HIRA to form a repression module that restricts expression of the *KNOX* genes *KNAT1/BREVIPEDICELLUS* (*BP*), *KNAT2* and *KNAT6* from primordia [14•,15,16]. A model for this repression activity was recently proposed: AS1 and AS2 were found to bind at two sites of the *BP* promoter that flank an enhancer element which is required for expression in leaves. The interaction between the two AS1-AS2 complexes would sequester the enhancer sequences into a DNA loop, recruit HIRA and convert the chromatin to an inactive state [17••]. However, in many plant species (and in *Arabidopsis* plants mutant for AS1 or AS2) are *KNOX* genes also expressed at early stages of leaf development, where they promote the formation of dissected leaves. In meristems, *AS1* is negatively regulated by *STM*, thereby permitting *KNOX* gene expression [15].

The downregulation of *KNOX* gene expression in most leaf primordia and the initiation of auxin controlled gene expression programs are interconnected. Auxin accumulation in organ primordia appears to act in parallel with the *AS1/AS2* module to repress activity of *KNOX* genes in leaves [18], while misexpressing *KNOX* genes in organs reduces local auxin accumulation [19]. Genetic analysis showed that the failure to initiate lateral organs on *pin1*-mutant inflorescences is at least partly owing to an extended expression of the *KNOX* gene *BP* at lateral positions [20]. Furthermore, live imaging of gene expression patterns in the shoot meristem of *Arabidopsis* revealed a strict complementarity of *PIN1* and *STM* expression patterns during organ initiation [2••].

Genes expressed in boundaries

JAGGED LATERAL ORGANS (*JLO*), another member of the *LBD* gene family, is expressed in boundaries between the SAM and lateral organs (Figure 2). Misexpression of *JLO* in leaves caused leaf lobing, indicating extension of meristematic capacity by upregulation of KNOX genes [21•]. The primary target genes of *JLO* are probably *PIN* genes, because *PIN1* and others were rapidly downregulated upon *JLO* induction, preceding activation of *STM* and *BP* expression (Figure 3). When *JLO* was converted into a transcriptional repressor, boundaries where not maintained, showing that antagonistic regulation of *PIN* and *KNOX* genes is required. *LATERAL ORGAN BOUNDARIES* (*LOB*), the founding member of the *LBD* gene family that carries a conserved DNA binding domain [22,23], is expressed at the base of all lateral organs, and also in a ring-shaped domain at the base of lateral roots. The function of *LOB* is not fully understood, but several genes of the *LBD* family were shown to mediate responses to auxin [24,25]. *LOB* expression is induced by the *AS1/AS2* module, and by *BP* [26].

A number of transcriptional regulators act in boundaries to repress cell divisions and growth (Table 1). Their expression has to be tightly regulated to allow for proper organ growth and development. Prominent examples are the *CUP-SHAPED COTYLEDON* (*CUC1,2,3*) genes of *Arabidopsis*, encoding NAC domain transcription factors [27,28]. They were identified first owing to their double mutant phenotypes. *cuc1 cuc2* embryos grow fused cotyledon, because a discrete boundary between these organs

Table 1

Genes and their functions in lateral organ development

Gene	Annotation	Protein class	Expression	Function
Meristem-specific genes				
CLV3	AT2G27250	CLE	CZ	Promotion of stem cell differentiation, ↓WUS
WUS	AT2G17950	HOMEODOMAIN TF	OC	Maintenance of stem cell pool, ↑ CLV3
STM	AT1G62360	CLASS I KNOX	SAM	Initiation and maintenance of SAM, ↓CUC/AS1/AS2
BP	AT4G08150	CLASS I KNOX	SAM, Stamen	Maintenance of SAM, ↑LOB
KNAT2	AT1G70510	CLASS I KNOX	Rib meristem flower	Maintenance of SAM
Boundary-specific genes				
KNAT6	AT1G23380	CLASS I KNOX	Boundary	Maintenance of SAM, organ separation
CUC1	AT3G15170	NAC DOMAIN	Boundary	Negative regulation of growth, organ separation, ↑ class I KNOX
CUC2	AT5G53950	NAC DOMAIN	Boundary	Negative regulation of growth, organ separation, ↑ class I KNOX
CUC3	AT1G76420	NAC DOMAIN	Boundary	Negative regulation of growth, organ separation, ↑ class I KNOX
LOB	AT5G63090	LOB DOMAIN	Boundary	Putative role in organ separation and development
JLO	AT4G00220	LOB DOMAIN	Boundary	Boundary specification, ↑ BP/STM, ↓PIN
LBD36	AT5G66870	LOB DOMAIN	Boundary	Putative role in regulation of BP
UFO	AT1G30950	F-BOX	Boundary	Specification of FM identity and floral organs
SUP	AT3G23130	ZINC FINGER	Boundary	Negative regulation of growth at the stamen-to-carpel boundary
Primordia-specific genes				
AS2	AT1G65620	LOB DOMAIN	Primordia (adaxial)	Ad/ab polarity, petal development, ↓BP/KNAT2/KNAT6;↑LOB; ↔ AS1
AS1	AT2G37630	MYB DOMAIN	Primordia	Determination of ad/ab polarity ↓BP/KNAT2/KNAT6;↑LOB;↔ AS2/HIRA
HIRA	AT3G44530	WD-REPEAT	Primordia/ vasculature	Chromatin re-organization ↓BP/KNAT2/KNAT6;↔ AS1
BOP1	AT3G57130	BTB/POZ	Lateral organ base	Regulation of organ cell fate and polarity ↓BP/KNAT2/KNAT6;↑AS1/AS2
BOP2	AT2G41370	BTB/POZ	Lateral organ base	Regulation of organ cell fate and polarity ↓BP/KNAT2/KNAT6;↑AS1/AS2
PTL	AT5G03680	TRIHELIX TF	Flower primordia sepal margin	Negative regulation of growth, organ separation
JAG	AT1G68480	ZINC FINGER	Primordia	Regulation of organ shape and organ tissue proliferation
RBE	AT5G06070	ZINC FINGER	Integument, petal primordia	Separation of petals, ↓AG
Genes involved in auxin transport				
PIN1	AT1G73590	EFFLUX CARRIER	SAM (L1), vasculature	Polar auxin transport
PID	AT2G34650	SER/THR KINASE	Primordia, vasculature	Positive regulation of auxin efflux, binary switch for PIN polarity
AUX1	AT2G38120	INFLUX CARRIER	SAM (L1), vasculature	Maintenance of auxin gradients
LAX1	AT5G01240	INFLUX CARRIER	SAM (L1), vasculature	Maintenance of auxin gradients
LAX2	AT2G21050	INFLUX CARRIER	Primordia, vasculature	Maintenance of auxin gradients
other genes				
miRNA 164	AT2G47585	/	Diverse	Directs degradation of NAC domain proteins (CUC1,CUC2)
PAN	AT1G68640	bZIP PROTEIN	SAM, FM, floral organ primordia	Regulation of floral organ number and meristem cell proliferation
TCP3	AT1G53230	bHLH PROTEIN	Diverse	↑ miRNA164 in organs

↑: Upregulation of expression; ↓: downregulation of expression; ↔: interaction; SAM: shoot apical meristem; FM: floral meristem; CZ: Central Zone; OC: Organising Centre; TF: transcription factor.

Figure 3

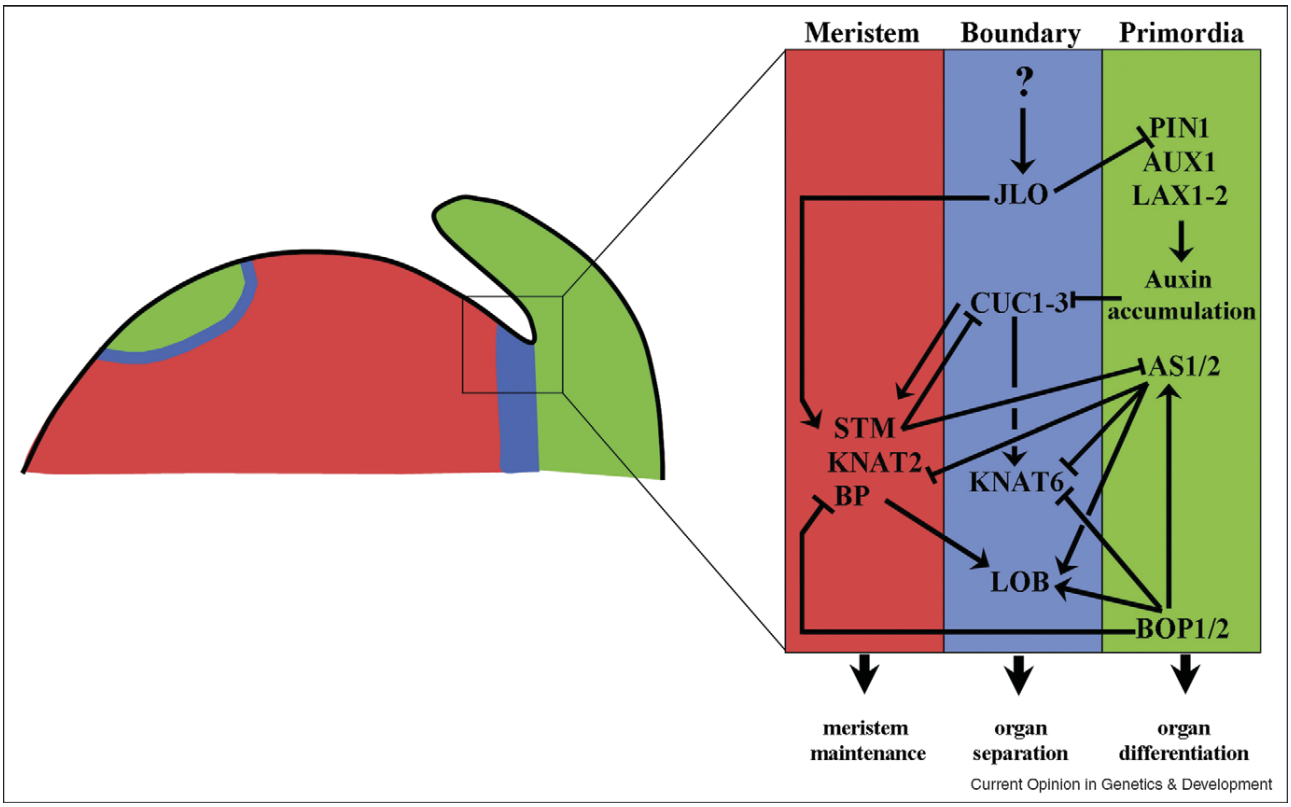

Genes controlling the separation of indeterminate (meristem) cells from determinate cells (organ). Undifferentiated cells in the meristem (red) express class I KNOX genes (*STM*/*BP* and *KNAT2*); lateral organ primordia (green) concentrate auxin and express genes that promote differentiation; boundary cells (blue) separate meristem and primordia from each other. During embryogenesis, *CUC* genes are required for the activation of *STM* in the SAM. Once expressed, *STM* downregulates *CUC* expression. In addition, *CUC* genes are negatively regulated by auxin dependent signalling, thus restricting *CUC* expression to the boundary region. Three more class I KNOX genes, *BP* and *KNAT2* and *KNAT6* (the only boundary expressed KNOX gene) are also positively regulated by *CUC* [27,28]. *STM* keeps cells in an undifferentiated state by repressing *AS1* and *AS2* in stem cells and their immediate derivatives. In turn, the AS1/AS2 complex promotes leaf development via repression of *KNOX* genes (*BP*/*KNAT2*/*KNAT6*) in leaf primordia, thus allowing differentiation [14•,15,16]. Additionally, localized auxin maxima act alongside *AS1*/*AS2* to promote leaf development, which is also partly dependent on *BP* downregulation [20] (not shown here). Auxin distribution is dependent on polar transport via the auxin efflux carrier PIN1 [2••], and auxin influx carrier of the AUX1/LAX1 family [7••]. Two members of the LBD family, *JLO* and *LOB*, are expressed in the boundary region [22,23]. *JLO* was shown to repress *PIN* gene expression, whereas *STM* and *BP* are upregulated by induced *JLO* misexpression. To date, regulators of *JLO* expression have not been identified (**?**) [21•]. The function of *LOB* in organ development is less understood, but its expression was shown to be induced by the *AS1*/*AS2* complex, *BP* and by *BOP1/2* [26,38]. *BOP1/2* are involved in the regulation of lateral organ cell fate and polarity via activation of *AS1*/*AS2* and repression of *KNOX* genes. Although *BOP1/2* are expressed in cells adjacent to the lateral organ boundary, they are required for expression of boundary-specific genes like *LOB* [37,38].

is missing. During embryogenesis, *CUC* genes are required for the activation of *STM* expression, and these genes later act together in a pathway controlling meristem initiation and organ separation. *CUC* genes are also required postembryonically in a partially redundant manner to promote boundary maintenance. It was found that the expression of *CUC2* is posttranscriptionally downregulated by members of the miRNA164 [29,30•], which play a dual role in spatially restricting and dampening the expression of growth inhibiting *CUC* genes. Accordingly, expression of a miRNA resistant version of *CUC2* increased the size of the boundary domain, indicating that *CUC2* is a central regulator of boundary size. There is an intricate interdependence between auxin-dependent organ initiation and *CUC* gene expression. Mutants with reduced directional auxin transport, such as *pin1* or *pinoid*, allow expansion of *CUC2* and *STM* expression to the periphery, where they suppress cotyledon and organ growth [31,32]. This suggests that *CUC* expression is negatively regulated by auxin dependent signaling. Furthermore, failure to downregulate *CUC2* expression in plants lacking miRNA164 affects phyllotactic patterning. We have discussed above that phyllotaxis is established via the creation of an auxin concentration landscape, but *CUC2* misexpression seems to act later and interfere with the (less understood) maintenance of

the phyllotactically correct angles between organs [30•,33•].

PETALLOSS (*PTL*) encodes a trihelix transcription factor that separates sepals from each other by suppressing growth in the boundary regions between them [34]. In *ptl* single mutants, but more frequently in double mutants with *cuc1* or *cuc2*, boundaries are not established, indicating that *PTL* and the *CUC* genes act in parallel pathways of growth repression. Normal organ development is only possible if *CUC* and *PTL* expression is repressed in organ primordia, and several factors appear to share this task, among them are *AS1* and *AS2*. This was revealed in *as1 jag* or *as2 jag* double mutants that allow *PTL*, *CUC1* and *CUC2* expression in organs, causing a severe reduction in organ size [35•]. In addition, several transcription factors of the *TCP* family regulate *CUC* expression by promoting expression of miRNA164 in organs [36•].

BLADE ON PETIOLE (*BOP*) *1* and *2*, two related genes encoding *BTB/POZ* domain and ankyrin-repeat containing proteins, are expressed at the base of lateral organs from where they regulate lateral organ cell fate and polarity [37,38]. *bop1 bop2* double mutants show ectopic tissue growth from the lamina, and lack a distinct petiole. The two *BOP* genes are functionally redundant and repress *KNOX* genes that confer meristematic fate via activation of *AS1* and *AS2* expression. Although the *BOP*s are expressed in cells adjacent to the lateral organ boundary [38], they are required for expression of the boundary genes *LOB* and *LBD36*. Interestingly, *BOPs* were shown to interact with *PERIANTHIA*, a TGA transcription factor that controls floral organ number and meristem cell proliferation [39]. Several genes have been identified that control boundary formation during flower development, but also expression of floral organ identity genes. The zinc-finger gene *SUPERMAN* (*SUP*) restricts cell proliferation at the stamen-to-carpel boundary [40], while the superman-like protein *RABBIT EARS* (*RBE*) acts downstream of *PTL* to separate first whorl organs and repress ectopic expression of the homeotic gene *AGAMOUS* [41,42].

The only gene of the *KNOX* family preferentially expressed in boundaries is *KNAT6*. Together with *STM*, *KNAT6* promotes SAM maintenance and organ separation [43•]. In a functional hierarchy, *KNAT6* acts after the *CUC* genes, and antagonistic to BP [44].

Conclusions: the role of boundaries in meristem and organ development

We have identified some of the genetic interactions between genes expressed in meristems, lateral organs and the boundary cells separating them. Cell fates at the meristem flank are altered with the local accumulation of auxin, controlled by PIN and AUX/LAX carrier proteins. This coincides with a downregulation of *KNOX* gene expression at these positions. Restricting meristematic gene expression from the periphery is mediated by the AS1/AS2 module. Gene expression boundaries are set and maintained by a whole set of transcription factors that interact with and regulate the expression of meristematic and organ-specific genes.

However, there are probably more roles for boundaries than just separating domains with differing transcription profiles. Detailed analysis of cell shapes revealed that the meristem apex surface displays mostly positive Gaussian curvature, and that primordia arise as small bulges on the meristem flank in a region with negative curvature that forms a shallow crease [45,46]. This creates the morphological boundary, which is characterized by reduced cell proliferation [47], cell elongation perpendicular to the radial axis, but formation of new cell walls parallel to the long axis of boundary cells. It is not yet clear if these morphological features are just a consequence of different tissue stress in the adjacent meristem and organ domains, or if generating a cell group with such distinct features enables the shaping of meristem and organ. Boundaries with distinct cell wall properties could also play a more passive role in filtering the flux of informational molecules, such as miRNAs or other small RNAs, between meristem and organ [48•]. Classic microsurgical experiments showed that a signal from the meristem is required to promote adaxial cell fate in lateral organs, which is possibly transmitted via the outermost cell layer [49•].

We found that our understanding of boundaries in plant organ development does not match with the philosophical concept of a boundary, because they are not just the extremity of anything (meristem or organ), they are unique entities consisting of many cells with specialized functions that require further studies to uncover all their secrets.

Acknowledgements

Funding of research in R.S. laboratory was provided by the DFG through SFB590, individual grants, and *SY-STEM*, a Marie-Curie Research and Training Network of the European Union.

References and recommended reading

Papers of particular interest, published within the period of review, have been highlighted as:

- • of special interest
- •• of outstanding interest

1. Galweiler L, Guan C, Muller A, Wisman E, Mendgen K, Yephremov A, Palme K: **Regulation of polar auxin transport by AtPIN1 in *Arabidopsis* vascular tissue**. *Science* 1998, **282**:2226-2230.

2. •• Heisler MG, Ohno C, Das P, Sieber P, Reddy GV, Long JA, Meyerowitz EM: **Patterns of auxin transport and gene expression during primordium development revealed by live imaging of the *Arabidopsis* inflorescence meristem**. *Curr Biol* 2005, **15**:1899-1911.

This study analyzes in detail the expression patterns of genes controlling flower primordia development. In addition, by monitoring the expression and polarity of PINFORMED1 (PIN1), an auxin efflux facilitator, and the

expression of the auxin-responsive reporter DR5, they reveal stereotypical PIN1 polarity changes. Auxin induction experiments suggest that cycles of auxin build-up and depletion direct different stages of primordium development.

3. Benkova E, Michniewicz M, Sauer M, Teichmann T, Seifertova D, Jurgens G, Friml J: **Local, efflux-dependent auxin gradients as a common module for plant organ formation**. *Cell* 2003, **115**:591-602.

4. Reinhardt D, Pesce ER, Stieger P, Mandel T, Baltensperger K, Bennett M, Traas J, Friml J, Kuhlemeier C: **Regulation of phyllotaxis by polar auxin transport**. *Nature* 2003, **426**:255-260.

5. Reinhardt D, Mandel T, Kuhlemeier C: **Auxin regulates the initiation and radial position of plant lateral organs**. *Plant Cell* 2000, **12**:507-518.

6. Leyser O: **Auxin distribution and plant pattern formation: how many angels can dance on the point of PIN?** *Cell* 2005, **121**:819-822.

7. •• Bainbridge K, Guyomarc'h S, Bayer E, Swarup R, Bennett M, Mandel T, Kuhlemeier C: **Auxin influx carriers stabilize phyllotactic patterning**. *Genes Dev* 2008, **22**:810-823.

This paper describes the role of the auxin influx transporter AUX1 and its paralogs LAX1, LAX2 and *LAX3* in the maintenance of the auxin gradient in the shoot. A characterization of different *aux1/lax* double, triple, and quadruple mutant combinations revealed that AUX1, LAX1 and LAX2, but not LAX3, have partially redundant functions in the organization of phyllotactic patterning. Analysis of auxin distribution and PIN1 localization further suggest that AUX LAX transporters act in the maintenance of a defined auxin maxima in the L1 layer of the shoot, leading to primordium initiation in a regular pattern.

8. Stahl Y, Simon R: **Plant stem cell niches**. *Int J Dev Biol* 2005, **49**:479-489.

9. • Leibfried A, To JP, Busch W, Stehling S, Kehle A, Demar M, Kieber JJ, Lohmann JU: **WUSCHEL controls meristem function by direct regulation of cytokinin-inducible response regulators**. *Nature* 2005, **438**:1172-1175.

This paper describes a link between the CLV/WUS network and hormonal control. The authors show that WUS, a positive regulator of stem cell fate, directly repress the transcription of several two-component ARABIDOPSIS RESPONSE REGULATOR genes (ARR5, ARR6, ARR7 and ARR15). These ARR genes were shown to act as negative regulators of cytokinin signaling in *Arabidopsis*. The authors suggest that repression of ARR genes by WUS might be necessary to maintain a functional meristem.

10. • Müller R, Bleckmann A, Simon R: **The receptor kinase CORYNE of *Arabidopsis* transmits the stem cell-limiting signal CLAVATA3 Independently of CLAVATA1**. *Plant Cell* 2008, **20**:1-13.

This paper provides a functional analysis of the receptor kinase CORYNE (*CRN*). Mutations in CRN cause stem cell proliferation, similar to clv1, clv2, and clv3 mutants. CRN is supposed to act together with CLV2, and in parallel with CLV1, to perceive the CLV3 signal for restriction of stem cell proliferation and promotion of differentiation. Furthermore, CRN has additional functions during plant development, including floral organ development that are shared with CLV2. Because the CRN protein lacks a distinct extracellular domain, the authors propose that CRN and CLV2 interact via their transmembrane domains to establish a functional receptor.

11. •• Reddy GV, Meyerowitz EM: **Stem-cell homeostasis and growth dynamics can be uncoupled in the *Arabidopsis* shoot apex**. *Science* 2005, **310**:663-667.

This paper shows that CLV3 restricts its own domain of expression (the CZ) by preventing differentiation of peripheral zone cells (PZ), which surround the CZ, into CZ cells, and restricts overall SAM size by a separate, long-range effect on cell division rate.

12. • Müller R, Borghi L, Kwiatkowska D, Laufs P, Simon R: **Dynamic and compensatory responses of *Arabidopsis* shoot and floral meristems to CLV3 signaling**. *Plant Cell* 2006, **18**:1188-1198.

A detailed analysis of the dynamics of *CLV3* signaling using an inducible gene expression system. It is shown that increasing the *CLV3* signal can very rapidly repress *WUS* expression during development and restrict meristem growth by promoting allocation of peripheral meristem cells into organ primordia. Meristem homeostasis seems to tolerate variation in *CLV3* levels over a 10-fold range. High-level *CLV3* signaling can be partially compensated with time, indicating that the level of *CLV3* expression communicates only limited information on stem cell number to the underlying OC cells.

13. Scofield S, Murray JA: **KNOX gene function in plant stem cell niches**. *Plant Mol Biol* 2006, **60**:929-946.

14. • Phelps-Durr TL, Thomas J, Vahab P, Timmermans MC: **Maize rough sheath2 and its *Arabidopsis* orthologue ASYMMETRIC LEAVES1 interact with HIRA, a predicted histone chaperone, to maintain knox gene silencing and determinacy during organogenesis**. *Plant Cell* 2005, **17**:2886-2898.

It is shown that RS2/AS1-mediated *KNOX* gene silencing involves epigenetic mechanism. These MYB domain proteins can form conserved protein complexes through interaction with ASYMMETRIC LEAVES2 (AS2), a predicted RNA binding protein (RIK), and a homologue of the histone chaperon HIRA. The data suggest that AS1, AS2, and HIRA act together to maintain *KNOX* gene silencing, likely by modulating chromatin structure.

15. Byrne ME, Barley R, Curtis M, Arroyo JM, Dunham M, Hudson A, Martienssen RA: **Asymmetric leaves1 mediates leaf patterning and stem cell function in *Arabidopsis***. *Nature* 2000, **408**:967-971.

16. Byrne ME, Simorowski J, Martienssen RA: **ASYMMETRIC LEAVES1 reveals knox gene redundancy in *Arabidopsis***. *Development* 2002, **129**:1957-1965.

17. •• Guo M, Thomas J, Collins G, Timmermans MC: **Direct repression of KNOX Loci by the ASYMMETRIC LEAVES1 complex of *Arabidopsis***. *Plant Cell* 2008, **20**:48-58.

This study is focused on the mechanism of AS1 complex-mediated KNOX gene silencing in *Arabidopsis*. The authors show that AS1 and AS2 form a repressor complex that binds directly to regulatory motifs at two sites in the promoters of the KNOX genes BREVIPEDICELLUS (BP) and KNAT2. The paper presents a model in which AS1-AS2 complexes interact to create a loop in the KNOX promoter. Recruitment of the chromatin remodeling factor HIRA leads then to the formation of a repressive chromatin state.

18. Scanlon MJ: **The polar auxin transport inhibitor N-1-naphthylphthalamic acid disrupts leaf initiation, KNOX protein regulation, and formation of leaf margins in maize**. *Plant Physiol* 2003, **133**:597-605.

19. Zgurski JM, Sharma R, Bolokoski DA, Schultz EA: **Asymmetric auxin response precedes asymmetric growth and differentiation of asymmetric leaf1 and asymmetric leaf2 *Arabidopsis* leaves**. *Plant Cell* 2005, **17**:77-91.

20. Hay A, Barkoulas M, Tsiantis M: **ASYMMETRIC LEAVES1 and auxin activities converge to repress BREVIPEDICELLUS expression and promote leaf development in *Arabidopsis***. *Development* 2006, **133**:3955-3961.

21. • Borghi L, Bureau M, Simon R: ***Arabidopsis* JAGGED LATERAL ORGANS is expressed in boundaries and coordinates KNOX and PIN activity**. *Plant Cell* 2007, **19**:1795-1808.

This paper describes the identification of the JLO gene, a member of the LATERAL ORGAN BOUNDARY DOMAIN gene family. JLO is expressed in boundaries between meristems and organ primordia. Misexpression of JLO correlates with ectopic expression of STM and KNAT1 in leaves and repression of PIN auxin export facilitators. The results indicate that JLO function is required to maintain the integrity of boundaries between cell groups with indeterminate or determinate fates.

22. Husbands A, Bell EM, Shuai B, Smith HM, Springer P: **LATERAL ORGAN BOUNDARIES defines a new family of DNA-binding transcription factors and can interact with specific bHLH proteins**. *Nucleic Acids Res* 2007:1-9.

23. Shuai B, Reynaga-Pena CG, Springer PS: **The lateral organ boundaries gene defines a novel, plant-specific gene family**. *Plant Physiol* 2002, **129**:747-761.

24. Inukai Y, Sakamoto T, Ueguchi-Tanaka M, Shibata Y, Gomi K, Umemura I, Hasegawa Y, Ashikari M, Kitano H, Matsuoka M: **Crown rootless1, which is essential for crown root formation in rice, is a target of an AUXIN RESPONSE FACTOR in auxin signaling**. *Plant Cell* 2005, **17**:1387-1396.

25. Okushima Y, Fukaki H, Onoda M, Theologis A, Tasaka M: **ARF7 and ARF19 regulate lateral root formation via direct activation of LBD/ASL genes in *Arabidopsis***. *Plant Cell* 2007, **19**:118-130.

26. Lin WC, Shuai B, Springer PS: **The *Arabidopsis* LATERAL ORGAN BOUNDARIES-domain gene ASYMMETRIC LEAVES2**

functions in the repression of KNOX gene expression and in adaxial-abaxial patterning. *Plant Cell* 2003, **15**:2241-2252.

27. Aida M, Ishida T, Tasaka M: **Shoot apical meristem and cotyledon formation during *Arabidopsis* embryogenesis: interaction among the CUP-SHAPED COTYLEDON and SHOOT MERISTEMLESS genes**. *Development* 1999, **126**:1563-1570.

28. Aida M, Tasaka M: **Genetic control of shoot organ boundaries**. *Curr Opin Plant Biol* 2006, **9**:72-77.

29. Laufs P, Peaucelle A, Morin H, Traas J: **MicroRNA regulation of the CUC genes is required for boundary size control in *Arabidopsis* meristems**. *Development* 2004, **131**:4311-4322.

30. • Sieber P, Wellmer F, Gheyselinck J, Riechmann JL, Meyerowitz EM: **Redundancy and specialization among plant microRNAs: role of the MIR164 family in developmental robustness**. *Development* 2007, **134**:1051-1060.
This paper shows the effects of elimination of all three members of the MIR164 family from *Arabidopsis*. It was found that a loss of miR164 activity leads to a severe disruption of shoot development, in contrast to the effect of mutation in any single MIR164 gene. This indicates that these miRNAs are functionally redundant. However, differences in the expression patterns of the individual MIR164 genes imply that redundancy among them is only partially. Furthermore, it is shown that the derepression of two of the miR164 targets, CUC1 and CUC2, in miR164 loss-of-function mutants is likely to account for most of the mutant phenotype.

31. Vernoux T, Kronenberger J, Grandjean O, Laufs P, Traas J: **PIN-FORMED 1 regulates cell fate at the periphery of the shoot apical meristem**. *Development* 2000, **127**:5157-5165.

32. Furutani M, Vernoux T, Traas J, Kato T, Tasaka M, Aida M: **PIN-FORMED1 and PINOID regulate boundary formation and cotyledon development in *Arabidopsis* embryogenesis**. *Development* 2004, **131**:5021-5030.

33. • Peaucelle A, Morin H, Traas J, Laufs P: **Plants expressing a miR164-resistant CUC2 gene reveal the importance of post-meristematic maintenance of phyllotaxy in *Arabidopsis***. *Development* 2007, **134**:1045-1050.
This paper describes a novel mechanism leading to changes in phyllotactic pattern. *CUC1* and *CUC2,* which are expressed in the boundary domain, are targets of the *miR164* mediated endonucleotide cleavage. Using plants expressing a *miR164*-resistant *CUC2* gene, the authors could show that ectopic *CUC2* expression cause changes in the phyllotactic pattern of the fully grown stem, despite the pattern of organ initiation by the meristem. This indicates that the phyllotaxy initiated at the meristem has to be maintained during stem growth and differentiation, and suggests that this requires the proper timing of *CUC2* expression.

34. Brewer PB, Howles PA, Dorian K, Griffith ME, Ishida T, Kaplan-Levy RN, Kilinc A, Smyth DR: **PETAL LOSS, a trihelix transcription factor gene, regulates perianth architecture in the *Arabidopsis* flower**. *Development* 2004, **131**:4035-4045.

35. • Xu B, Li Z, Zhu Y, Wang H, Ma H, Dong A, Huang H: ***Arabidopsis* genes AS1, AS2, and JAG negatively regulate boundary-specifying genes to promote sepal and petal development**. *Plant Physiol* 2008, **146**:566-575.
In this article, the authors present double mutant and overexpression analysis of *Arabidopsis thaliana* ASYMMETRIC LEAVES1 and 2 (AS1 and AS2) and JAGGED (JAG) genes. The results indicate that AS1/AS2 and JAG act in parallel to repress the boundary-specifying PETAL LOSS (PTL) and CUP-SHAPED COTYLEDONS1 and 2 (CUC1 and CUC2) genes in sepals and petals to define these organs from their boundaries.

36. • Koyama T, Furutani M, Tasaka M, Ohme-Takagi M: **TCP transcription factors control the morphology of shoot lateral organs via negative regulation of the expression of boundary-specific genes in *Arabidopsis***. *Plant Cell* 2007, **19**:473-484.
In this paper a gene silencing system, designated chimeric repressor gene-silencing technology (CRES-T), is used to study the function of TCPs in leaf morphogenesis.

37. Norberg M, Holmlund M, Nilsson O: **The BLADE ON PETIOLE genes act redundantly to control the growth and development of lateral organs**. *Development* 2005, **132**:2203-2213.

38. Ha CM, Jun JH, Nam HG, Fletcher JC: **BLADE-ON-PETIOLE 1 and 2 control *Arabidopsis* lateral organ fate through regulation of LOB domain and adaxial-abaxial polarity genes**. *Plant Cell* 2007, **19**:1809-1825.

39. Hepworth SR, Zhang Y, McKim S, Li X, Haughn GW: **BLADE-ON-PETIOLE-dependent signaling controls leaf and floral patterning in *Arabidopsis***. *Plant Cell* 2005, **17**:1434-1448.

40. Sakai H, Medrano LJ, Meyerowitz EM: **Role of SUPERMAN in maintaining *Arabidopsis* floral whorl boundaries**. *Nature* 1995, **378**:199-203.

41. Krizek BA, Lewis MW, Fletcher JC: **RABBIT EARS is a second-whorl repressor of AGAMOUS that maintains spatial boundaries in *Arabidopsis* flowers**. *Plant J* 2006, **45**:369-383.

42. Takeda S, Matsumoto N, Okada K: **RABBIT EARS, encoding a SUPERMAN-like zinc finger protein, regulates petal development in *Arabidopsis thaliana***. *Development* 2004, **131**:425-434.

43. • Belles-Boix E, Hamant O, Witiak SM, Morin H, Traas J, Pautot V: **KNAT6: an *Arabidopsis* homeobox gene involved in meristem activity and organ separation**. *Plant Cell* 2006, **18**:1900-1907.
This study provides a detailed analysis of KNAT6 and KNAT2 function in the *Arabidopsis* SAM. The identification of null alleles for both class I KNOX genes and the analysis of their interaction with STM indicate that KNAT6 but not KNAT2 contributes, redundantly with STM, to SAM maintenance and to the establishment of the boundaries via the STM/CUC pathway.

44. Ragni L, Belles-Boix E, Gunl M, Pautot V: **Interaction of KNAT6 and KNAT2 with BREVIPEDICELLUS and PENNYWISE in *Arabidopsis* inflorescences**. *Plant Cell* 2008, **20**:888-900.

45. Kwiatkowska D: **Flowering and apical meristem growth dynamics**. *J Exp Bot* 2008, **59**:187-201.

46. Grandjean O, Vernoux T, Laufs P, Belcram K, Mizukami Y, Traas J: ***In vivo* analysis of cell division, cell growth, and differentiation at the shoot apical meristem in Arabidopsis**. *Plant Cell* 2004, **16**:74-87.

47. Breuil-Broyer S, Morel P, de Almeida-Engler J, Coustham V, Negrutiu I, Trehin C: **High-resolution boundary analysis during *Arabidopsis thaliana* flower development**. *Plant J* 2004, **38**:182-192.

48. • Garcia D, Collier SA, Byrne ME, Martienssen RA: **Specification of leaf polarity in *Arabidopsis* via the trans-acting siRNA pathway**. *Curr Biol* 2006, **16**:933-938.
Previous studies identified different genes that are involved in the determination of adaxial/abaxial polarity in plants, for example the Myb domain gene PHANTASTICA (PHAN) which is required for adaxial fate. Here, the authors provide evidences that an alternative or redundant pathway for specification of leaf polarity exist, in which trans-acting siRNAs play an important role. Analysis of various mutant combinations and expression pattern revealed a network regulation in which expression of FILAMENTOUS FLOWER (FIL) is redundantly regulated by AS1 and ETTIN (ETT)/ARF3. ETT in turn is a target of the trans-acting siRNA gene TAS3. Furthermore, the data implicate ta-siRNA as a mobile signal in Arabidopsis development.

49. • Reinhardt D, Frenz M, Mandel T, Kuhlemeier C: **Microsurgical and laser ablation analysis of leaf positioning and dorsoventral patterning in tomato**. *Development* 2005, **132**:15-26.
The authors employed new microsurgical techniques to analyze the mechanism that are involved in phyllotactic patterning and leaf polarity. The results of these experiments indicate that existing primordia influence the size and position of new organs. In addition, L_1-specific cell ablation experiments suggest that the meristem L_1 layer is essential for the dorsoventral patterning of leaf primordia.

1.2.3. The *LATERAL ORGAN BOUNDARY DOMAIN GENE* (*LBD*) family

LATERAL ORGAN BOUNDARY (LOB) is a transcription factor which is expressed in boundaries of all above ground lateral organs and secondary roots (Shuai et al., 2002). Although the function of *LOB* in organ separation and development is less understood, its expression appears to be positively regulated by *ASYMMETRIC LEAVES 2 (AS2)* and *BLADE-ON PETIOLE1 (BOP1)* and *BOP2,* as well as *BREVIPREDICELLUS (BP)* (Lin et al., 2003a; Jun et al., 2010, Ha et al., 2007). Thus, both meristem and organ primordia specific genes concur to promote *LOB* expression in the boundaries between them (reviewed in Rast et al., 2008).

LOB is the founder of the *LATERAL ORGAN BOUNDARY DOMAIN* (*LBD*) gene family in *Arabidopsis.* All 43 *LBD* members share an N-terminal domain, termed LOB domain, of approximately 100 amino acids (AA). This LOB domain is conserved in plant evolution as homologues have been identified in the moss *Physcomitrella* as well as in higher plants (Iwakawa et al., 2002; Shuai et al., 2002; R. Simon pers. communication).The LOB domain contains conserved blocks of AA, called C-BLOCK and GAS-BLOCK. The C-BLOCK is a cystein-rich region with 4 cystein residues arranged in a CX2CX6CX3C motif (X = every amino acid) which are supposed to form a zincfinger to mediate DNA binding. The GAS-Block comprises 49 AA and owes its name to a conservation of the three AA, G, A and S. Further features include a predicted coiled coil domain at the end of the LOB domain. This coiled coil domain contains 4 leucine residues in a LX6LX3LX6L spacing that is reminiscent of a leucine zipper and is thought to provide protein interaction (Shuai et al., 2002).

Sequence alignments based on the AA sequence within the LOB domain showed that the LBD proteins can be grouped into two classes. Class II proteins lack the coiled coil domain; their function may therefore be distinct from the class I proteins. A phylogenetic tree that is based on the entire AA sequence revealed further subclasses within the LBD family (Iwakawa et al., 2002; Shuai et al., 2002). Notably, most *LBD* genes that group together in this phylogenetic tree are also immediate neighbors at genomic regions. This suggests duplication events among the LBD family members. Furthermore, several of these chromosomal mini-clusters are thought to result from large-scale duplications, indicating a functional conservation within the *LBD* gene family (Matsumura et al., 2009).

LBD proteins are suggested to execute their function in the nucleus. In line with this assumption, all analyzed LBD-fluorescent protein fusions localize to the nucleus (Iwakawa et al., 2002; Naito et al., 2007; Oh et al., 2010) and the LOB domain of LOB was shown to bind to DNA *in vitro* (Husbands et al., 2007). Recent studies implicated LBD family members in various developmental processes, such as gametophyte development (Evans, 2007; Oh et al., 2010), embryonic patterning (Borghi et al., 2007; Bureau et al., 2008), leaf and flower development (Ori et al., 2000; Semiarti et al., 2001; Xu et al., 2008; Chalfun-Junior et al., 2005), inflorescence branch formation (Bortiri et al., 2006), lateral root formation (Liu et al.,

2005; Okushima et al., 2007), tracheary element differentiation (Soyano et al., 2008) boundary delimitation (Shuai et al., 2002; Borghi et al., 2007) and photomorphogenesis (Mangeon et al., 2010). Furthermore, some LBD proteins were found to act in phytohormone signaling pathways. Expression of *LBD3* for example was shown to respond to cytokinin (Husbands et al., 2007; Naito et al., 2007), and microarray experiments identified a number of *LBD* genes that are regulated by auxin (Nemhauser et al., 2004; Paponov et al., 2008). Accordingly, *LBD16, LBD18* and *LBD29* act downstream of the *AUXIN RESPONSE FACTOR7 (ARF7*) and *ARF9* in lateral root formation (Okushima et al., 2005; Okushima et al., 2007) and *JAGGED LATERAL ORGANS (JLO/LBD30),* as well as *DOWN IN DARK AND AUXIN1 (DDA1/LBD25),* were shown to be involved in the control of auxin transport and signaling (Mangeon et al., 2010; Borghi et al., 2007; Bureau et al., 2008).

1.3. Organization of the Root Meristem (RM)

Similar to the SAM, the *Arabidopsis* root displays an organization in zones and layers. In transverse sections the root is composed of concentrically arranged, clonally distinct cell files, termed epidermis, cortex, endodermis, pericycle and vasculature (from outside to inside). Stereotyped cell divisions precisely maintain this radial pattern and each cell file can be traced back to one stem cell, also called initial. These root initials are organized around the quiescent center (QC) that is required to maintain their stem cell fate. Depending on their positions, initials form different tissue types. Columella cells derive from the distal initials whereas endodermis, cortex and vasculature derive from proximal initials. The proximal-lateral initials form the epidermis and lateral root cap (Fig. 1.3).

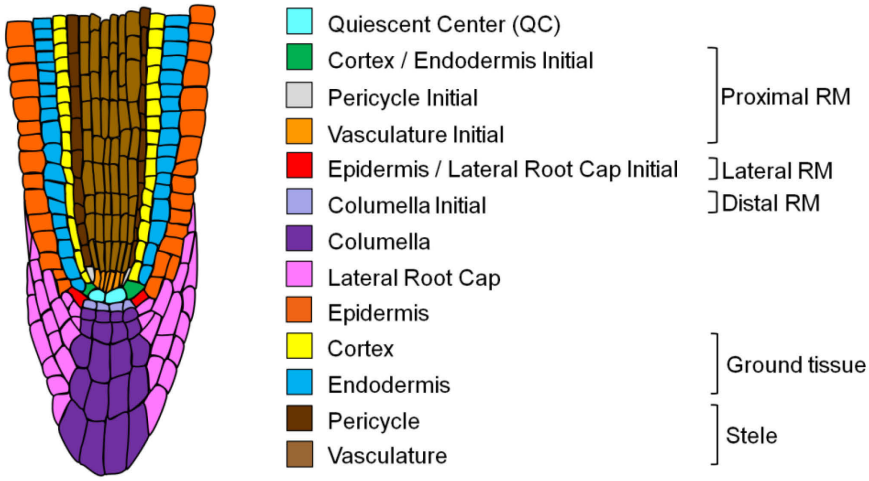

Fig. 1.3: Organization of the root meristem (RM). The *Arabidopsis* root is organized in concentrically arranged tissues: epidermis, cortex, endodermis, pericycle and vasculature (from outside to inside). Root initials are located at the basal tip and are in direct contact to the QC. With the exception of cortex and endodermis which derive from a common initial, every cell row can be traced back to a single initial. The proximal RM consists of the vasculature pericycle and endodermis/cortex initials; the lateral RM contains the epidermis/lateral root cap initial and the distal RM consists of columella initial cells. Differentiated columella cells serve as root protection and carry starch granules which are required for gravitropism response.

As the root grows, initial daughter cells are continuously replenished and displaced further away from the root tip. The youngest cells occupy the meristematic zone; the older cells pass the elongation zone where cells attain their final size. These elongated cells mature fully when they reach the differentiation zone. The distal end of this zone is marked by those epidermal cells that form root hairs (Dolan et al., 1993; Terpstra et al., 2009).

1.3.1. Establishment and maintenance of a functional RM

Establishment and maintenance of a functional RM depends on differential auxin distributions that are interpreted by transcriptional networks. The initial specification of the RM founder cell, the hypophysis, is mediated by an auxin maximum in the uppermost suspensor cell of globular stage embryos. This accumulation depends on combinatorial activities of the PINFORMED1/4/7 (PIN) efflux carriers. As pattern formation is disturbed in *pin* double, triple or quadruple mutant embryos, they are either lethal or develop into seedlings with severe defects and a non-functional root (Friml et al., 2003; Blilou et al., 2005).

BODENLOS (BDL) and MONOPTEROS (MP) are required to specify the hypophysis in response to auxin. *mp* loss-of-function and *bdl* gain-of-function mutants lose the embryonic root and carry reduced hypocotyls and vascular systems (Hardtke et al., 1998; Hamann et al., 2002). MP belongs to the AUXIN RESPONSE FACTOR (ARF) family which transcriptionally regulate auxin response genes by binding to auxin response elements (AuxRE) in promoters (Ulmasov et al., 1999, Liscum et al., 2002). *BDL* encodes the auxin-response regulator AUXIN/INDOLE-3-ACETIC ACID12 (Aux/IAA12), which dimerizes with MP to repress the regulation of auxin-inducible target genes. High auxin levels trigger the release of MP by promoting BDL degradation via the 26S proteasome (chapter 1.4; Dharmasiri et al., 2004; Weijers et al., 2005a). Notably, both MP and BDL are expressed in the adjacent proembryo rather than in the hypophysis itself. Thus, hypophysis specification requires cell to cell communication (Hamann et al., 2002).

Recent studies showed that two signals are involved in this cell-cell communication. One is the basic helix–loop–helix (bHLH) transcription factor, TARGET OF MP7 (TMO7). *TMO7* expression in the basal proembryo is directly regulated by MP but the protein moves from its site of synthesis into the hypophysis precursor (Schlereth et al., 2010). The other mobile signal is auxin itself, as MP dependent signaling promotes *PIN* expression and therefore the auxin transport toward the hypophysis (Weijers et al., 2006).

The *PLETHORA* genes (*PLT1-3* and *BABYBOOM* (*BBM*)) were identified as downstream effectors in auxin dependent RM formation. Mutations in two or more of these AP2-type transcription factors interfere with divisions of hypophysis descendants resulting in a failure to specify the QC. *PLT1/2* expression was shown to be auxin inducible, and embryonic transcription is dependent on *MP* and its close homolog *NONPHOTOTROPIC HYPOCOTYL 4*

(*NPH4/ARF7*). As *PLT/BBM* misexpression induces the formation of ectopic roots, these genes are thought to be master regulator in RM development (Galinha et al., 2007; Aida et al., 2004).

Postembryonically, PLT1-3 and BBM act in an additive and dosage dependent manner to maintain an active RM. High PLT protein levels promote stem cell identity; intermediate levels facilitate cell divisions of stem cell descendants; and low levels allow cell differentiation. These gradients in *PLT/BBM* expression are thought to be a graded read-out of the auxin distribution (Galinha et al., 2007). Auxin is transported though the root stele toward the basal root tips to generate a maximum at the QC, the surrounding initials and the columella cells. This transport is mediated by the basally localized PIN1/3/4 and PIN7 efflux carriers. A lateral redistribution from the columella is achieved by the laterally localized PIN3 and PIN7 proteins. The apical localization of PIN2 in epidermal cells redirects auxin upwards to the end of the meristematic zone in which PIN1, PIN3 and PIN7 recycle auxin again to the stele to create a loop of auxin flow (Vieten et al., 2005; reviewed in Tromas et al., 2010). Strikingly, PIN1/3/4 transcript levels are strongly reduced in *plt1/2/3* triple mutants (Galinha et al., 2007) while in turn *PLT1* was found to be misexpressed in *pin2/3/4/7* quadruple mutants (Blilou et al., 2005). This suggests a feedback regulation between the generation of the auxin concentration maxima via PIN activity and the positioning and maintenance of the root stem cell niche via PLT activity.

The homeobox transcription factor WUSCHEL-RELATED HOMEOBOX 5 (WOX5); a close homolog of WUS, is a major regulator of the root stem cell activity. WOX5 is expressed in the QC and maintains the surrounding stem cells. Restriction of WOX5 to the QC requires auxin signaling mediated through the activities of ARF10 and ARF16. WOX5 in turn promote the activity of *PLT1* and *PLT2*, thus creating an auxin dependent network of transcription factors that regulate the activity of the root stem cell niche (Ding et al., 2010).

Other factors required for QC establishment and maintenance are the GRAS family transcription factors SCARECROW (SCR) and SHORTROOT (SHR). These proteins appear to act in parallel to the PLT pathway (Aida et al., 2004; reviewed in Iyer-Pascuzzi et al., 2009).

1.4. Auxin perception and signal transduction

The phytohormone auxin, its transport and signaling plays a crucial role in almost all aspects of plant development. Auxin can be considered to act as a morphogen as it regulates patterning processes in a dose dependent manner (Rast et al., 2008; chapter 1.3.1). Various environmental signals, such as light or gravity, can influence auxin distribution through their effects on local auxin biosynthesis and intercellular auxin transport. This modulation provides a means for a higly flexible and adaptive plant development (reviewed in Vanneste et al., 2009)

At cellular level, direct interpretation of differential auxin concentrations requires the action of the TRANSPORT INHIBITOR RESPONSE1/ AUXIN SIGNALING F-BOX PROTEINS (TIR1/AFB) family. The *TIR1/AFB* genes encode F-Box proteins and are broadly transcribed throughout the plant (Dharmasiri et al., 2005b; Parry et al., 2009). TIR/AFB proteins are part of different $SCF^{TIR1/AFB}$ E3 ubiquitin ligase complexes (Skp1·cdc53/cullin·F-$box^{TIR1/AFB}$). For the TIR1 protein it was shown that auxin resides in a binding pocket to serve as "molecular glue" that stabilizes interaction with Aux/IAA proteins. Once bound to the $SCF^{TIR1/AFB}$ complexes, Aux/IAAs are ubiquitinated and subsequently degraded by the 26S proteasome (Gray et al., 2001; Dharmasiri et al., 2005a; Kepinski et al., 2005; Tan et al., 2007).

Aux/IAA proteins are small, short-living nuclear proteins. Typically, they contain four highly conserved domains from which two (domain III and IV) trigger homo- or heterodimerization between Aux/IAA and ARF proteins (Ulmasov et al., 1999; Liscum et al., 2002). Domain I allows recruitment of a transcriptional corepressor, such as TOPLESS (TPL), which has been shown to interact with BDL/IAA12 (Tiwari et al., 2004, Szemenyei et al., 2008). Domain II is required for auxin dependent degradation, as mutations in this domain result in a stabilization of Aux/IAA proteins (Gray et al., 2001; Ramos et al., 2001; Dharmasiri et al., 2005b). According to the current model, auxin triggers Aux/IAA turnover and thus activates ARF release. ARFs can then exert their function as transcriptional regulators by binding to the AuxREs on the promoters of auxin response genes (Ulmasov et al., 1997,Tiwari et al., 2003; Tiwari et al., 2004, Liscum et al., 2002).

The *Arabidopsis* genome encodes as much as 29 Aux/IAA and 23 ARF proteins (reviewed in Liscum et al., 2002). The genes studied to date revealed spatially and temporally restricted expression patterns. Different pairs of ARF and Aux/IAA proteins in given tissues may therefore regulate expression of a particular set of auxin responsive genes. In line with this assumption, individual Aux/IAA gain-of-function mutants display a high range of phenotypic defects. However, most of these defects can be found in *tir1, afb1, afb2, afb3* quadruple mutants. Thus, TIR/AFB auxin receptors act redundantly in different $SCF^{TIR1/AFB}$ complexes to mediate degradation of Aux/IAA proteins (reviewed in Weijers et al., 2005b).

Recent studies have identified AUXIN BINDING PROTEIN1 (ABP1) as an additional auxin receptor (Tromas et al., 2009). ABP1 is located at the plasma membrane (PM) and at the endoplasmic reticulum (ER) where it is involved in very early auxin mediated responses. However, the signaling cascade downstream of ABP1 is unknown. Further identified components of the auxin response machinery are MAP kinases, the IBR5 protein phosphatase or RAC GTPases, but these components have not yet been implicated in the short auxin signaling $SCF^{TIR1/AFB}$ pathway (reviewed in Tromas et al., 2010).

1.5. Aims of this study

The first part of this study aims at the functional characterization of the *LATERAL ORGAN BOUNDARY DOMAIN* gene family in *Arabidopsis thaliana.* To gain more information about possible gene functions, available insertion lines for the majority of the *LBD* genes will be systematically identified and characterized. Construction of transgenic plants that permit constitutive overexpression of *LBD* genes will allow studying the consequences of increased *LBD* function for plant development. Results from these complementary approaches will be used to select specific family members and to subject these genes to a more detailed characterization.

The *LBD* gene, *JAGGED LATERAL ORGANS* (*JLO*) was shown to integrate the control of *PIN* gene transcription with the regulation of class I *KNOX* gene expression. The second part of this study aims therefore at increasing our knowledge about this *JLO-PIN-KNOX* circuitry.

A key approach is to investigate the morphological and molecular phenotype of *JLO* loss-of-function mutants with respect to auxin related defects. Analysis of expression levels and patterns of components of the auxin transport, signaling and perception machinery in wild-type and mutant background will provide more information about *JLO*'s role in plant development. Response of these genes to high level *JLO* misexpression and cross-breedings with mutants impaired in auxin signaling will gain more insight into genetic interactions.

Previous studies indicate that JLO can interact with AS2, another member of the LBD family. One goal will be to confirm this interaction and to map the relevant interaction domains. Therefore the yeast-two hybrid system should be exploited. Additional *in planta* and *in vivo* approaches should verify the obtained results, and testing other proteins should provide information about the specificity of the observed interaction.

Analysis of the spatial expression pattern of *JLO* and *AS2* will elucidate the tissues in with interaction may occur. Phenotypic analysis of *jlo* and *as2* single or double mutants will help to learn more about the developmental role of the JLO-AS2 complex. Expression of known target genes in either single and double mutant background, as well as the effects of *JLO* misexpression in absence of AS2 will be studied.

CHAPTER II

MATERIALS AND METHODS

2. MATERIALS AND METHODS

2.1. Used materials

2.1.1. Chemicals

Chemicals were ordered in *pro analysis* quality from the following companies: Biozym (Oldendorf), Duschefa (Haarlem, NL), Fluka (Neu-Ulm), Invitrogen™ (Karlsruhe), Merck-Eurolab (Darmstadt), Roche Diagnostics (Mannheim), Roth (Karlsruhe), Serva (Heidelberg), Sigma-Aldrich® (Deisenhofen).

2.1.2. Enzymes

Enzymes were ordered from the following companies: New England Biolabs (Frankfurt); Roche Diagnostics (Mannheim); Invitrogen™ (Karlsruhe). All enzymes were used with the supplied buffers according to manufacturer's instructions.

2.1.3. Buffers and Media

Buffers, solutions and media were prepared following the protocols from Ausubel, 1996.

2.1.4. Antibodies

Name	Company	Dilution	Comment
Primary antibodies			
Anti-HA High Affinity	Roche (Mannheim)	1:1000	rat
Anti-Gal4 DNA-BD	BD Biosciences (Palo Alto, USA)	1:1000	mouse
Anti-Flag M2	Sigma Aldrich® (Deisenhofen).	1:1000	mouse
Anti-JLO	Eurogentec (Seraing, Belgien)	1:1000	rabbit
Anti-GFP IgG	Roche (Mannheim)	1:2000	mouse
Secondary antibodies			
Anti-mouse IgG	Dianova (Hamburg)	1:1250	ALP
Anti-rabbit IgG	Dianova (Hamburg)	1:1250	ALP
Anti-mouse	Invitrogen™ (Karlsruhe)	1:1000	Alexa 488
Anti-rabbit	Invitrogen™ (Karlsruhe)	1:800	Alexa 488
Anti-rat IgG	Dianova (Hamburg)	1:1000	HRP

Tab. 1: Antibodies

2.1.5. Molecular size standards

Name	Company	Size
GeneRuler™ 1kb DNA Ladder	Fermentas (St. Leon Rot)	250, 500, 750, 1000, 1500, 2000, 2500, 3000, 3500, 4000, 5000, 6000, 8000,10 000 [bp]
GeneRuler™ 50bp DNA Ladder	Fermentas (St. Leon Rot)	50, 100, 150, 200, 250, 300, 400, 500, 600, 700, 800, 900, 1031 [bp]
Precision Plus Protein Standards Dual Color	Bio-Rad (München)	10, 15, 20, 25, 37, 50, 75, 100, 150, 250 [kD]

Tab. 2: Molecular size standards

2.1.6. Membrane and Paper

Western blot analysis was performed using Roti-PVDF membrane (Roth; Karlsruhe) and 3mm Whatman paper (Maidstone, England).

2.1.7. Oligonucleotides

The oligonucleotides used in this work are listed in table Tab. 3. They were ordered from Eurofins MWG Operon (Ebersberg) or Eurogentec (Köln).

Name	Description	Sequence (5´ → 3´)
I. Vector cloning		
MR_LBD30F_TAG	pMR025, pMR027	ATGAGCAGTAGCGGAAACCCTAGCA
MR_LBD30R_FLAG1	pMR025, pMR027	TTGTAGTCTTCTCGTTTTATCACTGACGAGGC
MR_LBD30R_FLAG2	pMR025, pMR027	CTTGTCATCGTCATCCTTGTAGTCTTCTCG
MR_FLAG-attB2	pMR025, pMR027	AAGAAAGCTGGGTCCTTGTCATCGTCATCC
MR_LOB_EcoR1_f	pMR047 + 048	AAAAGAATTCGCAGTAGCGGAAACCC
MR_LOB_BamHI_r	pM046 - 048, pMR050 + 051	AAAGGATCCTAAGTGTGCTTGTAGATATGAAAGC
MR_LOB_NcoI_f	pMR046	AAAACCATGGGCAGTAGCGGAAACCC
MR_GAS_EcoRI_f	pMR050 +051	AAAAGAATTCGAGCGGCGCACTTCGCG
MR_AS2_LOBf-EcoRI	pMR055	AAAAGAATTCTCACCATGCGCCGCTTGC
MR_AS2_LOBr-BamHI	pMR055 +056	AAAGGATCCGAGCTCAGATTTAGCACAGCT
MR_AS2-GASf-EcoR1	pMR056	AAAAGAATTCTTCGCAAACGTTCACAAAGTG
MR_AS2-C-EcoRI-f	pMR057 + 058	AAAAGAATTCTCTAAGTACCAAAGCCTCGGTATCC
MR_AS2-C-BamHI-r	pMR057 + 058	AAAGGATCCTCAAGACGGATCAACAGTACGGC
MR_AS1-EcoRI-f	pMR061 + 062	AAAAGAATTCATGAAAGAGAGACAACGTTGGAGTG
MR_AS1-BamHI-r	pMR061 + 062	AAAGGATCCTCAGGGGCGGTCTAATCTGC
MR_LBD2-NdeI-f	pMR060	AAAACATATGATGATGCAAAGGAACTCTAACAACACC
MR_LBD2-BamHI-r	pMR060	AAAGGATCCTTAGAGTGGGAGATAGTGTTGTTTGAAACC
MR_LBD31-NdeI-f	pMR059	AAAACATATGATGAGCGGAAGCACCACCGGTTGTG
MR_LBD31-BamHI-r	pMR050	AAAGGATCCTTATATTAAAGAAGATGGTCGGTATTTGCCTCCGGTC
MR_AS1-f	pMR061 + 062	ATGAAAGAGAGACAACGTTGGAGTGGTGAAGAAGATGCAT TGT
MR_AS1-r	pMR061 + 062	TCAGGGGCGGTCTAATCTGCAACCCATTTGTTGTTCAAGA AAC
MR_AS1r_attB	pMR040 - 043	AAGAAAGCTGGGTCGGGGCGGTCTAATCTGCA
AttB1v2	adding AttB sites	GGGGACAAGTTTGTACAAAAAAGCAGGCT
ATTB2v2	adding AttB sites	GGGGACCACTTTGTACAAGAAAGCTGGGT
SeqL1	sequencing	TCGCGTTAACGCTAGCATGGATCTC
SeqL2	sequencing	GTAACATCAGAGATTTTGAGACAC
II. Probe amplification for WISH		
MB_jloF3	WISH	GGTGTACGACCTCTCCTCCA
MR_JLOC+T7r	WISH	CCAAGCTTCTAATACGACTCACTATAGGGAGATTCTCGTTTTATCACTGA
MR_JLON+T7r	WISH	CCAAGCTTCTAATACGACTCACTATAGGGAGAGAGGTTGTGGCAGCTCTA
III. RT-PCR		
MR_JLO_Cr	*JLO*	TTGCTCGGAGTCAAAGTAAGGAGCG
MR_JLO_GAS_r	*JLO*	TGTGAGAGACGCAGCCGTAGATAGGG
MR_JLO_C-Term-f	*JLO*	CACAACCTCAACCACCACAGGTTC
MB_jloF3	*JLO*	GGTGTACGACCTCTCCTCCA
RT-LBD13_f	*LBD13*	TGGGAATCAGGAGACATGTG
RT-LBD13_r	*LBD13*	GTGGCGTAGGATTTCCGTAC
RT-LBD14_f	*LBD14*	TTTTGCAGCCATTCACAAAG
RT-LBD14_r	*LBD14*	CAGACCAAGGAAAATTGACC
RT-LBD15_f	*LBD15*	GAATGTCCCTTTTCGCCATA
RT-LBD15_r	*LBD15*	TCTCACTTTCAATGTTGCCG
RT-LBD16_f	*LBD16*	TCGCAGCTATTCACAAGGTG
RT-LBD16_r	*LBD16*	CCTCCGGTTTGATGATGAGT
RT-LBD21_f	*LBD21*	CATGGTGAAGCTGTTCATGG

RT-LBD21_r	*LBD21*	TTTTGGGTCAGACCAAGGAG
eIF4A-F	control	TTCGCTCTTCTCTTTGCTCTC
eIF4A-R	control	GAACTCATCTTGTCCCTCAAGTA

IV. qRT-PCR

MR_RTP-JLO_f	*JLO*	TCACATCGTCTCTCTTCAGCA
MR_RTP-JLO_r	*JLO*	TGAGGTTGTGGCAGCTCTA
MR_RTP-AS2_f	*AS2*	CCCCTCTGAGCAACAGAAGC
MR_RTP-AS2_r	*AS2*	CCCCTCTGAGCAACAGAAGC
RM_RTP-LOB31_f	*LBD31*	TGGCTAGGCTTCGCGATCCCG
RM_RTP-LOB31_r	*LBD31*	GGACGTAAGCTAACTCCGCCTGATGTTGAA
RM_RTP-PIN1_f	*PIN1*	GGAAACTTATTCGTAATCCCAACTCT
RM_RTP-PIN1_r	*PIN1*	CAATGTTCCACTTGAAGGAAATGAG
RT_PIN3F	*PIN3*	TTCTATCTGATGCTGGTCTTGG
RT_PIN3R	*PIN3*	CCACAAGCGATTAATTTGGGT
RT_PIN4F	*PIN4*	CCTCTCCACTATCAAGACCG
RT_PIN4R	*PIN4*	GCTAAGGAGATTCGGATGGT
RTP_PIN7_5v2	*PIN7*	CGGTGAGATTCTTTACTGGAC
RTP_PIN7_3v2	*PIN7*	CAATGCAGCTTGAACAATGG
MR_AFB1_f	*AFB1*	CAGCTACTTGCAGGAACTTGAGAGTGT
MR_AFB1_r	*AFB1*	CTGGAAAATAGCTAAGCCAATCTCCTC
MR_AFB2_f	*AFB2*	GCTGAGATTCATGGTAGCCACCTTATT
MR_AFB2_r	*AFB2*	CCTATACTATCCAAAATCCATAACCGCTG
MR_AFB3_f	*AFB3*	CTAATTGCAGGCATCTTCGTGAGCTG
MR_AFB3_r	*AFB3*	TGGAAAACAGTTCAGCCATTGACCTC
MR_TIR1_f	*TIR1*	TCTTGTGCTTTCTTCCTGCGAAGG
MR_TIR1_r	*TIR1*	AGCTCTTTCAGATTCCTGCAAGTGG
MR_RTP_MP_f	*MP*	GCCATATCTACCGAGGGCAACCAA
MR_RTP_MP_r	*MP*	GACTTCTCATCCCTGATGAACAAAACA
RTP_IAA12/BDLf	*BDL*	GGCTTTTAGATGGATCATCAGACTTTGT
RTP_IAA12/BDLr	*BDL*	AGTTGATAAACATTCTCCATGGAACATCT
PLT1 rt F	*PLT1*	CTATTATCCCATAGATGAGCCT
PLT1 rt R	*PLT1*	ACAACGAACCTCGATCTAT
PLT2 F rt	*PLT2*	AAAAGTAGCGGATTCTCGCG
PLT2 R rt	*PLT2*	CCTTGCTTGCCATCTTCCAT
PLT3 F rt	*PLT3*	CTGTTTTGATCTGGCCGCTC
PLT3 R rt	*PLT3*	TCGAGGGTGACACCGAAAG
BBMFrt	*BBM*	GTAGATACGAGGCACATTTATGG
BBMRrt	*BBM*	TGTCATAACCTCCTTGTCTTCC
RTP_Nblack_f	*TIP41-like*	GTGAAAACTGTTGGAGAGAAGCAA
RTP_Nblack_r	*TP41-like*	TCAACTGGATACCCTTTCGCA

V. Plant genotyping

MR_NOS_R	*35SCaMV::LBD*	ACCGCGCGCGATAATTTATC
MR_LBD2_F	MR018	GAGACAGAAAGATCCGGTCCTT
MR_LBD7_F	GD047	AATAGACTTTCGAAGGAATTGCAG
MR_LBD13_F	MR019	CATCAGTGAGTTGTGATCAGCATGC
MR_LBD14_F	GD048	CCCTCAAGATGATCCTGGTTGTA
MR_LBD15_F	GD049	CAGCTCTACAACAACAAGTCCAAGC
MR_LBD16_F	GD050	TCAGTGTCTCTCCGATCGGTAG
MR_LBD17_F	MR020	CGTGCTACCACCAAATGGAAA
MR_LBD18_F	GD051	CCGCTCTTTTTCACTCCTCCTC
MR_LBD19_F	GD052	CTTGCTCATGTTCAAGCTCGTC
MR_LBD20_F	GD053	CGTTATGCAACAACAAACTCATC
MR_LBD21_F	GD054	CCATAGCGTCTCTGCAGAAGAAG
MR_LBD22_F	GD055	CTCTCGAGTTTTTCGAGTTCTTGTG

MR_LBD27_F	GD056	ACCAACAATAACAATGTTTGGGGTG
MR_LBD29_F	GD057	GCTGATTCACCAACATCAGAAAAC
MR_LBD31_F	GD058	TCAACTCTCAACATTACAAGGTCTTC
MR_LBD34_F	MR021	CGGAGCGACATCAAGAGTTC
MBGFP6-3'bis	MR031-038	TTTGTATAGTTCATCCATGCCATGTGTAATC
AB_mCherry-r	MR031-038	AAAGAGCTCTTACTTGTACAGCTCGTCCA
T-LBD2-F	*lbd2-1, lbd2-2*	ATAGTTACTTAGAGTGGGAG
T-LBD2-R	*lbd2-1, lbd2-2*	CTCTTAAATATGGAAGCCAC
T-LBD7-F	*lbd7*	GCTTTCAGATTCACTCTGAC
T-LBD7-R	*lbd7*	ATTTCTCTACCCACAACTCG
T-LBD13-F	*lbd13-1*	GGATCACCATTCAATCTCGT
T-LBD13-R	*lbd13-1*	TTAACGTACAAGAGCAGGAC
T-LBD15-F	*lbd15-11*	TGT CAA GAG AAA GGT ACG AAG TG
T-LBD15-R	*lbd15-11*	TAC ACC GGA TCT CTT AGC CTC
T-LBD16-R	*lbd16-1 – lbd16-3*	CAAACATGGATGTGTAGTAGAC
T-LBD16P-F	*lbd16-1 – lbd16-4*	CATGTAACCAAATATTCCTAAGCCA
T-LBD16P-R	*lbd16-4*	GAGCCATACTTATCGTTTCGTTTAT
T-LBD18-F	*lbd18-2, lbd18-3*	CCCATTGCAAAGTTACGAAG
T-LBD18-R	*bd18-2, lbd18-3*	GATATTGTAAATCCAGTCCCGT
T-LBD18F-Prom	*lbd18-1, lbd18-4*	TGATGGCTAATTTAAGTTGGACC
T-LBD18R-Prom	*lbd18-1, lbd18-4*	ACCTGTTGCTGAAGAGCAAAG
T-LBD20LP	*lbd20-1, lbd20-2*	CATTTAATTAGTCACCACTCACCAG
T-LBD20RP	*lbd20-1, lbd20-2*	GAGAGCAAGGATGGTTGAGAC
T-LBD20F-neu	*lbd20-3, lbd20-4*	GCTTGCAAGTTCTTGAGAAGG
T-LBD20R-neu	*lbd20-3, lbd20-4*	TCATTCAAATATTTCACGACAACTC
T-LBD29-F	*lbd29*	CCT TAGTAGTGTCTCCATAG
T-LBD29-R	*lbd29*	AGATTT GTCGAT TTCTTTAACA
T-LBD31-F	*lbd31-1 – lbd31-7*	TTA ACA TAA GCC CAT TTG GG
T-LBD31-R	*lbd31-1 – lbd31-7*	TAGCTTGTTTCT TGAGTGTG
T-LBD31-seqF	*lbd31-1 – lbd31-7*	GCATGTAAGTTTCTCCGACGGAA
T-LBD31-seqR	*lbd31-1 – lbd31-7*	GATGGTCGGTATTTGCCTCC
T-LBD33-F	*lbd33*	GATCGCTGCTATCACCATCTC
T-LBD33-R	*bd33*	CATAGATTAATTGTTCAAAATGATG
MB_jlo3148-	*jlo-2*	GGAAACAAACCTTGTAAACATTCAACAAAA
Ds5-1	*jlo-2*	ACGGTCGGGAAACTAGCTCTAC
Pst17018LB	*jlo-3*	TACTTTGGGGCAGTGAATTTC
Pst17018RB	*jlo-3*	GCGACACACTTCCTTCTCAAG
Pst19766LB	*jlo-4*	CCCTGACCCAAATATAGATTGC
Pst19766RB	*jlo-4*	TTTCCGCTACTGCTCATCTTC
Pst20504LB	*jlo-5*	CCATAAGATAGTTGTGTGGTTCG
Pst20504RB	*jlo-5*	TGCATGATGGGATATGATCC
Pst00432LB	*jlo-6*	CTTGAGAAGGAAGTGTGTCGC
Pst00432RB	*jlo-6*	TTGCGAACAGAGGAAGATTTG
Pst13957LB	*jlo-7*	TTTGTTAAGAAAACATGCATAAAGC
Pst13957RB	*jlo-7*	TCGTTTTATCACTGACGAGGC
Ds5-2a	*jlo-3- jlo-7*	TCCGTTCCGTTTTCGTTTTTTAC
Ds5-3	*jlo-3- jlo-7*	TACCTCGGGTTCGAAATCGAT
Ds3-2a	*jlo-3- jlo-7*	CCGGATCGTATCGGTTTTCG
Ds3-4	*jlo-3- jlo-7*	CCGTCCCGCAAGTTAAATATG
Ds5-2a	*jlo-3- jlo-7*	TCCGTTCCGTTTTCGTTTTTTAC
Ds5-3	*jlo-3- jlo-7*	TACCTCGGGTTCGAAATCGAT
Ds3-2a	*jlo-3- jlo-7*	CCGGATCGTATCGGTTTTCG
Ds3-4	*jlo-3- jlo-7*	CCGTCCCGCAAGTTAAATATG
MR_nph4 LP	*nph4-1*	AGTGGATGAATATGCAGCAGCAGAAC
MR_nph4 RP	*nph4-1*	GTTGAAGAGGAAGGTGCATCTCCTC
MR_tir1-1-f	*tir1-1*	ATGCAGAAGCGAATAGCCTTGTCGTTTCC

MR_tir1-1-r	*tir1-1*	ATGCAGAAGCGAATAGCCTTGTCGTTTCC

Tab. 3: Oligonucleotides

2.1.8. Plasmids

All vectors were created using the GATEWAY® cloning system (Invitrogen™) or by using restriction endonucleases and ligation. All methods were performed according to manufacturer's instructions.

2.1.8.1. Basic vectors used for cloning purposes

Name	Description	Reference / Origin
Yeast interaction studies		
pGADT7	Y2H vector; Gal4-AD and HA Tag	Clonetech
pGBKT7	Y2H vector; Gal4-BD and c-Myc Tag	Clonetech
pTFT1	Y3H vector, ADH1 promoter	Egea-Cortines et al., 1999
Entry clones		
pDONR201		Invitrogen™
Destination clones		
pMDC7	ß-Estradiol inducible	Curtis et al., 2003
pMDC32	35SCaMV promoter	Curtis et al., 2003
pABindGFP	i35S::C-term-GFP	Bleckmann et al., 2010
pABindmCherry	i35S::C-term-mCherry	Bleckmann et al., 2010
pABindFRET	i35S::C-Term-GFP-mCherry	Bleckmann et al., 2010
pGreen*nos*-Kan	includes pBluescript II KS+ polylinker	John Innes Centre

Tab. 4: List of empty vectors used for cloning purposes

Name	Annotation	Description	Reference / Origin
pGD012	AT1G06280	*LBD2* cDNA in pENTR/D-TOPO	G.Dai
pGD014	AT2G30340	*LBD13* cDNA in pENTR/SD/D-TOPO	G.Dai
pGD018	AT2G42440	*LBD17 cDNA* in pENTR/D-TOPO	G.Dai
pGD027	not annotated	*LBD34* cDNA in pENTR/SD/D-TOPO	G.Dai
pGD047	AT1G72980	*LBD7* cDNA in pMDC32*	G.Dai
pGD048	AT2G31310	*LBD14* cDNA in pMDC32*	G.Dai
pGD049	AT2G40470	*LBD15* cDNA in pMCD32*	G.Dai
pGD050	AT2G42430	*LBD16* cDNA in pMDC32*	G.Dai
pGD051	AT2G45420	*LBD18* cDNA in pMDC32*	G.Dai
pGD052	AT2G45410	*LBD19* cDNA in pMDC32*	G.Dai
pGD053	AT3G03760	*LBD20* cDNA in pMDC32*	G.Dai
pGD054	AT3G11090	*LBD21* cDNA in pMDC32*	G.Dai
pGD055	AT3G13850	*LBD22* cDNA in pMDC32*	G.Dai
pGD056	AT3G47870	*LBD27* cDNA in pMDC32*	G.Dai
pGD057	AT3G58190	*LBD29* cDNA in pMDC32*	G.Dai
pGD058	AT4G00210	*LBD31* cDNA in pMDC32*	G.Dai
pENTR-AS2	AT1G65620	*AS2* cDNA in pENTR/D- TOPO	A. Betzhold diploma thesis

Tab. 5: List of vectors used for cloning purposes and misexpression experiments*

2.1.8.2. Generated vectors

All vectors generated in this work are listed in Tab. 6 and Tab. 7. Amplification of coding sequences for cloning purposes was performed using Col-0 cDNA. All GATEWAY vectors were cloned in the cassette B reading frame (Invitrogen™).

Name	Insert	Entry vector / Destination vector
Entry clones		
pMR044	*JLO (CDS – STOP)*	
pMR041	*JLO (CDS + STOP)*	
pMR025	*JLO (CDS + FLAG)*	
pMR045	*AS1 (CDS - STOP)*	
Expression clones		
I. Misexpression experiments		
pMR027	*JLO (CDS + FLAG)*	pMR025 / pMDC7
pMR018	*LBD2*	pGD012 / pMD32
pMR019	*LBD13*	pGD014 / pMD32
pMR020	*LBD17*	pGD018 / pMD32
pMR021	*LBD34*	pGD027 / pMD32
II. Localization studies and FRET analysis		
pMR028	*JLO (CDS - STOP)*	pMR044 / pABindGFP
pMR029	*JLO (CDS - STOP)*	pMR044 / pABindmCherry
pMR030	*JLO (CDS - STOP)*	pMR044 / pABindFRET
pMR031	*AS2 (CDS - STOP)*	pENTR-AS2 / pABindGFP
pMR032	*AS2 (CDS - STOP)*	pENTR-AS2 / pABindmCherry
pMR033	*AS2 (CDS - STOP)*	pENTR-AS2 / pABindFRET
pMR034	*LBD31 (CDS - STOP)*	pGD026 / pABindGFP
pMR035	*LBD31 (CDS - STOP)*	pGD026 / pABindmCherry
pMR036	*LBD31 (CDS - STOP)*	pGD026 / pABindFRET
pMR037	*LBD2 (CDS - STOP)*	pGD012 / pABindGFP
pMR038	*LBD2 (CDS - STOP)*	pGD012 / pABindmCherry
pMR039	*LBD2 (CDS - STOP)*	pGD012 / pABindFRET
pMR040	*AS1 (CDS - STOP)*	pMR045 / pABindGFP
pMR042	*AS1 (CDS - STOP)*	pMR045 / pABindmCherry
pMR043	*AS1 (CDS - STOP)*	pMR045 / pABindFRET

Tab. 6: List of created GATEWAY compatible vectors

Name	Insert	Fragment [bp]	Restriction sites	Backbone
Yeast interaction studies				
pMR046	*JLO (LOB)*	5-354	NcoI/BamHI	pGBKT7
pMR047	*JLO (LOB)*	5-354	EcoRI/BamHI	pGADT7
pMR048	*JLO (LOB)*	5-354	EcoRI/BamHI	pTFT1
pMR049	*JLO (C-Block)*	5-126	NcoI/BamHI	pGBKT7
pMR050	*JLO (GAS-BLOCK)*	128-354	NcoI/BamHI	pGBKT7
pMR051	*JLO (GAS-BLOCK)*	128-354	EcoRI/BamHI	pGADT7
pMR053	*AS2 (CDS)*	1-601	EcoRI/BamHI	pGADT7
pMR054	*AS2 (CDS)*	1-601	EcoRI/BamHI	pGBKT7
pMR055	*AS2 (LOB)*	22-327	EcoRI/BamHI	pGADT7
pMR056	*AS2 (GAS-BLOCK)*	112-327	EcoRI/BamHI	pGADT7
pMR057	*AS2 (C-Term)*	328-601	EcoRI/BamHI	pGADT7
pMR058	*AS2 (C-Term)*	328 -601	EcoRI/BamHI	pGBKT7

pMR059	*LBD31 (CDS)*	1-663	NdeI/BamHI	pGBKT7
pMR060	*LBD2 (CDS)*	1-621	NdeI/BamHI	pGBKT7
pMR061	*AS1 (CDS)*	1-1104	EcoRI/BamHI	pGADT7
pMR062	*AS1 (CDS)*	1-1104	EcoRI/BamHI	pGBKT7
WISH experiments				
pMR052	*JLO (CDS)*	1-687	EcoRI/BamHI	pGreenII

Tab. 7: List of created vectors

2.1.9. Microorganism

The *Saccharomyces cerevisiae* (*S. cerevisiae*) strains listed in Tab. 8 were used for yeast two-hybrid and yeast three-hybrid experiments. The *Escherichia coli* (*E. coli*) strains were used for cloning and plasmid amplification. Stable transformation of *Arabidopsis thaliana* or transient transformation of *Nicotiana benthamiana* leaves was performed with the *Agrobacterium tumefaciens* (*A. tumefaciens*) strains.

Strain	Description
S. cerevisiae	
AH109	*MATa, trp1-901, leu2-3,112, ura3-52, his3-200, gal4Δ, gal80Δ, LYS2::GAL1$_{UAS}$ -GAL1$_{TATA}$-HIS3, MEL1, GAL2$_{UAS}$ -GAL2$_{TATA}$-ADE2, URA3::MEL1$_{UAS}$-MEL1$_{TATA}$-lacZ*
YST1	*MATa,ura3-52, his3-200, ade2-101, trp1-901, leu2-3,112, gal4Δmet-, gal80Δ, URA3::GAL1$_{UAS}$ -GAL1$_{TATA}$-lacZ, MEL1*
E. coli	
DB3.1	F– *gyr*A462 *end*A1 Δ(sr1-*rec*A) *mcr*B *mrr hsd*S20(rB–, mB–) *sup*E44 *ara*-14 *gal*K2 *lac*Y1 *pro*A2 *rps*L20(SmR) *xyl*-5 λ– *leu mtl*1
DH5α	F– Φ80*lac*ZΔM15 Δ(*lac*ZYA-*arg*F) U169 *rec*A1 *end*A1 *hsd*R17 (rK–, mK+) *pho*A *sup*E44 λ– *thi*-1 *gyr*A96 *rel*A1
A. tumefaciens	
GV3101 (pMP90)	*C58C1, pMK90*, *Rif^r, Gm^r* (Koncz, 1986)
GV3101 (pMP90RK)	*C58C1, pMK90RK*, *Rif^r, Gm^r, Km^r* (Koncz, 1986)

Tab. 8: Microorganism

2.1.10. Plants

The *Arabidopsis thaliana* (*A. thaliana*) ecotypes Columbia (Col-0*),* Landsberg *erecta* (L*er*-0) and Nossen (No-0) were used as wild-type. Plants carrying a T-DNA or transposon insertion are listed in Tab. 9. This seeds were ordered from the Nottingham Arabidopsis Stock Center (NASC) or from the T-DNA express center (The Salk Institute, La Jolla, California).

Name	Ecotype	Description	Reference / Origin
jlo-2	L*er*-0	*Ds* transposon insertion AT4G00220, Exon1	NASC: N174918
jlo-3	No-0	*Ds* transposon insertion AT4G00220, Promoter	RIKEN: *pst17018*
jlo-4	No-0	*Ds* transposon insertion AT4G00220, Promoter	RIKEN: *pst19766*
jlo-5	No-0	*Ds* transposon insertion AT4G00220, Exon1	RIKEN: *pst20504*
jlo-6	No-0	*Ds* transposon insertion AT4G00220, Intron	RIKEN: *pst00432*
jlo-7	No-0	*Ds* transposon insertion AT4G00220, Exon2	RIKEN: *pst13957*
lbd2-1	Col-0	T-DNA insertion AT1G06280, 5'UTR	SALK_149880
lbd2-2	Col-0	T-DNA insertion AT1G06280, 5'UTR	SALK_149878
lbd7	Col-0	T-DNA insertion AT1G72980, 3`Bereich	SALK_075629
lbd13-1	Col-0	T-DNA insertion AT2G30340, Intron	SALK_050601

lbd15-11	Col-0	T-DNA insertion AT2G40470, Exon2	SALK_019954
lbd16-1	Col-0	T-DNA insertion AT2G42430, Intron	SALK_095791
lbd16-2	Col-0	T-DNA insertion AT2G42430, Exon2	SALK_133690
lbd16-3	Col-0	T-DNA insertion AT2G42430, Exon2	SALK_040739
lbd16-4	Col-0	T-DNA insertion AT2G42430, Promotor	Sail_679_G07
lbd18-1	Col-0	T-DNA insertion AT2G45420, 5'UTR	SALK_112078
lbd18-2	Col-0	T-DNA insertion AT2G45420, Exon2	SALK_016088
lbd18-3	Col-0	T-DNA insertion AT2G45420, Intron	Sail_182_C06
lbd18-4	Col-0	T-DNA insertion AT2G45420, Intron	Sail_269_H02
lbd20-1	Col-0	T-DNA insertion AT3G03760, Promotor	SALK_054710
lbd20-2	Col-0	T-DNA insertion AT3G03760, Exon	Sail_708_G05
lbd20-3	Col-0	T-DNA insertion AT3G03760, Intron	SALK_005646
lbd27	Col-0	T-DNA insertion AT3G47870, Exon	SALK_019070
lbd29	Col-0	T-DNA insertion AT3G58190, Promotor	SALK_071133
lbd31-1	Col-0	T-DNA insertion AT4G00210, 3`UTR	SALK_016145
lbd31-2	Col-0	T-DNA insertion AT4G00210, Exon 2	SALK_126485
lbd31-3	Col-0	T-DNA insertion AT4G00210, Intron	SALK_067808
lbd31-4	Col-0	T-DNA insertion AT4G00210, Exon 2	SALK_128165
lbd31-5	Col-0	T-DNA insertion AT4G00210, Exon 2	SALK_076504
lbd31-6	Col-0	T-DNA insertion AT4G00210, Exon1	SALK_021150
lbd31-7	Col-0	T-DNA insertion AT4G00210, Exon 2	SALK_152471
lbd33	Col-0	T-DNA insertion AT5G06080, downstream	SALK_015831
plt1-4	L*er*	T-DNA insertion	Aida et al., 2004
plt2-2	L*er*	T-DNA intertion	Aida et al., 2004

Tab. 9: T-DNA and transposon insertion lines

Other mutant or transgenic *A. thaliana* lines used in this work are listed in Tab. 10.

Name	Ecotype	Description	Reference / Origin
as2-1	An	x-rays	NASC: N3117
as2-2	L*er*-0	x-rays	NASC: N3118
tir1-1	L*er*-0	substitution	Ruegger et al., 1998
nph4-1	Col-0	X-rays	Harper et al., 2000
mpBS1354	L*er*-0	substitution	T. Berleth
mpG12	L*er*-0	substitution	T. Berleth
BDL:bdl-GUS	Col-0	transgene	Dharmasiri et al., 2005b
DR5rev::GFP	Col-0	transgene	B. Scheres
PIN1::PIN1-GFP	Col-0	transgene	J.Friml
PIN4::PIN4-GFP	Col-0	transgene	J.Friml
PIN7::PIN7-GFP	Col-0	transgene	J.Friml
AUX1::AUX1-YFP	Col-0	transgene	L. Colombo
WOX5::NLS-GFP	Col-0	transgene	F. Tax
PLT1::PLT1-YFP	Col-0	transgene	Galinha et al., 2007
PLT2::PLT2-YFP	Col-0	transgene	Galinha et al., 2007
PLT3::PLT3-YFP	Col-0	transgene	Galinha et al., 2007
BBM::BBM-YFP	Col-0	transgene	Galinha et al., 2007
PLT1::CFP	Col-0	transgene	Galinha et al., 2007
PLT2::CFP	Col-0	transgene	Galinha et al., 2007
PLT3::CFP	Col-0	transgene	Galinha et al., 2007
BBM::CFP	Col-0	transgene	Galinha et al., 2007
MP::MP-GFP	Col-0	transgene	D. Weijers
BDL::BDL-GUS	Col-0	transgene	Dharmasiri et al., 2005b
TIR1::TIR1-GUS	Col-0	transgene	Parry et al., 2009
TIR1::GUS	*tir1-1*	transgene	Parry et al., 2009
AFB1::AFB1-GUS	Col-0	transgene	Parry et al., 2009
AFB1::GUS	Col-0	transgene	Parry et al., 2009

AS2::GUS	L*er*-0	transgene	Jun et al., 2010
BP::GUS	L*er*-0	transgene	M. Tsiantis
STM::GUS	L*er*-0	transgene	W. Werr
QC184	Col-0	transgene	INRA
GD047	Col-0	*35S::LBD7*	G. Dai
GD048	Col-0	*35S::LBD14*	G. Dai
GD049	Col-0	*35S::LBD15*	G. Dai
GD050	Col-0	*35S::LBD16*	G. Dai
GD051	Col-0	*35S::LBD18*	G. Dai
GD052	Col-0	*35S::LBD19*	G. Dai
GD053	Col-0	*35S::LBD20*	G. Dai
GD054	Col-0	*35S::LBD21*	G. Dai
GD055	Col-0	*35S::LBD22*	G. Dai
GD056	Col-0	*35S::LBD27*	G. Dai
GD057	Col-0	*35S::LBD29*	G. Dai
GD058	Col-0	*35S::LBD31*	G. Dai

Tab. 10: Mutants and transgenic *Arabidopsis* lines

All transgenic lines constructed in this work are listed in Tab. 11.

Name	Ecotype	Description
MR018	Col-0	*35S::LBD2*
MR019	Col-0	*35S::LBD13*
MR020	Col-0	*35S::LBD17*
MR021	Col-0	*35S::LBD34*
MR027	Col-0	ß-estradiol inducible *iJLO-FLAG*
MR028	*as2-1*	ß-estradiol inducible *iJLO-FLAG*
MR029	*as2-2*	ß-estradiol inducible *iJLO-FLAG*
MR030	Col-0	ß-estradiol inducible *iJLO-GFP*
MR031	Col-0	ß-estradiol inducible *iJLO-mCherry*
MR032	Col-0	ß-estradiol inducible *iJLO-GFP-mCherry*
MR033	Col-0	ß-estradiol inducible *iAS2-GFP*
MR034	Col-0	ß-estradiol inducible *iAS2-mCherry*
MR035	Col-0	ß-estradiol inducible *iAS2-GFP-mCherry*
MR036	Col-0	ß-estradiol inducible *iAS1-GFP*
MR037	Col-0	ß-estradiol inducible *iAS1-mCherry*
MR038	Col-0	ß-estradiol inducible *iAS1-GFP-mCherry*

Tab. 11: Constructed transgenic Arabidopsis lines

2.1.11. Software

Microsoft Word, Excel and PowerPoint software was used to organize experimental data. Images were processed in ImageJ software and assembled in Adobe Photoshop CS2. Vector NTI (Invitrogen™) was used for vector maps and sequence analysis. Databank gene researches were performed on TAIR (The Arabidopsis Information Resource, http://www.arabidopsis.org/) and NCBI (http://www.ncbi.nlm.nih.org/).

2.2. Methods

2.2.1. Genetic methods

2.2.1.1. Plant growth conditions

A. thaliana plants were grown on soil under constant light conditions at 21°C or 16°C. For analysis of root phenotypes or for selection of transgenic plants, seeds were surface sterilized (chlorine gas) and then imbibed in 0.1 % (v/v) agarose for 2 days at 4°C. Seeds were then plated onto 0.5 x Murashige and Skoog (MS) medium with Gamborgs no. 5 vitamins (Duchefa), 0.5 g/l 2-(N-morpholino) ethanesulfonic acid (MES), 1 % (w/v) sucrose and 1.2 % (w/v) plant agar. For analysis of root phenotypes, plates were incubated vertically in a growth chamber with constant light at 21°C for 3–9 days. *Nicotiana benthamiana* (*N. benthamiana*) plants were grown on soil under long day conditions.

2.2.1.2. *In planta* transformation of *A. thaliana*

A. thaliana transformation was performed according to the “floral dip” method as described in Clough et al., 1998.

2.2.1.3. Selection of transgenic *A. thaliana* plants

Transgenic plants were selected with antibiotics diluted in growth medium (Hygromycin 20µg/ml or Kanamycin 50µg/ml). After germination antibiotic resistant plants were transferred to soil.

2.2.1.4. Transient transformation of *N. benthamiana* leaves

Abaxial sides of leaves of 4 week old *N. benthamiana* plants were infiltrated as described in Bleckmann et al., 2010. To avoid transgene gene silencing, cultures were mixed in a 1:1 ratio with an *Agrobacterium* culture that allows expression of the silencing suppressor p19 (Voinnet et al., 2003).

2.2.1.5. Induction of transgene expression

The induction system used in this work is the estrogen receptor-based XVE system. The chimeric transcription activator, XVE, was assembled by fusion of the DNA-binding domain of the bacterial repressor LexA (X), the acidic transactivating domain of VP16 (V) and the regulatory region of the human estrogen receptor (E; ER). The transactivating activity of the chimeric XVE factor, whose expression is controlled by the strong constitutive promoter G10-90, is strictly regulated by estrogens. Upon induction by ß-estradiol, XVE is transported into the nucleus, binds to the -46 35S promoter and thereby activates transgene expression (Zuo et al., 2000). Induction of transgenic plants was performed by spraying with 20 µM ß-estradiol, 0.1% Tween20.

2.2.2. Basic molecular methods

2.2.2.1. Preparation of plasmid DNA

Plasmid DNA extraction from *E.coli* was performed with the QIAprep Spin Miniprep or the QIAGEN Plasmid Midi Kit (Qiagen, Hilden).

2.2.2.2. Preparation of genomic DNA

Extraction of genomic DNA from *A. thaliana* leaves was performed following a modified protocol from Delaporta et al., 1983.

2.2.2.3. Isolation of DNA fragments

Isolation and purification of DNA fragments from agarose gels was performed using GFX DNA Purification Kit (Amersham, Braunschweig).

2.2.2.4. Isolation of total RNA from plant tissue

Isolation of total RNA from different plant tissues was performed with the RNeasy Plant Mini Kit (Qiagen, Hilden).

2.2.2.5. Synthesis of cDNA

Synthesis of cDNA from total RNA was performed with SuperScriptII (Invitrogen^{TM}) according to manufacturer's instructions**.**

2.2.2.6. Isolation of proteins from plant tissue

For extraction of proteins, plant tissue was homogenized in 750 µl extraction buffer (0.1M Tris-HCl pH8.3; 0.5M NaCl; 5mM DTT; 5mM EDTA, Protease Inhibitor Cocktail (SIGMA-ALDRICH®) using the Precellys Homogenizator (Peqlab, Erlangen). Following 2h solubilization at 4°C, 6x loading buffer (0.3M Tris-HCl pH6.8; 10% (w/v) SDS; 30 % (v/v) Glycerin; 0.6M DTT; 0.01% (w/v) Bromphenolblau) was added and the protein extract was denaturized for 10 minutes at 94°C. Protein separation was carried out by SDS-Page.

2.2.2.7. Immunoblot procedures

Western blot analysis was performed as described in Ausubel, 1996. All SDS-Page Gels were run with Mini-PROTEAN tetra cell (Biorad) and proteins were transferred onto PVDF-membranes (Roth) with Trans-Blot SD semi dry transfer cell (Biorad).

2.2.2.8. Molecular biology standard methods

All molecular standard methods like DNA/RNA separation, PCR reactions, phenol-chloroform extractions, ethanol precipitations, DNA sequencing, gel electrophoresis, quantification nucleic acids concentrations, preparation of competent cells for heat-shock and electro- transformation were performed following the protocols from Ausubel, 1996.

2.2.2.9. Cloning methods and vector generation

Template amplification for cloning purposes was performed using the Phusion® High-Fidelity DNA Polymerase (Finnzymes). The cloning methods used in this work are DNA restriction, dephosphorylation of 5´ends and ligation or GATEWAY® BP and LR recombination (Invitrogen™). All methods were performed according to manufacturer's instructions.

2.2.2.10. Quantitative real time PCR (qRT-PCR)

qRT-PCR was performed in biological triplicates using oligonucleotides spanning exon-exon borders (Tab. 3). The MESA blue Mastermix (Eurogentec) was used for amplification in a Chromo4-real-time PCR machine (Bio-Rad). Expression levels were normalized to the reference gene *TIP41-like* (At4g34270) (Czechowski et al., 2005). Calculation of the mean normalized expression (MNE) and the standard error was performed according to (Muller et al., 2002).

2.2.2.11. Whole mount RNA *in situ* hybridization (WISH)

Conditions for whole mount *in situ* hybridizations were described in Hejatko et al., 2006. The method was carried out with an automated system (InSituPro; Intavis AG).

2.2.2.12. Antibody Immunodetection

Immunodetection experiments were performed with an automated system (InSituPro; Intavis AG). For details about used antibodies see Tab. 1.

2.2.2.13. ß-Glucoronidase (GUS) assay

Detection of ß-Glucuronidase (GUS) activity was performed as described in Stahl et al., 2009. For microscopic analysis, embryos and roots were cleared in a 70% (w/v) chloral hydrate, 10% (v/v) glycerol solution. Green tissues were first cleared with an EtOH series from 50% (v/v) to 100% (v/v) (1-3 hours at RT) followed by 50% to 100% (v/v) Roti®- Histol (1-3 hours at RT) and an overnight incubation in immersion oil.

2.2.3. Protein interaction studies

2.2.3.1. Gal4 based Yeast Two-hybrid and Yeast Three-hybrid system

All yeast techniques were performed as described in the yeast protocols handbook of the Clonetech Matchmaker system (http://www.clontech.com/images/pt/PT3024-1.pdf). The yeast strains YST1 and AH109 were used for yeast two-hybrid studies (mating), the yeast strain AH109 was used for three-hybrid assays (co-transformation). Expression of all fusion proteins was confirmed by western blotting (Tab. 1).

2.2.3.2. Fluorescence Resonance Energy Transfer (FRET)

Quantification of the fluorescence resonance energy transfer (FRET) was used to study protein interactions *in planta* and *in vivo*. FRET describes the effect of a nonradiative transfer of energy between two chromophores that are in close proximity (less than 10nm) to each other. This energy transfer can occur if the emission photon energy of a chromophore (donor) overlaps with the excitation spectrum of another chromophore (acceptor) (Förster, 1948). FRET can be parameterized by the Förster radius (R_0), i.e. the donor–acceptor distance at which the energy transfer via FRET is 50%. In case of the GFP (donor) and mCherry (acceptor) pair used in this work, R_0= 5.1nm (Albertazzi et al., 2009). As the FRET transfer efficiency is with the 6th power directly related to the distance between donor and acceptor, even modest reorientations or changes in relative distances of the chromophores results in detectable changes in FRET transfer efficiency.

Monitoring protein complex formation was achieved by labeling the putative interaction partners with the GFP or mCherry fluorophore, respectively (Tab. 6). For calculation of the FRET efficiency (E_{FRET}), GFP fluorescence intensity was measured directly before (GFP_{before}) and after (GFP_{after}) destroying the acceptor by photobleaching. If FRET was initially present, a resultant increase in GFP fluorescence will occur upon photobleaching of the acceptor. The percentage change of the GFP intensity was quantified as:

$E_{FRET} = (GFP_{after} - GFP_{before})/GFP_{after} \times 100$

***Experimental procedures*:**

Transgene expression was induced 2 days after transient transformation of *N. benthamina* leaves or at 5DAG in stable transformed *A. thaliana* plants (chapter 2.2.1.5). Integrity of the fusion proteins was verified by western blotting. Acceptor photobleaching experiments were performed at nucleus according to Bleckmann et al., 2010.

2.2.4. Histological and Cytological techniques

2.2.4.1. Phenotypic analysis of *A. thaliana* embryos

For analyses of embryo phenotypes, siliques were dissected under a stereomicroscope (Zeiss) to collect the immature seeds. Embryos were excised from the ovules and cleared in 70% (w/v) chloral hydrate, 10% (v/v) glycerol solution. Fluorescence analyses were performed in the F2 or F3 generation after genetic crossing with different marker lines using the confocal microscope LSM510 Meta^{MK4} (Zeiss).

2.2.4.2. Phenotypic analysis of *A. thaliana* roots

Starch granules were visualized using a 1:5 dilution of Lugol's solution (5g I_2, 10g KI in 100ml dH_2O) in 70% (w/v) chloral hydrate, 10% (v/v) glycerol, or with the mPSPI method

(Truernit et al., 2008). Analysis of fluorescence reporter expression was performed using a LSM510 Meta^{MK4} confocal microscope. Counterstaining of cell walls was achieved by mounting roots in 10µM propidium iodide.

2.2.4.3. Cell size measurements

Petals were printed with 1.5% (v/v) agarose, negatives were examined using a Zeiss Axioskop Mot Plus, photographed and cell areas were measured with the ImageJ software.

2.2.5. Microscopy

Normarsky microscopy

The microscope used for this work is the *Axioskop* (*Zeiss*). Pictures were taken with the *Zeiss Axiocam* digital camera and saved with the *Axio Vision* software.

Scanning electron microscopy (SEM)

The LEO (Zeiss) scanning electron microscope was used for this work, together with the provided software.

Confocal microscopy

The LSM 510 META^{MK4} (Zeiss) scanning confocal microscope was used for this work, together with the provided Software. Excitation and emission spectra are listed below.

Fluorphore/Dyes	Excitation	Emission
GFP	488 nm argon laser	meta channel 496 nm – 550 nm
mCherry	561 nm cw laser diode	meta channel 571 nm – 636 nm (leaves) LP 575 nm (root)
DAPI	405 nm cw laser diode	BP 480 nm – 520 nm
PI	561 nm cw laser diode	LP 575nm

Tab. 12: Excitation and emission spectra

CHAPTER III

FUNCTIONAL CHARACTERIZATION OF THE *LBD* GENE FAMILY

3. FUNCTIONAL CHARACTERIZATION OF THE *LBD* GENE FAMILY

The first part of this study contributes to a collaborative project and aimed to determine the function of the *LBD* gene family in *A. thaliana*. Together with the lab of P. Springer (University of California, USA) gain- and loss-of-function mutants for the majority of the *LBD* genes were systematically identified and characterized. Starting from this broad analysis of gene function, I focused my efforts on specific members of the *LBD* gene family (*LBD15* and *JLO/LBD30*), and subjected them to a more detailed analysis.

3.1. Results

3.1.1. Isolation of *LBD* gain- and loss-of-function mutants

Misexpression of a gene outside of its normal temporal and spatial expression domain can provide important information about its function. The *35SCaMV* (*35S*) promoter was therefore used to overexpress different *LBD* genes in wild-type (Col-0) background. In total, 16 *Arabidopsis* lines carrying a *35S::LBD* transgene were established (Tab. 10 and Tab. 11). In this screen, only misexpression of *LBD14* and *LBD16* resulted in phenotypic alterations.

35S::LBD14 plants developed aerial leaf rosettes but were otherwise phenotypically wild-type (Fig. 3.1E/G). Plants carrying a *35S::LBD16* transgene developed lobed leaves, an indicator for *KNOX* gene misexpression and displayed a reduction of apical dominance (Fig. 3.1F/H). As apical dominance requires auxin mediated regulation, this phenotype may result from interference with auxin signaling. Consistent with this notion, Okushima et al., 2007 reported on *LBD16* as a target of *ARF7* and *ARF19* in lateral root formation. However, although PCR based genotyping confirmed the homozygosis of the *35S::LBD14* and *35S::LBD16* lines, and increased *LBD* transcript levels could be shown by reverse transcriptase (RT) PCR (Fig. 3.1E/F), the frequency of plants with mutant phenotypes was relatively low (*35S::LBD14*: 5% and *35S::LBD16*: 7%; the T3 progeny of three independent transformation events was analyzed respectively, N = 45 for each line). Notably, RT-PCR analyses revealed only a moderate increase in *LBD* expression levels in *35S::LBD* plants which appeared phenotypically wild-type (Fig. 3.1E/F; P1) compared to those with morphological defects (Fig. 3.1E/F; P2*). Thus, the *LBD14* and *LBD16* gain-of-function phenotypes likely depend on the level of transgene expression. A similar effect could explain the absence of phenotypic alterations in the other *35S::LBD* lines. Indeed when T3 plants of three different *35S::LBD* lines (*LBD13*, *LBD15* and *LBD21*) were analyzed by RT-PCR, only a slight upregulation of *LBD* expression was detectable (Fig. 3.1B-D; P1-P2).

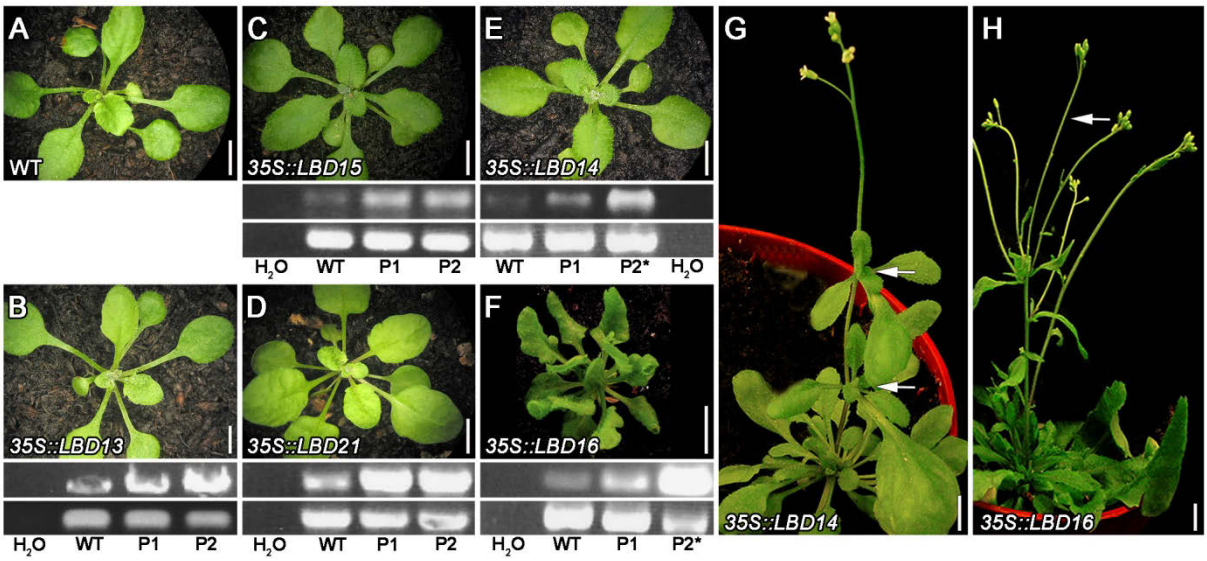

Fig. 3.1: LBD gain-of-function phenotypes. Wild-type (WT; A) and *35S::LBD* plants (C-F) at 25 days after germination (DAG). Plants misexpressing *LBD13* (B), *LBD15* (C), *LBD21* (D) and *LBD14* (E) were indistinguishable from wild-type (A) at vegetative stage of development while *35S::LBD16* (F) developed lobed leaves. The *LBD* transcript levels in the different *35S::LBD* lines were analyzed by RT-PCR (indicated below the pictures of the *35S::LBD* plants: The upper panels show the *LBD* transcript levels in wild-type (WT) and in two (P1-P2) *35S::LBD* plants (P2*: plant with morphological defects), respectively. Lower panels show the control (eIF4A)). (G-H) *35S::LBD14* (G) and *35S::LBD16* plants at 40 DAG. (G) *35SS::LBD14* plants develop aerial leaf rosettes (arrows). (H) *35S::LBD16* revealed a reduced apical dominance (arrow). Scale bars: A-F = 1cm; G-H = 2cm; DAG: days after germination.

As a next step towards elucidating the function of *LBD* family members, available T-DNA and *Ds*- transposon insertion lines were analyzed in a reverse genetics approach. With exception of *JLO* (*LBD30),* all verified single gene knock-outs in *LBD* genes were aphenotypic under standard growth conditions (Tab. 13). This observation could indicate a high level of redundancy among the *LBD* family members. As phylogenetic analyses revealed the existence of subclades within the *LBD* family (Shuai et al., 2002), a combination of multiple knock-outs between these genes might be required to uncover their function. A detailed phenotypic description of the *jlo-3* to *jlo-7* alleles is provided in chapter 5.1.3.1.

LBD	Annotation	Name	Insertion	Mutant phenotype
LBD2	AT1G06280	*lbd2-1*	5' UTR	no
LBD2	AT1G06280	*lbd2-1*	5' UTR	no
LBD5	AT1G36000	*lbd5-1*	promoter	no
LBD7	AT1G72980	*lbd7-1*	3' region	no
LBD13	AT2G30340	*lbd13-1*	intron	no
LBD15	AT2G40470	*lbd15-11*	exon 2	no
LBD16	AT2G42430	*lbd16-1*	intron	no
LBD16	AT2G42430	*lbd16-2*	exon 2	no
LBD16	AT2G42430	*lbd16-3*	exon 2	no
LBD16	AT2G42430	*lbd16-4*	promoter	no
LBD18	AT2G45420	*lbd18-1*	5' UTR	no
LBD18	AT2G45420	*lbd18-2*	exon 2	no
LBD18	AT2G45420	*lbd18-3*	intron	no
LBD18	AT2G45420	*lbd18-4*	intron	no
LBD20	AT3G03760	*lbd20-1*	promoter	no
LBD20	AT3G03760	*lbd20-2*	exon	no
LBD20	AT3G03760	*lbd20-3*	intron	no
LBD27	AT3G47870	*lbd27-1*	exon	no
LBD29	AT3G58190	*lbd29-1*	promoter	no
LBD30	AT4g00220	*jlo-3*	promoter	yes
LBD30	AT4g00220	*jlo-4*	promoter	yes
LBD30	AT4g00220	*jlo-5*	exon 1	yes
LBD30	AT4g00220	*jlo-6*	intron	yes
LBD30	AT4g00220	*jlo-7*	exon 2	yes
LBD31	AT4G00210	*lbd31-1*	3' UTR	no
LBD31	AT4G00210	*lbd31-2*	exon 2	no
LBD31	AT4G00210	*lbd31-3*	intron	no
LBD31	AT4G00210	*lbd31-4*	exon 2	no
LBD31	AT4G00210	*lbd31-5*	exon 2	no
LBD31	AT4G00210	*lbd31-6*	exon1	no
LBD31	AT4G00210	*lbd31-7*	exon 2	no
LBD33	AT5G06080	*lbd33-1*	downstream	no

Tab. 13: Analysis of *LBD* Insertion mutants. Given are the *LBD* numbers, gene annotations, names and insertion positions of verified *LBD* insertion lines. Seeds from each line were planted, genotyped for the presence of a T-DNA or *Ds* element and investigated for phenotypic alterations (T2 and T3 generation).

3.1.2. Assigning function to *LBD15*

In yeast one hybrid screens, *LBD15* was identified as a putative regulator of *PINFORMED7 (PIN7)* and *BODENDLOS (BDL)* expression (Jiri Friml and Gerd Jürgens, unpublished data). *PIN7* encodes an auxin efflux carrier that is involved in polar auxin transport (Blilou et al., 2005). BDL is a member of the auxin-response regulator AUXIN/INDOLE-3-ACETIC ACID (Aux/IAA) protein family and is required for hypophysis specification during embryogenesis (Hamann et al., 2002). Based on this information, a more detailed analysis of *LBD15* function was performed.

3.1.2.1. *PIN7* is a possible LBD15 target gene

In the reverse genetic approach, the *lbd15-11* T-DNA insertion line could be isolated (Tab. 13). This allele carries an insertion in the second exon, within the conserved LOB region of the gene (Fig. 3.2A, red underlined). RT-PCR analysis revealed that a shortened RNA, consisting of sequences 3' to the T-DNA insertion is still detectable in the homozygous mutants

(Fig. 3.2B). This RNA may derive from transcription out of a constitutive promoter on the inserted T-DNA but would encode a protein that lacks a functional LOB domain which normally provides DNA binding activity (Husbands et al., 2007).

Based on the potential binding of LBD15 to the promoter of *PIN7* and *BDL*, their expression levels in *lbd15-11* mutants were quantified via quantitative *real time* (qRT) PCR (Fig. 3.2K). This assay showed a reduction of *PIN7* transcript levels in *lbd15-11* mutant background while *BDL* expression remained unchanged. To verify that the downregulation of *PIN7* transcription causes a reduction in PIN7 protein levels, I investigated the expression of a *PIN7::PIN7-GFP* reporter. In wild-type roots, PIN7 mainly resides at the membranes of vascular cells in the meristematic and elongation zone, as well as in the columella cells of the basal root tip (Fig. 3.2I/I'). This expression pattern was unaltered in *lbd15-11* roots, but the PIN7-GFP signal was slightly reduced in the columella cells (Fig. 3.2J/J'). Thus, *LBD15* might indeed function to promote *PIN7* expression. In contrast, a role for *LBD15* as regulator of *BDL* expression could not be confirmed.

pin7 mutants show strong patterning defects that can be traced back to the earliest stage of embryogenesis, at which the apical daughter cell is specified (Hamann et al., 1999; Friml et al., 2003). Therefore, the embryonic development of *lbd15-11* mutants was monitored, to see whether, and at which developmental stage an embryonic defect occurs. *lbd15-11* mutants exhibited wild-type like embryos at all stages (N = 456, data not shown). Similarly, no morphological defects could be observed during postembryonic development. The reduction of *PIN7* expression in *lbd15-11* loss-of-function mutants does therefore not have an obvious phenotypic consequence.

3.1.2.2. Expression pattern of *LBD15*

In publicly available RT-PCR datasets *LBD15* was shown to be expressed in all tissues, although at variable levels (Shuai et al., 2002). To get a more precise idea of the spatial expression pattern, I analyzed the expression of an *LBD15::NLS3xGFP* reporter gene (provided by G. Jürgens). *LBD15* expression was not detected before heart stage of embryogenesis (Fig. 3.2C), thus *LBD15* cannot be involved in early embryonic pattern formation. From heart stage onwards *LBD15::NLS3xGFP* activity was detected in cells of the primary root meristem (Fig. 3.2D/E; arrowhead). During postembryonic root development, *LBD15* was found to be expressed in columella cells and the lateral root cap of the primary root (Fig. 3.2F/G) as well as the tips of young side roots (Fig. 3.2H, arrowhead). Notably, this expression pattern overlaps with that of *PIN7* during later stage of embryogenesis (Blilou et al., 2005) and in the columella cells of postembryonic root. However, as mentioned earlier, *PIN7* is already expressed and plays an important role during the earliest stages of embryogenesis. LBD15 might therefore not be required for the initial regulation of *PIN7* expression during early proembryo stages but is likely to play a role during later stages of development.

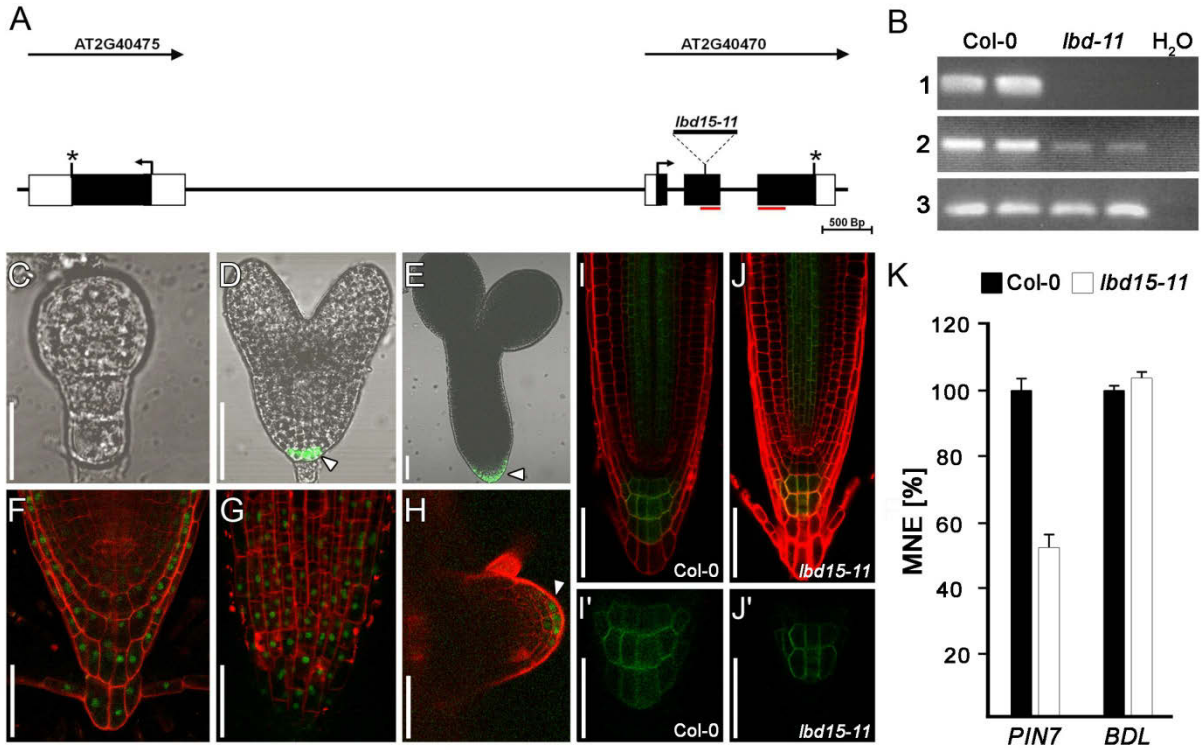

Fig. 3.2: *PIN7::PIN7-GFP* activity in *lbd15-11* mutants and spatial expression of *LBD15*. (A) Gene structure of *LBD15* (*At2g40470*) and the neighboring gene on chromosome 2. The positions of the T-DNA (*lbd15-11*) insertion within the conserved LOB motif (red underlined) is indicated. (B) RT-PCR was performed with total RNA isolated from seedlings of the indicated genetic background. No full length transcript (1) could be identified in homozygous *lbd15-11* mutants but a shortened RNA, consisting of sequences 3' to T-DNA insertion (2) is still detectable. (3) control: elf4a. (C-H) Expression of an *LBD15::NLS3xGFP* reporter during wild-type embryogenesis and root development. *LBD15* expression was not detected before heart stage of embryogenesis. From heart stage onwards, *LBD15* is expressed in cells of the primary root meristem (D and E, arrowhead). In postembryonic roots, *LBD15::NLS3xGFP* activity was observed in columella cells (F) and the lateral root cap (G, the same root as in F in another focus level) as well as in columella cells of lateral roots (H, arrowhead). (I/I'-J/J') *PIN7::PIN7-GFP* reporter expression in the primary root of wild-type (I) and *lbd15-11* (J) plants. PIN7-GFP protein localization is unaltered in *lbd15-11* mutant background. (I') and (J') represent close ups of (I) and (J) without PI counterstaining, to visualize PIN7-GFP protein in columella cells. PIN7 expression is reduced in columella cells of *lbd15-11* roots (J'). Note the overlap of *LBD15* and *PIN7* expression in columella cells. (K) qRT-PCR analysis revealed downregulation of *PIN7* expression in homozygous *lbd15-11* mutant seedlings (5DAG) compared to wild-type (Col-0). By contrast, expression of *BDL* was unaltered in mutant background (N ≥ 3). Standard errors are indicated; MNE: Mean Normalized Expression; DAG: days after germination; Scale bars: 50µm

3.2. Discussion

The *LATERAL ORGAN BOUNDARY DOMAIN (LBD)* gene family defines a large, plant-specific family which is conserved in a variety of evolutionary divergent plant species. LBD proteins are characterized by their N-terminal LOB domain which contains two motifs, a DNA-binding zinc finger and a leucine zipper which is likely to mediate protein interactions (Shuai et al., 2002; Matsumura et al., 2009). The *LBD* genes therefore are considered to encode DNA-binding transcription factors which are capable to interact with other proteins (Gong et al., 2004; Husbands et al., 2007; Guo et al., 2008). During the last years, substantial progress has been made in unraveling the functions of *LBD* family members in *Arabidopsis thaliana.* LBD transcription factors were implicated in the regulation of almost all aspects of plant development, including embryo, root, leaf and inflorescence development (reviewed in Majer et al., 2010). Two family members, which have been functionally characterized in more detail, are *AS2* and *JLO* (Chalfun-Junior et al., 2005; Ori et al., 2000; Semiarti et al., 2001; Byrne et al., 2002; Borghi et al., 2007; Bureau et al., 2008; Bureau et al., 2010). Here, two approaches were used to gain more insight into the function of different *LBD* genes: The isolation of *lbd* loss-of-function mutants and the construction of transgenic *Arabidopsis thaliana* lines that permit constitutive *LBD* overexpression.

3.2.1. *LBD* family members regulate specific developmental processes

The majority of the *LBD* insertion lines examined in this study exhibited no obvious phenotypic alterations (chapter 3.1.1). Because the effect of each mutation has not been analyzed on RNA level, it cannot be excluded that some of the *lbd* insertion mutants still generate full length transcripts. Nevertheless, a number of lines analyzed contain insertions in exons or the conserved LOB domain, raising the question why such mutants do not show morphological defects. This could be explained by two possible scenarios: First, redundant functions, shared by members of the *LBD* gene family, mask a loss-of-function phenotype. This notion is consistent with phylogenetic analyses that indicated a functional conservation among some *LBD* family members (Shuai et al., 2002; Matsumura et al., 2009). Several studies reported on redundant functions of *LBD* genes. For example *lbd36* loss-of-function mutants are aphenotypic, whereas the analysis of *lbd36 as2* double mutants showed that these genes act redundantly to control cell fate determination in petals (Chalfun-Junior et al., 2005). Moreover, I found that three *LBD* genes, *LBD15, JLO* and *AS2* play a role in the regulation of *PIN7* transcription (chapter 3.1.2.1 and chapter 5.1.3.10). Thus, some *LBD* family members indeed have overlapping functions.

On the other hand, the examination of expression profiles by RT-PCR and qRT-PCR assays showed that closely related *LBD* family members are differentially expressed in various tissues (Shuai et al., 2002; Matsumura et al., 2009). Consistent with this, *JLO* and *LBD18*, which were considered to be duplicated genes, can be implicated in different developmental

processes. Although both genes were recently suggested to play a role during tracheary element (TE) differentiation (Soyano et al., 2008), they function independently from each other in other developmental processes. The expression of both genes do e.g. not overlap during embryogenesis, and in contrast to *jlo* mutants, loss of *LBD18* function does not cause embryonic patterning defects (Borghi et al., 2007; Matsumura et al., 2009; Bureau et al., 2010). This leads to the conclusion that closely related *LBD* genes can have overlapping, but also diverse functions during plant development. Still, the failure to identify morphological defects in most of the insertion mutants is not entirely explainable by functional redundancy.

A second explanation is that several *LBD* family members are involved in the regulation of very specific developmental processes, so that these *lbd* mutations cause only subtle phenotypic changes. This is the case for *LBD16,* which was reported to promote lateral root development. *LBD16* knock out alleles show a reduction in lateral root number (Lee et al., 2009; Okushima et al., 2007). Since there was no previous indication of an involvement in lateral root development, these mild phenotypic defects in *ldb16* mutants was not noticed in this study. Similar subtle phenotypes could exist in other *LBD* insertion lines. Furthermore, several *LBD* family members function in developmental processes that were not analyzed here. For example, recent studies showed that *LBD27* is involved in microspore development (Oh et al., 2010).

The analyses of *LBD* overexpression lines did not provide more information about *LBD* functions, because most of the transgenic plants appeared to be aphenotypic. I found that *LBD* transcript levels were only moderately increased in different *35S::LBD* lines tested (chapter 3.1.1). Thus, the level of ectopic *LBD* transcription in the *35S* lines was likely not sufficient to trigger a detectable phenotypic effect. The fact that the transgene expression in the few *35S::LBD14* and *35S::LBD16* plants with morphological defects was higher than in those which appeared phenotypically wild-type supports this conclusion. Choosing another promoter for misexpression will probably help to overcome this problem.

Although the analyses of *LBD* gain-of-function phenotypes can provide information about potential gene functions, these misexpression experiments do not necessarily reflect the genuine gene activity. This assumption is based on the following observations: As shown in chapter 5.1.3.5, I found that overexpression of *JLO* interferes with its normal function in *KNOX* gene repression by disturbing AS2 activity. This leads to the conclusion that correct target gene expression depends on a balance between the JLO and AS2 proteins. In addition, published data showed that ectopic expression of various *LBD* genes causes similar morphological defects. Although these genes (*JLO, LOB, LBD3, LBD16, LBD18, LBD14*) were implicated into various different developmental processes, all transgenic plants were dwarfed, produced short petioles and their leaves were lobed (Borghi et al., 2007; Naito et al., 2007; Okushima et al., 2007; Shuai et al., 2002; Soyano et al., 2008). Moreover, I found

that ectopic expression of *LBD14* occasionally caused the formation of aerial leaf rosettes, while published RT-PCR data provides evidence for a root specific function (Shuai et al., 2002). This indicates that specific *LBD* functions correlate with their separate expression pattern. Because of the high homology among different *LBD* family members, ectopic expression likely affects regulatory pathways which are normally regulated by other LBD proteins. That is probably why overexpression of different *LBD* genes causes very similar phenotypes. The results obtained by ectopic expression can therefore generally uncover regulatory pathways in which *LBD* family members are involved. Nevertheless, whether the ectopically expressed LBD transcription factor indeed executes this regulatory role or whether closely related *LBD* genes fulfill this function requires subsequent experiments.

3.2.2. Conclusions

By phenotypic analyses of *LBD* loss- and gain-of-function mutants, I tried to assign functions to specific family members. Such screens are commonly used and can provide first insights into the biological relevance of proteins with unknown function. Nevertheless, I encountered problems with both reverse genetic approaches. The identification of morphological defects in *lbd* mutants appeared to be difficult without a priori indication about potential gene functions. At the most basic level, this objective will be more efficient by precisely elucidating the spatial and temporal *LBD* gene expression patterns. These studies will allow a more specific examination of the phenotypic consequences associated with *LBD* loss-of-function and gain-of-function mutations. In this respect, expression analyses by RNA *in situ* hybridization experiments will probably not be so easy. It was shown that LBD family members share a 25% to 82% identity throughout the LOB domain, and closely related LBD proteins exhibit more that 35% indentify in their C-terminal halves (Shuai et al., 2002; Matsumura et al., 2009). Because of these homologies, RNA *in situ* hybridizations experiments can result in the detection of unspecific signals. Controls experiments like for example signals obtained in knock-out mutants, or RNA *in situ* hybridizations performed with antisense probes are therefore required. Moreover, I failed to detect *JLO* RNA in early embryos with this technique (chapter 4; Bureau et al., 2010), thus *LBD* expression levels in specific tissues or stages could be too low for this detection system. A more advisable approach could be the construction of reporter lines by cloning the endogenous promoters of the different *LBD* family members. Based on these results, the generation of multiple knock-outs mutants will uncover redundant gene activities. The identification of targets by microarray experiments, followed by a confirmation of direct targets using chromatin immunoprecipitation (ChIP), will then provide more information about the regulatory roles of the LBD transcription factors during *Arabidopsis* development.

CHAPTER IV

THE ROLE OF *JLO* IN AUXIN SIGNAL TRANSDUCTION

The results presented in this chapter are in parts published in:

Bureau, M., Rast, M.I., Illmer, J., and Simon, R. (2010). *JAGGED LATERAL ORGANS* (*JLO*) controls auxin dependent patterning during development of the *Arabidopsis* embryo and root. Plant Mol Biol **74,** 479-491.

4. THE ROLE OF *JLO* IN AUXIN SIGNAL TRANSDUCTION

The *LBD* family member *JAGGED LATERAL ORGANS* (*JLO/LBD30*) was shown to be involved in numerous auxin dependent developmental processes. These comprise a function in embryonic development, organ primordia delimitation and differentiation of vascular precursors (Borghi et al., 2007; Soyano et al., 2008). Altered *JLO* activity in gain-of-function mutants suggested a role in *PIN* gene regulation but whether *JLO* acts directly upon *PIN* gene expression or interferes in general with auxin signal transduction remained unclear. The aim of the second part of my study was to determine the role of *JLO* in auxin mediated development. The results of these analyses are in part published in the enclosed paper (Bureau et al., 2010) and the most important conclusions are summarized in chapter 4.1.1.

4.1. Results

4.1.1. Summary of results published in Bureau et al., 2010

Previous results showed that the *jlo-1* loss-of-function mutation cause an arrest at globular stage of embryogenesis (Borghi et al., 2007). In order to gain more insight into JLO functions at later developmental stages, we used the phenotypically milder *jlo-2* allele for further studies. Our analyses revealed altered cell division planes in the early proembryo or in the suspensor when *JLO* activity was compromised (Fig. 1). Consequently, these mutant embryos did not beyond heart stage, thus implicating *JLO* again in patterning of the early embryo. Nevertheless, most of the homozygous *jlo-2* mutants displayed milder morphological defects from heart stage onwards (Fig. 2). These defects comprise a delayed initiation of the provascular system, a reduced number of provascular cell files as well as a reduction in hypocotyl length. At seedling stage, *jlo-2* mutants showed a defective cotyledon development; vascular defects and a premature arrest of shoot and root meristem activity (Fig. 3). Collectively, these results provide evidence for a continuous requirement for JLO function throughout embryogenesis and postembryonic development.

The *jlo-2* phenotype resembles those of mutants compromised in polar auxin transport, signal transduction or biosynthesis. Therefore, we monitored the expression of synthetic auxin response reporter *DR5rev::GFP* in *jlo* mutant background (Ulmasov et al., 1997). Indeed, *DR5rev::GFP* signal intensity was severely reduced in *jlo* mutant embryos (Fig. 5A-D) and roots (Fig. 6A/E). The observation that exogenously applied auxin did not restore the mutant phenotype suggest that *jlo-2* seedlings do not simply suffer from a reduced auxin biosynthesis (Suppl. Fig. $6A_1$-B_4). We conclude that JLO function is required to facilitate auxin transport and/or signaling.

The temporal and spatial distribution of auxin largely depends on the activity of members of *PIN* family which encode auxin efflux carrier (Wisniewska et al., 2006). Our analyses of reporter gene activity and qRT-PCR assays showed a reduced expression of several *PIN*

genes in the mutant embryos (Fig. 5E-J) and roots (Fig. 6B-D/F-I). Furthermore, inducible misexpression revealed that *JLO* activity is sufficient to upregulate *PIN1* and *PIN3* transcription in roots (Fig. 6J). *JLO* might therefore, at least in part, exert its role during plant development by promoting *PIN* gene expression. Notably, members of the *PLETHORA* (*PLT*) gene family, which respond to auxin signaling and direct *PIN* gene expression (Galinha et al., 2007), are also less expressed *jlo-2* mutant roots (Fig. 7A-L). In addition, induction of *JLO* misexpression resulted in an upregulation of *PLT* expression (Fig. 7M). This suggests that *JLO* can affect *PIN* gene transcription in roots via the regulation of *PLT* gene expression.

We then modified the auxin content and distribution in roots by treatments with synthetic auxin (IAA), the auxin transport inhibitor (NPA) and the non-transportable auxin analogue 2,4-D. *PIN* and *PLT* genes displayed only a very damped response to this treatment in absence of JLO (Suppl. Fig. 6 and 7*),* indicating that JLO function is essential for the full response of these auxin target genes. However, we found that *JLO* transcription itself is only mildly auxin inducible. Thus, the normal rapid increase of *PIN* gene expression upon auxin treatment cannot be easily explained by an upregulation of *JLO* (Fig. 6K).

The expression of auxin response genes was shown to be regulated by the antagonistic activities of ARF and Aux/IAA proteins (Weijers et al., 2005b). One of these pairs, BDL and MP, is required for hypophysis specification during embryogenesis which gives rise to parts of the RM. Phenotypically, *mp* loss-of-function and *bdl* gain-of-function mutants resemble *jlo-2* mutants (Suppl. Fig. 8). Consistent with this, our genetic studies showed that *JLO* and *BDL/MP* act partially in a common pathway (Suppl. Tab. 2, Suppl. Fig. 8). Nevertheless, the discrete hierarchy of these genes within the pathway still needs to be determined. Taken together, the presented data show that *JLO* acts in part through the BDL/MP pathway to mediate auxin responses and eventually regulate *PLT* and *PIN* gene expression.

4.1.2. *JAGGED LATERAL ORGANS* (*JLO*) controls auxin dependent patterning during development of the *Arabidopsis* embryo.

The paper Bureau et al., 2010 was published in *Plant Molecular Biology* (impact factor: 3.5). The manuscript was written by me and overworked by Prof. Dr. R. Simon.

Author's contribution:

M. Bureau initially isolated the *jlo-2* allele and studied *DR5rev::GFP*, *PIN::PIN-GFP* and *WOX5::NLS-GFP* reporter expression in embryos (Fig. 5; Suppl. Tab. 1; Suppl. Fig. 3). J. Illmer characterized the *jlo-2* seedling and root phenotype (Fig. 3A-F; J-K; N), monitored *DR5rev::GFP*, *PIN::PIN-GFP* and *PLT::PLT-GFP* reporter expression in roots and analyzed the response to exogenous auxin treatment (Fig. 6A-H; Fig. 7A-L; Suppl. Fig. 6; Suppl. Fig. 7). I performed all other experiments.

Plant Mol Biol
DOI 10.1007/s11103-010-9688-2

JAGGED LATERAL ORGAN (*JLO*) controls auxin dependent patterning during development of the *Arabidopsis* embryo and root

Marina Bureau · Madlen I. Rast · Jasmin Illmer · Rüdiger Simon

Received: 20 August 2010 / Accepted: 6 September 2010

Abstract The plant hormone auxin plays a role in virtually every aspect of plant growth and development. Temporal and spatial distribution of auxin largely depends on the dynamic expression and subcellular localization of the PIN auxin-efflux carrier proteins. We show here that the *Arabidopsis thaliana JAGGED LATERAL ORGAN* (*JLO*) gene, a member of the *LATERAL ORGAN BOUNDARY DOMAIN (LBD)* gene family, is required for coordinated cell division during embryogenesis. *JLO* promotes expression of several *PINFORMED (PIN)* genes during embryonic and root development. Inducible *JLO* misexpression reveals that *JLO* activity is sufficient for rapid and high level *PIN1* and *PIN3* transcription. Genes of the *PLETHORA (PLT)* family respond to auxin and direct *PIN* expression, but *PLT* genes were severely underexpressed in *jlo* mutants. *JLO* controls embryonic patterning together with the auxin dependent *MONOPTEROS/BODENLOS* pathway, but is itself only mildly auxin inducible. We further show that all known auxin responses in the root require *JLO* activity. We thereby identify *JLO* as a central regulator of auxin distribution and signaling throughout plant development.

Marina Bureau, Madlen I. Rast contributed equally to this work.

Electronic supplementary material The online version of this article (doi:10.1007/s11103-010-9688-2) contains supplementary material, which is available to authorized users.

M. Bureau · M. I. Rast · J. Illmer · R. Simon (✉)
Institut für Genetik, Heinrich-Heine-Universität, Universitätstr. 1, 40225 Düsseldorf, Germany
e-mail: ruediger.simon@uni-duesseldorf.de

M. Bureau
Institut de Biologie Moléculaire des Plantes UPR-CNRS2357, 12 rue du Général Zimmer, 67084 Strasbourg Cedex, France

Keywords *LBD* · *MP* · *BDL* · *PIN* · *PLT* · Auxin signaling · Embryo development · Root development

Introduction

Embryogenesis establishes the basic seedling body organization of *Arabidopsis thaliana*. Following the asymmetric division of the zygote, the smaller apical daughter cell will give rise to the proembryo, while the larger basal daughter cell divides to form the suspensor. At early globular stage, the uppermost suspensor cell adjacent to the proembryo, the hypophysis, adopts an embryonic fate and generates the basal region of the embryo and the primary root meristem (Weijers and Jurgens 2005). The mature embryo consists of four distinct structures: the cotyledons, the shoot meristem, hypocotyl, and the root harboring the root meristem.

The shoot and root are further elaborated postembryonically from the two primary meristems, and new structures such as flowers, leaves, shoot branches and lateral roots are formed after germination to complete the plant body. Both shoot and root can modify their growth behavior in response to environmental signals such as nutrient availability, light or gravity. This highly flexible and adaptive development allows to compensate for a plant's sessile lifestyle.

The spatial and temporal distribution of the phytohormone auxin directs the formation of plant organs and mediates patterning processes during embryonic and postembryonic development (Sabatini et al. 1999; Friml et al. 2002; Benkova et al. 2003; Blilou et al. 2005). Dynamic auxin gradients are created and upheld by active polar auxin transport, which requires the activity of auxin transport facilitators of the PINFORMED (PIN) family (Galweiler et al. 1998; Paponov et al. 2005; Zazimalova

Published online: 19 September 2010

et al. 2007; Feraru and Friml 2008). The direction of auxin flux is determined by cell type-specific expression and subcellular localization of PIN proteins (Friml et al. 2003). Coordinated expression and polar localization of PIN proteins in turn is established through a self-organizing auxin-mediated feedback loop (Paciorek et al. 2005; Vieten et al. 2005; Sauer et al. 2006; Kleine-Vehn et al. 2008c). Furthermore, localization and stability of PIN proteins is controlled by reversible phosphorylation (Michniewicz et al. 2007), endocytotic recycling (Geldner et al. 2001; Jaillais et al. 2007), vesicle trafficking and protein turnover (Kleine-Vehn and Friml 2008; Kleine-Vehn et al. 2008a, b).

Two types of gene families direct the expression of auxin response genes. Members of the auxin response factor (ARF) protein family interact with auxin response elements (AuxREs) (Tiwari et al. 2003; reviewed by Liscum and Reed 2002). ARFs work in combination with AUX/IAA repressors, which heteromerize with ARF proteins in the absence of auxin. Thus, ARF proteins are sequestrated and inactivated by AUX/IAA proteins (Gray et al. 2001; Tiwari et al. 2001, 2004; Weijers et al. 2005; reviewed by Reed 2001). The presence of auxin stimulates proteasome dependent degradation of the AUX/IAA proteins via the auxin-$SCF^{TIR1/ABP1}$-E3 ligase complex (Kepinski and Leyser 2004; Dharmasiri et al. 2005a, b; Kepinski and Leyser 2005).

The function of several pairs of AUX/IAA and ARF proteins has been studied in detail. Genetic and protein interaction analysis showed that BODENLOS (BDL/IAA12) acts antagonistically to MONOPTEROS (MP/ARF5) during embryogenesis. BDL and MP are involved in the specification of the hypophysis, which initiates the formation of the primary root meristem. Both homozygous *mp/arf5* mutants and dominant *bdl/iaa12* gain-of-function alleles lose the embryonic root and carry reduced hypocotyls and vascular systems (Hardtke and Berleth 1998; Hamann et al. 2002; Weijers et al. 2005). Auxin signaling through the *BDL/MP* dependent pathway positively regulates *PLETHORA* (*PLT*) gene expression. The *PLT* family encodes AP2-domain transcription factors that regulate QC identity and stem cell maintenance. Activity of the four family members *PLT1*, *PLT2*, *PLT3* and *BABYBOOM* (*BBM*) is largely additive and dosage dependent. High levels of PLT activity promote stem cell identity and maintenance; lower levels promote mitotic activity of stem cell daughters; and further reduction in levels is required to allow cell differentiation (Aida et al. 2004; Galinha et al. 2007). *PLT1, 2* and *3* redundantly control expression levels of *PIN* genes during embryonic and post-embryonic root development (Galinha et al. 2007). Hence, PLT proteins are involved in an auxin-mediated feedback regulation that triggers *PIN* gene expression at sites of high auxin concentrations.

High level expression of the *JAGGED LATERAL ORGAN* (*JLO*) gene of *Arabidopsis,* which encodes a member of the LATERAL ORGAN BOUNDARY DOMAIN (LBD) family of transcription factors (Shuai et al. 2002), reduces apical-basal transport of auxin in the shoot system (Borghi et al. 2007). This effect is at least in part mediated by repression of *PIN* gene transcription. Furthermore, early embryo arrest of *jlo-1* mutants indicated that *JLO* function is essential for embryo organization, and that *JLO* is required for the accumulation of auxin in the hypophysis (Borghi et al. 2007). During later stages of development, *JLO* appears to promote differentiation of vascular precursors into tracheary elements (Soyano et al. 2008), and delimits organ primordia from the shoot and floral meristems (Borghi et al. 2007). *JLO* thus contributes at several positions to auxin-dependent developmental pathways. We now show that *JLO* exerts an important role during early patterning of the *Arabidopsis* embryo and in the seedling root by modulating the activity of the auxin-controlled *BDL/MP* pathway to regulate *PLT* and *PIN* gene expression.

Results

Novel *jlo* alleles

We previously reported on the *jlo-1* T-DNA insertion line (SALK_020930) that causes an arrest at globular stage of embryogenesis (Borghi et al. 2007). Due to this early termination, we were unable to examine *JLO* functions at later developmental stages in more detail. A phenotypically slightly milder allele, *jlo-2* (JIC_GT.9713) carries a *Ds* element insertion in the 3′ part of the first exon, within the conserved LOB region of the gene (Suppl Fig. 1). RT–PCR analysis revealed that a shortened RNA, consisting of sequences 3′ to the T-DNA insertion is still detectable, which might allow residual *JLO* function (Suppl Fig. 2). However, this RNA would encode a protein lacking a functional LOB domain, which normally provides DNA binding activity. We used the *jlo-2* mutant for all further studies.

Plants heterozygous for the *jlo-2* mutation appeared phenotypically wild-type. Among the progeny of *jlo-2/+* plants, 85% of the seedlings (n = 2446) were phenotypically normal, while 15% of the F2 seedlings showed a mutant phenotype with strong growth retardation (see below). Since the observed number of mutant seedlings was smaller than the 25% expected for a recessive allele, we analyzed developing siliques of *jlo-2/+* plants and found a high number (15%) of aborted embryos (Fig. 1). This suggests embryonic lethality of the homozygous *jlo-2* mutants, similar to the *jlo-1* allele (Borghi et al. 2007).

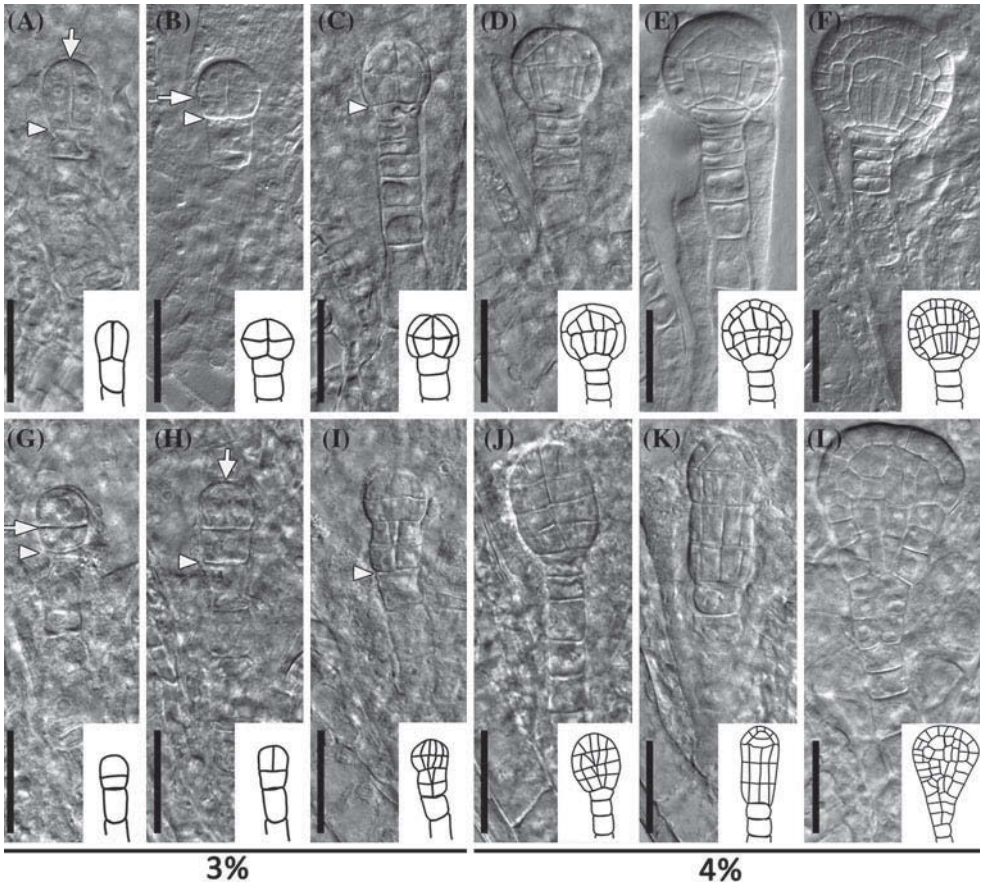

Fig. 1 Early stages of *jlo-2* embryogenesis. Histological analysis of embryos from individual siliques of *jlo-2/+* plants. **a–f** Stages of wild-type embryogenesis and **g–l** *jlo-2* mutants: (**a/g**) 2 cell stage, (**b/h**) 4 cell stage; (**c/i**) 16 cell stage, (**d–f/j–l**) early to late globular stages. In *jlo-2* embryos, the apical daughter cell of the zygote often divides horizontally instead of vertically, resulting in elongated embryos (*arrow* in **a/g**, and **i/j**). Later cell division patterns are often irregular. White *arrowhead* mark (**a–c/g–f**) the cell wall resulting from the division of the zygote. White *arrows* (**a–b/g–h**) mark the orientation of the first cell divisions. *Insets* show a schematic representation of the respective embryo. Frequency of occurrence is indicated below as percentage of total embryos analysed. *Scale bars*: 20 μm

The embryo arrest of *jlo-1* and *jlo-2* could be due to closely linked mutations (Soyano et al. 2008). Functional complementation assays, i.e. rescue of *jlo*-mutants by introducing a wild-type gene copy was not achievable because the required *JLO* promoter sequences could neither be cloned, nor obtained by PCR amplification from *Arabidopsis* genomic DNA. However, transheterozygosis of *jlo-1* with *jlo-2* failed to complement the embryo mutant phenotypes observed in both *jlo-1* and *jlo-2* homozygotes, indicating that embryo arrest is indeed due to reduced or missing *JLO* function, and not due to linked mutations (Table 1).

Development of *jlo-2* mutants and *JLO* expression

jlo-2 homozygotes often developed duplications of the proembryo, indicating aberrations of early cell divisions even before the octant stage (Fig. 1). In siliques growing on *jlo-2/+* plants after selfing, 3% of all embryos showed altered cell division planes in the early proembryo stage, or vertical divisions in the suspensor (Fig. 1g, h, i; n = 333; this phenotype was not observed among 773 embryos in wild-type siliques). During globular and early heart stage, 4% of all embryos were elongated or pear-shaped, due to abnormal divisions in the basal embryo domain (Fig. 1j, k, l; n = 1285), and did not develop beyond heart stage. When wild-type siblings had reached heart stage, 12% of all embryos showed delayed initiation of the provascular system, reduced number of vascular cell files and a reduced hypocotyl, giving rise to V-shaped embryos (Fig. 2e, f; Suppl Table 1; n = 627). Towards the end of embryogenesis, 23% (n = 165) were delayed in development and carried a shorter and narrow hypocotyl region, indicating that *JLO* function is required throughout embryonic patterning.

At the seedling stage, *jlo-2* homozygotes developed asymmetric (1%), fused (7%) or atrophic (92%) cotyledons (Fig. 3a–f). Notably, the vascular system in cotyledons was always interrupted and less branched (Fig. 3g–i). Seedling

Table 1 Allelism test between *jlo-1* and *jlo-2*

Parental genotype	Embryonic phenotype			
	WT	Mutant		Total
(A). Embryonic development				
jlo-1/+ x *jlo-2*/+	77% (67)	23% (20)		87
P-value	0.64			
Parental genotype	Kanamycin sensitive	Kanamycin resistant		
	WT or *jlo-1*/+	*jlo-2*/+	*jlo-1*/*jlo-2*	Total
(B). Postembryonic development				
jlo-1/+ x *jlo-2*/+	51% (35)	23% (16)	26% (18)	69.00
P-value	0.90			

(A) Embryonic development in F1 siliques resulting from genetic crossings between *jlo-1*/+ and *jlo-2*/+ plants. Given are the ratios (%) and total numbers of wild-type and mutant embryos. Chi-squared (χ^2) test proved that the observed segregation does not significantly differ from the expected 3:1 for two allelic mutations. (B) Postembryonic development of the F1 progeny obtained from crossing between *jlo-1*/+ and *jlo-2*/+ plants. To select for the *jlo-2 Ds* transposon insertion, seedlings were grown on media supplemented with kanamycin. Given are the ratio (%) the total numbers of seedlings for each genotype respectively. The observed segregation was analyzed with Chi-squared (χ^2) test

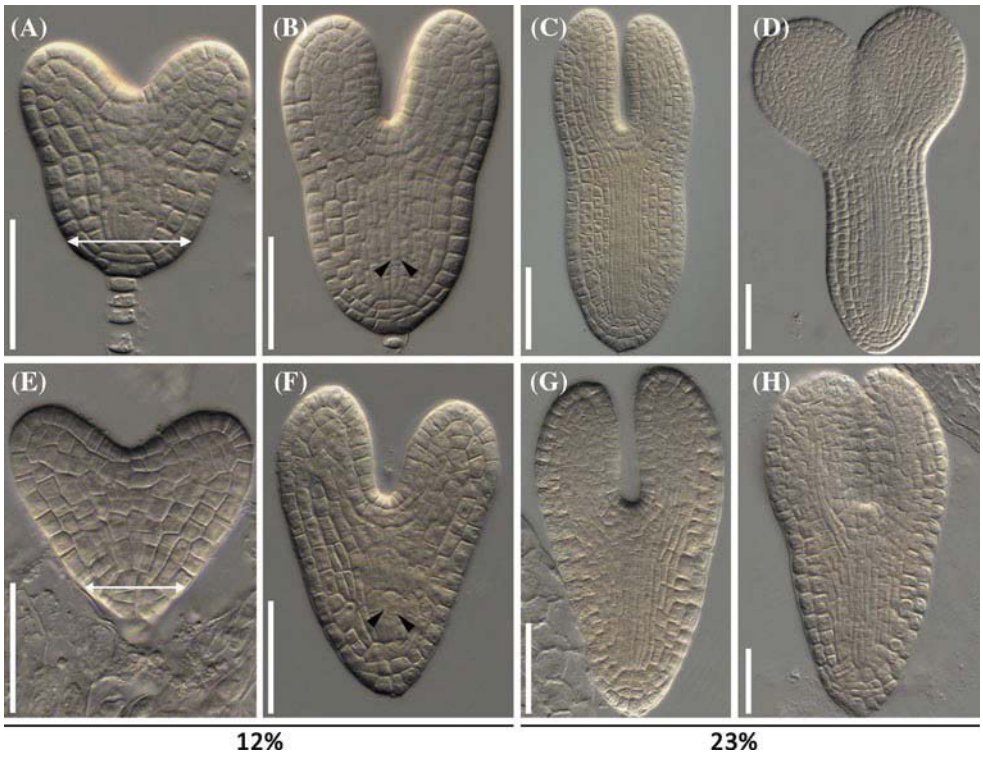

Fig. 2 Late stages of *jlo-2* embryogenesis. Embryos were isolated from siliques of *jlo-2*/+ plants after selfing. **a–d** Embryonic stages of wild-type siblings and **e–h** *jlo-2* mutants: **a/e** early heart stage, **b/f** late heart stage, **c/g** torpedo stage, **d/h** and bent cotyledon stage. *jlo-2* mutant embryos show an overall developmental delay. Hypocotyl diameter (**a/e**, *white arrow*) and length (**c–d/g–h**) of *jlo-2* embryos is reduced. Typical long and thin cells of provasculature are missing in *jlo-2* mutants at heart stage (**b/f**, *black arrowheads*), but become discernible at torpedo stage (**g**, compare to **c**). Frequency of occurrence is indicated below as percentage of total embryos analysed. *Scale bars*: 50 μm

shoots initiated several malformed organs before final arrest (Fig. 3f, arrowhead). All mutant roots were severely reduced in size and stopped growth within 5 days after germination (DAG) (root lengths: wt = 29.8 mm ± 0.9; *jlo-2* = 2.2 mm ± 0.2; n = 30). *jlo-2* root meristems appeared disorganized (Fig. 3j, k). In wild-type, columella stem cells are found between the quiescent center (QC) and the layers of differentiated columella cells that contain

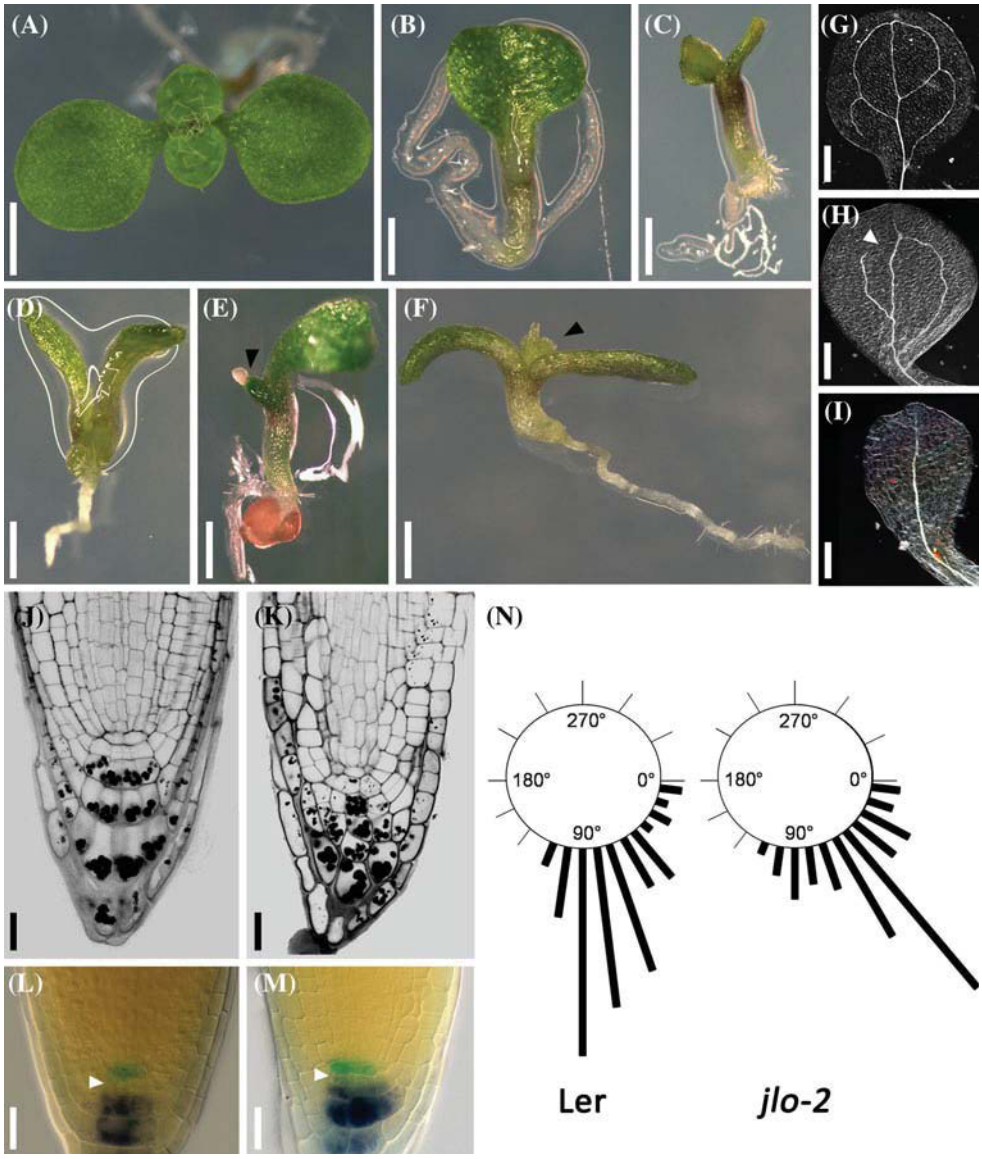

Fig. 3 Postembryonic development of *jlo-2* mutants. Wild-type (**a**) and homozygous *jlo-2* mutants (**b–f**) at seedling stage (5 DAG). Mutant seedlings develop asymmetric (**b–e**, *arrowhead* in **e**), atrophic (**c**) or fused (**d**) cotyledons and short hypocotyls. (**g–i**) Vasculature of wild-type (**g**) and *jlo-2* cotyledons (**h/i**). The vascular system is interrupted (**h**, *arrowhead*) or reduced to a single strand (**i**). (**j/k**) Root architecture of wild-type (**j**) and *jlo-2* mutants (**k**), starch granules are stained via mPSPI (*black dots*). (**l/m**) A columella stem cell layer (*white arrowhead*) separates the QC (*light blue* staining of marker QC184) from the starch carrying (*dark blue*) columella cells in the wild-type (**l**). In *jlo-2* roots (**m**), starch granules are juxtaposed to the QC. (**n**) Gravitropism response of wild-type and *jlo-2* mutants (5DAG) within 1 day after re-orientation by 90°. *Scale*: **a**: 1 mm; **b–f**: 2 mm; **g–i**: 200 μm; **j–m**: 20 μm

starch granules (Fig. 3l). *jlo-2* mutant roots lacked columella stem cells and carried starch granules in cells next to the QC (Fig. 3m). Consistent with defects in columella development, the root response to gravitational changes was strongly diminished in *jlo-2* seedlings (Fig. 3n).

In summary, we found that *JLO* is required for early embryonic patterning along the apical-basal axis, cotyledon initiation, vascular development and organization and maintenance of the root meristem. Overall, we noted that all *jlo-2* mutant phenotypes, ranging from embryo lethality to patterning defects, were milder when plants were grown at only 16°C, compared to our standard growth conditions of 21°C. The observed mutant phenotypes strongly resemble those of mutants affected in auxin signaling or directional auxin transport.

We analyzed *JLO* expression during wild-type development via RNA in situ hybridization (Fig. 4). With this technique, we so far failed to detect *JLO* RNA in early embryos, probably due to low expression at these stages (Borghi et al. 2007). From heart stage onwards, *JLO* is expressed in the provasculature, and later accumulates at the root tip during torpedo stage. A weak signal remains detectable in the embryonic vasculature (Fig. 4a–c). We could not detect *JLO* mRNA in *jlo-2* loss-of function mutants (Fig. 4d, e) which confirms the specificity of the observed signal.

Patterning defects in *jlo* embryos indicate a role in auxin mediated development

The phenotypic defects of *jlo* mutants could be explained by a failure in organized auxin transport or auxin signaling. We therefore examined local auxin distribution during embryogenesis using the synthetic auxin response reporter

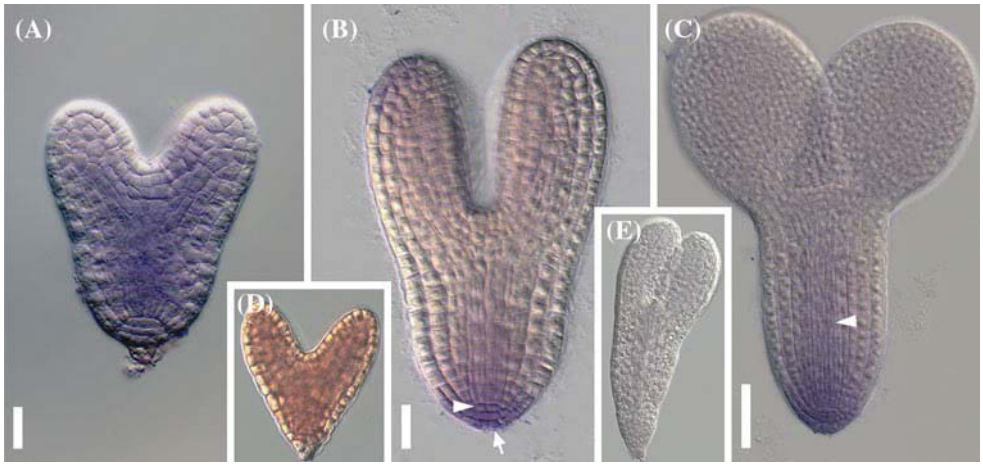

Fig. 4 *JLO* expression pattern during embryogenesis. *JLO* expression during embryo development analyzed by whole-mount RNA in situ hybridization. (**a–c**) Wild-type embryos of (**a**) heart stage, (**b**) torpedo stage and (**c**) bent cotelydon stage. During early heart stage, *JLO* transcripts can be detected in provascular cells (**a**). From torpedo stage on, expression becomes restricted to the basal root tip (**b–c**) and is detectable in the QC (**b**, *arrowhead*) with the surrounding initials as well as in the embryonic columella cells (**b**, *arrow*). Higher probe concentrations detected *JLO* also in the stele (**c**, *arrowhead*). *jlo-2* mutant embryos of heart (**d**) and bent cotyledon stage (**e**) analyzed with the same *JLO* probe. No signal is observable confirming probe specificity. *Scale bars*: 20 μm in **a** and **b**; 50 μm in **c**

DR5rev::GFP (Ulmasov et al. 1997; Friml et al. 2003). In wild-type globular stage embryos, auxin accumulates in the hypophysis and upper suspensor cells, as indicated by a strong *DR5rev::GFP* signal. *jlo-1* embryos at this stage concentrate auxin in the suspensor, and the hypophysis cannot be identified (Fig. 5a, b). PIN1 is expressed throughout the globular stage embryo of wild-type, but at reduced levels in *jlo-1* mutants (Fig. 5g, h). At heart stage, strong *DR5rev::GFP* signal is detected at the root pole with an intensity maximum in the uppermost suspensor cell. The pattern of *DR5rev* activity was unaltered in *jlo-2* mutants, but signal intensity was strongly reduced (Fig. 5c, d). We analyzed the expression pattern of PIN1 and PIN4, which control embryonic auxin transport (reviewed by Moller and Weijers 2009). In wild-type heart stage embryos, PIN4 is expressed in the prospective QC and in the provasculature. Heart stage *jlo-2* embryos expressed PIN4 in the QC, but lacked provascular expression (Fig. 5e, f; white arrowhead). This is consistent with the observed defects in provasculature development of *jlo-2* and overlaps with *JLO* expression during this stage of development (Fig. 4a). *jlo-2* mutant embryos expressed *PIN1::PIN1-GFP* in an unchanged pattern, but overall signal intensity was reduced to about 60% wild-type levels (Fig. 5i, j, Suppl Fig. 3).

The homeodomain transcription factor WOX5 maintains QC activity and inhibits differentiation of adjacent columella stem cells. *WOX5* expression is auxin regulated and restricted to the QC by *PLT1* and *PLT2* (Sarkar et al. 2007). Compared to wild-type, the *WOX5::NLS-GFP* reporter was more widely expressed in *jlo-2*, indicating that *JLO* is also required to confine *WOX5* expression to the QC domain (Fig. 5k, l).

JLO is required for *PIN* expression in the root

Wild-type roots accumulate auxin in a gradient with a maximum at the root tip. The gradient is formed and stabilized through the combined activities of PIN1,3,4 and 7, and interpreted by differential expression of PLT-family transcription factors. *PIN* gene expression depends in turn on auxin and *PLT* activity, thus creating a regulatory and self stabilising circuitry (Blilou et al. 2005; Vieten et al. 2005; Galinha et al. 2007).

DR5rev::GFP is strongly expressed in the stele, the QC with the adjacent stem cells and in columella cells. The patterning of this auxin maximum was unaltered in *jlo-2* mutants, but expression levels of *DR5rev::GFP* were drastically reduced (Fig. 6a, e). Next, we investigated the expression of the *PIN1::PIN1-GFP*, *PIN4::PIN4-GFP* and *PIN7::PIN7-GFP* reporters in postembryonic roots. In wild-type, PIN1 mainly resides at the basal end of vascular cells (Fig. 6b). PIN4 was detected around the QC, the stem cells surrounding it and in the first two layers of differentiated columella cells (Fig. 6c). PIN7 is localized at membranes of provascular cells in the meristem and elongation zone, as well as in the columella cells of the root tip (Fig. 6d). Expression of these PIN reporters was detectable in *jlo-2* in an unaltered pattern, but at very low levels (Fig. 6f–h). Using quantitative reverse transcriptase PCR assays, we found that *PIN1*, *PIN3, PIN4* and *PIN7*

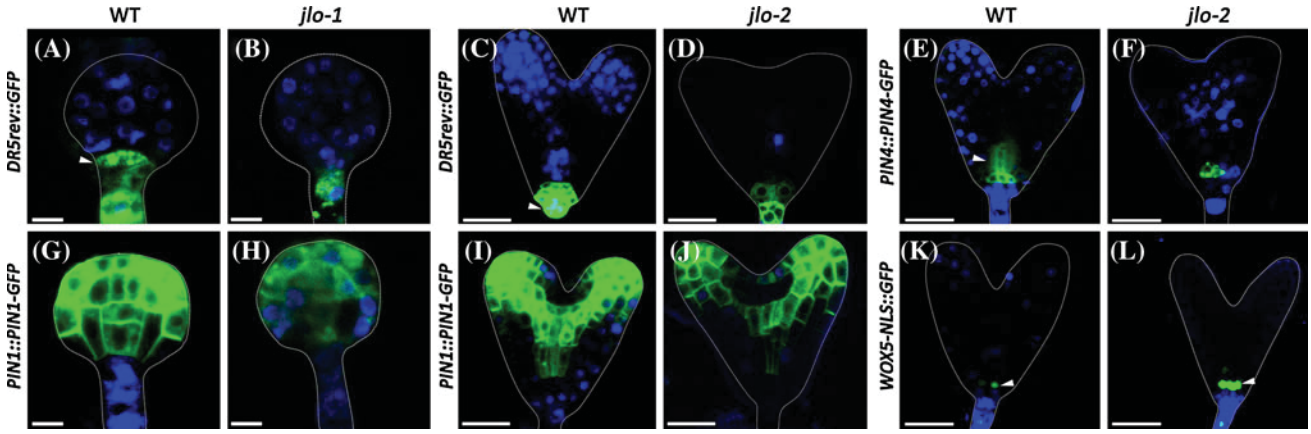

Fig. 5 Expression of auxin controlled genes in *jlo* mutant embryos. (**a–d**) Expression pattern of *DR5rev::GFP*, (**e–f**) *PIN4::PIN4-GFP*, (**g–j**) *PIN1::PIN1-GFP* and (**k–l**) *WOX5::NLS-GFP* in wild-type and *jlo* mutant embryos. Shapes of embryos are outlined. (**a**) In wild-type globular stage embryos *DR5rev::GFP* is expressed in the hypophysis (*arrowhead*) and upper suspensor cells. (**b**) *jlo-1* embryos at this stage concentrate auxin in the suspensor, but lack *DR5rev::GFP* signal in the hypophysis. In wild-type heart stage embryos (**c**), auxin concentrates in the root primoridum with maximum *DR5rev::GFP* fluorescence in the upper suspensor cell (*white arrowhead*). Heart stage *jlo-2* embryos (**d**) show only a weak signal at the root pole. (**e**) PIN4 is expressed in the QC and pro-vascular cells (*arrowhead*) of wild-type heart stage embryos. (**f**) *jlo-2* mutants lack *PIN4* expression in provascular cells. (**g**) PIN1 expression in wild-type globular stage embryo. (**h**) *jlo-1* show severely reduced PIN1 expression. (**i**) PIN1 concentrates to cotyledon tips and provascular cells in wild-type heart stage embryos. (**j**) *jlo-2* mutants show a similar PIN1 distribution, but reduced expression levels. (**k**) *WOX5::NLS-GFP* expression in the QC (*arrowhead*) of wild-type heart stage embryos. (**h**) In the *jlo-2* mutants, *WOX5* signal (*arrowhead*) expression is increased and laterally expanded. Scales bar: 20 µm; green: GFP fluorescence, blue: DAPI

transcript levels are already significantly reduced in *jlo-2/+* seedling roots, and further downregulated in *jlo-2* homozygotes, compared to wild-type (Fig. 6i). These results together with the previous observations show that JLO is an essential transcriptional regulator required for *PIN* gene expression.

To analyze if *JLO* expression is also sufficient to increase *PIN* RNA levels in the root, we misexpressed *JLO* using *Arabidopsis* seedlings that carry an estradiol inducible *i35S::JLO-FLAG* transgene. Inducible production of the JLO-FLAG fusion protein was confirmed by Western blotting with an anti-FLAG-antibody (Suppl Fig. 4). RNA was extracted from roots of 5 day old seedlings at 0, 1, 4 and 12 h after induction (HAI) of JLO-FLAG expression. qRT-PCR analysis of *PIN* RNA revealed a robust increase of expression for *PIN1* and *PIN3* within 4 HAI (Fig. 6j), while either no response or even a reduction of RNA levels was found for *PIN7* and *PIN4*, respectively, within 12 HAI. Because *PIN* gene expression depends on *PLT* gene activity, we also analyzed *PLT1,2,3* and *4* (*BBM*) RNA levels upon induction of high-level *JLO* expression. Expression of the four *PLT* genes tested was at least 1.5-fold increased within 2–4 HAI (Fig. 7m).

We conclude that *JLO* activity is required for *PIN1,3,4* and *7* transcription, and limiting for expression levels of *PIN1* and *PIN3*. Furthermore, this increased expression of *PIN* genes may be mediated by increased *PLT* gene expression in response to *JLO*.

Notably, the overall response of *PIN* genes to *JLO* must strongly depend on the developmental context, because *JLO* represses *PIN1* expression in shoot tissues (Suppl Fig. 5; Borghi et al. 2007).

JLO mediates auxin regulation of *PLT* and *PIN* expression

Members of the *PLETHORA* (*PLT/BBM*) gene family were shown to redundantly control expression of *PIN* genes in embryonic and postembryonic roots (Galinha et al. 2007). To analyze the relationship between *JLO* and *PLT* genes, we compared the expression patterns of *PLT1*, *2* and *BBM/PLT4* in wildtype roots and homozygous *jlo-2* mutants. All *PLT* genes studied were less expressed in *jlo-2*, both at the transcriptional and protein level (Fig. 7). The reduced expression of the *DR5rev::GFP* reporter, *PIN* genes and the *PLT* genes could suggest that auxin is limiting in *jlo* mutant roots. We therefore modified auxin content and distribution via treatment of roots with auxin (IAA), auxin transport inhibitors (NPA) or the transport-independent auxin analogue 2,4-D. We found that *DR5rev::GFP* expression is strongly upregulated by these treatments in wild-type roots, but only very mildly in *jlo-2* mutants (Suppl Fig. 6). Similarly, *PIN* and *PLT* gene expression showed a very dampened response to artificially increased availability of auxin in *jlo-2* mutants (Suppl Figs. 6, 7). Together, this indicated that auxin itself was not lacking or

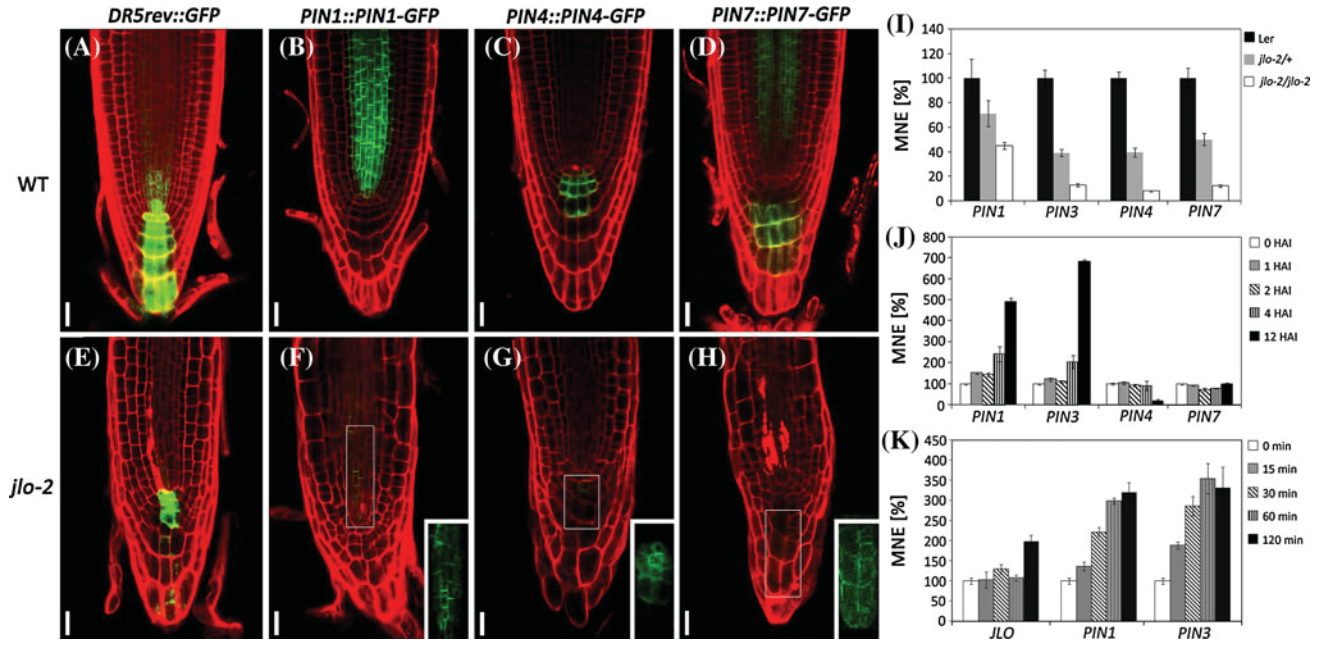

Fig. 6 Auxin signaling and *PIN* expression are regulated by *JLO*. (**a/e**) *DR5rev::GFP* activity in the primary root of wild-type (**a**) and *jlo-2* (**e**) mutants (5DAG). Auxin accumulation in *jlo-2* mutants is severely reduced. Expression of *PIN1::PIN1-GFP* (**b/f**), *PIN4::PIN4-GFP* (**c/g**) and *PIN7::PIN7-GFP* (**d/h**) in wild-type (**b–d**) and *jlo-2* mutants (**f–h**). Insets in **f**, **g** and **h** show GFP fluorescence obtained by increased laser excitation. Expression of all three PIN proteins analyzed is severely reduced in *jlo-2* mutant background, but not completely abolished (insets). Localization of the proteins is not affected by the *jlo-2* mutation. (**i**) qRT-PCR reveal downregulation of *PIN1*, *PIN3*, *PIN4* and *PIN7* transcript level in *jlo-2* mutant seedlings (5DAG) compared to wild-type. Note the reduction in *PIN* expression in heterozygous *jlo-2*/+ seedlings, although these roots are morphologically wild-type. (**j**) Analysis of *PIN1*, *PIN3*, *PIN4* and *PIN7* transcript levels in roots after induced misexpression of JLO-FLAG. Expression levels were normalized to uninduced controls prepared at the same time points. *PIN1* and *PIN3* are upregulated within 12 HAI whereas *PIN7* expression is unaltered and *PIN4* is downregulated between 4 HAI and 12 HAI. (K) Wild-type seedlings (5DAG) were incubated in 20 µM IAA for 0–120 min. *JLO* expression in roots increases within 2 h. *PIN1* and *PIN3* expression is induced within 15 min. *Scale bars*: 20 µm; GFP fluorescence, *red*: propidium iodide staining MNE: Mean Normalized Expression, HAI: hours after induction; *Bars* in (**i–k**) indicate standard error

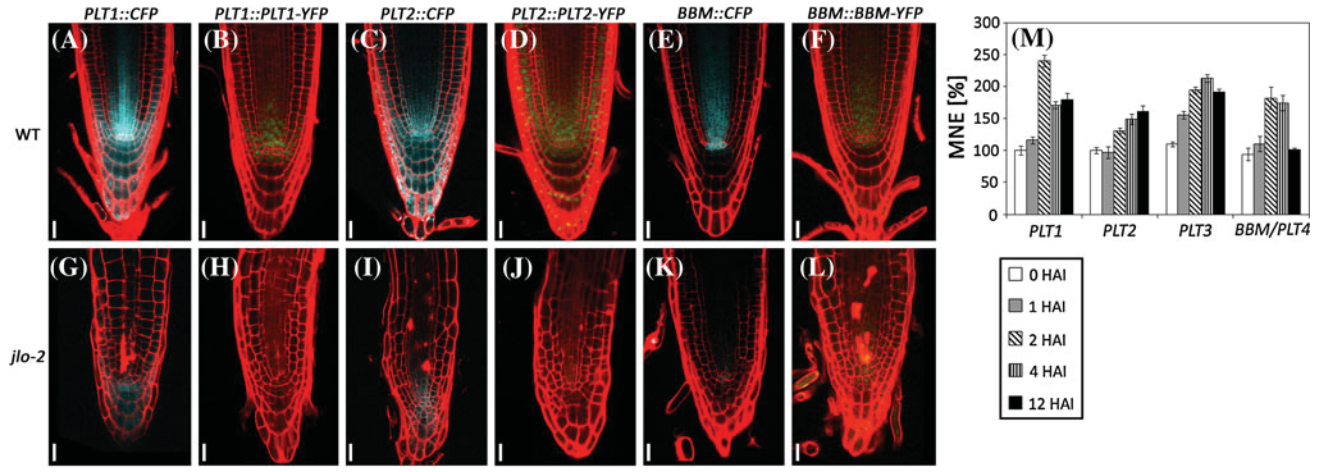

Fig. 7 *JLO* activates *PLT* expression. Expression of transcriptional *PLT::CFP* and translational *PLT::PLT-YFP* fusions in wild-type (**a–f**) and *jlo-2* mutant (**g–l**) roots (5DAG). (**a/g** and **b/h**): *PLT1* expression; (**c/i** and **d/j**): *PLT2* expression; (**e/k** and **f/l**): *BBM/PLT4* expression. Pictures of wild-type and the corresponding *jlo-2* mutant roots were taken with the same settings. Transcription and protein accumulation of all three *PLT* genes analyzed is strongly reduced in *jlo-2* roots. (**m**) Analysis of *PLT1*, *PLT2*, *PLT3* and *BBM/PLT4* transcript levels in roots after induced misexpression of JLO-FLAG. Expression levels were normalized to uninduced controls prepared at the same time points. *PLT* transcript levels increased at least 1.5 fold within 2–4 HAI. *Scale bars*: 20 µm; GFP fluorescence, *red*: propidium iodide staining; MNE: Mean Normalized Expression, HAI: hours after induction; *Bars* in (m) indicate standard error

limiting in *jlo-2* mutants, but that *JLO* acted in an auxin perception or signaling pathway. To analyze if auxin also regulates *JLO* expression levels, we quantified *JLO* mRNA amounts in roots of wild-type plants that were treated with IAA (Fig. 6k). *JLO* transcripts increased two-fold by 2 HAI. In parallel, we analyzed expression changes for *PIN1* and *PIN3*, which showed a drastic increase already within 15 min after induction. Thus, although *JLO* expression responds to added auxin, this response is temporally delayed and is not sufficient to explain the rapid changes in *PIN* gene expression levels.

We conclude that *JLO* is necessary to mediate auxin signaling. It is possible that some residual *JLO* activity in *jlo-2* mutants could allow for a minor transcriptional response of *PIN* and *PLT* genes to exogenous auxin.

BDL/MP act in a *JLO* dependent pathway

The severe embryonic phenotype exhibited by both strong (*jlo-1*) and weaker (*jlo-2*) mutations in *JLO* resembled those observed in *bdl* or *mp* mutants of *Arabidopsis*. Furthermore, our auxin induction experiments had shown that *JLO* is required for the full response of known auxin target genes. We used genetics to investigate if *JLO* interacts with *BDL* and *MP*. Gain-of-function mutations of *BDL* result in a stabilization of the IAA12/BDL protein (Hamann et al. 2002). Seedlings carrying a single *BDL::bdl-GUS* copy resembled wild-type, and those containing two *BDL::bdl-GUS* copies displayed the typical *bdl* phenotype (Suppl Fig. 8b; Suppl Table 2). The F2 progeny of a *jlo-2*/+; *BDL::bdl-GUS*/+ plant, which was phenotypically wild-type, was analyzed at the seedling stage (n = 677). We were not able to identify seedlings homozygous for both the *jlo-2* and *BDL::bdl-GUS* alleles, suggesting that double mutant embryos are not viable. Wild-type seedlings occurred at the expected ratio, but *BDL::bdl-GUS/BDL::bdl-GUS* and *BDL::bdl-GUS/BDL::bdl-GUS; jlo-2/+* seedlings displayed the same range of phenotypes, which were also indistiguishable from those of *jlo-2/jlo-2* seedlings, with or without one copy of *BDL::bdl-GUS*. Similarly, double mutants of *jlo-2* with *mp*-alleles were lethal, while the single mutants were epistatic to each other, but remained recessive (Suppl Table 3). In line with this, an *MP::MP-GFP* reporter (Schlereth et al. 2010) was expressed in a normal pattern in the *jlo-2* mutant root (Suppl Fig. 8f, g).

Genetics did not allow us to unravel the discrete genetic hierarchy of gene activities. However, since *jlo-1* mutants are fully embryo lethal, we conclude that *JLO* is essential for embryo patterning and that a part of *JLO* function is mediated through *BDL* and *MP*.

Discussion

The basic elements composing the *Arabidopsis* embryos, namely cotyledons, shoot meristems, root meristem and hypocotyl, originate after a series of stereotypic cell divisions. The zygote that was generated during fertilization first divides into a small apical cell that gives rise to the proembryo, and a larger basal cell that remains attached to the surrounding sporophytic tissues and forms the suspensor. Cell division orientation now drastically differs between the apical and basal cell line. The suspensor is formed by transversal divisions that generate an elongated file of cells. The apical cell undergoes two vertical cell divisions, followed by a transversal division that generates the first eight cells of the proembryo. Although highly regular, the division orientation may not be an essential prerequisite for the generation of an organized embryo later on. Several mutants were identified that exhibit altered cell division patterns during development of the proembryo, typically a change from vertical to transversal orientation of the first cell wall. The genes affected, *GNOM, BDL, MP* and *PIN* have all been shown to participate in auxin signaling, perception or directional transport (reviewed by Moller and Weijers 2009). However, the mechanism that controls the position and orientation of a new cell wall is not known.

We observed similar misoriented cell divisions when *JLO* activity was compromised, implicating *JLO* in patterning of the early embryo. *JLO* exerts its function, similarly to *MP* and *BDL*, at least in part by controlling auxin distribution. We observed that auxin signaling when monitored by *DR5rev::GFP* expression analysis was severely reduced in *jlo*-mutant embryos at all stages. Wild-type expression levels of the auxin efflux carriers PIN1 and PIN4 depended on *JLO* function, while their intracellular localization remained unaltered. Consistent with this, we found a reduced hypocotyl diameter, an underdeveloped vascular domain and misregulated *WOX5* expression in *jlo-2* mutants.

The morphology of *jlo*-2 mutant roots was strongly affected and therefore deviant from wild-type. The changes in reporter gene expression that we noted in the roots are similar to those observed during embryogenesis, and likely reflect a continuous requirement for JLO function throughout root growth.

At later stages, *JLO* was required to maintain activity of both shoot and root meristems. Aberrant development of the shoot comprised fused or missing cotyledons, formation of filamentous organs and vascular defects. Roots remained short, exhibited a reduced gravitropic response and carried misarranged cells in the root meristem due to differentation of stem cells. These seedling defects of *jlo-2*

mutants were again indicative for defects in auxin transport or signaling.

Our studies with auxin inhibitors, auxin addition and auxin analogues revealed that *jlo* mutants do not simply suffer from a reduced auxin biosynthesis. Because addition of 2,4-D was able to increase the response of a *DR5rev::GFP* reporter, although not to wild-type levels, we concluded that *JLO* is required to facilitate both auxin transport and perception or transduction.

We also noted that *JLO* is necessary for the expression of *PIN1,3,4,7* in roots. Expression of a inducible JLO-GR fusion protein repressed PIN transcripts in the root, indicating that the fusion to the GR domain interferes with normal JLO function (Bureau and Simon 2008). JLO is only sufficient to upregulate *PIN1* and *PIN3*. The fact that *PIN4* and *PIN7* expression are not increased upon *JLO* induction indicates that *JLO* requires cofactors for its function. In line with this hypothesis we observed a differential response of *PIN1* to *JLO* induction in roots and shoots, suggesting again a requirement for tissue specific cofactors. Candidate proteins could be other members of the LBD protein family. Although it was not shown to date whether LBD proteins directly interact with each other, several LBD proteins were found to function in similar developmental processes. LBD16 and LBD29 for example jointly contribute to lateral root development, and both LBD6/AS2 and LBD36 promote the differentiation of leaves and petals (Chalfun-Junior et al. 2005; Okushima et al. 2007). The protein showing closest sequence homology to JLO in *Arabidopsis* is LBD18. However, the expression pattern of *LBD18* does not overlap with that of *JLO* during embryogenesis. Furthermore, loss-of *LBD18* function does not cause embryonic patterning defects, indicating that *JLO* acts independently of *LBD18* in embryo development. Both *JLO/ASL19* and *LBD18/ASL20* were recently shown to be expressed during tracheary element (TE) development. Increased *JLO/ASL19* activity was shown to promote TE cell differentiation (Soyano et al. 2008). However, this might at least in part be explained by *JLO* affecting local auxin transport via regulation of *PIN* gene expression in the shoot.

PLT genes are central regulators of *PIN* gene expression (Blilou et al. 2005). *PLT* gene expression in the root depended largely on *JLO* activity, and increased *JLO* expression was able to upregulate *PLT* genes at least twofold. Thus, *JLO* can affect *PIN* gene expression via regulation of *PLT* genes. Because auxin alone was unable to promote *PIN* and *PLT* expression in the absence of *JLO*, we conclude that *JLO* is an essential factor that mediates auxin responses during plant development.

How *JLO* acts at the molecular level is still not understood. Mutants in *JLO*, *MP* and *BDL* are phenotypically alike, and both *bdl* and *mp* mutants enhanced embryo lethality of the phenotypically weaker *jlo-2* allele, suggesting that all three genes may act in a common pathway to regulate auxin signalling during early embryo development. However, strong (loss-of-function) *jlo*-mutants are embryo lethal and arrest at the globular stage of development, whereas dominant *bdl* mutants and loss-of-function *mp* mutants still develop into seedlings. This indicates that *JLO* performs also *BDL* and *MP* independent functions, possibly via regulation of, or interaction with, other ARF and IAA proteins (Shin et al. 2007). Interestingly, sequential activity of two auxin response moduls controls organogenesis during lateral root development (De Smet et al. 2010), and a similar scenario can be envisaged for early embryo development (Ploense et al. 2009).

During shoot and floral development, *JLO* is expressed in the boundaries between developing lateral organs and the remainder of the meristem. Cells that establish these boundaries are characterized by division along their longer axis, giving rise to narrow domains of elongated cells that form a physical and transcriptional barrier between functional domains. *JLO* was implicated here in the regulation of *PIN* gene expression, possibly resulting in a depletion of auxin from the boundary domain. Expression of a dominant negative acting JLO protein inhibited boundary formation and maintenance and thereby also organ initiation (Borghi et al. 2007). This late function of *JLO* may parallel its earlier function during embryo development. Here, *JLO* is required for the correct positioning and orientation of the first cell division in the proembryo, for further organized divisions and hypophysis specification. *JLO* shares this role in early embryo patterning with *MP, BDL, GN* and at least 4 *PIN* genes, which together control auxin distribution and signaling, and coordinate stereotypical cell division (reviewed by Moller and Weijers 2009).

Experimental procedures

Plant Accessions

The *jlo-1* mutant (S_020930) in *Columbia* (*Col-0*) background and the *jlo-2* mutant (JIC_GT.9713) in *Landsberg erecta* (*Ler*) background were obtained from the Nottingham *Arabidopsis* Stock Centre (NASC, UK) and confirmed by PCR based genotyping. Both mutant lines were maintained as heterozygous populations. The origins of the marker lines and mutants are as follows: *DR5rev::GFP* (Ben Scheres), *PIN1::PIN1-GFP*, *PIN4::PIN4-GFP* and *PIN7::PIN7-GFP* (Jiri Friml); *WOX5::NLS-GFP* (Frans Tax); *PLT1::PLT1-YFP*, *PLT1::CFP*, *PLT2::PLT2-YFP*, *PLT2::CFP*, *BBM::BBM-YFP* and *BBM::CFP* (Galinha et al. 2007); *QC184* promoter trap line (Institut National de Recherche Agronomique T-DNA collection), *MP::MP-GFP* (Dolf

Weijers), *BDL::bdl-GUS* (Gerd Jürgens), *mpBS1354*, *mpG12* (Thomas Berleth).

Plant growth conditions

Arabidopsis thaliana plants were grown on soil under constant light conditions at 21°C. For roots analysis, seeds were surface sterilized with chlorine gas or by washing with 70% EtOH, 0.1% Tween 20 and then imbibed in 0.1% agarose for 2 days at 4°C. After that, seeds were plated onto 0,5× Murashige and Skoog (MS) medium with Gamborgs no. 5 vitamins (Duchefa), 0,5 g/l 2-(N-morpholino) ethanesulfonic acid (MES), 1% (w/v) sucrose and 1.2% (w/v) plant agar. Plates were incubated vertically in a growth chamber with constant light at 21°C for 3–9 days. For hormone containing plates, IAA, 2,4-D and NPA (Sigma) were added to a final concentration of 10 µM (IAA and NPA) or 1 µM (2,4-D). For selection of plants carrying the *jlo-2 Ds* transposon insertion, seedlings were grown on media supplemented with Kanamycin (50 µg/µl).

Chimeric constructs and molecular techniques

For *LexA35S::JLO-FLAG* transgene construction, the *JLO* (AT4g00220) coding region without stop codon was amplified from *Col-0* genomic DNA with the primers JLO_for (5′-ATG AGC AGT AGC GGA AAC CCT AGC A-3′) and JLO_rev (5′-TTC TCG TTT TAT CAC TGA CGA GGC AGA-3′). The C-terminal FLAG tag (GCCTC GTCAGTGATAAAACGAGAAGACTACAA) and the attB recombination sites were added via PCR-mediated ligation. According to the manufacturer‘s instructions (Gateway manual; Invitrogen) the PCR fragment was recombined into pDONR201 and finally into the binary plant transformation vector pMDC7 (Curtis and Grossniklaus 2003). Subsequent transformation of *Col-0* was carried out with the floral dip method (Clough and Bent 1998).

For RNA extraction from root tissue, T2 seedlings (5 DAG) were induced by spraying with 20 µM ß-estradiol, 0.1% Tween20. Isolation of total RNA from *jlo-2* mutant seedlings and the corresponding wild-type control was performed at 5 DAG. RNA was extracted with the RNeasy kit (Qiagen). Conditions for cDNA synthesis were described previously (Muller et al. 2008). The MESA blue Mastermix (Eurogentec) was used for qRT-PCR according to the manufacturer's instructions. All individual reactions were performed as triplicates. Expression levels were normalized to those of *TIP41-like* (At4g34270) (Czechowski et al. 2005). Primers for all amplifications were located on an exon-exon border to prevent amplification of potentially contaminating genomic DNA.

Conditions for protein extraction and western blot analysis have been described previously (Bleckmann et al. 2010). To verify JLO-FLAG induction a primary anti-FLAG antibody (Sigma) and a secondary anti-mouse alkaline phosphatase conjugated antibody (Dianova) were used.

Embryo analysis

For the analysis of embryo phenotypes plants were grown under continous light conditions at 16°C. Siliques were dissected under a stereomicroscope to collect the immature seeds and embryos were excised from the ovules for microscopic analysis. Embryos were then cleared in 70% (w/v) chloral hydrate, 10% (v/v) glycerol solution. Fluorescence analysis of the embryos was performed in the F2 and F3 generation after genetic crossing with the different marker lines. Embryos were stained with DAPI and analyzed with a confocal microscope LSM510 Meta (Zeiss).

Expression analysis

Whole mount in situ hybridizations were carried out according to published methods (Hejatko et al. 2006) with an automated system (InSituPro liquid-handling robot; Intavis AG). The complete coding region of *JLO* (AT4g 00220) was amplified from cDNA and cloned as EcoRI - BamHI fragment into pGreenII, giving rise to plasmid pMR52. The plasmid pMR52 was used as template to amplify the C-terminal part of the *JLO* coding region fused to the T7 promoter sequence (forward primer: 5′-GGT GTA CGA CCT CTC CTC CA-3′ and reverse primer +T7: 5′-CCA AGC TTC TAA TAC GAC TCA CTA TAG GGA GAT TCT CGT TTT ATC ACT GA-3′). Probe preparation was performed as described (Hejatko et al. 2006).

Analysis of fluorescence reporter expression in seedling roots was performed using a LSM510 Meta confocal microscope. Counterstaining of cell walls was achieved by mounting roots in 10 µM propidium iodide. Histochemical analysis of ß-glucuronidase (GUS) activity in enhancer trap line *QC184* was carried out by incubation of seedling roots in GUS staining solution [0,05 M $NaPO_4$ (pH7.0), 5 mM $K_3[Fe(CN)_6]$, 10 mM $K_4[Fe(CN)_6]$, 10 mM X-glucuronidase at 37°C until blue staining was visible, followed by clearing in 70% (w/v) chloral hydrate, 10% (v/v) glycerol for microscopy.

Starch staining

Starch granules and cell walls in the root tips were stained with the mPSPI method and imaged with a confocal microscope as described (Truernit et al. 2008). Lugol's staining was carried out by mounting root tips in a 1:5 dilution of Lugol's solution in 70% (w/v) chloral hydrate, 10% (v/v) glycerol and analyzed after 1 h incubation.

Microscopy

Image acquisition was carried out with an Axiocam HR camera attached to a Zeiss Axioscope II microscope. Confocal images were taken with a Zeiss LSM 510 Meta laser scanning microscope. Images were processed in ImageJ software and assembled in Adobe Photoshop.

Acknowledgments We are grateful to Carin Theres and Cornelia Gieseler for technical support and to members of the R.S. laboratory for critical comments. We specifically thank Jiri Friml, Frans Tax, Thomas Berleth, Gerd Jürgens, Dolf Weijers and Ben Scheres for generously supplying plant materials. This work was funded through an EU Marie Curie Research and Training Network "SyStem", grant number MCRTN-CT-2004005336, and the DFG through grants Si677/2-1, 2-2 and Si947/3-1.

References

Aida M, Beis D, Heidstra R, Willemsen V, Blilou I, Galinha C, Nussaume L, Noh YS, Amasino R, Scheres B (2004) The PLETHORA genes mediate patterning of the Arabidopsis root stem cell niche. Cell 119:109–120

Benkova E, Michniewicz M, Sauer M, Teichmann T, Seifertova D, Jurgens G, Friml J (2003) Local, efflux-dependent auxin gradients as a common module for plant organ formation. Cell 115:591–602

Bleckmann A, Weidtkamp-Peters S, Seidel CA, Simon R (2010) Stem cell signaling in Arabidopsis requires CRN to localize CLV2 to the plasma membrane. Plant Physiol 152:166–176

Blilou I, Xu J, Wildwater M, Willemsen V, Paponov I, Friml J, Heidstra R, Aida M, Palme K, Scheres B (2005) The PIN auxin efflux facilitator network controls growth and patterning in Arabidopsis roots. Nature 433:39–44

Borghi L, Bureau M, Simon R (2007) Arabidopsis JAGGED LATERAL ORGANS is expressed in boundaries and coordinates KNOX and PIN activity. Plant Cell 19:1795–1808

Bureau M, Simon R (2008) JLO regulates embryo patterning and organ initiation by controlling auxin transport. Plant Signal Behav 3:145–147

Chalfun-Junior A, Franken J, Mes JJ, Marsch-Martinez N, Pereira A, Angenent GC (2005) ASYMMETRIC LEAVES2-LIKE1 gene, a member of the AS2/LOB family, controls proximal-distal patterning in Arabidopsis petals. Plant Mol Biol 57:559–575

Clough SJ, Bent AF (1998) Floral dip: a simplified method for Agrobacterium-mediated transformation of Arabidopsis thaliana. Plant J 16:735–743

Curtis MD, Grossniklaus U (2003) A gateway cloning vector set for high-throughput functional analysis of genes in planta. Plant Physiol 133:462–469

Czechowski T, Stitt M, Altmann T, Udvardi MK, Scheible WR (2005) Genome-wide identification and testing of superior reference genes for transcript normalization in Arabidopsis. Plant Physiol 139:5–17

De Smet I, Lau S, Voss U, Vanneste S, Benjamins R, Rademacher EH, Schlereth A, De Rybel B, Vassileva V, Grunewald W, Naudts M, Levesque MP, Ehrismann JS, Inze D, Luschnig C, Benfey PN, Weijers D, Van Montagu MC, Bennett MJ, Jurgens G, Beeckman T (2010) Bimodular auxin response controls organogenesis in Arabidopsis. Proc Natl Acad Sci USA 107: 2705–2710

Dharmasiri N, Dharmasiri S, Estelle M (2005a) The F-box protein TIR1 is an auxin receptor. Nature 435:441–445

Dharmasiri N, Dharmasiri S, Weijers D, Lechner E, Yamada M, Hobbie L, Ehrismann JS, Jurgens G, Estelle M (2005b) Plant development is regulated by a family of auxin receptor F box proteins. Dev Cell 9:109–119

Feraru E, Friml J (2008) PIN polar targeting. Plant Physiol 147:1553–1559

Friml J, Wisniewska J, Benkova E, Mendgen K, Palme K (2002) Lateral relocation of auxin efflux regulator PIN3 mediates tropism in Arabidopsis. Nature 415:806–809

Friml J, Vieten A, Sauer M, Weijers D, Schwarz H, Hamann T, Offringa R, Jurgens G (2003) Efflux-dependent auxin gradients establish the apical-basal axis of Arabidopsis. Nature 426: 147–153

Galinha C, Hofhuis H, Luijten M, Willemsen V, Blilou I, Heidstra R, Scheres B (2007) PLETHORA proteins as dose-dependent master regulators of Arabidopsis root development. Nature 449:1053–1057

Galweiler L, Guan C, Muller A, Wisman E, Mendgen K, Yephremov A, Palme K (1998) Regulation of polar auxin transport by AtPIN1 in Arabidopsis vascular tissue. Science 282:2226–2230

Geldner N, Friml J, Stierhof YD, Jurgens G, Palme K (2001) Auxin transport inhibitors block PIN1 cycling and vesicle trafficking. Nature 413:425–428

Gray WM, Kepinski S, Rouse D, Leyser O, Estelle M (2001) Auxin regulates SCF(TIR1)-dependent degradation of AUX/IAA proteins. Nature 414:271–276

Hamann T, Benkova E, Baurle I, Kientz M, Jurgens G (2002) The Arabidopsis BODENLOS gene encodes an auxin response protein inhibiting MONOPTEROS-mediated embryo patterning. Genes Dev 16:1610–1615

Hardtke CS, Berleth T (1998) The Arabidopsis gene MONOPTEROS encodes a transcription factor mediating embryo axis formation and vascular development. EMBO J 17:1405–1411

Hejatko J, Blilou I, Brewer PB, Friml J, Scheres B, Benkova E (2006) In situ hybridization technique for mRNA detection in whole mount Arabidopsis samples. Nat Protoc 1:1939–1946

Jaillais Y, Santambrogio M, Rozier F, Fobis-Loisy I, Miege C, Gaude T (2007) The retromer protein VPS29 links cell polarity and organ initiation in plants. Cell 130:1057–1070

Kepinski S, Leyser O (2004) Auxin-induced SCFTIR1-Aux/IAA interaction involves stable modification of the SCFTIR1 complex. Proc Natl Acad Sci USA 101:12381–12386

Kepinski S, Leyser O (2005) The Arabidopsis F-box protein TIR1 is an auxin receptor. Nature 435:446–451

Kleine-Vehn J, Friml J (2008) Polar targeting and endocytic recycling in auxin-dependent plant development. Annu Rev Cell Dev Biol 24:447–473

Kleine-Vehn J, Langowski L, Wisniewska J, Dhonukshe P, Brewer PB, Friml J (2008a) Cellular and molecular requirements for polar PIN targeting and transcytosis in plants. Mol Plant 1:1056–1066

Kleine-Vehn J, Leitner J, Zwiewka M, Sauer M, Abas L, Luschnig C, Friml J (2008b) Differential degradation of PIN2 auxin efflux carrier by retromer-dependent vacuolar targeting. Proc Natl Acad Sci USA 105:17812–17817

Kleine-Vehn J, Dhonukshe P, Sauer M, Brewer PB, Wisniewska J, Paciorek T, Benkova E, Friml J (2008c) ARF GEF-dependent transcytosis and polar delivery of PIN auxin carriers in Arabidopsis. Curr Biol 18:526–531

Liscum E, Reed JW (2002) Genetics of Aux/IAA and ARF action in plant growth and development. Plant Mol Biol 49:387–400

Michniewicz M, Zago MK, Abas L, Weijers D, Schweighofer A, Meskiene I, Heisler MG, Ohno C, Zhang J, Huang F, Schwab R, Weigel D, Meyerowitz EM, Luschnig C, Offringa R, Friml J

(2007) Antagonistic regulation of PIN phosphorylation by PP2A and PINOID directs auxin flux. Cell 130:1044–1056

Moller B, Weijers D (2009) Auxin control of embryo patterning. Cold Spring Harb Perspect Biol 1:a001545

Muller R, Bleckmann A, Simon R (2008) The receptor kinase CORYNE of Arabidopsis transmits the stem cell-limiting signal CLAVATA3 independently of CLAVATA1. Plant Cell 20: 934–946

Okushima Y, Fukaki H, Onoda M, Theologis A, Tasaka M (2007) ARF7 and ARF19 regulate lateral root formation via direct activation of LBD/ASL genes in Arabidopsis. Plant Cell 19:118–130

Paciorek T, Zazimalova E, Ruthardt N, Petrasek J, Stierhof YD, Kleine-Vehn J, Morris DA, Emans N, Jurgens G, Geldner N, Friml J (2005) Auxin inhibits endocytosis and promotes its own efflux from cells. Nature 435:1251–1256

Paponov IA, Teale WD, Trebar M, Blilou I, Palme K (2005) The PIN auxin efflux facilitators: evolutionary and functional perspectives. Trends Plant Sci 10:170–177

Ploense SE, Wu MF, Nagpal P, Reed JW (2009) A gain-of-function mutation in IAA18 alters Arabidopsis embryonic apical patterning. Development 136:1509–1517

Reed JW (2001) Roles and activities of Aux/IAA proteins in Arabidopsis. Trends Plant Sci 6:420–425

Sabatini S, Beis D, Wolkenfelt H, Murfett J, Guilfoyle T, Malamy J, Benfey P, Leyser O, Bechtold N, Weisbeek P, Scheres B (1999) An auxin-dependent distal organizer of pattern and polarity in the Arabidopsis root. Cell 99:463–472

Sarkar AK, Luijten M, Miyashima S, Lenhard M, Hashimoto T, Nakajima K, Scheres B, Heidstra R, Laux T (2007) Conserved factors regulate signalling in Arabidopsis thaliana shoot and root stem cell organizers. Nature 446:811–814

Sauer M, Balla J, Luschnig C, Wisniewska J, Reinohl V, Friml J, Benkova E (2006) Canalization of auxin flow by Aux/IAA-ARF-dependent feedback regulation of PIN polarity. Genes Dev 20:2902–2911

Schlereth A, Moller B, Liu W, Kientz M, Flipse J, Rademacher EH, Schmid M, Jurgens G, Weijers D (2010) MONOPTEROS controls embryonic root initiation by regulating a mobile transcription factor. Nature 464:913–916

Shin R, Burch AY, Huppert KA, Tiwari SB, Murphy AS, Guilfoyle TJ, Schachtman DP (2007) The Arabidopsis transcription factor MYB77 modulates auxin signal transduction. Plant Cell 19:2440–2453

Shuai B, Reynaga-Pena CG, Springer PS (2002) The lateral organ boundaries gene defines a novel, plant-specific gene family. Plant Physiol 129:747–761

Soyano T, Thitamadee S, Machida Y, Chua NH (2008) ASYMMETRIC LEAVES2-LIKE19/LATERAL ORGAN BOUNDARIES DOMAIN30 and ASL20/LBD18 regulate tracheary element differentiation in Arabidopsis. Plant Cell 20:3359–3373

Tiwari SB, Wang XJ, Hagen G, Guilfoyle TJ (2001) AUX/IAA proteins are active repressors, and their stability and activity are modulated by auxin. Plant Cell 13:2809–2822

Tiwari SB, Hagen G, Guilfoyle T (2003) The roles of auxin response factor domains in auxin-responsive transcription. Plant Cell 15:533–543

Tiwari SB, Hagen G, Guilfoyle TJ (2004) Aux/IAA proteins contain a potent transcriptional repression domain. Plant Cell 16:533–543

Truernit E, Bauby H, Dubreucq B, Grandjean O, Runions J, Barthelemy J, Palauqui JC (2008) High-resolution whole-mount imaging of three-dimensional tissue organization and gene expression enables the study of Phloem development and structure in Arabidopsis. Plant Cell 20:1494–1503

Ulmasov T, Murfett J, Hagen G, Guilfoyle TJ (1997) Aux/IAA proteins repress expression of reporter genes containing natural and highly active synthetic auxin response elements. Plant Cell 9:1963–1971

Vieten A, Vanneste S, Wisniewska J, Benkova E, Benjamins R, Beeckman T, Luschnig C, Friml J (2005) Functional redundancy of PIN proteins is accompanied by auxin-dependent cross-regulation of PIN expression. Development 132:4521–4531

Weijers D, Jurgens G (2005) Auxin and embryo axis formation: the ends in sight? Curr Opin Plant Biol 8:32–37

Weijers D, Benkova E, Jager KE, Schlereth A, Hamann T, Kientz M, Wilmoth JC, Reed JW, Jurgens G (2005) Developmental specificity of auxin response by pairs of ARF and Aux/IAA transcriptional regulators. EMBO J 24:1874–1885

Zazimalova E, Krecek P, Skupa P, Hoyerova K, Petrasek J (2007) Polar transport of the plant hormone auxin—the role of PIN-FORMED (PIN) proteins. Cell Mol Life Sci 64:1621–1637

4.1.3. Supplemental Data (Bureau et al., 2010)

4.1.3.1. Supplemental Tables

Hypocotyl diameter of heart stage embryos	
Wild-type [µm]	*jlo-2* [µm]
46,9 (+/- 0,9)	40,6 (+/- 1,6)

Suppl. Tab. 1: Hypocotyl diameter of wild-type and *jlo-2* heart stage embryos. Measurement of hypocotyl diamenter [µm] was performed with the ImageJ software as indicated in Fig. 2A and 2E (white arrow).

A. Parental Genotype: *BDL::bdl-GUS/+* (selfing)

Seedling Phenotype	WT		*bdl*		Total
n counted	51		16		67
n expected	50		16		67
GUS staining	positive	negative	positive	negative	Total
n counted	36	15	16	0	67
n expected	34	17	17	0	67

B. Parental Genotype: *mpBS1354/+* (selfing)

Seedling Phenotype	WT	*mp*	Total
n counted	451	104	555
n expected	451	150	601

C. Parental Genotype: *mpG12/+* (selfing)

Seedling Phenotype	WT	*mp*	Total
n counted	269	52	321
n expected	269	90	359

Suppl. Tab. 2: Segregation of *bdl* and *mp* mutations. Segregation of mutant phenotypes in the progeny of *BDL::bdl-GUS*/+ (A); *mpBS1354*/+ (B) and *mpG12*/+ (C). Given are the total numbers of wild-type (WT) and mutant seedlings as counted for each mutation and the expected number based on a 3:1 segregation for recessive alleles. The *BDL::bdl-GUS* transgene was further identified by GUS staining. (A) Segregation analysis revealed that *BDL::bdl-GUS* behaves like a recessive allele at seedling stage. (B) *mpBS1354/+* plants show embryonic lethality with a frequency of 8%. The *mpG12* allele is stronger since 11% of seedlings are missing in the progeny of a *mpG12*/+ plant (C).

A. Parental Genotype: *jlo-2/+* x *BDL::bdl-GUS/+*

	Kanamycin Sensitive				Kanamycin Resistant								
Seedling Phenotype	WT		*bdl*		WT		*bdl**		*jlo-2*		*bdl/jlo-2*		Total
n counted	124		45		254		175		44		0		642
n expected	127		42		254		85		127		42		677
GUS staining	+	-	+	-	+	-	+	-	+	-	+	-	Total
n counted	84	40	45	0	172	82	175	0	0	44	/	/	642
n expected	85	42	42	0	169	85	85	0	85	42	42	0	677

* potential Genotypes: *BDL::bdl-GUS/BDL::bdl-GUS; jlo-2/+* and *BDL::bdl-GUS*/+; *jlo-2/jlo-2*

B. Parental Genotype: *jlo-2/+* x *mpBS1354/+*

	Kanamycin Sensitive		Kanamycin Resistant				
Seedling Phenotype	WT	*mp*	WT	*mp**	*jlo-2*	*mp/jlo-2*	Total
n counted	106	33	201	114	34	0	488
n expected	101	34	201	67	101	34	536

* potential Genotypes: *mpBS1354/mpBS1354; jlo-2/+* and *mpBS1354*/+; *jlo-2/jlo-2*

C. Parental Genotype: *jlo-2/+* x *mpG12/+*

	Kanamycin Sensitive		Kanamycin Resistant				
Seedling Phenotype	WT	*mp*	WT	*mp**	*jlo-2*	*mp/jlo-2*	Total
n counted	217	55	465	137	67	0	941
n expected	233	78	465	155	233	78	1240

* potential Genotypes: *mpG12/mpG12; jlo-2/+* and *mpG12*/+; *jlo-2/jlo-2*

Suppl. Tab. 3: Segregation analysis of *jlo-2 bdl* and *jlo-2 mp* double mutants. Segregation of mutant phenotypes in the F2 progeny of a *jlo-2/+*; *BDL::bdl-GUS*/+ (A); *jlo-2/+*; *mpBS1354*/+ (B) and *jlo-2/+*; *mpG12*/+ (C) plant. Given are the total numbers of seedling phenotypes as counted for each crossing and the expected numbers. Resistance to kanamycin due to the *jlo-2* Ds transposon insertion was used for segregation analysis. GUS staining of the *jlo-2/+; BDL::bdl-GUS/+* progeny was used for identification of the *BDL::bdl-GUS* allele. (A) Wild-type seedlings occurred at the expected ratio and no seedlings homozygous for both alleles could be identified. *jlo-2/+; BDL::bdl-GUS/ BDL::bdl-GUS* seedlings were phenotypically indistiguishable from those of *jlo-2/jlo-2; BDL::bdl-GUS/+* seedlings. (B-C) Similar results were obtained for both *jlo-2/+ mp/+* crossings.
+ GUS positive; - GUS negative

4.1.3.2. Supplemental Figures

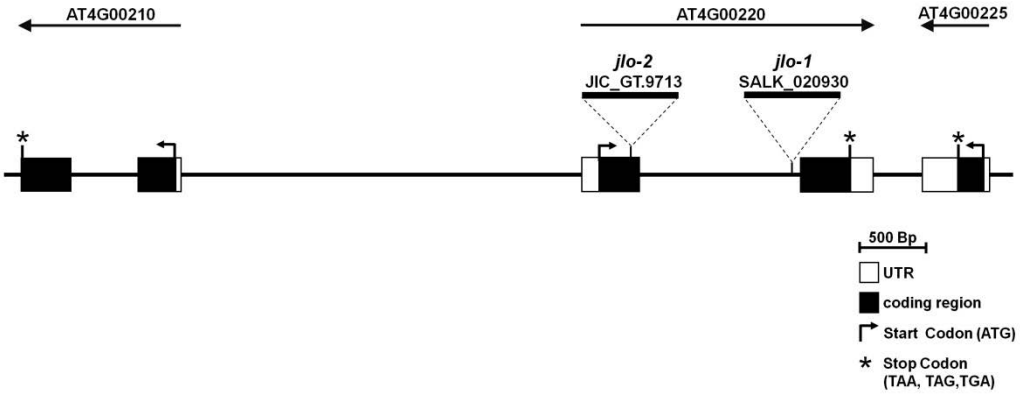

Suppl, Fig. 1: Mutations in the *JLO* (At4g00220) gene. Exon-intron structure of *JLO* and the neighboring genes on chromosom 4. The *jlo-1* T-DNA (SALK_090930) is inserted in the end of the intron. The *Ds* element insertion in *jlo-2* (JIC_GT.3713) is positioned in the first exon. Both insertion sites were confirmed by sequencing of genomic DNA fragments amplified by PCR.

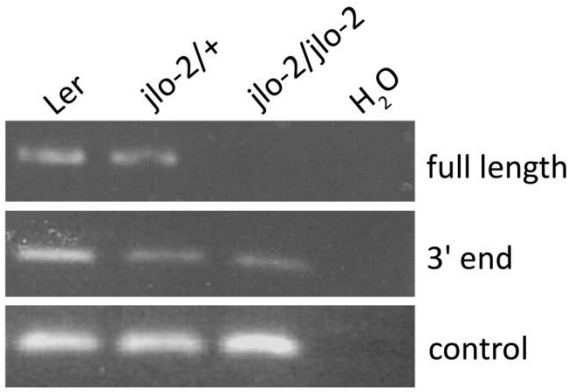

Suppl. Fig. 2: RT-PCR analysis. RT-PCR was performed with total RNA isolated from seedlings (5DAG) of the indicated genetic backgrounds to examine *JLO* expression. No full length transcript could be identified in homozygous *jlo-2* mutants but a shortened RNA, consisting of sequences 3´ to the T-DNA insertion is still detectable. control: EIF4A

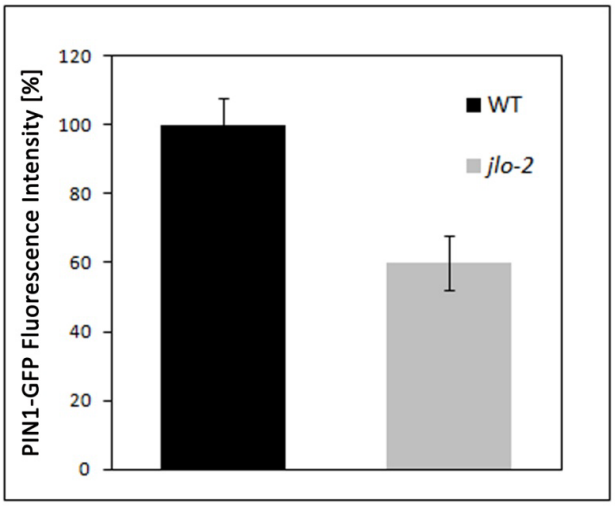

Suppl. Fig. 3: *PIN1::PIN1-GFP* fluorescence intensity in heart stage embryos. Measurement of the GFP fluorescence intensity was performed with the ImageJ software. *PIN1::PIN1-GFP* expression is reduced to 60% of wild-type the level. Bars indicate standard error.

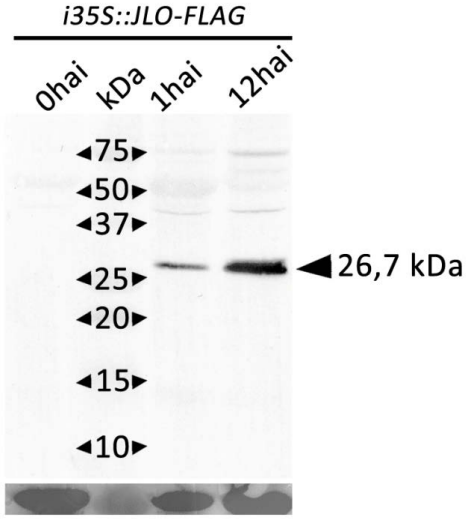

Suppl. Fig. 4: Western blot analysis. Western blot analysis with an anti-FLAG antibody to confirm the presence of the JLO-FLAG fusion protein (expected size: 26.7 kDa), one hour or twelve hours after induction (HAI). Protein was extracted from *Arabidopsis thaliana* roots (5DAG). The PonceauS stained protein bands of Ribulosebisphophatecarboxylase (Rubisco) is shown as loading control.

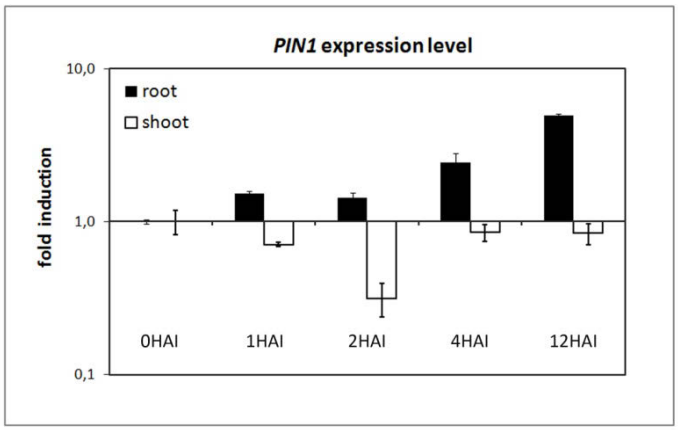

Suppl. Fig. 5: Transcriptional regulation of *PIN1* by JLO in inflorescences and roots. (A) qRT-PCR showing that regulation of *PIN1* expression by *JLO* is dependent on the developmental context. In roots, *PIN1* is upregulated after induction of JLO-FLAG misexpression, whereas *PIN1* expression in inflorescences decreases after induction. HAI: hours after induction; Bars indicate standard error.

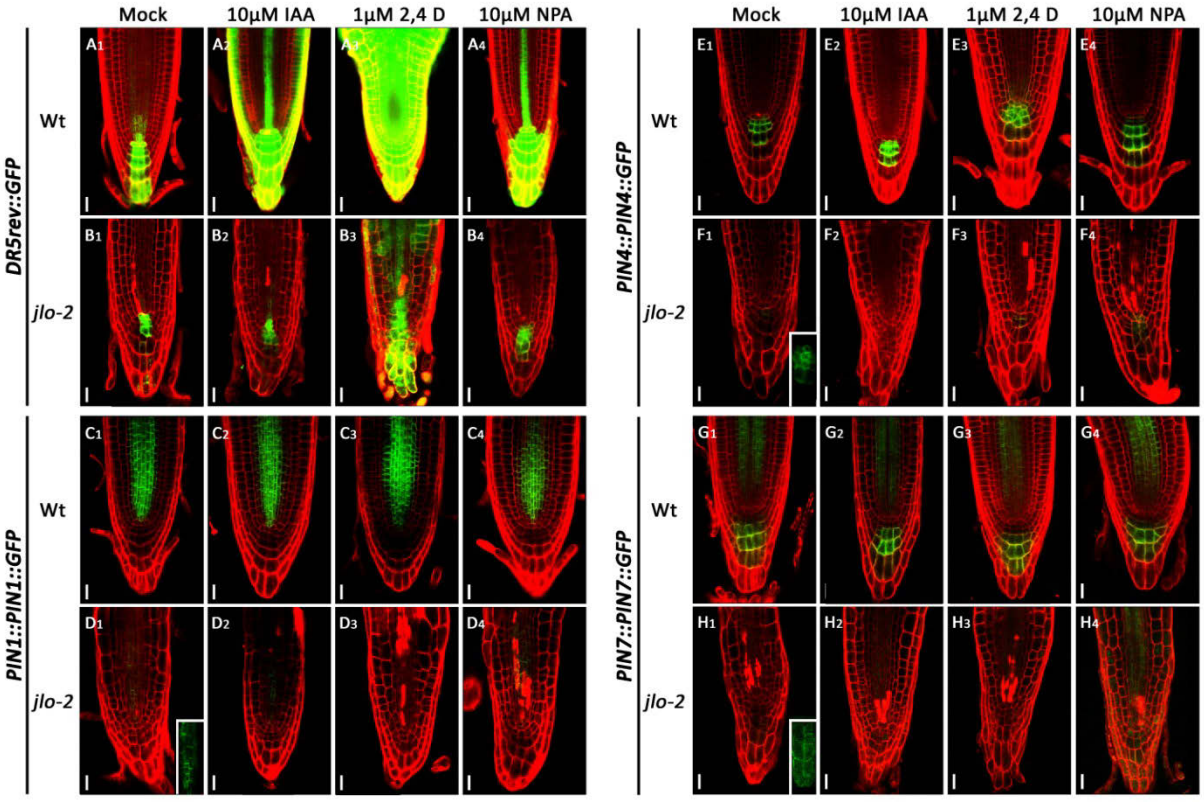

Suppl. Fig. 6: Auxin distribution and *PIN* expression in response to exogenous auxin treatment. Expression of *DR5rev::GFP* in wild-type roots (A_1-A_4) and *jlo-2* mutants (B_1-B_4): (A_1/B_1) untreated control; (A_2/B_2) overnight treatment with IAA (10µM), (A_3/B_3) 2,4-D (1µM) and (A_4/B_4) NPA (10µM). The *DR5rev* promoter activity clearly responds to the modified auxin distribution in wild-type roots. *jlo-2* roots show a severely reduced *DR5rev::GFP* expression around the QC and no upregulation of *DR5rev::GFP* expression in response to external (10µM) IAA; (B3) overnight treatment with 1µM 2,4-D increases the *DR5rev::GFP* signal in *jlo-2* mutants, indicating that auxin perception is not completely abolished. (B_4) no upregulation of *DR5rev::GFP* signal after NPA (10µM) treatment. (C_1-C_4) Expression of *PIN1::PIN1-GFP* in wild-type roots. Untreated control (C_1); overnight treatment with 10µM IAA (C_2); 1µM 2,4-D (C_3) and 10µM NPA (C_4). (D_1-D_4) Expression of *PIN1::PIN1-GFP* in

jlo-2 mutants (D_1) is strongly downregulated, but not completely lost (inset). The amount of PIN1-GFP protein is not increased after treatment with 10µM IAA (D_2); 1µM 2,4-D (D_3) and 10µM NPA (D_4). (E_1–E_4) Expression of *PIN4::PIN4-GFP* in wild-type and (F_1–F_4) *jlo-2* mutant roots without hormone treatment (E_1 and F_1) and with 10µM IAA (E_2 and F_2), 1µM 2,4-D (E_3 and F_3) or 10µM NPA (E_4 and F_4) treatment. (G_1–G_4) Expression of *PIN7::PIN7-GFP* in wild-type and (H_1–H_4) *jlo-2* mutant roots without hormone treatment (G_1 and H_1) and with 10µM IAA (G_2 and H_2), 1µM 2,4-D (G_3 and H_3) or 10µM NPA (G_4 and H_4) treatment. Treatment with IAA, 2,4-D and NPA did not restore the expression of *PIN* genes in *jlo-2* mutants. Pictures of wild-type and the corresponding *jlo-2* mutant roots were taken with the same settings. Insets in D_1, F_1 and H_1 show images obtained by increasing laser intensities to enhance GFP signals. Note that PIN1, PIN4 and PIN7 expression is not lost in *jlo-2* mutants, and that localization of the proteins is unaffected. Cell walls were stained with propidium iodide (red); Scale bars: 20µm

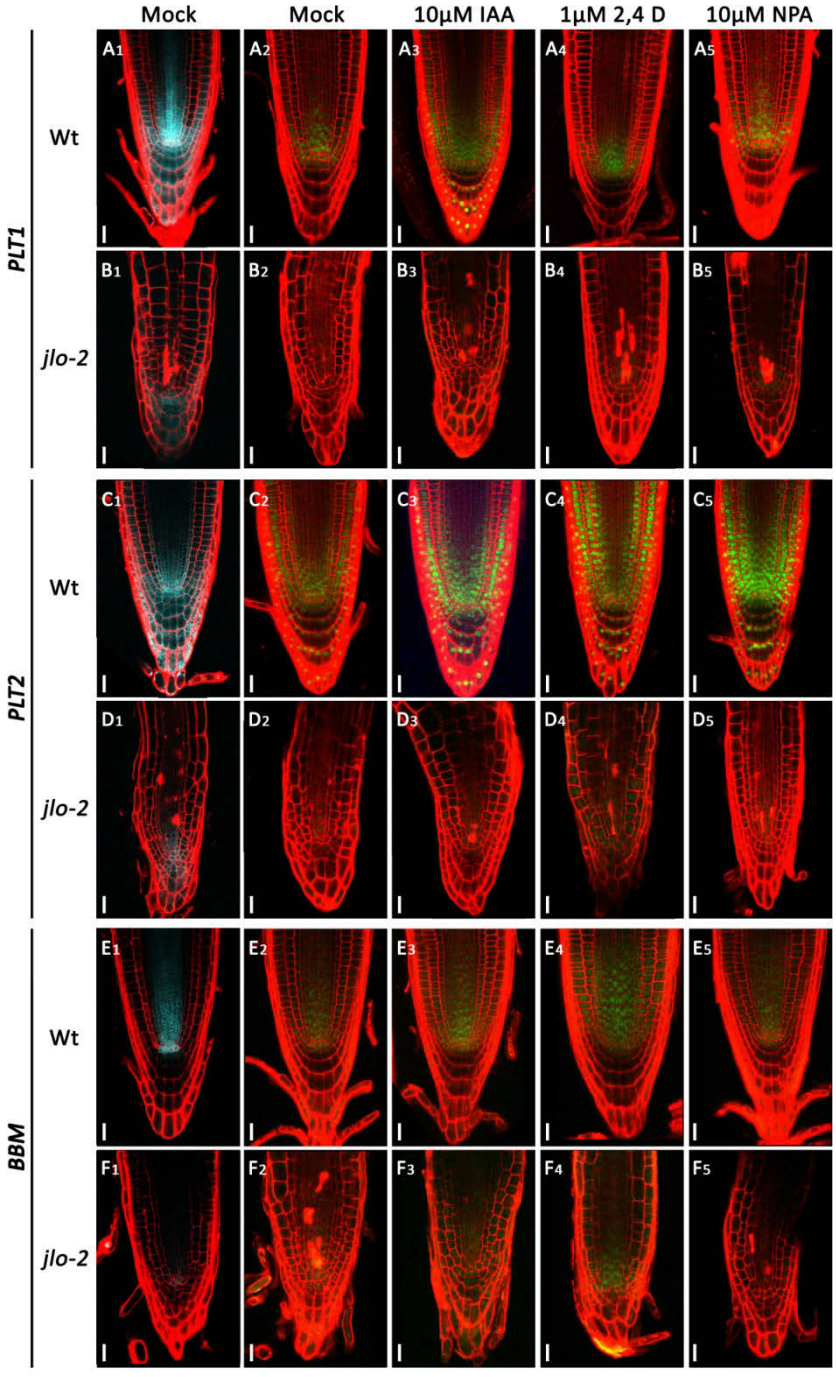

Suppl. Fig. 7: *PLT* expression in response to exogenous auxin treatment. (A_1 and B_1) Expression of transcriptional *PLT1::CFP* and translational *PLT1::PLT1-YFP* (A_2 and B_2) fusions in wild-type and *jlo-2* mutants.

PLT1 expression is downregulated in *jlo-2* mutants. Treatment with 10µM IAA (A3 and B3); 1µM 2,4-D (A4 and B4) and 10µM NPA (A5 and B5) does not significantly increase PLT1-YFP expression in wild-type or *jlo-2* mutant roots. (C_1/D_1 and C_2/D_2) Expression of *PLT2::CFP* and *PLT2::PLT2-YFP* in wild-type and *jlo-2* roots. (C_3- C_5) PLT2-YFP protein accumulation is increased after modification of the auxin gradient in wild-type roots. (C_3) 10µM IAA; (C_4) 1µM 2,4-D and (C_5) 10µM NPA. (D_3- D_5) PLT2-YFP response to IAA (D_3) or NPA (D_5) treatment is not detectable in *jlo-2* mutants. Only high amounts of 2,4-D (D_4) slightly increase PLT2-YFP protein concentration in *jlo-2* mutants in comparison to the untreated control. (E_1/F_1 and E_2/F_2) Expression of *BBM::CFP* and *BBM::BBM-YFP* in wild-type and *jlo-2* roots. (E_3- E_5) Response of BBM-YFP expression to IAA (E_3), 2,4-D (E_4) or NPA (E_5) treatment in wild-type roots. A prominent increase in BBM protein amount was observed with 2,4-D treatment. (F_3- F_5) Hormone treatment also increased BBM-YFP expression in *jlo-2* mutants, although to a lesser extent than in wild-type. Cell walls were stained with propidium iodide (red); Scale bars: 20 µm

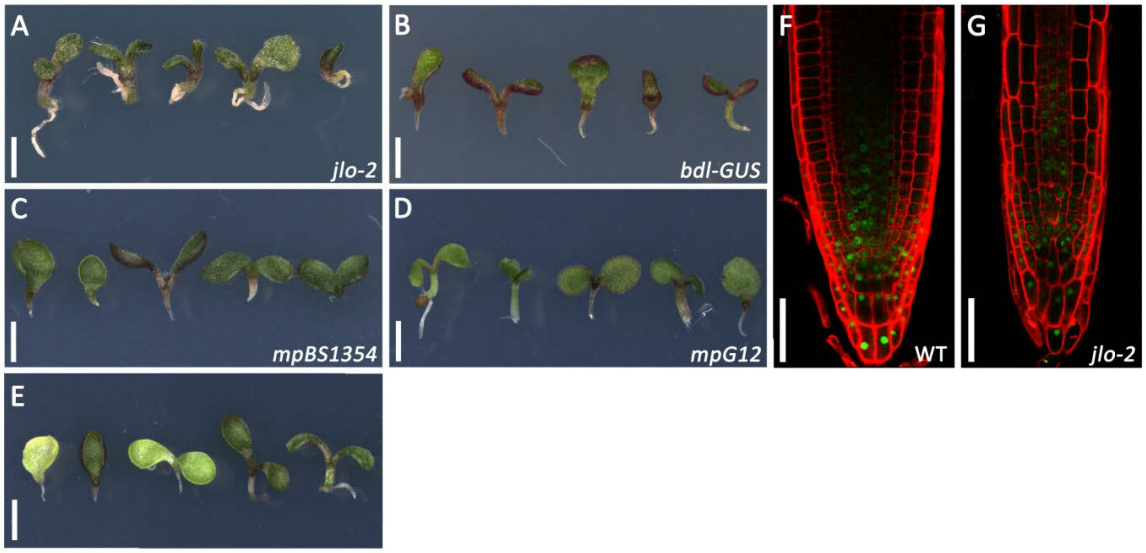

Suppl. Fig. 8: Seedling phenotypes of *jlo-2 bdl* and *jlo-2 mp* double mutants. Seedling phenotypes (5DAG) of *jlo-2* (A), *BDL::bdl-GUS* (B), a weak *mp* allele (*mpBS1354)* (C), a stronger *mp* allele (*mpG12*) (D) and F2 seedlings deriving from *jlo-2 BDL::bdl-GUS* crossing. The *BDL::bdl-GUS* transgene carries a mutation within domain II of IAA12 resulting in a stabilization of the protein. Seedlings containing a single *BDL::bdl-GUS* copy resembled wild-type, whereas seedlings containing two copies resemble *bdl* gain-of function mutants (B). A similar range of seedling phenotypes was observed after selfing of *mpBS1354/+* and *mpG12/+* plants (C/D). Note the phenotypic similarity between *jlo-2* and *bdl* or *mp* single mutants. (E) F2 progeny of a *jlo-2/+*; *BDL::bdl-GUS*/+ plant. To select for the *jlo-2 Ds* transposon insertion, seedlings were grown on media supplemented with kanamycin. Seedlings with the genotype +/+; *BDL::bdl-GUS/BDL::bdl-GUS* (light green) phenotypically resemble seedlings that carry additionally the *jlo-2* mutation (*jlo-2/+; BDL::bdl-GUS/BDL::bdl-GUS*) or seedling homozygous for the *jlo-2* allele with or without one copy of *BDL::bdl-GUS* transgene (*jlo-2/jlo-2*; *BDL::bdl-GUS/+* or *jlo-2/jlo-2;* +/+). Seedlings resistant to kanamycin appear dark green, seedlings sensitive to kanamycin appear light green. (F/G) Expression of *MP::MP-GFP* in wild-type and *jlo-2* mutant roots. The *MP* expression pattern is not altered in *jlo-2* mutants. Cell walls in F/G were stained with propidium iodide (red). Scale bars: A-D 1mm; E-F 50µm.

4.1.4. Outcomes from prior studies

Based on the previous work JLO is considered to be an important regulator of auxin signaling during plant development. Nevertheless, it remained unclear how JLO can be directly implicated in the auxin signal transduction. Furthermore, little is known about the external cues that trigger JLO activity. With the following experiments, I tried to answer these open questions. As most of these studies were performed in postembryonic roots, I initially assayed the *JLO* expression pattern in these tissues.

4.1.5. *JLO* expression in postembryonic roots

JLO is expressed in provascular cells during early heart stage of embryogenesis. From torpedo stage onwards, expression becomes restricted to the basal root tip while only a weak signal remains detectable in the embryonic vasculature (Bureau et al., 2010). To unravel the spatial expression pattern of *JLO* in postembryonic roots, whole mount RNA *in situ* hybridization (WISH) was performed. The *JLO* transcripts were detected in all root tissues proximal to the QC with slightly higher signal intensity in the epidermis, cortex and endodermis (Fig. 4.1A). As expected, no *JLO* mRNA was detectable in *jlo-2* loss-of-function mutants, confirming the specificity of the observed signals (Fig. 4.1B).

Immunolocalization experiments were carried out to further explore the spatial expression and subcellular localization of the JLO protein in wild-type roots. The antibody used for these experiments was raised against the non conserved C-terminus of the JLO protein (Tab. 1). Western blot analysis ensured functionality of the JLO antibody as only one specific band of the expected size was detected in protein extracts of wild-type and *JLO* misexpressing plants (Fig. 4.1G). Monitoring Alexa 488 signals after immunodetection of the JLO protein showed both, a nuclear and cytoplasmic localization (Fig. 4.1C/C', insets). Spatially, the JLO protein was predominately detected in the outer root layers but weak signals also appeared in the inner root stele while differentiated columella cells showed only background signals (Fig. 4.1C/C'). No comparable results were obtained using *jlo-2* mutant roots, thus these signals are most likely specific (Fig. 4.1D/D').

Unfortunately, no appropriate positive control to test the quality of tissue permeabilization was available. Therefore an insufficient antibody penetration cannot be excluded. Nevertheless, the mRNA expression pattern obtained by WISH analysis resembles the results of the immunodetection experiments. Collectively, these results show that *JLO* is clearly expressed in postembryonic roots. This is consistent with the role of *JLO* in root meristem maintenance.

4.1.6. JLO response to exogenous auxin treatment

In contrast to the transcriptional response of *PIN1* and *PIN3* to exogenous IAA treatment, the *JLO* response is temporally delayed (Bureau et al., 2010). Therefore, the induction of *JLO* expression by auxin is not sufficient to explain the rapid changes in *PIN* gene expression. To

test if auxin influences JLO activity on protein level, immunodetection of the JLO protein in auxin treated roots (5DAG; 20µM IAA for 12h) were carried out. This analysis revealed no apparent difference concerning signal intensities (Fig. 4.1F/F'). Because this experiment would not allow to distinguish intact JLO proteins from degradation products, western blot analysis was performed to monitor protein stability upon auxin treatment. To obtain a sufficient protein amount, *JLO* was misexpressed using the ß-estradiol inducible *iJLO-FLAG* line (Bureau et al., 2010). Induced seedlings (12 hours after induction (HAI)) were incubated in 20µM IAA for 0-120 min and extracted proteins were analyzed using the anti-JLO antibody. The results showed no altered protein abundance or protein degradation upon auxin treatment, suggesting that JLO is not regulated by auxin at the protein level (Fig. 4.1H).

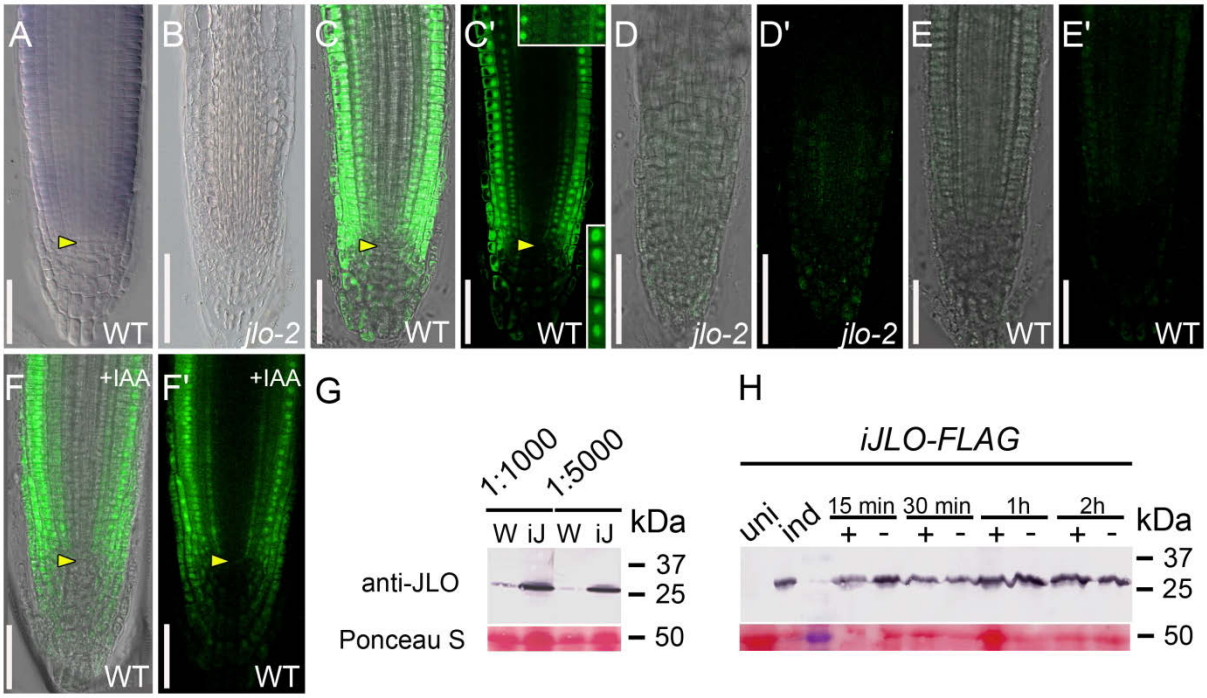

Fig. 4.1: *JLO* expression pattern in postembryonic roots. (A-B) *JLO* expression pattern in wild-type (WT; A) and *jlo-2* mutant roots (D) analyzed by whole mount RNA *in situ* hybridization (5DAG). (A) *JLO* transcripts can be detected in all root tissues proximal to the QC (arrowhead). (B) No signal is observable in homozygous *jlo-2* mutants confirming the probe specificity. (C/C') Immunodetection of JLO in roots (5DAG) using a primary anti-JLO antibody and a secondary anti-rabbit-Alexa488 antibody. JLO localizes to the nucleus and cytoplasm (lower inset in C'). Signals are predominantly detectable in the outer root tissues (epidermis, endodermis and cortex). Upper inset shows Alexa488 signals in the root vasculature obtained by increased laser excitation. (D/D') Immunodetection of JLO using homozygous *jlo-2* mutants. (F/F') Immunodetection experiment without the primary anti-JLO antibody. (E/E') Immunodetection of JLO in wild-type roots treated with 20µM IAA (12h). (G) Western blot analysis of wild-type (W) and *iJLO-FLAG* (iJ) plant protein extracts using the anti-JLO antibody (expected size: W = 25kDa; iJ = 27 kDa.) (H) Western blot analysis with the anti-JLO antibody. Proteins were extracted from induced *iJLO-FLAG* plants treated with 20µM IAA (+) for the indicated time. Mock treated controls (-) are shown for each time point. The Ponceau S stained proteins bands of Rubisco are shown as loading control. kDa: Kilo Dalton; uni: uninduced; ind: ß-estradiol induced *iJLO-FLAG* plants; DAG: days after germination; Scale bars: 50µm; yellow arrowheads indicate the position of the QC in wild-type roots.

4.1.7. Genetic interaction between *JLO* and members of the *PLT* family

From previous results, genes belonging to the *PLT* family (*PLT1, PLT2* and *BBM*) are strongly downregulated in *jlo-2* mutant background (Bureau et al., 2010). Therefore, the expression of a fourth member of the *PLT* family, *PLT3*, was monitored using a *PLT3::CFP* reporter. In wild-type, *PLT3* is highly expressed in the stem cell niche and the columella cells at the basal root tip. Graded expression is also detectable in epidermal and vascular tissues (Fig. 4.3A/A'). In *jlo-2* roots, *PLT3* was expressed in an unaltered pattern but at lower levels (Fig. 4.3E/E'). Furthermore, qRT-PCR analysis showed a downregulation of all four *PLT* genes in *jlo-2* mutant background and revealed already a reduction in *jlo-2/+* heterozygotes plants (5DAG, Fig. 4.2M). Thus, JLO is an essential factor required for *PLT* gene expression.

The *PLT* genes contribute redundantly and dosage dependent to root growth and root meristem (RM) maintenance. Therefore, single mutants display only mild defects while roots of double or triple mutants show strong patterning defects (Aida et al., 2004; Galinha et al., 2007). The RM disorganization of various *plt/bbm* allelic combinations partially resembles that observed in *jlo-2* mutants. To further disclose the genetic relationship between *JLO* and the *PLT* genes, cross-breedings of *jlo-2/+* with the *plt1-4* and *plt2-2* loss-of function alleles was performed. The F3 progeny of a *jlo-2/+ plt1-4*, a *jlo-2/+ plt2-2* and a *jlo-2/+ plt1-4 plt2-2* plant was examined at seedling stage (5DAG). Segregation analyses showed that loss of *PLT1; PLT2* or *PLT1/2* function did not enhance the frequency of embryonic lethality observed in the *jlo-2* allele (Fig. 4.2O). For further studies, root lengths were measured and the root morphology was examined. These analyses revealed a root length reduction of *jlo-2/+ plt1-4* and *jlo-2/+ plt2-2* plants with respect to either single mutant (Fig. 4.2N). Moreover, both *jlo-2/+ plt* combinations showed an enhanced disorganization of the RM (Fig. 4.2G/H). These defects resembled those of the *plt1-4 plt2-2* mutant roots (Fig. 4.2I/N). Because *JLO* promotes the expression of all four *PLT* genes, this effect could depend on a reduction of the redundant PLT proteins in *jlo-2/+* mutants. The *jlo-2/+ plt1-1 plt2-2* root phenotype was only mildly increased compared to *plt1-4 plt2-2* mutants (Fig. 4.2I/O/N).

98.8% of the homozygous *jlo-2 plt1-4* and *jlo-2 plt2-2* mutants were indistinguishable from *jlo-2* mutants, but 1.2% of the seedlings lacked a primary root (Fig. 4.2J/K/N/O). 58.6% of the homozygous *jlo-2 plt1-4 plt2-2* mutants resembled the *jlo-2* phenotype, while 35.2% lacked the root and 6.2% lacked the root and the hypocotyl (Fig. 4.2L/N/O). Such a phenotype was not found in *jlo-2* single mutants but it was reported that *plt* triple mutants that miss *BBM* function lack both, the root and the hypocotyl (Galinha et al., 2007). The milder *jlo-2* phenotype could be therefore explained by a dosage effect because of residual *PLT* expression in *jlo-2* mutants (Fig. 4.2M). Alternatively, *JLO* and the *PLT/BBM* genes may act in both a common and a parallel pathway.

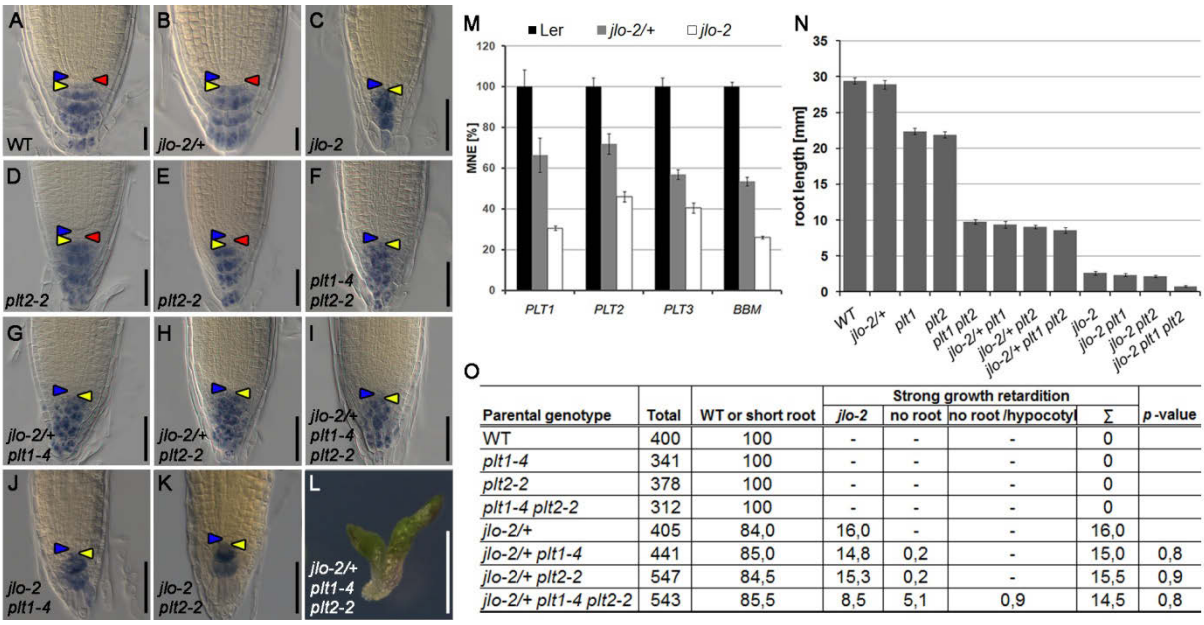

O

Parental genotype	Total	WT or short root	Strong growth retardation				p-value
			jlo-2	no root	no root /hypocotyl	Σ	
WT	400	100	-	-	-	0	
plt1-4	341	100	-	-	-	0	
plt2-2	378	100	-	-	-	0	
plt1-4 plt2-2	312	100	-	-	-	0	
jlo-2/+	405	84,0	16,0	-	-	16,0	
jlo-2/+ plt1-4	441	85,0	14,8	0,2	-	15,0	0,8
jlo-2/+ plt2-2	547	84,5	15,3	0,2	-	15,5	0,9
jlo-2/+ plt1-4 plt2-2	543	85,5	8,5	5,1	0,9	14,5	0,8

Fig. 4.2: Genetic interaction between *JLO* and the *PLT* genes. (A-L) Root phenotypes of seedlings (5DAG) with the indicated genotype. Lugol staining was used to visualize starch granules in differentiated columella cells. Red arrow: QC, Blue arrow: columella stem cells (CSC) lacking stainable starch granules; Yellow arrow: first differentiated columella cells. *jlo-2/+* roots (B) appear aphenotypic compared to wild-type (WT; A). Roots of *jlo-2* (C) mutants are unorganized and starch granules are juxtaposed to the QC. Roots of *plt1-4* (D) and *plt2-2* (E) mutants show only mild defects. (F) *plt1-4 plt2-2* mutants show a defective root patterning. (G-H) *jlo-2/+ plt1-4* and *jlo-2/+ plt2-2* reveal increased disorganization of the root. (I) The *jlo-2/+ plt1-4 plt2-2* roots are comparable to *plt1-4 plt2-2* (F) roots. (J-K) 98.8% of the *jlo-2 plt1-4* and *jlo-2 plt2-2* roots resembled the *jlo-2* mutants. (L) *jlo-2 plt1-4 plt2-2* lacking a root and parts of the hypocotyl. (M) qRT-PCR analysis of *PLT/BBM* transcript levels showed a reduced expression in *jlo-2/+* and a further reduction in *jlo-2* seedlings (N ≥ 3; 5DAG). (N) Root length measurements of the indicated seedling genotypes (N ≥ 25, for each measurement). (O) Segregation analyses of the F3 progeny of plants with the indicated genotype. Given are the total numbers of counted seedlings (2. column) and the obtained frequencies (%) of phenotypes (3.-6. column). The frequencies of wild-type seedlings (WT) and seedlings that with a wild-type like shoot organization but a root length reduction are given in the 3. column. Seedlings with a phenotype that resembles *jlo-2* mutants or which lacked the root or the root and hypocotyl are categorized as strong growth retardations. Chi-Test was used for statistic analyses (last column). Scale bars: 50µm; MNE: Mean Normalized Expression; DAG: days after germination; Bars in (M/N) indicate standard error.

4.1.8. Several auxin regulated genes are misexpressed in *jlo-2* mutants

To learn more about the *JLO* function, the expression of genes involved in RM development and maintenance was monitored. The permease AUX1 act as auxin import carrier (Marchant et al., 2002) and similar to *jlo-2* mutants, *aux1* loss-of-function results in a strongly diminished root gravitropism response (Bennett et al., 1996). *AUX1* is expressed in the root stele, in columella cells and lateral root cap cells (Fig. 4.3B/B'). The *jlo-2* mutant roots expressed a *AUX1::AUX1-YFP* reporter gene in an unaltered pattern but at a lower level (Fig. 4.3F/F') suggesting that JLO function is required to promote AUX1 mediated auxin import.

The homeodomain transcription factor WOX5 is specifically expressed in the QC and acts to inhibit differentiation of adjacent columella stem cells (Fig. 4.3C/C'; Sarkar et al., 2007). Restriction of *WOX5* to the QC requires auxin signal transduction (Ding et al., 2010). In *jlo-2* roots, the expression domain of *WOX5* was expanded, indicating that JLO is required to spatially confine *WOX5* expression (Fig. 4.3G/G').

The stem cell niche in the root is specified and maintained by two parallel pathways (Aida et al., 2004). One comprises the *PLT* family members (Blilou et al., 2005), the other requires the activity of the *SCARECROW* (*SCR*) and *SHORTROOT* (*SHR*) (Sabatini et al., 2003). *SCR* expression in the endodermis, the endodermis/cortex initial and the QC is activated by the SHR protein which moves from the root stele moves into the adjacent tissues. SCR in turn blocks SHR movement by sequestering it into the nucleus via protein-protein interaction (Helariutta et al., 2000; Cui et al., 2007). Disruption of this regulatory pathway results in aberrant radial patterning and loss of QC identity (Di Laurenzio et al., 1996). To explore whether loss of *JLO* function interferes with the SHR/SCR pathway, I analyzed the expression of a *SCR::SCR-YFP* reporter gene. Similar to wild-type, SCR-YFP signals were detected in a single cell layer of *jlo-2* mutant roots (Fig. 4.3D/D' and H/H'). This cell layer, which likely has endodermis identity, was located directly adjacent to the vascular tissues. The *jlo-2* mutants also showed *SCR::SCR-YFP* reporter gene activity in cells of the presumptive QC, suggesting that JLO is not involved in the regulation of *SCR* expression. As *SCR* expression requires SHR activity, it is unlikely *SHR* expression is altered in *jlo*-2 mutants.

Together, these results show that impaired JLO activity causes a reduced *PIN*, *AUX1* and *PLT* expression and a failure to restrict *WOX5* to the QC. In contrast, loss of *JLO* function may not affect the SCR/SHR pathway.

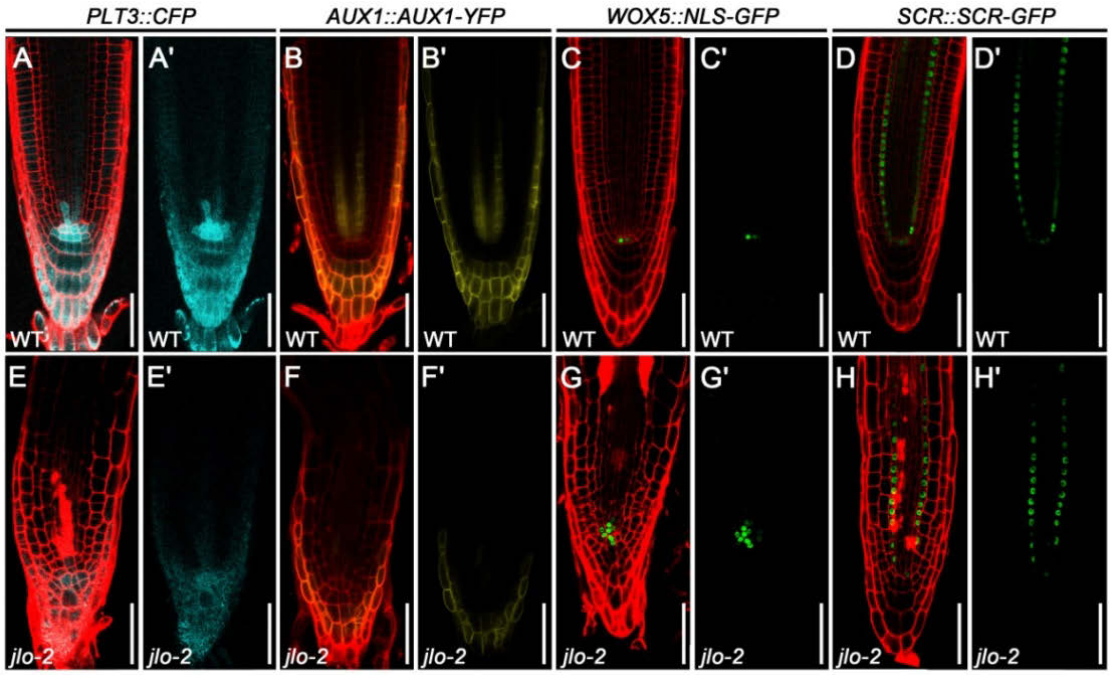

Fig. 4.3: Expression of genes required for RM development and maintenance in *jlo-2* mutant roots. (A-H) Expression pattern of *PLT3::CFP* (A/A' and E/E'), *AUX1::AUX1-YFP* (B/B' and F/F'), *WOX5::NLS-GFP* (C/C' and G/G') and *SCR::SCR-GFP* (D/D' and H/H') in wild-type (WT; A-D) and *jlo-2* (E-H) mutant roots. Compared to wild-type (A/A') the *PLT3::CFP* expression in *jlo-2* mutants is reduced (E/E'). Overall expression of *AUX1* is reduced in *jlo-2* mutants (B/B'compared to F/F'). *WOX5::NLS-GFP* expression domain is expanded in the *jlo-2* root meristem (C/C' compared to G/G'). *SCR::SCR-GFP* expression is unaltered in *jlo-2* mutants compared to wild-type (D/D' compared to H/H'). Scale bar: 50µm. Roots were counterstained with PI.

4.1.9. JLO function is partially mediated by the BDL/MP pathway

The previous work indicates that JLO acts in part through the BDL/MP pathway to regulate *PLT* and *PIN* gene expression (Bureau et al., 2010). This observation raised three possibilities: (1) JLO could promote *MP* expression. This explanation can be excluded because the expression of a *MP::MP-GFP* reporter in *jlo-2* mutants root was unaltered compared to wild-type (Bureau et al., 2010). (2) JLO may negatively regulate *BDL* expression. (3) Because *bdl* gain-of-function mutation causes a stabilization of the BDL protein (Hamann et al., 2002), JLO could be required for auxin dependent BDL degradation. I assayed *BDL* expression in *jlo-2* mutants to distinguish between these two remaining alternatives.

4.1.9.1. JLO is required of auxin dependent BDL degradation

To examine whether *JLO* regulates *BDL* expression, I introduced a *BDL::BDL-GUS* reporter into the *jlo-2* mutant background. The BDL-GUS protein was detected in the stele of *jlo-2* seedling roots (5DAG, Fig. 4.4H). This expression pattern was similarly observed in the corresponding wild-type control and closely resembles previously published data (Fig. 4.4A; Dharmasiri et al., 2005b). This result suggests that JLO does not act as a transcriptional repressor of *BDL*. Analysis of *BDL* transcript levels by qRT-PCR also supports this conclusion. *BDL* transcript levels were neither significantly increased in *jlo-2* mutant background nor altered upon induction of JLO-FLAG misexpression (data not shown).

The auxin content in wild-type and *jlo-2* roots was modified to examine whether *JLO* loss-of-function interferes with the auxin dependent BDL degradation. To this end, seedlings where incubated in liquid GM media supplemented with 20µm IAA. As published in Dharmasiri et al., 2005b, BDL-GUS was destabilized in wild-type roots by a 1h treatment with IAA (Fig. 4.4B; 100%; N = 69), whereas the Mock treated controls showed a clear blue staining in the root stele (Fig. 4.4A; 100%; N = 67). Additional application of the proteasome inhibitor MG132 confirmed that this auxin-dependent BDL degradation requires the proteasome. Wild-type roots that were pretreated for 1h with medium containing 50µM MG132, followed by incubation in 20µM IAA displayed GUS signals comparable to the untreated controls (Fig. 4.4C; 100%; N = 32).

Together my analyses showed that *jlo-2* mutants are deficient in degradation of BDL-GUS. In 78% of the analyzed *jlo-2* roots (N = 139), GUS signals were still present after 1h incubation in 20µm IAA (Fig. 4.4I). This stabilization support the hypothesis that JLO functions upstream of BDL in auxin response. However, compared to untreated *jlo-2* mutants (96%; N = 123), fewer roots revealed GUS staining after auxin treatment. Furthermore, pretreatment with MG132 slightly increased the number of GUS stained *jlo-2* roots after IAA application (82%; N = 48; Fig. 4.4J). This indicates that some residual JLO activity in *jlo-2* mutants allow minor response to exogenous auxin treatment.

We previously showed that at least 4 *PIN* genes are less expressed in *jlo-2* mutants (Bureau et al., 2010). Thus, the deficiency in BDL-GUS degradation could be due to a failure to transport the exogenous applied IAA. I repeated the GUS assay using the transport-independent auxin analogue 2,4-D (10µM). After 1h incubation, GUS signals were still strongly detectable in the wild-type control (Fig. 4.4D; N = 36). For this reason, I prolonged the incubation times to 2h, 4h and 6h (Fig. 9E-G; N ≥ 25 for each experiment). As shown in Fig. 4.4G, even after 6h 2,4-D treatment, a faint GUS staining remained detectable in wild-type roots. Nevertheless, GUS signal intensity was drastically reduced relative to the time of 2,4-D treatment. This clear reduction was not visible in homozygous *jlo-2* mutants (Fig. 4.4K-N; N ≥ 25 for each experiment). Together, these results demonstrate that JLO is required for auxin dependent degradation of BDL.

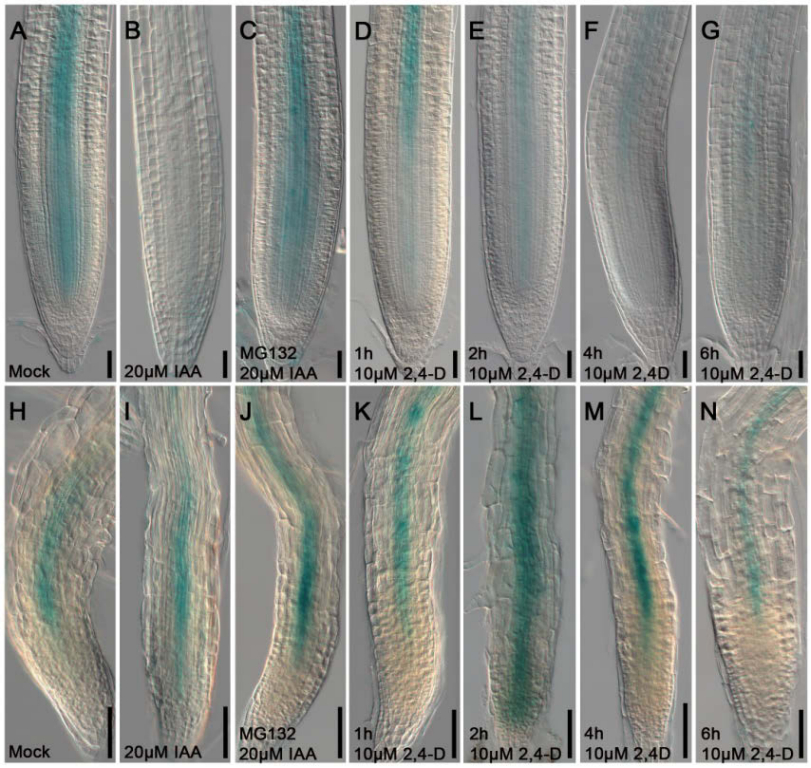

Fig. 4.4: BDL-GUS activity in wild-type and *jlo-2* seedling roots (5DAG). Seedlings in (A) and (H) were Mock treated, whereas seedlings in (B) and (I) were incubated in 20µM IAA for 1h. No GUS signals are detectable in wild-type (WT) roots, while BDL-GUS remains stable in homozygous *jlo-2* mutants. To confirm proteasome dependent BDL degradation, seedlings in (C) and (J) were pretreated with 50µM MG132 for 1h, followed by 1h incubation in 20µM IAA. (D-G and K-N) Expression of BDL-GUS in wild-type (D-G) and *jlo-2* (K-N) roots that were treated with 10µM 2,4-D for 1h (D/K), 2h (E/L), 4h (F/M) and 6h (G/N). In contrast to wild-type, *jlo-2* mutants reveal no clear reduction of GUS signals. Scale bar: 50µm

4.1.10. Genetic interaction between *JLO* and *NPH4 (ARF7)*

The phenotypically stronger *jlo-1* mutants do not develop beyond globular stage of embryogenesis while *bdl* and *mp* mutants still develop into seedlings. Thus, *JLO* performs also *BDL* and *MP* independent functions. I therefore analyzed the genetic interaction between *JLO* and *NPH4* (*ARF7*), a close homolog of *MP*. *nph4-1* loss-of-function mutants do not display an obvious mutant phenotype during embryogenesis or at early seedling stage (Fig. 4.5F-J). However, the *nph4-1* mutation enhanced the phenotypic severity of *mp* mutants, suggesting that both *MP* and *NPH4* are capable of controlling embryo patterning (Hardtke et al., 2004).

Analyses of the F3 progeny of a *jlo-2/+ nph4-1* plant showed no new phenotypic classes or enhanced morphological defects with respect to the embryonic and seedling phenotypes of

jlo-2 mutants. Similarly, the frequency of embryo phenotypes did not significantly differ between *jlo-2 nph4-1* and *jlo-2* mutants (Fig. 4.5; Tab. 14). It might therefore be possible that both genes function in a common pathway.

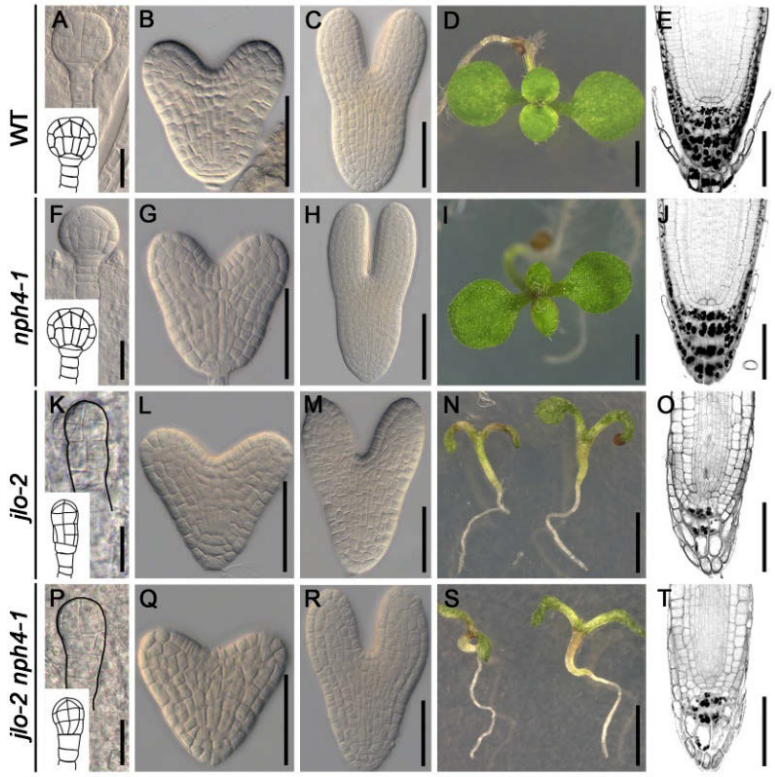

Fig. 4.5: Genetic interaction of *JLO* and *NPH4*. Embryo development of wild-type (WT; A-C); *nph4-1* (F-H); *jlo-2* (K-M) and *jlo-2 nph4-1* mutants (P-R). Embryonic stages: globular stage (A/F/K/P); heart stage (B/G/L/Q); torpedo stage (C/H/M/R). *nph4-1* embryos are aphenotypic. *jlo-2* and *jlo-2 nph4-1* embryos reveal altered cell division planes at globular stage (K/P, insets show the respective embryo schematically). These embryos did not develop beyond heart stage. From heart stage onwards, *jlo-2* and *jlo-2 nph4-1* embryos displayed reduced hypocotyl diameter and length and an overall developmental delay. Seedling phenotypes of WT (D/E), *nph4-1* (I/J), *jlo-2* (N/O) and *jlo-2 nph4-1* mutants (S/T) at 5DAG. *nph4-1* mutants are aphenotypic (I/J). *jlo-2* and *jlo-2 nph4-1* mutants show strong growth retardations and a defective RM organization (N-T). Roots were stained via mPSPI; black dots indicate starch granules. Scale bars: (A-R/E-T): 50µm; (D-S): 1mm

A)	**embryonic phenotypes**			
Parental genotype	**2-8 cell**	**globular**	**heart**	**torpedo**
WT	0% (142)	0% (316)	0% (987)	0% (137)
nph4-1	0% (224)	0% (456)	0% (498)	0% (481)
jlo-2/+	3% (333)	4% (1285)	12% (729)	23% (279)
jlo-2/+ nph4-1	2% (409)	4% (657)	11% (888)	23% (378)
p-value		0,9		

B)	**counted seedling phenotypes**				**expected seedling phenotypes**		
Parental genotype	**Total**	**WT**	***jlo-2***	***p*-value**	**Total**	**WT**	***jlo-2***
WT	377	100% (377)	-		377	100% (377)	-
nph4-1	365	100% (365)	-		365	100% (365)	-
jlo-2/+	1399	86% (1205)	14% (194)		1607	75% (1205)	25% (402)
jlo-2/+ nph4-1	445	87% (387)	13% (58)	0,8	516	75% (387)	25% (129)

Tab. 14: Segregation analysis of *nph4-1, jlo-2* and *jlo-2 nph4-1* mutants. (A) Frequencies of embryonic defects among the progeny of the indicated genetic background. Plants were analyzed in the F3 generation after genetic crossing or selfing. Given are the frequencies (%) of mutant embryos and the total numbers of analyzed embryos (brackets) at different developmental stages. The homozygous *nph4-1* mutation did not significantly enhance the frequencies of *jlo-2* embryonic phenotypes as proven with the Chi-squared test. (B) Segregation of seedling phenotypes (5DAG) in F3 progeny of plants with the indicated genetic background. Given are the frequencies (%) and total numbers (brackets) of wild-type (WT) and mutant seedlings as counted, and the expected numbers based on a 3:1 segregation. The observed segregation of seedling phenotypes does not significantly differ between *jlo-2* and *jlo-2 nph4-1* mutants as analyzed by Chi-squared test. DAG: days after germination

4.1.11. JLO is required for the expression of *TIR1/AFB1* family members

Members of *TIR1/AFB* family act as auxin receptors that directly link auxin perception to the degradation of Aux/IAA proteins via the $SCF^{TIR1/AFB}$ complex (Dharmasiri et al., 2005a; Kepinski et al., 2005). Because the BDL protein is not degraded in *jlo-2* mutants, I analyzed the expression levels of four *TIR1/AFB* genes (*TIR1*, *AFB1*, *AFB2* and *AFB3*) in *jlo-2* mutant background (5DAG). qRT-PCR assays showed reduced *TIR1* and *AFB1* RNA levels in *jlo-2/+* seedlings and further reduction in *jlo-2* homozygotes (Fig. 4.6I). In contrast, expression levels of *AFB2* and *AFB3* were unaltered in *jlo-2* mutant background. Thus, *JLO* could mediate auxin dependent BDL protein turnover by promoting expression of the auxin receptors *TIR1* and *AFB1*. To confirm these results, the *TIR1* and *AFB1* expression in wild-type and *jlo-2* mutant roots was analyzed using GUS reporters (Fig. 4.6A-H; Parry et al., 2009). In wild-type, *TIR1* and *AFB1* are broadly expressed throughout the basal root tip (Fig. 4.6A/C and E/G). The *TIR1* expression pattern was unaltered in homozygous *jlo-2* mutant roots (Fig. 4.6B/D), but both the transcriptional and protein levels were strongly reduced. GUS staining of the *AFB1* reporter lines showed no significant downregulation compared to the wild-type control (Fig. 4.6E-H), indicating that the reduction in *AFB1* expression is too weak to be detected with a GUS assay.

To explore whether *JLO* is sufficient to upregulate *TIR1* and *AFB1* expression, their RNA levels were examined upon induction of JLO-FLAG misexpression. For this purpose, *iJLO-FLAG* plants (5DAG) were induced and roots for RNA extraction were collected at 0, 1, 2 and 4 HAI. qRT-PCR analyses showed a 2.6-fold increase in *TIR1* expression within 2 HAI. In contrast, *AFB1* responded only slightly to JLO-FLAG misexpression and the RNA levels of *AFB2* and *AFB3* remained unchanged (Fig. 4.6J). These results suggest that of the *TIR1/AFB* genes, JLO primarily promotes *TIR1* expression.

4.1.12. Genetic interaction between *JLO* and *TIR1*

To gain more insight into the genetic interaction of *JLO* and *TIR1*, *jlo-2/+* plants were crossed with the *tir1-1* loss-of-function mutant. The *tir1-1* allele carries an amino acid substitution that causes mild morphological defects in lateral root formation (Ruegger et al., 1998). The F3 progeny of a *jlo-2/+ tir1-1* plant was examined at seedling stage (5DAG). A segregation analysis revealed no significant enhancement of the *jlo-2* mutation concerning the phenotypic frequencies (Fig. 4.6O). Furthermore, *jlo-2 tir1-1* double mutants were phenotypically indistinguishable from the *jlo-2* single mutants (Fig. 4.6N) supporting the hypothesis that *JLO* and *TIR1* function in the same pathway. Studies with the auxin analogue 2,4-D confirmed this assumption (Fig. 4.6K). Consistent with previously published results, the *tir1-1* root elongation was significantly less affected than that of wild-type seedlings (5DAG) when grown on media containing 0.2µM 2,4-D (Ruegger et al., 1998). Similarly, *jlo-2/+* roots were less sensitive to the growth inhibitory effects of 2,4-D. Elimination of *TIR1* function from *jlo-2/+* mutants

further decreased the auxin response. However, the observed auxin response, measured as root length reduction, was similar in both *jlo-2* and *jlo-2 tir1-1* mutants. This indicates that loss of *TIR1* function does not affect auxin response when the seedling is already lacking *JLO* function. These results are consistent with the assumption that JLO is an upstream regulator of *TIR1* expression.

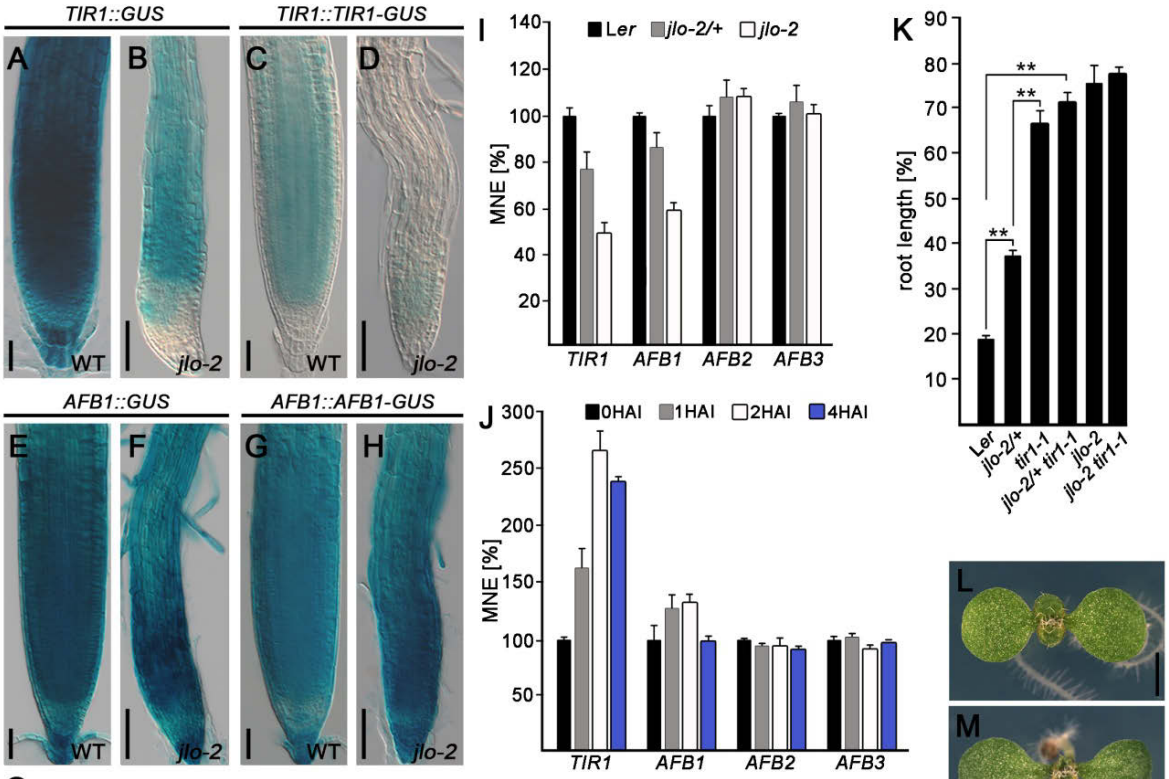

O

	counted seedling phenotypes				expected seedling phenotypes		
Parental genotype	Total	WT	*jlo-2*	*p* -value	Total	WT	*jlo-2*
WT	321	100% (321)	-		321	100% (321)	-
tir1-1	156	100% (156)	-		156	100% (156)	-
jlo-2/+	240	86% (206)	14% (34)		275	75% (206)	25% (69)
jlo-2/+ tir1-1	207	87% (180)	13% (27)	0,8	240	75% (180)	25% (60)

Fig. 4.6: *JLO* promote expression of *TIR1/AFB1* family member. (A-H) Expression of *TIR1::GUS* (A/B), *TIR1::TIR1-GUS* (C/D), *AFB1::GUS* (E/F) and *AFB1::ABF1-GUS* (G/H) in wild-type (WT; A/C/E/G) and *jlo-2* mutant roots (B/D/F/H). Expression of *TIR1* is severely reduced in *jlo-2* mutants. No visible change in *AFB1* reporter activity was observed in *jlo-2* mutants compared to wild-type. (I) qRT-PCR revealed a downregulation of *TIR1* and *AFB1* but not of *AFB2* and *AFB3* transcript levels in *jlo-2* mutants (5DAG; N ≥ 3). Note that expression of both genes is already reduced in *jlo-2/+* seedlings. (J) qRT-PCR analysis of *TIR1, AFB1, AFB2* and *AFB3* RNA levels upon induction of JLO-FLAG misexpression. Expression levels were normalized to uninduced controls prepared at the same time points. *TIR1* is 2.6 fold upregulated within 2HAI while *AFB1* reveal only a minor response to JLO-FLAG induction. *AFB2* and *AFB3* expression level remained unaltered (N ≥ 3). (K) Root elongation in response to 2,4-D. Each bar represents the relative root length of auxin treated seedlings (%) compared to untreated seedling of the same genotype (N ≥ 55 for each measurement). Significance** (p<0.001) was proven using the T-test. Wild-type (L), *tir1-1* (M), *jlo-2* (N, two seedlings left) and *jlo-2 tir1-1* (N, two seedlings right) seedlings (5DAG). (O) Segregation of seedling phenotypes in F3 progeny of plants with the indicated genetic background. Given are the frequencies (%) and total numbers (brackets) of wild-type (WT) and mutant seedlings as counted, and the expected numbers based on a 3:1 segregation. The observed segregation of seedling phenotypes does not significantly differ between *jlo-2* and *jlo-2 tir1-1* mutants as analyzed by Chi-squared test. Scale bars: (A-H): 50µm; (L-N): 1mm; MNE: Mean Normalized Expression; DAG: days after germination; Bars in H-J indicate the standard errors.

4.1.13. *TIR1* expression is already reduced during *jlo-2* embryogenesis

Because *jlo-2* mutants show auxin related patterning defects from early embryo stages onwards, I monitored *TIR1* and *AFB1* expression during embryonic development. At globular stage of wild-type embryogenesis, *TIR1::GUS* was expressed throughout the proembryo but not in the suspensor (Fig. 4.7A). Heart stage embryos also displayed GUS signals in the complete proembryo with an intensity maximum in the basal region (Fig. 4.7B). From torpedo stage onwards, a GUS staining maximum was visible at the basal root tip (Fig. 4.7C/D, arrowhead) and in the embryonic SAM. The GUS pattern in the *AFB1::GUS* line was more restricted to the basal part of the embryo. At globular stage, GUS staining appeared predominantly in the basal part of the pro-embryo (Fig. 4.7G). I could not detect a staining in the cotyledons from early heart stage onwards (Fig. 4.7H). Toward the end of embryogenesis, *AFB1* expression is restricted to the basal root tip and only a faint staining is detectable in the embryonic hypocotyl (Fig. 4.7J, arrowhead).

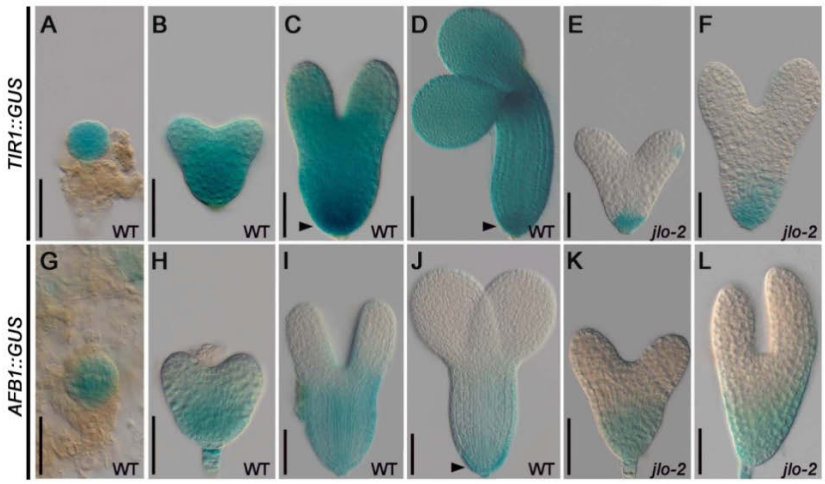

Fig. 4.7: Embryonic expression pattern of *TIR1* and *AFB1*. (A-F) *TIR1::GUS* in wild-type (WT; A-D) and *jlo-2* (E-F) embryos. (G-L) *AFB1::GUS* in WT (G-J) and *jlo-2* (K-L) embryos. (A-D) *TIR1::GUS* is expressed throughout the WT proembryo. From heart stage onwards, a maximum of expression can be detected in the basal root tip (B-D, arrowheads). (E-F) *TIR1::GUS* expression is strongly reduced in *jlo-2* mutants with only a residual staining in the root tip. (G-J) *AFB1::GUS* expression is predominantly localized to the basal embryo with a maximum in the root tip at bend cotelydon stage (J, arrowhead). Expression in *jlo-2* embryos is comparable to that of WT embryos at the respective stages (K-L). Stages of embryogenesis: (A/G): globular stage; (B/H and E/K): heart stage; (C/I and F/L): early torpedo stage; (D/J): bend cotelydon stage. WT: wild-type; Scale bars: 50µm

Compared to wild-type, *TIR1::GUS* activity was strongly reduced in *jlo-2* heart stage and torpedo stage embryos (Fig. 4.7E/F). GUS expression was excluded from the cotyledons and the embryonic hypocotyl and only a faint signal appeared in the mutant root tip. Notably this residual GUS staining overlaps with the observed *TIR1* expression maximum at the basal root tip of wild-type embryos. In contrast, expression of *AFB1::GUS* in *jlo-2* mutant embryos was almost comparable to that in wild-type embryos (Fig. 4.7K/L). Taken together, these results suggest that JLO is required to promote embryonic and postembryonic *TIR1* transcription while loss of *JLO* function does not or only mildly affect *AFB1* expression.

4.2. Discussion

The dynamic and differential distribution of the phytohormone auxin controls many aspects of plant growth and development. Auxin signals were shown to regulate the formation of the embryonic apical-basal axis (reviewed by Moller et al., 2009), the outgrowth of lateral organs (Vernoux et al., 2000; Reinhardt et al., 2003; Heisler et al., 2005), the vascular differentiation (Mattsson et al., 1999) and the patterning of the root meristem (reviewed in Benfey et al., 2000). These patterning processes are collectively disturbed in mutants of the *LBD* family member *JLO* (*jlo-2*), suggesting that *JLO* plays an important role in auxin mediated development and is continuously required throughout *Arabidopsis* development (Bureau et al., 2010).

4.2.1. JLO regulates auxin dependent gene expression

To gain more insight into the role of *JLO*, the expression of auxin regulated genes was monitored in *jlo-2* mutants. These analyses showed that at least four members of the *PIN* family of auxin efflux carriers are severely downregulated in *jlo-2* mutant background (Bureau et al., 2010). Moreover, I found a reduced expression of the auxin influx carrier AUX1 in *jlo-2* roots (chapter 4.1.8), indicating that JLO exerts its function at least in part by controlling polar auxin transport. Nevertheless, studies with exogenously applied auxin revealed that *jlo-2* mutants do not simply suffer from reduced polar auxin transport. Treatment with the transport independent auxin analogue 2,4-D was insufficient to restore auxin signaling in *jlo-2* mutants, as monitored by *DR5rev::GFP* expression analyses (Bureau et al., 2010). Thus, JLO is required to facilitate both auxin transport and perception or signal transduction.

Consistent with this, the auxin regulated members of the *PLT* family were found to be less expressed in *jlo-2* mutant roots (Bureau et al., 2010; chapter 4.1.7). Published studies showed that the activity of *PLT1, PLT2, PLT3* and *BBM* is largely additive and dosage dependent. Loss-of-function mutations in two or more of these genes cause a disorganization of the root meristem (RM) due to a differentiation of stem cells (Aida et al., 2004; Galinha et al., 2007). This mutant phenotype partially resembles that of *jlo-2* mutant roots (Bureau et al., 2010). Furthermore, my analyses of *jlo-2, plt1-4* and *plt2-2* double and triple mutants confirmed that *JLO* can act through the *PLT* pathway. However, I noted that some of the *jlo-2, plt1* and *plt2-2* double and triple mutants exhibited clearly additive defects. This observation raises two possible explanations. As qRT-PCR analyses showed that *PLT* gene expression is strongly downregulated but not absent in *jlo-2* mutant roots, the *jlo-2* phenotype might be enhanced by a complete removal of the *PLT1* and *PLT2* function. Alternatively, *PLT1* and *PLT2* could also act partially independent of *JLO*. Further experiments, e.g. the analyses of *jlo-2 plt3* or *jlo-2 bbm* mutants should help to elucidate the genetic relationship between *JLO* and the *PLT* family.

It was reported that the *PLT* and *SCR/SHR* pathways provide parallel inputs in root stem cell niche specification and maintenance (Aida et al., 2004). Since I could not detect an alter-

ation in *SCR* expression in *jlo-2* mutant roots (chapter 4.1.8), loss of *JLO* function seems to specifically interfere with the auxin dependent regulation of root development. To verify this notion, it will be important to also monitor *SHR* expression in *jlo-2* mutants.

Another gene, *WOX5*, is misexpressed in *jlo-2* mutant embryos (Bureau et al., 2010) and roots (chapter 4.1.8). Restriction of *WOX5* to the QC of the root meristem was shown to depend on the activity of the auxin response factors ARF10 and ARF16 (Ding et al., 2010). This result is therefore again indicative for defects in auxin signaling. Although it was reported that *WOX5* acts from the QC to maintain the distal stem cell population, and overexpression blocks differentiation of stem cell descendants (Sarkar et al., 2007), I found a premature differentiation of columella stem cells in *jlo-2* mutants (Bureau et al., 2010). Thus, ectopic expression of *WOX5* in *jlo-2* mutants is insufficient to inhibit stem cell differentiation, suggesting that *JLO* function is essential for stem cell maintenance. Taken together these data provide evidence that JLO is required to control auxin dependent gene expression programs.

4.2.2. JLO facilitates auxin dependent BDL degradation

Phenotypically the *jlo-2* and *mp* loss-of-function as well as *bdl* gain-of-function mutants are very similar (Hamann et al., 1999; Bureau et al., 2010). The reason for this is as follows. My double mutant analyses showed that that these genes act in a common pathway (Bureau et al., 2010). Furthermore, I found that exogenously applied auxin was insufficient to promote the degradation of BDL in absence of JLO function (chapter 4.1.9.1). This leads to the conclusion that JLO is an upstream regulator in the *BDL/MP* pathway and required to mediate auxin dependent BDL protein turnover. The failure to release the ARF transcription factor MP from BDL repression is likely in part the cause for the misregulation of auxin induced target genes in *jlo-2* mutants. Consistent with this assumption, it was reported that auxin signaling through the BDL/MP dependent pathway positively regulates *PIN* and *PLT* gene expression (Aida et al., 2004; Weijers et al., 2006). Nevertheless, the phenotypically stronger *jlo-1* loss-of-function mutants arrest at the globular stage of embryogenesis while *mp* or *bdl* mutants still develop into seedlings (Hamann et al., 2002; Borghi et al., 2007). Thus, JLO also performs BDL and MP independent functions. A hypothesis that should be tested is that JLO regulates the auxin dependent protein turnover of other Aux/IAA proteins besides BDL.

It was shown that the residual axial patterning in *mp* mutants is due to the activity of its close homologue *NPH4* (*ARF7*). Similar as *jlo-1* mutants, strong *mp nph4-1* double mutants lack a functional root and fail to initiate cotyledons during embryogenesis (Hardtke et al., 2004; Borghi et al., 2007). A complete loss of MP and NPH4 function in *jlo-1* mutants via stabilization of their Aux/IAA repressors could partially explain the strong patterning defects. I found that *nph4-1* mutants do not enhance the *jlo-2* mutant phenotype in the double mutant combination (chapter 4.1.10). However, because *nph4-1* mutants appear aphenotypic during embryogenesis and early seedling stage, it is not possible to conclude that *JLO* and *NPH4*

function in a common pathway. Further experiments are required to examine whether loss of *JLO* function interferes with the activity of both MP and NPH4. Together, these data so far provide evidence that JLO mediates auxin dependent BDL protein turnover. Whether JLO also facilitates degradation of other Aux/IAA proteins remains to be determined.

4.2.3. JLO mediates auxin perception by promoting *TIR1* expression

My studies showed that *JLO* regulates the transcription of the auxin receptor *TIR1* (chapter 4.1.11). The *TIR1* gene encodes the F-Box subunit of the SCF^{TIR1} complex that ubiquitinates Aux/IAA proteins for proteasomal degradation (reviewed in Weijers et al., 2004). A reduced auxin perception, due to the down-regulation of *TIR1,* therefore explains the stabilization of BDL and potentially other Aux/IAA proteins in *jlo-2* mutants. Because redundantly acting SCF complexes ($SCF^{AFB1–AFB3}$) are involved in auxin response, *tir1-1* mutants show only mild morphological defects, in contrast to *jlo-2* mutants (chapter 4.1.12; Ruegger et al., 1998; Dharmasiri et al., 2005b; Parry et al., 2009; Bureau et al., 2010). I found no evidence for JLO regulating the transcription of *AFB2* or *AFB3*, two other auxin receptors. Furthermore, *AFB1* expression was only slightly decreased in *jlo-2* mutant background. Thus, the *jlo-2* phenotype cannot depend on a combined reduction of *TIR1* and *AFB1-3* transcription.

Phylogenetic studies revealed six members of the F-box protein subclass that includes TIR1 (Gagne et al., 2002; Parry et al., 2009). The two additional AFB proteins, AFB4 and AFB5, were recently shown to be capable of binding to Aux/IAA proteins (Greenham et al., 2011). Furthermore, *AFB5* was found to be strongly expressed from the earliest stages of embryogenesis onwards (D. Weijers, pers. communication), so the possibility that JLO regulates *AFB4* and *AFB5* expression should be tested. Alternatively, *JLO* may be involved in regulation of *SKP1, CULLIN* or the *RING-BOX PROTEIN1* (*RBX1*), which are the additional components of the $SCF^{TIR1/AFB}$ complexes (reviewed in Tromas et al., 2010). The *AUXIN RESISTANT 1* (*AXR1*) gene is also a possible candidate target gene. *ARX1* encodes a subunit of the RUB1 activating enzyme that regulates the activity of SCF^{TIRAFB} protein complexes (Leyser et al., 1993; del Pozo et al., 2002; Schwechheimer et al., 2002).

Another possible explanation for the phenotypic differences between *jlo-2* and *tir1-1* is provided by the studies presented in chapter 5. I found that JLO homomeric and JLO/AS2 (and potentially AS1) heteromeric complexes regulate *PIN* gene expression. This could indicate that JLO is not only involved in Aux/IAA protein turnover but also regulates auxin inducible target genes more directly. Alternatively, AS2 and AS1 might regulate the expression of *TIR1/AFB* family members together with JLO. Based on the current results, I cannot exclude either possibility. Nevertheless, *PIN* gene expression responded differentially to JLO homomeric and JLO/AS2 heteromeric complexes, suggesting that both proteins do not exclusively act to promote auxin perception via regulation of *TIR1/AFB* gene expression. JLO might therefore contribute at several positions to the auxin signal transduction pathway (Fig.

4.8). This would explain the apparent differences in *tir1-1* and *jlo-2* mutant phenotypes. The identification of direct target genes should help to further unravel the role of JLO in auxin related development. Transgenic lines have been generated that will allow Chromatin immunoprecipitation (ChIP) analyses.

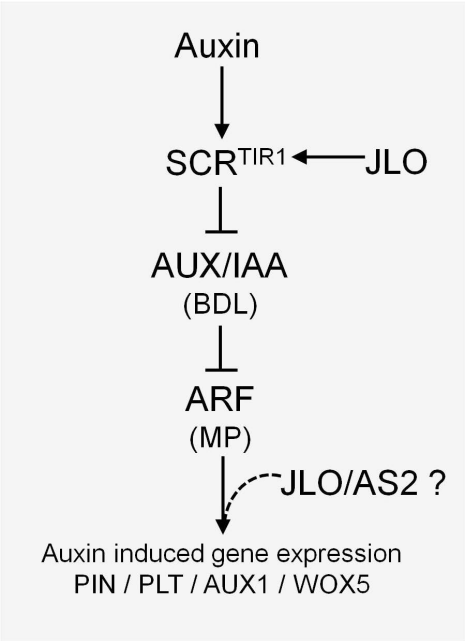

Fig. 4.8: A model for JLO function. Auxin triggers the degradation of Aux/IAA proteins, as for example BDL, by stabilizing the interaction between SCF^{TIR1} complex and Aux/IAA proteins. The SCF^{TIR1} complex ubiquitinates Aux/IAA proteins and marks them for proteasome dependent degradation. Degradation of Aux/IAA allows transcriptional activities of ARFs like MP. Auxin signaling is required to control the expression of genes like *PLT, PIN, AUX1* and *WOX5.* JLO promotes the regulation of auxin-responsive genes through positive regulation of *TIR1* transcription. JLO homomeric and heteromeric complexes may also regulate auxin responsive genes (e.g. *PIN* genes) more directly.

4.2.4. Conclusions

There are several lines of evidence that link JLO to auxin signal transduction, such as the regulation of *TIR1* expression, the stabilization of BDL in *jlo-2* mutants, and a number of auxin regulated genes that are misexpressed in a *jlo* mutant background. Nevertheless, to date the external cues that trigger JLO activity remain unclear. Although *JLO* transcription responds to exogenously applied auxin, this response is temporally delayed compared to that observed for *PIN1* and *PIN3* (Bureau et al., 2010). Moreover, I found that JLO activity is not regulated by auxin on the protein level (chapter 4.1.6). In view of the results presented in this thesis, it might be possible that auxin affects JLO activity by regulating tissue specific co-factors. Therefore, it should be tested whether the activity of AS2, AS1 or LBD31, the proteins identified to interact with JLO (chapter 5), can be modulated by auxin. The identification of additional interaction partners will also help to elicit how JLO acts at the molecular level.

CHAPTER V

JLO AND AS2 ACT TOGETHER TO PROMOTE ORGAN DEVELOPMENT AND AUXIN TRANSPORT

The results presented in this chapter are part of the yet unpublished manuscript:

Rast, M.I. and Simon, R. (2011). JAGGED LATERAL ORGANS (JLO) and ASYMMETRIC LEAVES 2 (AS2) act together to promote organ development and auxin transport in *Arabidopsis.*

5. JLO AND AS2 ACT TOGETHER TO PROMOTE ORGAN DEVELOPMENT AND AUXIN TRANSPORT

JLO was isolated as an important regulator of shoot development by its gain-of-function phenotype. Previous studies showed that *JLO* overexpressing plants develop small and lobed leaves due ectopic activation of the class I *KNOX* genes *SHOOT MERISTEMLESS (STM)* and *BREVIPEDICELLUS* (*BP*) (Borghi et al., 2007). Several lines of evidence suggested that this *KNOX* gene upregulation is not a direct consequence. This assumption was supported by experiments performed by M. Bureau, which indicated that the *JLO* gain-of-function phenotype requires the activity of *ASYMMETRIC LEAVES 2 (AS2*), another member of the *LBD* gene family (pers. communication). Based on this information, A. Betzhold initiated a yeast two hybrid interaction analysis and found evidence for an interaction between JLO and AS2. Therefore, the last part of my study aimed on detailed analysis of this protein interaction and the examination of the role of *JLO* during shoot development. The results of these studies are presented in the enclosed manuscript “JAGGED LATERAL ORGANS (JLO) and ASYMMETRIC LEAVES 2 (AS2) act together to promote organ development and auxin transport in *Arabidopsis”*.

Author’s contribution:

I performed all presented experiments and wrote the manuscript which was overworked by Prof. Dr. R. Simon.

5.1. Manuscript Rast et al., 2011

5.1.1. Abstract

Organ initiation requires the specification of a group of founder cells at the flanks of the SAM and the creation of a functional boundary that separates the incipient primordia from the remainder of the meristem. Organ development is closely linked to a downregulation of class I *KNOTTED1 LIKE HOMEOBOX* (*KNOX*) genes and accumulation of auxin at sites of primordia initiation. Here we show that the *Arabidopsis thaliana JAGGED LATERAL ORGANS* (*JLO*) gene, a member of the *LATERAL ORGAN BOUNDARY DOMAIN* (*LBD*) gene family, is required for coordinated organ development in shoot and floral meristems. Loss of *JLO* function results in an ectopic expression of the *KNOX* genes *SHOOT MERISTEMLESS* (*STM*) and *BREVIPEDICELLUS* (*BP*), suggesting that JLO acts to restrict *KNOX* gene expression. JLO acts in a trimeric protein complex with ASYMMETRIC LEAVES 2, another LBD protein, and ASYMMETRIC LEAVES 1 (AS1) to suppress *BP* expression in lateral organs. In addition to its role in *KNOX* gene regulation, we found a new role for AS2 in regulating *PINFORMED* (*PIN*) gene expression, together with JLO. We propose that different JLO and AS2 protein complexes, together with other LBD proteins, coordinate *KNOX* gene expression and auxin distribution during *Arabidopsis* development.

Key words: *JAGGED LATERAL ORGANS; LBD, AS2, PIN, KNOX*, lateral organ development, root development

5.1.2. Introduction

Organ formation and growth requires a continuous supply of new cells. The shoot apical meristem (SAM) of higher plants can provide these through a pool of pluripotent stem cells in the central zones. When these stem cells divide, daughter cells are displaced towards the periphery where they can be recruited to form organ primordia. There, cells undergo rapid divisions, expansion and ultimately differentiation. Cell fate appears to be determined by the position within the SAM, and morphological boundaries separate the emerging organs from the remaining meristem (reviewed in Rast et al., 2008).

The initiation of a new organ in the peripheral zone is controlled by two critical events: the accumulation of auxin in a group of founder cells and a simultaneous change in gene expression programs. Local auxin maxima are generated by active polar transport mediated through auxin efflux carriers of the PIN (PINFORMED) family (Galweiler et al., 1998; Paponov et al., 2005; Zazimalova et al., 2007). The direction of auxin flux within the L1 layer of the SAM is mainly determined by the subcellular localization of PIN1 (Benkova et al., 2003; Friml et al., 2003; Reinhardt et al., 2003). Live imaging of PIN1-GFP revealed the formation of an expression focus at the flanks of the SAM that raises auxin levels in organ founder cells and depletes auxin from the vicinity. As primordia growth starts, PIN1 polarity reverses to form a new auxin peak at a distant position. Thus, phyllotactic pattering requires dynamic PIN1 polarity changes to generate new auxin peaks (Heisler et al., 2005).

Meristematic and organ founder cells are further distinguished by the expression of specific gene sets. These contrasting patterns depend on a mutual repression between meristem and organ specific genes. For example, *SHOOT MERISTEMLESS* (*STM*), a member of the class I *KNOTTED LIKE HOMEOBOX* (*KNOX*) family, is specifically expressed in meristematic tissues and excluded from organ primordia. *stm* mutants lack a functional SAM due to ectopic expression of the MYB domain protein ASYMMETRIC LEAVES1 (AS1) which is normally confined to organ primordia (Byrne et al., 2000). *AS1* in turn restricts the *KNOX* genes *BREVIPEDICELLUS* (*BP)*, *KNAT2* and *KNAT6* from organ initials (Belles-Boix et al., 2006, Byrne et al., 2000; Ori et al., 2000; Byrne et al., 2002). This repression of *KNOX* genes depends on a molecular interaction of AS1 with ASYMMETRIC LEAVES2 (AS2), belonging to LATERAL ORGAN BOUNDARY DOMAIN (LBD) family of *Arabidopsis* that shares the plant specific LOB domain (Xu et al., 2003, Shuai et al., 2002; Guo et al., 2008).

All LBD proteins analyzed localize to the nucleus (Iwakawa et al., 2002; Naito et al., 2007; Borghi et al., 2007) and the LOB domain was shown to bind to DNA in vitro (Husbands et al., 2007). Heteromers of AS1 and AS2 can directly interact with the promoter regions of *BP* and *KNAT2*. This binding is suggested to recruit the chromatin remodeling factor HIRA, resulting in stable repression of *KNOX* genes in lateral organs (Guo et al., 2008; Phelps-Durr et al., 2005).

The downregulation of *KNOX* genes in organ primordia and auxin controlled gene expression programs are interconnected. Auxin activity appears to act in parallel with the AS1/AS2 module to exclude *BP* expression from lateral organs (Hay et al., 2006). Furthermore, leaf defects of plants that misexpress *KNOX* genes are in part caused by the disruption of local auxin gradients in the leaf margins (Tsiantis et al., 1999; Zgurski et al., 2005). Correct cell fate allocation therefore requires the combined activities of auxin and AS1/AS2 activity in the cells of lateral organs, and an antagonistic activity of *KNOX* genes in meristematic cells.

An important part of this regulation may take place at the boundaries between organ primordia and the meristem (Aida et al., 2006). A number of boundary specific genes were shown to be involved in meristem homeostasis and organ development. Among them are *CUP-SHAPED COTYLEDON1* (*CUC1*), *CUC2* and *CUC3* which are already required during early stages of embryogenesis to activate and later delineate *STM* expression (Aida et al., 1999). Furthermore, boundary specific expression of *LATERAL ORGAN BOUNDARIES* (*LOB*), the founding member of the LBD family, is promoted by BP and by AS2 (Lin et al., 2003b).

The *LBD* family gene *JAGGED LATERAL ORGANS* (*JLO/LBD30*) was shown to be required for auxin mediated development from earliest stages of embryogenesis onwards. *JLO* loss-of-function mutants (*jlo-1* and *jlo-2*) arrest during embryogenesis or early seedling stages due to an aberrant cell division pattern and meristem cell differentiation. These defects are at least in part caused by interfering with the auxin controlled BODENLOS/MONOPTEROS (BDL/MP) pathway, and a resulting failure of auxin signaling. As a consequence, expression of members of the *PIN* and *PLETHORA (PLT)* gene families is severely reduced in *jlo* mutants roots (Bureau et al., 2010). During shoot development, *JLO* is expressed at sites of organ initiation and later in meristem-to-organ boundaries. Ectopic high level expression of *JLO* in organ primordia causes leaf lobing and misexpression of both *STM* and *BP* in developing organs. This indicates that *JLO* could act from the boundary to orchestrate gene expression patterns (Borghi et al., 2007). However, all *jlo* mutants described so far grossly disturbed embryogenesis and arrested at early stages, so that *JLO* functions during postembryonic development were not yet understood.

We have here characterized an allelic series of *jlo* mutants, which allowed us to uncover an important role for *JLO* during organ development in shoot and floral meristems. We find that *JLO* integrates the promotion of *PIN* gene transcription with the regulation of *KNOX* gene expression. We demonstrate that JLO and AS2 interact molecularly, and form multimeric complexes with AS1 to suppress KNOX gene expression. Furthermore, we uncover a previously unsuspected role for AS2, together with JLO, in controlling auxin transport in seedling roots.

5.1.3. Results

5.1.3.1. Isolation and phenotypes of novel *jlo* alleles

The embryonic or early seedling lethality of *jlo-1* and *jlo-2* mutants interfered with any functional analysis during later stages of development (Borghi et al., 2007; Bureau et al., 2010). Thus, most of our conclusions regarding the function of *JLO* in the shoot were drawn from misexpression experiments. We now characterized a series of novel *jlo* alleles which reveal phenotypically milder defects (*jlo-3* to *jlo-7,* Fig. 1A) and allowed to dissect *JLO* functions during later development. Reverse Transcriptase PCR analyses of RNA isolated from seedlings showed that insertions located 5' to the *JLO* transcriptional start (*jlo-3* and *jlo-4*) cause a reduction in RNA levels, which are more severe in the *jlo-4* allele. Homozygous *jlo-5* to *jlo-7* mutants produced transcripts that were truncated 5´ and 3´ to the insertions, indicating that these alleles may encode proteins that lack parts of the conserved LOB domain (Suppl. Fig. 1A).

jlo-4 homozygotes showed phenotypic alterations from early stages of seedling development onwards. Similar to the previously described *jlo-2* allele (Bureau et al., 2010), *jlo-4* seedlings were smaller than wild-type seedlings with a disorganized root and narrow cotyledons. However, although growth and leaf development was strongly impaired, homozygous *jlo-4* mutants were eventually able to bolt (Fig. 1D-D''). *jlo-7* seedlings generated fused and curled leaves as well as aberrant vein patterning (Fig. 1G/G'). The other *jlo* mutants studied here displayed normal vegetative development.

After the transition to flowering, all novel *jlo* alleles displayed related defects that were categorized into three classes. Class I includes floral meristem identity defects, e.g. an indeterminacy of the meristem (Fig. 1D'', inset). This phenotype appeared with a low frequency (4.4%; N = 18/405) and mainly within the first four flowers of *jlo-3* and *jlo-4* mutants (Suppl. Fig. 1C). Notably, homozygous mutants of both alleles initiated fewer side shoots than the wild-type indicating a premature but incomplete switch from side shoot to flower production. Some of the flower were subtended by cauline leaves, supporting this assumption (Fig. 1C'').

Class II comprises homeotic transformations of petals and stamen which appeared mostly on the first flowers of *jlo* mutants (3.9%; N = 16/405; Fig. 1C'' inset; Suppl. Fig. 1C). However, the majority of mutant flowers exhibited a reduced number and size of sepals, petals and stamens, or displayed organ fusions (55.8%; N = 226/405; class III; Fig. 1E''- G'', insets). Occasionally, we noted an aberrant orientation of petals (14.3%; N = 87/405). In wild-type, the concave adaxial surface of petals usually faces inwards, but in *jlo* mutant flowers it faced other directions instead (Fig. 1E'' inset). This phenotype may result from polarity defects of the petal primordia and was also regarded as class III.

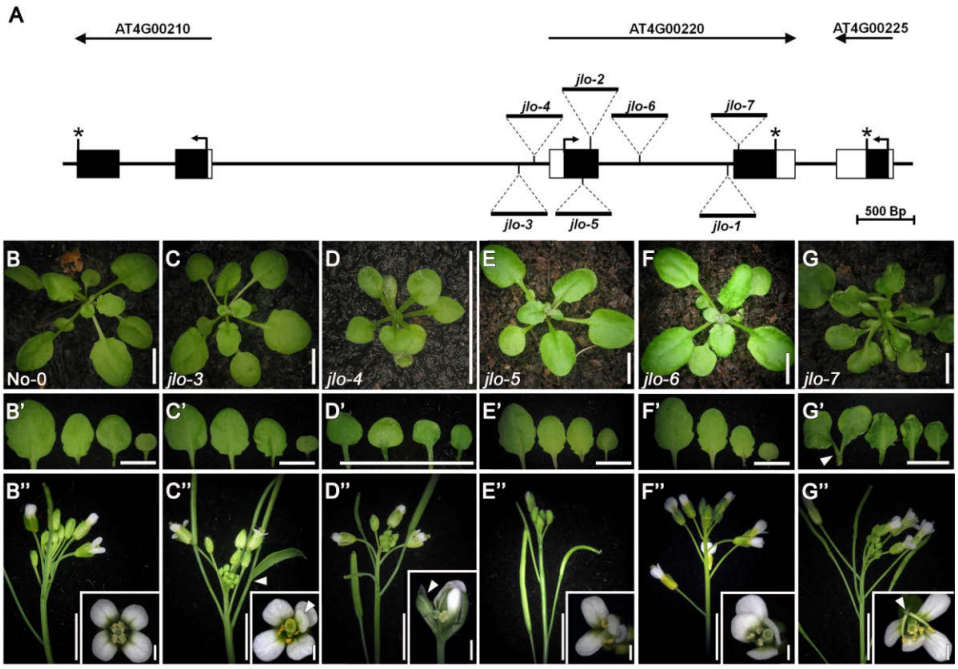

Fig. 1: Analysis of *jlo* mutant alleles. (A) Gene structure of *JLO* (*At4g00220*) and the neighboring genes on chromosome 4. The positions of *Ds* element (*jlo-2* to *jlo-7*) or T-DNA (*jlo-1*) insertions are indicated. The *jlo-1* and *jlo-2* alleles have been described previously. Black boxes: exons; white boxes: UTRs; black arrows: start codon; asterisk: stop codon. (B/B'-G/G') Three-week-old wild-type plants (No-0) compared with homozygous *jlo-3* to *jlo-7* mutants and corresponding first four leaves. *jlo-4* mutants are very small and develop misshaped leaves (D/D'). *jlo-7* leaves curl upwards and are occasionally fused (G/G', arrowhead). (B''-G'') Inflorescences and flowers of wild-type and *jlo* mutants. Phenotypes comprised floral meristem identity defects (C'', D'' inset arrowheads), homeotic transformations (C'' inset arrowhead), reduced number of floral organs (E''/F''), organ fusions (G'' inset, arrowhead) or polarity defects (E'', inset). Scale bars: 1mm

5.1.3.2. The *jlo* mutant phenotype is dosage dependent

jlo loss-of-function mutants arrest during embryogenesis or early seedling stages (*jlo-1* and *jlo-2*) whereas reduced *JLO* activity causes leaf and floral defects (*jlo-3* to *jlo-7*). In addition, we previously found altered target gene expression in heterozygous *jlo-2/+* plants (Bureau et al., 2010), suggesting that plant development may be very sensitive to the level of *JLO* activity. We therefore compared shoot development of wild-type, *jlo-2/+* and *jlo-2* plants to test this notion. Heterozygous *jlo-2/+* mutants appeared aphenotypic during vegetative development. However, after floral transition, *jlo-2/+* flowers displayed defects that were comparable to those of *jlo-3* to *jlo-7* mutants, namely: homeotic transformations of second and third whorl organs; reduction in floral organ number; organ fusions and aberrant petal polarities. Floral buds opened prematurely due to smaller sepals and petals, and stamen size was notably reduced (Suppl. Fig. 2).

In contrast, *jlo-2* homozygous mutants show a severe retardation of growth. Scanning electron micrographs (SEM) revealed that mutant meristems initiated primordia at arbitrary positions, indicating phyllotactic defects (Fig. 2A-D). Most of these organs failed to grow out, the remaining primordia gave rise to radialized organs (Fig. 2B-D). We were unable to detect a functional shoot meristem at 25 days after germination (DAG). We conclude that *JLO* acts in

a dosage dependent manner. Both, *jlo-2/+* and *jlo-2* plants exhibit defects in organ development, albeit with different severity. These phenotypes might either depend on premature meristem differentiation or defective organ maturation.

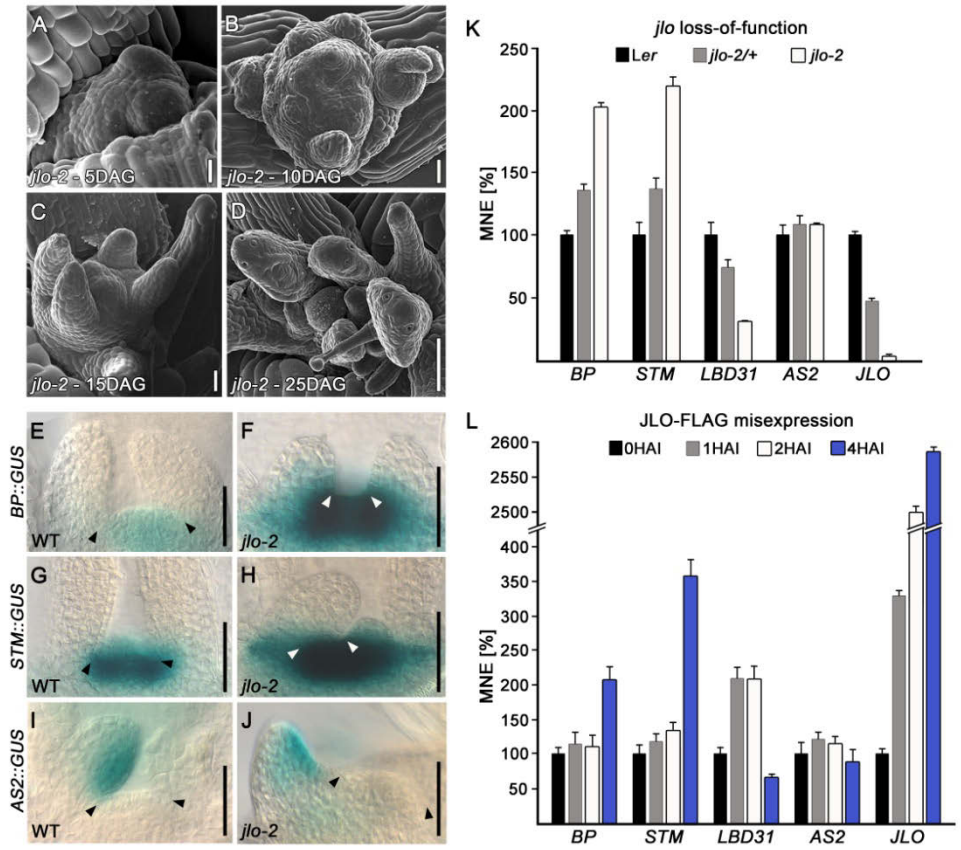

Fig. 2: Shoot development and gene expression analysis of *jlo-2* mutants. (A-D) Scanning electron micrographs of *jlo-2* shoot apical meristems (SAM). (A) Meristems reveal phyllotactic defects at 5DAG. (B/C) At 10 and 15 DAG, the shoot apex is expanded and organs are initiated, but fail to grow out or appear radialized. (D) Some organs display leaf-like structures at 25DAG. (E-F) *BP::GUS* (G-H) *STM::GUS* and (I-J) *AS2::GUS* expression in WT and *jlo-2* mutants. *BP* and *STM* expression is increased but still excluded from lateral organs. *AS2* expression is unaltered. Arrowheads mark meristem boundaries. (K) qRT-PCR confirms reduction of *JLO* transcript levels in *jlo-2* mutants. Expression of *BP* and *STM* is upregulated and *LBD31* expression is downregulated in *jlo-2* mutant seedlings compared to wild-type (5DAG). Note that gene expression is already altered in *jlo-2/+* seedlings. *AS2* transcription is unaffected. (L) Analysis of *BP, STM, LBD31, AS2* and *JLO* transcript levels upon JLO-FLAG induction. Expression levels were normalized to uninduced controls prepared at the same time points. *JLO* expression levels are strongly increased within 1HAI. *BP, STM* and *LBD31* are upregulated within 4 HAI whereas *AS2* expression is unaltered. Scale bars: 50µm; MNE: Mean Normalized Expression; HAI: hours after induction; WT: wild-type; Bars in (K/L) indicate standard error (N ≥ 3).

5.1.3.3. Class I *KNOX* genes are upregulated and ectopically expressed in *jlo* mutants

An active meristem requires expression of class I *KNOX* genes, such as *STM* or *BP* in meristematic cells, and their precise downregulation in lateral organs. The arrest of meristem activity in the *jlo-2* mutants could be caused by changes in the activity or expression levels of these genes. Thus, we examined *BP* and *STM* expression in homozygous *jlo-2* loss-of-function mutants. In wild-type, both *BP::GUS* and *STM::GUS* were expressed only in

meristematic tissue and down-regulated in organ primordia at 5DAG (Fig. 2E/G). In contrast, *BP::GUS* and *STM::GUS* signal intensity was strongly increased in *jlo-2* meristems and expanded to the basis of lateral organ primordia (Fig. 2F/H). At 15 DAG, *BP* and *STM* were expressed throughout the enlarging apex and at the basis of organ primordia (data not shown).

Using quantitative RT-PCR assays we found that transcript levels of *BP* and *STM* are at least 2-fold increased in *jlo-2* mutants. Furthermore, we observed an upregulation of both genes in *jlo-2/+* and in *jlo-4* to *jlo-7* mutant seedlings (Fig. 2K, Suppl. Fig.1B). This misexpression of *KNOX* genes indicate that the defective organ formation of *jlo* mutants is rather the result of a failure to properly differentiate than of premature meristematic differentiation.

The separation of organ primordia from the meristem is critical for their development. During shoot and floral development, *JLO* and its close homologue *LBD31* (*At4g00210*) are similarly expressed in meristem-to-organ boundaries (Borghi et al., 2007; data not shown). Knock-out mutants of *LBD31* are aphenotypic (unpublished data), suggesting that *JLO* and *LBD31* perform independent functions. However, we noted that *LBD31* transcripts are downregulated in *jlo* mutant background und increased upon *JLO* misexpression (Fig. 2K/L), indicating that *JLO* function is required to control meristem and boundary specific gene expression patterns.

5.1.3.4. Genetic interaction between *JLO* and *AS2*

Plants defective in *AS2* function grow lobed leaves that accumulate *BP* transcripts (Semiarti et al., 2001). Furthermore, *as2* mutants develop a defective vascular system and flowers that open prematurely due to reduced petal and sepal sizes (Ori et al., 2000). Thus, *jlo* and *as2* mutants share several characteristics. Because expression of both genes overlaps in newly initiated organ primordia, we hypothesized that they might act in the same pathway to direct organ development (Borghi et al., 2007; Iwakawa et al., 2007; Soyano et al., 2008).

We generated *jlo-2 as2-1* and *jlo-2 as2-2* double mutants to analyze genetic interactions. Both double mutant combinations displayed similar genetic interactions (see below), and only the *jlo-2 as2-2* double mutants will be further discussed. Compared to wild-type, *jlo-2* embryogenesis is strongly impaired with aberrant patterning from the first cell division of the proembryo onwards, and an overall delay in development (Fig. 3K-M; Bureau et al., 2010). *as2-2* single mutants are aphenotypic during embryo development (Fig. 3F-I). *jlo-2 as2-2* mutant embryos were indistinguishable from *jlo-2* mutant embryos (Fig. 3P-R). Similarly, the severe defects observed in *jlo-2* seedlings remained unaltered in *jlo-2 as2-2* double mutants, suggesting that both genes may function in a common pathway (Fig. 3D/O and S/T).

To analyze a genetic interaction during later stages of development we combined the *as2-2* mutation with the weaker *jlo-3* allele (Fig. 3V-Y). We found increased leaf lobing and ectopic

leaflet-formation in the *jlo-3 as2-2* double mutant which is indicative for an enhanced *KNOX* gene misexpression. Using qRT-PCR analyses we observed a moderate increase in *BP* but not in *STM* transcript levels in *jlo-3* mutant leaves. As we did not observe altered leaf morphology in *jlo-3* mutants, the level of ectopic *BP* activity might be too low to affect leaf development. The inappropriate expression of *BP* was higher in *as2-2* mutant leaves and substantially higher in *jlo-3 as2-2* leaves (Fig. 3U). This result suggests that both JLO and AS2 are involved in the repression of *BP* during leaf morphogenesis.

We further found synergistic effects when we analyzed flowers of *jlo-2/+ as2-2* double mutants. With respect to either single mutant, *jlo-2/+ as2-2* sepals, petals and stamens were reduced in size and cell length was decreased (Suppl. Fig.2). These synergistic effects indicate that JLO and AS2 can function partially independently to direct leaf and flower development.

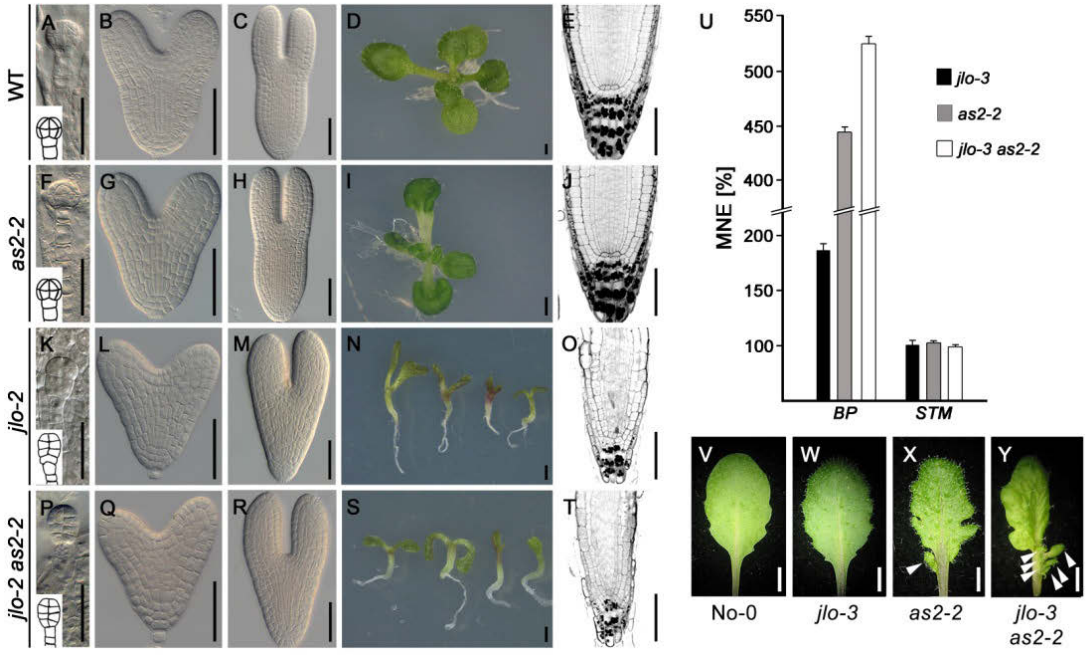

Fig. 3: Genetic interaction of *JLO* and *AS2*. Embryo development of wild-type (WT; A-C); *as2-2* (F-H); *jlo-2* (K-M) and *jlo-2 as2-2* mutants (P-R). Embryonic stages: 16 cell stage (A/F/K/P); heart stage (B/G/L/Q); torpedo stage (C/H/M/R). *as2-2* embryos are aphenotypic; *jlo-2* and *jlo-2 as2-2* embryos reveal altered cell division planes at early proembryo stage (K/P, insets show the respective embryo schematically). These embryos did not develop beyond heart stage. From heart stage onwards, *jlo-2* and *jlo-2 as2-2* embryos displayed reduced hypocotyl diameter and length and showed an overall developmental delay. Phenotypes of wild-type (D/E), *as2-2* (I/J), *jlo-2* (N/O) and *jlo-2 as2-2* mutants (S/T) at 5 DAG. *as2-2* mutants developed lobed leaves (I), but normal roots. *jlo-2* and *jlo-2 as2-2* mutants developed asymmetric and atrophic cotyledons, short hypocotyls and a defective root organization (N/S). Roots were stained via mPSPI; black dots indicate the starch granules in differentiated columella cells. (U) qRT-PCR analyses of *BP* and *STM* expression in mature leaves. *BP* expression is elevated in *jlo-3* leaves, more upregulated in *as2-2* leaves and even stronger increased in *jlo-3 as2-2* leaves. *STM* expression remained unaltered. Expression levels were normalized to those of L*er* and No-0 respectively. (V-Y) Mature leaves of No-0 (V); *jlo-3* (W); *as2-2* (X) and *jlo-3 as2-2* mutants (Y). Arrowhead in (X) and (Y) indicate leaflet formation. Scale bars: (A/F/K/P): 20µm; (B/C; G/H; L/M; Q/R; E/J/O/T): 50µm; (D/I/N/S): 1mm; (V-Y): 0.5 cm; MNE: Mean Normalized Expression; WT: wild-type; Bars in (U) indicate standard error (N ≥ 3).

5.1.3.5. *AS2* function is required for the *JLO* overexpression phenotype

The fact that *STM* and *BP* gene expression is upregulated in *jlo* mutant seedlings suggested that JLO normally acts to downregulate these two homeobox genes. However, this is in contrast to our previous observation that inducible misexpression of a fusion between JLO and the hormone binding domain of the glucocorticoid receptor (GR) causes a drastic upregulation of *STM* and *BP* expression (Borghi et al., 2007). To exclude that fusion to the GR domain interferes with the normally *KNOX* gene repressing function of *JLO*, we designed an estradiol inducible *i35S::JLO-FLAG* transgene (Bureau et al., 2010). However, JLO-FLAG misexpressing plants revealed strongly lobed leaves, resembling the JLO-GR misexpression phenotype (Suppl. Fig. 3F) and showed enhanced transcript levels of *BP* and *STM* upon JLO-FLAG induction (Fig. 2L). Within 1 hour after induction (HAI) both JLO RNA and protein were strongly upregulated (Fig. 2L; Suppl. Fig. 3G). *KNOX* gene expression levels significantly increased within 4HAI, suggesting an indirect mechanism for upregulation (Fig. 2L). We therefore propose that high level expression of JLO might interfere with regulatory pathways that restrict *KNOX* gene expression. *JLO* requires AS2 for this activity because induction of JLO-FLAG in *as2-2* mutants did not affect the typical *as2* leaf phenotype in 96% of all F2 plants analyzed (N = 53, Suppl. Fig. 3E).

We conclude that *JLO* regulates *KNOX* gene expression together with AS2. Ectopic JLO expression could either inhibit *AS2* transcription or interfere with *AS2* dependent regulation. qRT-PCR analysis showed that *AS2* transcript levels are not altered in *jlo-2* mutants or upon JLO-FLAG misexpression (Fig. 2K/L) and we therefore tested the possibility that both proteins physically interact.

5.1.3.6. JLO and AS2 can physically interact in yeast

We performed GAL4-based yeast two-hybrid experiments to assay a potential interaction between AS2 and JLO. AS2 was fused to the GAL4 activation domain (GAL4-AD) and used as bait. Since full length JLO protein was unstable and the JLO C-terminus was activating transcription by itself, we used only the N-terminal LOB domain, fused to the GAL4 DNA-binding domain (GAL4-BD), as prey. In this assay, AS2 was able to interact with the JLO LOB domain, as demonstrated by growth on selective medium lacking Leu, Trp, His and Ade (Fig. 4B).

To map the domains relevant for interaction, we tested several truncations of both proteins. Interaction was observed when AS2 was combined with JLO versions carrying the GAS BLOCK and Coiled Coil (CC) domain, which are highly conserved amino acid regions within the LOB domain (Fig. 4B; Shuai et al., 2002). None of the AS2 truncations including only parts or the complete LOB domain were able to interact with JLO. This suggests that functional domains within the AS2 C-terminus mediate the interaction. However, the AS2 C-terminus fused to the GAL4-AD appeared to be toxic for yeast (Fig. 4B). Thus, we performed

yeast two hybrid experiments with AS2 GAL4-BD fusions as prey. Interaction with JLO was obtained with full length AS2 or only the C-terminal domain of AS2 (Fig. 4C).

We noted that LBD proteins are capable of interactions in variable combinations (unpublished results). Both, JLO and AS2, can also interact with LBD31 in yeast, opening up the possibility that LBD proteins can form higher order complexes and act in a combinatorial fashion. However, we also noted that interactions are not random between LBD proteins, as e.g. LBD2 was not able to bind JLO or AS2 in yeast assays (Suppl. Fig.4).

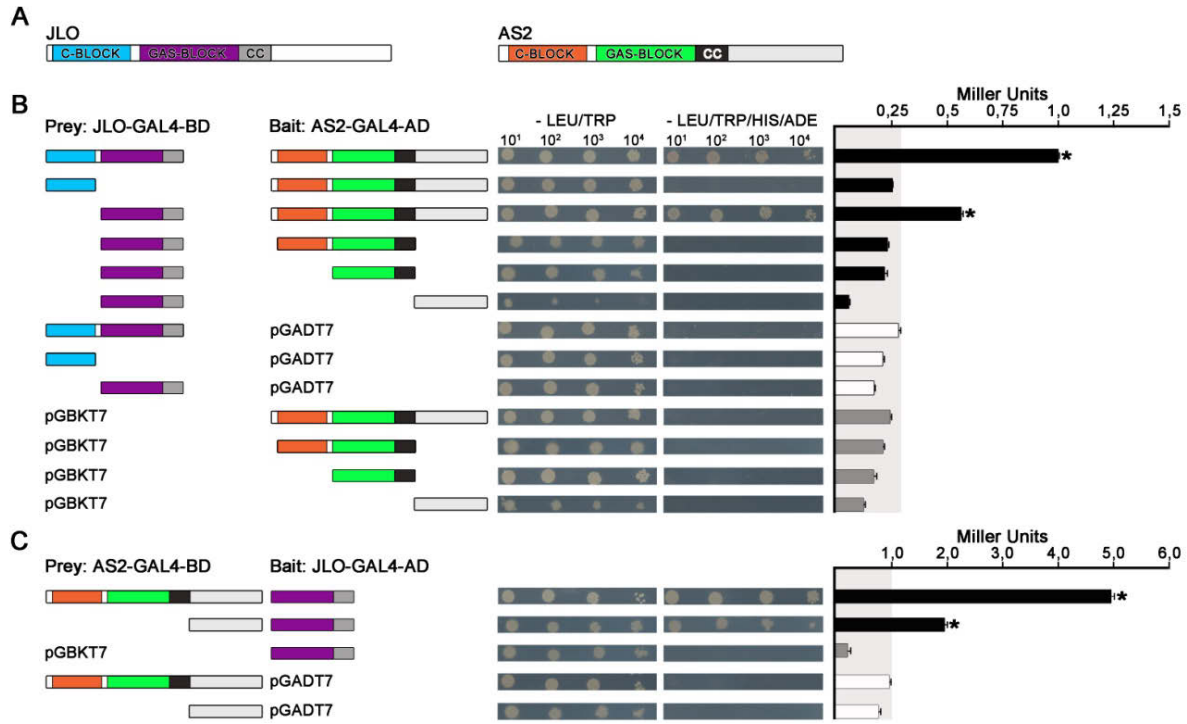

Fig. 4: Mapping JLO-AS2 Interaction domains. (A) Protein structure of JLO and AS2. The LOB domain at the N-terminus of each protein consists of C-BLOCK (blue/red), GAS-BLOCK (lilac/green) and Coiled Coil (CC; grey black) domain. (B-C) GAL4 based yeast two-hybrid study. Maiting with empty pGADT7 and pGBKT7 vectors excludes autoactivation. Growth on -LEU/TRP media was used to select for both plasmids. (B) Growth on selective media (-LEU/TRP/HIS/ADE) was only detected for JLO versions including the GAS-BLOCK and Coiled Coil domain. AS2 C-terminus fused to Gal4-AD appeared to be toxic. (C) AS2 full length or a C-terminal truncation was able to interact with JLO. All results were verified via calculation of Miller Units in a liquid culture assay (black bars). Maiting with pGADT7 (white bars) and pGBKT7 (grey bars) were used to calculate the background (grey shadowed). Asterisks indicate a significant difference to background ($p \geq 0.05$; analyzed by Student's t-test). Bars indicate standard error ($N \geq 3$). Leu: Leucine; Trp: Tryptophan; His: Histidine; ADE: Adenine.

5.1.3.7. JLO interaction with AS1 is mediated by AS2

Complex formation between AS2 and AS1 was shown to be required for *BP* repression in lateral organs (Xu et al., 2003; Guo et al., 2008). Co-expression of AS2 and AS1 allowed yeast growth on selective media, thus verifying the previously published data. However, we did not observe interaction between JLO and AS1 (Fig. 5).

We therefore performed a yeast three-hybrid assay to test whether JLO, AS2 and AS1 have the potential to form a multimeric complex. Yeast was able to grow on selective medium

when all three proteins were expressed, showing that the interaction between JLO and AS1 can be mediated by AS2. High level *JLO* misexpression in WT background may therefore interfere with the activity of the AS1/AS2 complex, and result in a *KNOX* gene misexpression phenotype as we observed for *iJLO-FLAG* plants (Suppl. Fig. 3F).

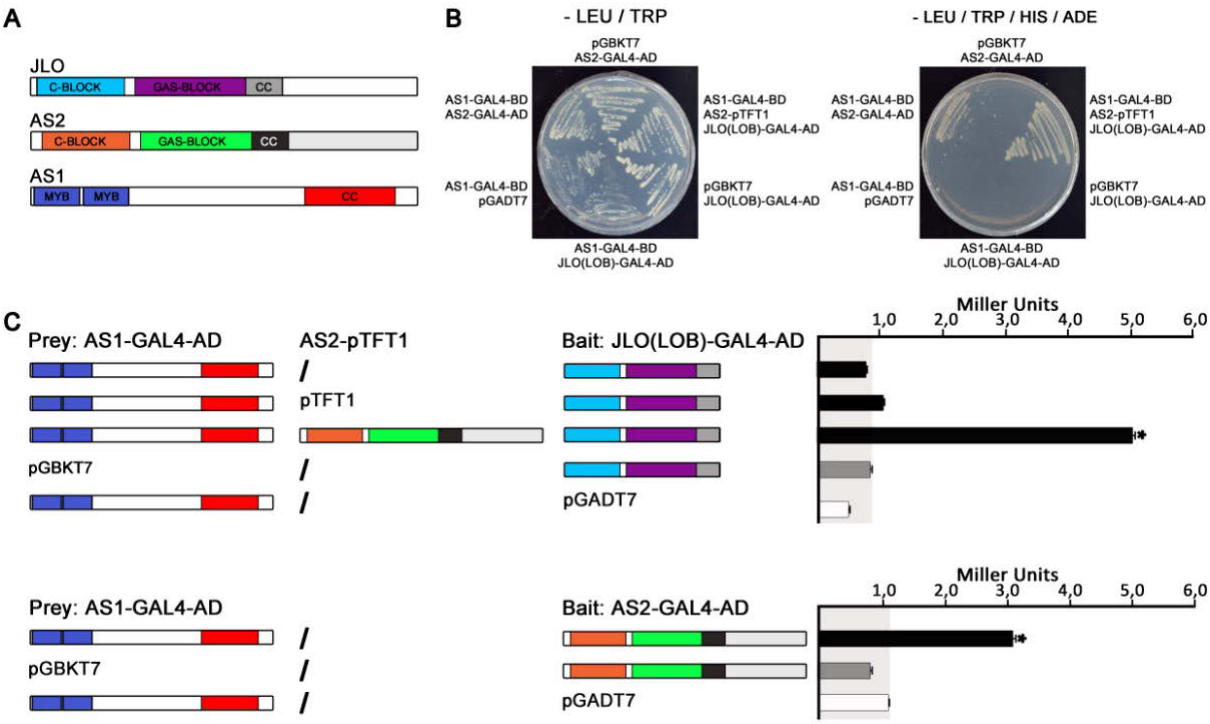

Fig. 5: Yeast three-hybrid assay. (A) Protein structure of JLO, AS2 and AS1. JLO and AS2: C-BLOCK (blue/red), GAS-BLOCK (lilac/green); Coiled Coil domain (CC; grey black). AS1: MYB domain (blue), Coiled Coil domain (CC, red). (B) GAL4 based yeast studies revealed interaction between AS2 and AS1 but not between JLO and AS1. A yeast three hybrid assay showed that AS2 can bridge the interaction between JLO and AS1. AS2 was cloned in the pTFT1 vector and co-transformed with AS1-GAL4-AD and JLO(LOB)-GAL4-BD vectors into yeast. Growth on -LEU/TRP media was used to select for GAL4-AD and GAL4-BD constructs. Growth on selective media (-LEU/TRP/HIS/ADE) was used to monitor interactions. Co-transformation with empty pGADT7 and pGBKT7 vectors exclude autoactivation. (C) All results were verified via calculation of Miller Units in a liquid culture assay (black bars). Co-transformation with pGADT7 (white bars) and pGBKT7 (grey bars) were used to calculate the background (grey shadowed). Asterisks indicate a significant difference to background ($p \geq 0.05$, analyzed by Student's t-test). Bars indicate standard error ($N \geq 3$). Leu: Leucine; Trp: Tryptophan; His: Histidine; ADE: Adenine

5.1.3.8. Intracellular Localization of fluorescent protein tagged JLO, AS2 and AS1

To analyze protein interaction *in planta,* JLO, AS2 and AS1 were fused to the fluorescent proteins (FP) GFP or mCherry and transiently expressed in *N. benthamiana* leaf epidermal cells. We used a ß-estradiol expression system to limit overexpression artifacts and unspecific interactions (Bleckmann et al., 2010). Integrity of the different fusion proteins was confirmed by western blotting using an anti-GFP antibody (Suppl. Fig.5G).

JLO and AS2 fusion proteins were found in the cytoplasm and enriched in the nucleoplasm (Fig. 6E/G). AS1 was exclusively localized to the nucleus with higher protein abundance in

the nucleolus (Fig. 6H). Consistent with previously published results, the presence of AS2 caused a re-localization of the AS1 protein to the nucleoplasm (Zhu et al., 2008; Fig. 6F). In contrast, JLO did not affect the AS1 localization, supporting the notion that JLO and AS1 do not directly interact (Fig. 6C).

We used inducible misexpression in stably transformed *Arabidopsis* plants to test the fusion proteins for functionality. In all cases, we obtained the previously described gain-of-function phenotypes, indicating that the fusion proteins are fully active. The observed subcellular localizations in root epidermal cells resembled those in *N. benthamiana* (Fig. 6I-N). Similarly, co-expression of AS2/AS1 (Fig. 6L) but not of JLO/AS1 (Fig. 6I) resulted in a re-localization of AS1 to the nucleoplasm. These findings are again consistent with a direct interaction of JLO/AS2 and AS2/AS1 and no direct binding of JLO to AS1.

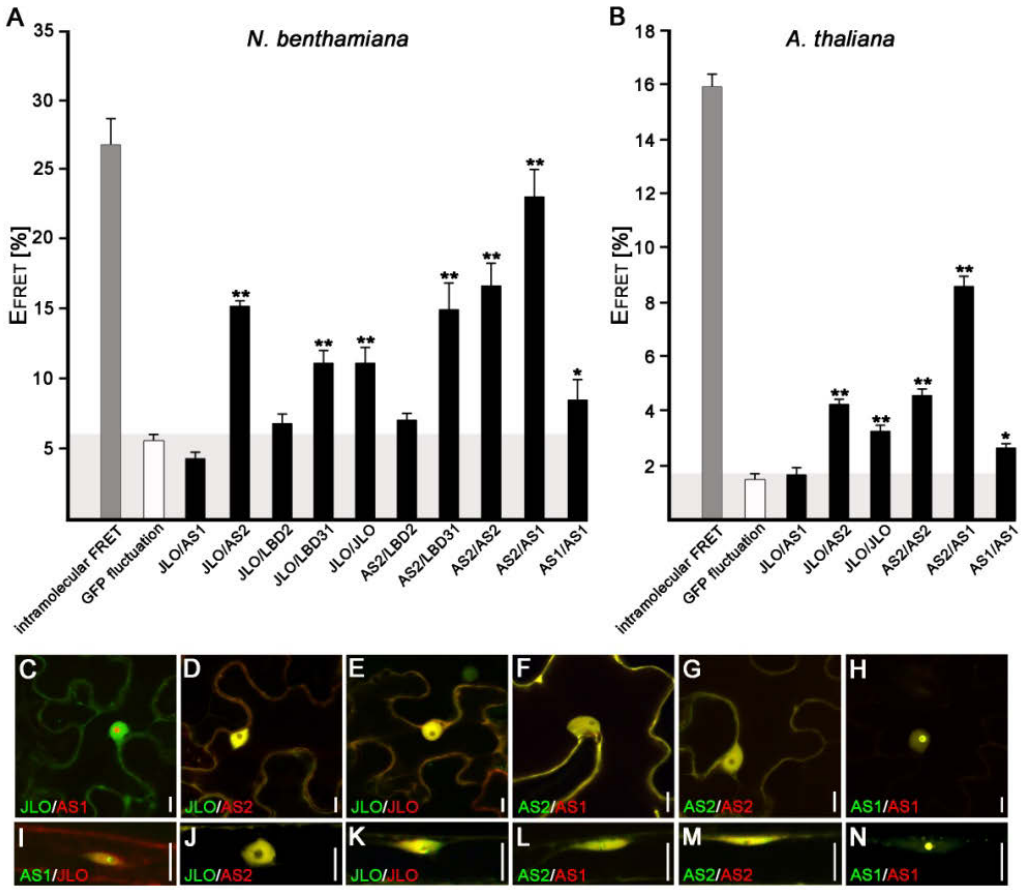

Fig. 6: Intracellular protein localization and FRET-based protein interaction analysis. (A-B) Protein interaction revealed by E_{FRET} [%]. Intramolecular E_{FRET} between obtained by direct fusion of GFP to mCherry (grey bars) and GFP background fluctuation (white bars) were calculated as positive and negative controls. (A) E_{FRET} measured with a transient expression of FP-tagged protein in epidermis cells of *N. benthamiana* (N ≥ 35 for each combination) (B) E_{FRET} measured in root epidermis cells of stable transformed *Arabidopsis* plants (N ≥ 25 for each combination). Grey shadowed area indicates background fluctuation level of GFP. Asterisks mark a significant difference from background ($p \leq 0.05$*; $p \leq 0.01$**; analyzed by Student's t-test). (C-H) Colocalization of the FP-tagged proteins in *N. benthamiana* epidermis cells. (I-N) Colocalization of the FP-tagged proteins in *Arabidopsis* root epidermis cells. Scale Bars: 10µm; Bars in (A/B) indicate standard error.

5.1.3.9. FRET-based protein interaction analysis

Next, we measured FRET efficiencies (E_{FRET}) between the GFP and mCherry pairs (Albertazzi et al., 2009). E_{FRET} was calculated as percentage increase of GFP (donor) fluorescence after photobleaching of mCherry (acceptor) (Bleckmann et al., 2010). All photobleaching experiments and E_{FRET} measurements were performed in the nucleus.

In *N. benthamiana* leaf epidermal cells, fluorescent signals were first detectable at 1HAI and remained stable within 12HAI (Suppl. Fig.5E). Upon extended induction (≥ 24 HAI), some cells carried fluorescent aggregates indicating protein overexpression (Suppl. Fig.5F, arrowhead). Therefore all measurements were performed within 12HAI. As E_{FRET} depends on orientation and distance of both chromophores to each other, we measured intramolecular E_{FRET} as control for the minimal distance. To this end, GFP and mCherry were fused to the C-termini of all tested proteins. The intramolecular E_{FRET} we measured ranged from 26% to 28%. Calculation of GFP fluorescence fluctuation during photobleaching in absence of the donor revealed a maximal background of 6%. Thus, only E_{FRET} significantly higher than 6% was regarded to indicate a close proximity or physical interaction of two proteins (Fig. 6A).

The results we obtained confirmed our yeast GAL4 interaction studies and showed a clear JLO/AS2 (E_{FRET} = 15% ± 0.5%) and AS2/AS1 (E_{FRET} = 23.0% ± 2%) interaction in both GFP/mCherry combinations. By contrast, we did not observe a significant E_{FRET} for JLO/AS1 (4.3% ± 0.8%). Measurements performed at 1HAI, 2HAI, 4HAI and 12HAI revealed that E_{FRET} remained stable over time (Suppl. Fig. 5H), thus E_{FRET} did not depend on protein overexpression. Interestingly, JLO (E_{FRET} = 11% ± 1.0%), AS2 (E_{FRET} = 17% ± 1.7%) and AS1 (E_{FRET} = 8.9% ± 1.5%) showed significant homomerization (Fig. 6A), suggesting that various homomers and heteromers may coexist within the nucleus.

FP tagged LBD31 and LBD2 proteins were used to further test the specificity of the observed interactions. Both proteins localized to the nucleus and cytoplasm, thus resembling subcellular localizations of JLO and AS2 (Suppl. Fig.5A-D). In line with our yeast studies, we found interaction between JLO/LBD31 (11.1% ± 1.0%) and AS2/LBD31 (15.0% ± 1.9%). E_{FRET} values for JLO/LBD2 (6.8% ± 0.7%) and AS2/LBD2 (7.1% ± 1.0%) were close to background (Fig. 6A).

Overall, we noted a reduction of E_{FRET} in root epidermal cells of stably transformed *Arabidopsis* plants compared to *N. benthamiana* (Fig. 6B). The intramolecular E_{FRET} we measured ranged only from 15% to 17%. The GFP background fluctuation was also only maximal 1.5%. However, we verified heteromerization of JLO/AS2 (4.1% ± 0.2%) and AS2/AS1 (8.6% ± 0.4%) as well as homomerization of JLO (3.1 ± 0.3%), AS2 (4.4 ± 0.3%) and AS1 (2.4 ± 0.1%). E_{FRET} values for JLO/AS1 (1.6% ± 0.4%) were in the range of background level.

We conclude that JLO and AS2 specifically interact in yeast, *N. benthamiana* and *Arabidopsis*.

5.1.3.10. Both *AS2* and *JLO* control auxin transport

Our studies show a complex formation between JLO and AS2 in *Arabidopsis.* To examine in which tissues this interaction could take place, we analyzed expression of an *AS2::GUS* reporter gene construct (Jun et al., 2010). GUS signals appeared on the adaxial side of cotyledons and organ primordia during embryonic and postembryonic development. In addition, *AS2::GUS* was expressed in cells of the suspensor and the embryonic root tip (Fig. 7C-D; Jun et al., 2010). After germination, *AS2* is expressed in the tips of seedling roots (Fig. 7E).

JLO expression in embryos was analyzed through whole-mount RNA *in situ* hybridization. At early heart stage, *JLO* is expressed in the entire embryo with a stronger transcript accumulation in the basal domain (Fig. 7A). Later on, expression is confined to the embryo axis and stronger in the developing vasculature and the root pole (Fig. 7B). Thus, the *JLO* and *AS2* expression domain coincides at heart stage and in the basal root tip of later embryo stages. Neither expression domain nor expression levels of *AS2* are altered in *jlo-2* mutant background. Similarly, *JLO* expression levels are unaltered in *as2-2* mutants (Fig. 7M).

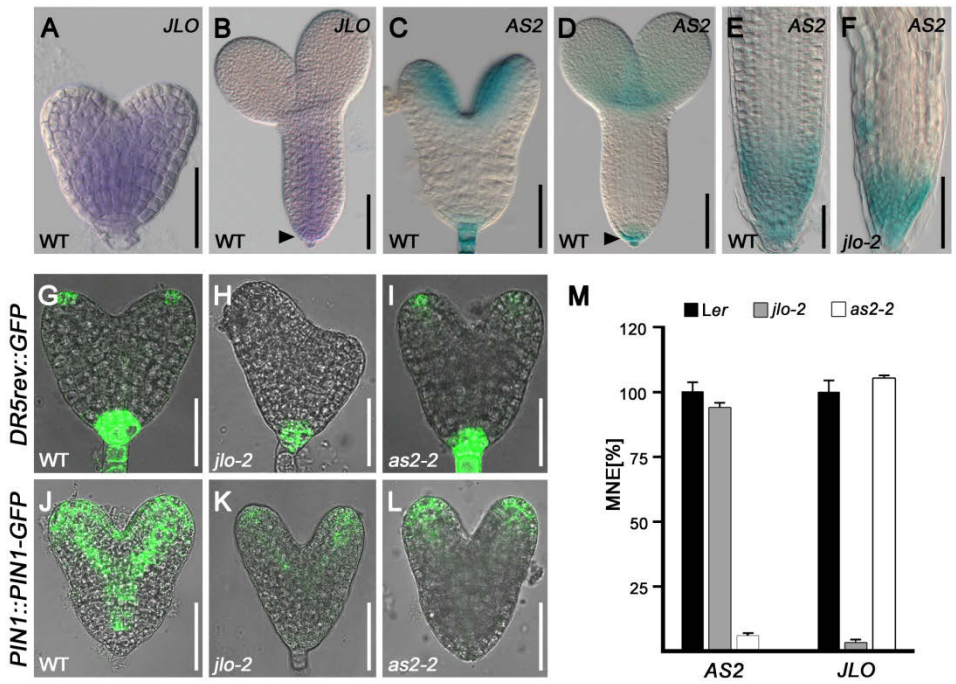

Fig. 7: Gene expression analyses during embryonic and root development. Embryonic stages: (A/C and G-L): heart stage; (B/D): bent cotyledon stage. (A-B) Embryonic expression pattern of *JLO* analyzed by whole-mount RNA in situ hybridization. (A) At heart stage, *JLO* transcripts are detectable in provascular cells. (B) Later on, expression becomes restricted to the basal root tip (B; arrowhead) and the stele. (C-D) During embryogenesis, *AS2::GUS* is expressed at the adaxial side of cotyledons and the basal root tip (arrowhead in D) including suspensor. (E) AS2 expression at tip of wild-type roots. (F) *jlo-2* roots reveal an unaltered AS2 expression. (G-I) *DR5rev::GFP* expression in heart stage embryos. (G) In wild-type, auxin concentrates in the root primordium and suspensor as well as in the tips of the cotelydons. (H) *jlo-2* embryos reveal only a weak signal at the root pole. (I) *as2-2* embryos show unaltered *DR5rev* activity. (J-L) *PIN1::PIN1-GFP* expression in heart stage embryos. (J) PIN1 concentrates to the cotelydon tips and provascular cells in wild-type. (K) *jlo-2* and (L) *as2-2* mutants show

similar PIN1 distributions but reduced expression levels. (M) qRT-PCR analysis of *JLO* and *AS2* transcript levels (5DAG). *JLO* expression is strongly reduced in *jlo-2* mutants but unaltered in *as2-2* mutant background. Similarly, *AS2* expression is downregulated in *as2-2* mutants but unchanged in *jlo-2* seedlings. Scale bars: 50µm; WT: wild-type; MNE: Mean Normalized Expression; Bars in (O) indicate standard error (N ≥ 3).

The severe patterning defects of *jlo-2* embryos and roots result from a failure in auxin signaling and transport (Bureau et al., 2010). Thus, we examined auxin distribution in *as2-2* mutants using the synthetic auxin response reporter *DR5rev:GFP* (Ulmasov et al., 1997). In WT heart stage embryos, auxin accumulates at the root pole with an intensity maximum in the uppermost suspensor cell (Fig. 7G). Unlike *jlo-2* mutants, *as2-2* embryos displayed an unaltered *DR5rev* activity (Fig. 7H/I). Postembryonic roots exhibit a maximum of *DR5rev::GFP* expression in the QC, the adjacent stem cells and columella cells. Again, *DR5rev* activity was unaltered in seedling roots of *as2-2* mutants (Fig. 8A/E). Because auxin accumulation is controlled by several PIN proteins, we analyzed their expression in more detail (Vieten et al., 2005). We previously identified JLO as an important regulator of these efflux carriers (Bureau et al., 2010). Consistent with this, expression levels of *PIN1/3/4* and *PIN7* were reduced in the novel *jlo-3* to *jlo-7* alleles (Suppl. Fig. 1B). We analyzed the expression of *PIN1::PIN1-GFP*, *PIN4::PIN4-GFP* and *PIN7::PIN7-GFP* reporters in the *as2-2* mutant background. We found a decreased PIN1-GFP signal in *as2-2* embryos and roots (Fig. 7L, Fig. 8F). PIN7-GFP expression in *as2-2* roots was also reduced, whereas PIN4-GFP signals were strongly increased (Fig. 8G-H). Thus, *AS2* and *JLO* are similarly required for *PIN1/7* expression, but they differ in their capacity to regulate *PIN4* expression.

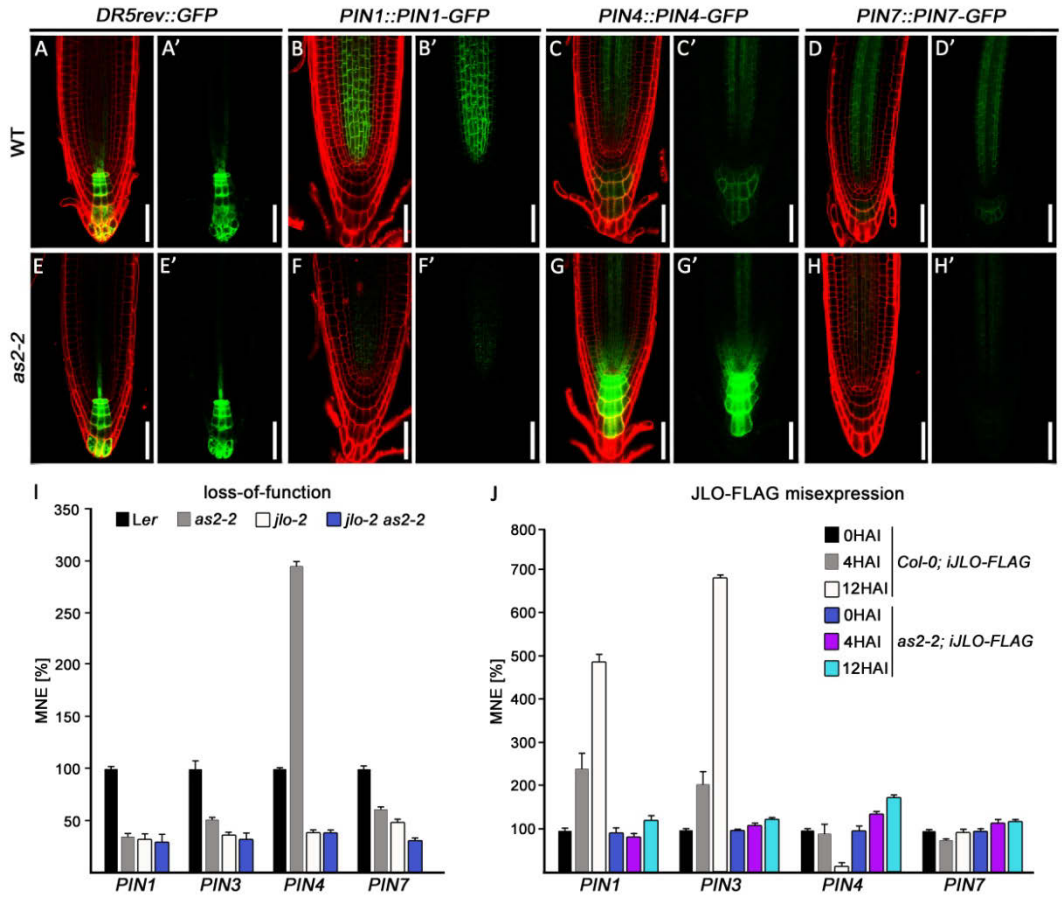

Fig. 8: *PIN* gene expression is regulated by a JLO/AS2 complex. Expression of *DR5rev::GFP* (A/A' and E/E'); *PIN1::PIN1-GFP* (B/B' and F/F'); *PIN4::PIN4-GFP* (C/C' and G/G') and *PIN7::PIN7-GFP* (D/D' and H/H') in wild-type (A-D) and *as2-2* (E-H) mutants (5DAG). Auxin accumulation is unaltered in *as2-2* mutants (E/E'). PIN1-GFP and PIN7-GFP signals are severely reduced (F/F' and H/H') while PIN4-GFP signal is strongly increased (G/G') in *as2-2* roots. (I) qRT-PCR analysis reveals a downregulation of *PIN1, PIN3, PIN7* and an upregulation of *PIN4* in *as2-2* roots. In contrast, transcript levels of all *PIN* genes studied are strongly reduced in *jlo-2* and *jlo-2 as2-2* roots. Note that *PIN1, PIN3* and *PIN4* expression is similar in *jlo-2* and *jlo-2 as2-2* mutants while *PIN7* transcript levels are further reduced in the double mutant. (J) Analysis of *PIN1, PIN3, PIN4* and *PIN7* transcript levels in roots after induced misexpression of JLO-FLAG in wild-type (Col-0) and *as2-2* mutants. Expression levels were normalized to uninduced controls prepared at the same time points. In wild-type, *PIN1* and *PIN3* are upregulated within 12HAI, while no response is detectable in *as2-2* background. *PIN4* is downregulated in wild-type roots but slightly upregulated in *as2-2* mutants. *PIN7* expression remained unaltered in both genetic backgrounds. Scale bars: 50µm; WT: wild-type; MNE: Mean Normalized Expression; HAI: hours after induction; Bars in (I/J) indicate standard error (N ≥ 3).

5.1.3.11. The JLO-AS2 complex is required for *PIN* gene regulation

We sought to analyze whether JLO and AS2 function together in the regulation of *PIN* genes. To this end, we first performed qRT-PCR analysis on *jlo-2* and *as2-2* single and double mutant roots (Fig. 8I). *PIN1* and *PIN3* transcript levels are severely reduced in *jlo-2* mutants and we found a similar downregulation of these genes in the *as2-2* mutant background. *jlo-2 as2-2* double mutants revealed no further decrease in *PIN1* and *PIN3* transcription suggesting that JLO and AS2 act together to promote *PIN1* and *PIN3* expression. However, *PIN4* expression was reduced in *jlo-2* mutants, but nearly 3-fold upregulated in *as2-2* mutants. In *jlo-2 as2-2* double mutants, *PIN4* expression levels resembled those of *jlo-2* single mutants.

This indicates that JLO is essential for *PIN4* expression and that JLO/AS2 heteromers may act to restrict *PIN4* levels. *PIN7* transcription is notably reduced in both *jlo-2* and *as2-2* mutant roots but further decreased in the double mutant, indicating that JLO act partially independent of AS2 to promote *PIN7* expression.

To further identify AS2 dependent functions of JLO, we analyzed *PIN* gene expression in roots (5DAG) upon JLO-FLAG misexpression (Fig. 8J). Increased JLO activity was shown to be sufficient for *PIN1* and *PIN3,* but not for *PIN7* upregulation in WT roots (Bureau et al., 2010). In *as2-2* mutant background, *PIN1* and *PIN3* did not respond to JLO-FLAG induction suggesting that JLO requires AS2 for this function. Expression of *PIN4* was first insensitive to JLO induction and decreased after prolonged *JLO* induction (12HAI). In *as2-2* mutants, that already express higher levels of *PIN4* before induction, JLO-FLAG misexpression caused a further increase in *PIN4* RNA levels. We propose that JLO contributes to complexes that promote PIN4 expression, and that these complexes compete with JLO/AS2 in the regulation of *PIN4.* This hypothesis would implicate that correct target gene expression requires a tight balance of various complexes that involve JLO. Interference via JLO misexpression may increase JLO/AS2 dimerization, thus repressing *PIN4,* while absence of AS2 in *as2-2* mutants would preferentially allow the formation of *PIN4* promoting complexes (Fig. 9).

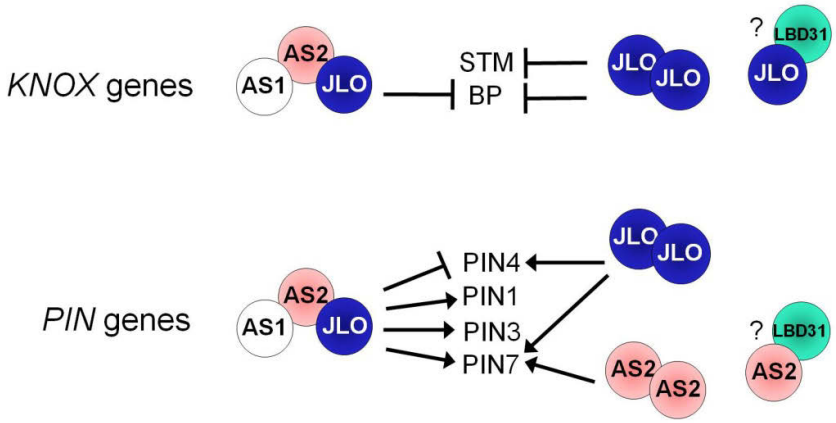

Fig. 9: A model for *KNOX* and *PIN* gene regulation through different JLO and AS2 homomeric and JLO/AS2/AS1heteromeric complexes. The interaction between JLO and AS1 is mediated through AS2. The JLO/AS2/AS1 complex represses *BP* and *PIN4* expression and promotes *PIN1, PIN3* and potentially *PIN7* expression. JLO homomers repress *STM, BP* and promote *PIN4* and *PIN7* expression. AS2 homomeric complexes may promote *PIN7* expression independently. Correct target gene expression requires a tight balance between the various protein complexes. LBD31 can bind to JLO and AS2, but the regulatory function of these complexes is so far unknown.

5.1.4. Discussion

Organ initiation requires the accumulation of auxin and downregulation of class I *KNOX* gene expression in organ anlagen, as well as the establishment of boundaries that separate cells with different cell fates (reviewed in Rast et al., 2008). Several lines of evidence suggest that *JLO* plays an essential role during cell fate regulation. (1) *JLO* is expressed early at sites of organ initiation, in meristem-to-organ boundaries and weakly in mature leaves (Borghi et al., 2007; Soyano et al., 2008). (2) Compromised *JLO* activity causes pleitropic defects that can be classified to affect meristem activity, organ identity and polarity, organ growth and separation. (3) These defects are accompanied by ectopic expression of *STM* and *BP* and decreased expression of several *PIN* genes.

We now conclude that *JLO* controls the downregulation of class I *KNOX* genes at the time of leaf initiation, because *STM* and *BP* expression were expanded into the basal domain of organ primordia in *jlo-2* mutants. This *KNOX* gene misexpression is likely to be responsible for organ developmental defects in *jlo-2* mutant meristems (Williams, 1998). The elevated levels of *BP* in mature leaves of the weaker *jlo-3* allele (which still permits organ formation due to residual JLO activity) implicate a role for *JLO* in the maintenance of *BP* repression. *JLO* shares this role with AS2, another LBD protein, that interacts with the MYB protein AS1 to repress *BP* expression during leaf morphogenesis (Ori et al., 2000; Xu et al., 2003; Guo et al., 2008).

Our studies showed that JLO and AS2 can physically interact *in vivo.* Furthermore, we found that AS2 can mediate the interaction between JLO and AS1. A simple scenario could therefore be that the JLO/AS2/AS1 complex represses *BP* expression in developing organs. However, the synergistic effects in *jlo-3 as2-2* and *jlo-2/+ as2-2* mutants indicate that JLO can act also independently of AS2. Furthermore, *STM* was found to be misexpressed in *jlo* mutant backgrounds, but not in *as2-2* mutants (Ori et al., 2000). This suggests that both JLO/AS2/AS1 heteromeric complexes as well as JLO homomers regulate *KNOX* gene expression in the shoot.

The evidence for JLO acting as a negative regulator of *BP* and *STM* expression is entirely based on the loss-of-function data, thus likely reflecting genuine JLO activity. We found that *JLO* acquires the capacity to interfere with *KNOX* gene repression when overexpressed. Ectopic JLO activity therefore disturbs regulatory networks that are required for *KNOX* gene restriction in leaves. Since organ development is also highly sensitive to reduced *JLO* gene dosage, we conclude that JLO expression levels must be normally strictly regulated. Our misexpression experiments showed that JLO induction in *as2-2* mutant background did not enhance the *as2-2* leaf phenotype, indicating again that *KNOX* gene regulation requires balanced expression of both JLO and AS2 proteins.

Our studies of JLO and AS2 function during root development support the hypothesis that both proteins act together in a heteromeric complex. They also revealed AS2 independent activities of JLO. Mutant studies showed that JLO and AS2 act together to promote *PIN1* and *PIN3* expression, and that further *PIN1* and *PIN3* upregulation by JLO overexpression requires the presence of AS2. We found increased *PIN4* expression in *as2-2* single mutants, but a decrease in *jlo-2* or *jlo-2 as2-2* double mutants. A simple interpretation of these results is that JLO homomers strongly promote *PIN4* transcription, JLO/AS2 heteromers control normal PIN4 levels, and that AS2 homomers (or complexes involving AS1) repress PIN4 expression. This notion is supported by the observation that JLO induction in absence of AS2 further increased *PIN4* transcription. To this end, it is noteworthy that PIN proteins are to some extent functionally interchangeable, and that loss of *PIN* gene expression can be compensated by other *PIN* genes (Blilou et al., 2005, Vieten et al., 2005). Thus, *PIN4* expression may be enhanced by JLO homomers in *as2-2* mutants, which may compensate for reduced expression of *PIN1*, *PIN3* and *PIN7*. Based on our *jlo-2 as2-2* double mutant analysis, JLO and AS2 act at least partially independently to direct *PIN7* expression.

We reported previously that *PIN* gene expression is already reduced at early stages of *jlo* embryogenesis (Bureau et al., 2010). Similarly, we showed here reduced *PIN1* expression in *as2-2* heart stage embryos. Thus, JLO and AS2 complexes likely regulate *PIN* expression from embryogenesis onwards. We also noted that the SAM of *jlo-2* mutants initiated filamentous organs with a disturbed phyllotaxis and eventually arrested organ formation. Similar defects were reported for *pin1* mutants (Reinhardt et al., 2003; Vernoux et al., 2000). Therefore, the overall reduction in *PIN1* transcription, which we showed for *jlo-2* mutant seedlings (Bureau et al., 2010), likely also contributes to the aberrant *jlo-2* shoot development. The epistatic genetic interaction of *jlo-2* to *as2-2* at embryonic and seedling stages, combined with our analysis of root development, suggests a continuous requirement for JLO homomeric and JLO/AS2 heteromeric complexes throughout plant development.

Our results show that JLO and AS2 regulate a similar set of target genes and act in a combinatorial manner. This raises the question how the JLO/AS2 complexes are modulated to obtain their specific functions. A possible explanation is that the interaction with additional factors is responsible for the modulation of DNA-binding specificity or transcriptional regulation. Similar combinatorial activities were reported for MADS-Box proteins which determine the identity of floral organs (Theissen et al., 2001). The formation of the multimeric JLO/AS2/AS1 complex in yeast supports this assumption. AS1 is expressed in developing organ primordia, leaves and in roots (Iwakawa et al., 2007). Thus, JLO/AS2 could function with AS1 to control *KNOX* and *PIN* gene expression in both shoots and roots. Indeed, the *as2* and *as1* mutant leaf phenotypes were not fully suppressed by *bp* mutants, suggesting that both genes regulate other targets besides *BP* (Ori et al., 2000; Byrne et al., 2002). In

addition, auxin activity is asymmetrically distributed at the distal leaf tip of *as1* or *as2* mutants (Zgurski et al., 2005). These observations could be explained by postulating a role for AS2 and AS1 in *PIN* gene regulation, which is strongly supported by our data presented here. In the root system, where no *as1* mutant phenotype was described so far, other MYB genes may replace AS1 function and contribute to *PIN* gene regulation.

We found that both JLO and AS2 can interact with LBD31 *in vivo*. *LBD31* expression is first detectable at sites of organ initiation and later in meristem-to-organ boundaries. This expression pattern overlaps with that of *JLO*, *AS2* and *AS1* during early organ development and later with that of *JLO* in the boundary (Borghi et al., 2007; Iwakawa et al., 2007; Xu et al., 2008; Jun et al., 2010). Whether higher order complexes with LBD31 are formed as not been analyzed so far. However, we envisage that LBD proteins can undergo a wide range of combinatorial interactions with each other. In contrast to *jlo* or *as2* and *as1* mutants, knock out alleles of *LBD31* were aphenotypic (unpublished data), indicating that either *JLO* can compensate for the loss of its close homologue *LBD31*, or that other related LBD proteins can substitute for LBD31 in heteromeric complexes. Further experiments are required to distinguish between these possibilities.

Reduced JLO activity interfered with the establishment of boundaries, resulting in leaf and floral organ fusions in the different *jlo* alleles. Boundary formation requires a depletion of auxin from the cells encompassing the organ primordia (Heisler et al., 2005). Boundary cells act not only as morphological barriers, they also provide signals that regulate the development of adjacent tissues (reviewed in Aida et al., 2006). The failure to separate cells with different identities, combined with a loss of boundary specific gene expression will then result in aberrant organ development of *jlo* mutants. Somewhat similar effects were reported for the trihelix transcription factor PETAL LOSS (PTL), which is expressed in sepal boundaries. *ptl* loss-of-function mutants develop fused sepals, but display also a reduced organ number as well as polarity defects (Brewer et al., 2006).

Taken together, our data show that *JLO* function is required for patterning processes throughout plant development. We demonstrate that JLO can act in homomeric as well as in heteromeric complexes with AS2 and AS1, and serves to coordinate *KNOX* gene expression and regulation of essential components of the auxin transport pathway during shoot and root development in *Arabidopsis*.

5.1.5. Experimental Procedures

Plant Material and Growth Conditions

The *jlo-2* (L*er*, Bureau et al., 2010), *as2-1* (An) and *as2-2* (L*er*) *(*Iwakawa et al., 2002) mutants were obtained from NASC. The *jlo-3* (*pst17018*), *jlo-4* (*pst19799*), *jlo-5* (*pst20504*), *jlo-6* (*pst00432*) and *jlo-7* (*pst13957*) mutations are in Nossen (No-0) background and belong to the RIKEN collection. Origins of marker lines are as follows: *DR5rev::GFP* (B. Scheres), *PIN1::PIN1-GFP*, *PIN4::PIN4-GFP* and *PIN7::PIN7-GFP* (J. Friml), *AS2::GUS* (J.C. Fletcher), *STM::GUS* (W. Werr) and *BP::GUS* (M. Tsiantis). *A. thaliana* plants were grown on soil under constant light conditions at 21°C. For root analyses, seeds were surface sterilized with chlorine gas, imbibed in 0.1% agarose and plated onto GM medium (0,5x MS medium with Gamborgs no. 5 vitamins (Duchefa), 0,5 g/l 2-(N-morpholino) ethanesulfonic acid (MES), 1% (w/v) sucrose; 1.2% (w/v) plant agar). Plates were incubated vertically in a growth chamber. *N. benthamiana* plants were grown for 4 weeks in a greenhouse under controlled conditions.

Binary Constructs and Plant Transformation

For protein localization and interaction studies, attB sites were added via PCR-mediated ligation to coding regions of *JLO* (*At4g00220*), *AS2* (*At1G65620*), *AS1* (*At2G37630*), *LBD31* (*At4G00210*) or *LBD2 (At1G06280).* PCR products were introduced into pDONR201 and eventually recombined into pABindGFP, pABindCherry or pABindFRET (Bleckmann et al., 2010). Binary vectors were transformed in *A. tumefaciens* GV3101 pMP90 (Koncz et al., 1984) according to manufactures instructions (Invitrogen^{TM}). Abaxial leaf sides of *N. benthamiana* plants were infiltrated as described in Bleckmann et al., 2010. Transgene expression was induced 48h after infiltration by spraying with 20µM ß-estradiol, 0.1% Tween20 and analyzed within 12HAI. Production of fusion proteins was confirmed by Western blotting (primary antibody: anti-GFP (Roche); secondary antibody: anti mouse ALP conjugated (Dianova)). *A. thaliana* plants were transformed using the floral dip method (Clough et al., 1998). Transgenic plants were selected on GM medium containing Hygromycin (15mg/mL). For *JLO* misexpression experiments, a *LexA35S::JLO-FLAG* transgene (Bureau et al., 2010) was transformed into Col-0 or *as2-2* plants. Induction of transgene expression was performed by spraying with 20µM ß-estradiol, 0.1% Tween20 and verified by Western Blot analysis (primary antibody: anti-FLAG (Sigma); secondary antibody: anti-mouse ALP conjugated antibody (Dianova)).

E_{FRET} Measurements via Acceptor Photobleaching

N. benthamiana leaf epidermal cells and *A. thaliana* root epidermal cells were examined with a 40x1.3 numerical aperture Zeiss oil-immersion objective using a Zeiss LSM 510 Meta confocal microscope. E_{FRET} was measured via GFP fluorescence intensity increase after photobleaching of the acceptor mCherry (Bleckmann et al., 2010). The percentage change of

the GFP intensity directly before and after bleaching was analyzed as E_{FRET} = (GFP_{after} - GFP_{before})/GFP_{after} x 100. All photobleaching experiments were performed in the nucleus. A minimum of 25 measurements were performed for each experiment. Significance was analyzed using Student's t-test.

Yeast Interaction Studies

Full length coding sequences or fragments of genes tested in yeast interaction studies were amplified by PCR from Col-0 cDNA. The forward and reverse primers used for this amplification carried a restriction site that permitted to clone the PCR product into pGADT7, pGBKT7 or pTFT1 (Egea-Cortines et al., 1999). For Yeast-Two-Hybrid studies, GAL4-BD and GAL4-AD clones were transformed into the yeast strains YST1 and AH109 (Clonetech). Expression of the fusion proteins was confirmed by western blotting (GAL4-BD: anti-Gal4 DNA-BD (Clonetech)/ anti-mouse-ALP conjugated (Dianova); GAL4-AD: anti-HA (Roche)/ anti-rat-HRP conjugated (Dianova)). After mating, interaction was studied by plating serial dilutions of yeasts on medium lacking Leu, Trp, His and Ade. Three-hybrid assays were performed in yeast strain AH109. Constructs were cotransformed and selected on Yeast Synthetic Dropout (YSD) medium. Interactions were assayed on quadruple dropout medium. All other techniques were performed according to the Matchmaker protocols handbook (Clonetech).

Gene Expression Analysis

Reporter gene analysis was performed in the F3 generation after genetic crossing. Detection of GUS activity was performed with GUS staining solution [0.05M $NaPO_4$ (pH7.0), 5mM $K_3[Fe(CN)_6]$, 10mM $K_4[Fe(CN)_6]$. For microscopic analysis of embryos and roots, tissue was cleared with 70% (w/v) chloral hydrate, 10% (v/v) glycerol solution. For microscopic analysis of green tissues, chlorophyll was removed using an ethanol series from 50% (v/v) to 100% (v/v). Tissues were then cleared with 50% to 100% (v/v) Roti®- Histol followed by overnight incubation in immersion oil. Analysis of fluorescence reporter expression was performed using a LSM510 Meta confocal microscope. Counterstaining of root cell walls was achieved by mounting roots in 10µM propidium iodide (PI). The RNeasy plant mini kit (Quiagen) was used for RNA extraction. RNA was treated with DNase (Fermentas) and transcribed into cDNA using SuperScriptII (Invitrogen™). qRT-PCR was performed in triplicates using the Mesa Blue Sybr Mix (Eurogentec) and a Chromo4 real-time PCR machine (Bio-Rad). Expression levels were normalized to the reference gene *At4g34270* (Czechowski et al., 2005).

Phenotypic Analysis and Microscopy

Analyses of embryos was performed as described in Bureau et al., 2010. SEM analyses was performed according to Kwiatkowska, 2004. Root architecture was studied with the mPSPI method (Truernit et al., 2008) and imaged with a Zeiss LSM 510 Meta laser scanning microscope. For size measurements, floral organs were separated from each other and imaged

with an AxioCam ICC1 camera (Zeiss) mounted onto a Zeiss Stemi 2000C. Comparison of cell sizes was achieved by printing petals with 1.5% agarose. Image acquisition was carried out with an Axiocam HR camera attached to a Zeiss Axioscope II microscope. Images were processed in ImageJ software and assembled in Adobe Photoshop.

Supplemental Data

The following materials are available in the online version of this article.

Supplemental Figure 1: Molecular and phenotypic analyses of the novel *jlo* alleles.

Supplemental Figure 2: *jlo-2/+ as2-2* double mutant analysis.

Supplemental Figure 3: The *JLO* gain-of-function phenotype requires AS2 activity.

Supplemental Figure 4: Interaction of JLO and AS2 with LBD31 and LBD2.

Supplemental Figure 5: Intracellular localizations of LBD31 and LBD2 and time course experiment.

Acknowledgements

We are grateful to Cornelia Gieseler and Carin Theres for technical support and members of the R. Simon and D. Schubert laboratory for critical comments. We specifically thank Jennifer C. Fletcher and JiHyung Jun for providing the *AS2::GUS* line, Andrea Bleckmann for the modified pMDC7 vectors and for the help with confocal microscopy, Yvonne Stahl for the help with whole mount RNA *in situ* hybridization and Stefan Schmid for information's about the analyses of LBD protein interactions. We thank Jiri Friml, Miltos Tsiantis and Wolfgang Werr for generously supplying plant materials. This work was supported by a grant from the Deutsche Forschungsgemeinschaft (DFG, Si 947/4-1) to R.S.

5.1.6. References

Aida, M., and Tasaka, M. (2006). Genetic control of shoot organ boundaries. Curr Opin Plant Biol **9,** 72-77.

Aida, M., Ishida, T., and Tasaka, M. (1999). Shoot apical meristem and cotyledon formation during Arabidopsis embryogenesis: interaction among the CUP-SHAPED COTYLEDON and SHOOT MERISTEMLESS genes. Development **126,** 1563-1570.

Albertazzi, L., Arosio, D., Marchetti, L., Ricci, F., and Beltram, F. (2009). Quantitative FRET analysis with the EGFP-mCherry fluorescent protein pair. Photochem Photobiol **85,** 287-297.

Belles-Boix, E., Hamant, O., Witiak, S.M., Morin, H., Traas, J., and Pautot, V. (2006). KNAT6: an Arabidopsis homeobox gene involved in meristem activity and organ separation. Plant Cell **18,** 1900-1907.

Benkova, E., Michniewicz, M., Sauer, M., Teichmann, T., Seifertova, D., Jurgens, G., and Friml, J. (2003). Local, efflux-dependent auxin gradients as a common module for plant organ formation. Cell **115,** 591-602.

Bleckmann, A., Weidtkamp-Peters, S., Seidel, C.A., and Simon, R. (2010). Stem cell signaling in Arabidopsis requires CRN to localize CLV2 to the plasma membrane. Plant Physiol **152,** 166-176.

Blilou, I., Xu, J., Wildwater, M., Willemsen, V., Paponov, I., Friml, J., Heidstra, R., Aida, M., Palme, K., and Scheres, B. (2005). The PIN auxin efflux facilitator network controls growth and patterning in Arabidopsis roots. Nature **433,** 39-44.

Borghi, L., Bureau, M., and Simon, R. (2007). Arabidopsis JAGGED LATERAL ORGANS is expressed in boundaries and coordinates KNOX and PIN activity. Plant Cell **19,** 1795-1808.

Brewer, P.B., Heisler, M.G., Hejatko, J., Friml, J., and Benkova, E. (2006). In situ hybridization for mRNA detection in Arabidopsis tissue sections. Nat Protoc **1,** 1462-1467.

Bureau, M., Rast, M.I., Illmer, J., and Simon, R. (2010). JAGGED LATERAL ORGAN (JLO) controls auxin dependent patterning during development of the Arabidopsis embryo and root. Plant Mol Biol **74,** 479-491.

Byrne, M.E., Simorowski, J., and Martienssen, R.A. (2002). ASYMMETRIC LEAVES1 reveals knox gene redundancy in Arabidopsis. Development **129,** 1957-1965.

Byrne, M.E., Barley, R., Curtis, M., Arroyo, J.M., Dunham, M., Hudson, A., and Martienssen, R.A. (2000). Asymmetric leaves1 mediates leaf patterning and stem cell function in Arabidopsis. Nature **408,** 967-971.

Clough, S.J., and Bent, A.F. (1998). Floral dip: a simplified method for Agrobacterium-mediated transformation of Arabidopsis thaliana. Plant J **16,** 735-743.

Czechowski, T., Stitt, M., Altmann, T., Udvardi, M.K., and Scheible, W.R. (2005). Genome-wide identification and testing of superior reference genes for transcript normalization in Arabidopsis. Plant Physiol **139,** 5-17.

Egea-Cortines, M., Saedler, H., and Sommer, H. (1999). Ternary complex formation between the MADS-box proteins SQUAMOSA, DEFICIENS and GLOBOSA is involved in the control of floral architecture in Antirrhinum majus. Embo J **18,** 5370-5379.

Friml, J., Vieten, A., Sauer, M., Weijers, D., Schwarz, H., Hamann, T., Offringa, R., and Jurgens, G. (2003). Efflux-dependent auxin gradients establish the apical-basal axis of Arabidopsis. Nature **426,** 147-153.

Galweiler, L., Guan, C., Muller, A., Wisman, E., Mendgen, K., Yephremov, A., and Palme, K. (1998). Regulation of polar auxin transport by AtPIN1 in Arabidopsis vascular tissue. Science **282,** 2226-2230.

Guo, M., Thomas, J., Collins, G., and Timmermans, M.C. (2008). Direct repression of KNOX loci by the ASYMMETRIC LEAVES1 complex of Arabidopsis. Plant Cell **20,** 48-58.

Hay, A., Barkoulas, M., and Tsiantis, M. (2006). ASYMMETRIC LEAVES1 and auxin activities converge to repress BREVIPEDICELLUS expression and promote leaf development in Arabidopsis. Development **133,** 3955-3961.

Heisler, M.G., Ohno, C., Das, P., Sieber, P., Reddy, G.V., Long, J.A., and Meyerowitz, E.M. (2005). Patterns of auxin transport and gene expression during primordium development revealed by live imaging of the Arabidopsis inflorescence meristem. Curr Biol **15,** 1899-1911.

Husbands, A., Bell, E.M., Shuai, B., Smith, H.M., and Springer, P.S. (2007). LATERAL ORGAN BOUNDARIES defines a new family of DNA-binding transcription factors and can interact with specific bHLH proteins. Nucleic Acids Res **35,** 6663-6671.

Iwakawa, H., Iwasaki, M., Kojima, S., Ueno, Y., Soma, T., Tanaka, H., Semiarti, E., Machida, Y., and Machida, C. (2007). Expression of the ASYMMETRIC LEAVES2 gene in the adaxial domain of Arabidopsis leaves represses cell proliferation in this domain and is critical for the development of properly expanded leaves. Plant J **51,** 173-184.

Iwakawa, H., Ueno, Y., Semiarti, E., Onouchi, H., Kojima, S., Tsukaya, H., Hasebe, M., Soma, T., Ikezaki, M., Machida, C., and Machida, Y. (2002). The ASYMMETRIC LEAVES2 gene of Arabidopsis thaliana, required for formation of a symmetric flat leaf lamina, encodes a member of a novel family of proteins characterized by cysteine repeats and a leucine zipper. Plant Cell Physiol **43,** 467-478.

Jun, J.H., Ha, C.M., and Fletcher, J.C. (2010). BLADE-ON-PETIOLE1 coordinates organ determinacy and axial polarity in arabidopsis by directly activating ASYMMETRIC LEAVES2. Plant Cell **22,** 62-76.

Koncz, C., Kreuzaler, F., Kalman, Z., and Schell, J. (1984). A simple method to transfer, integrate and study expression of foreign genes, such as chicken ovalbumin and alpha-actin in plant tumors. Embo J **3,** 1029-1037.

Kwiatkowska, D. (2004). Surface growth at the reproductive shoot apex of Arabidopsis thaliana pinformed 1 and wild type. J Exp Bot **55,** 1021-1032.

Lin, W.C., Shuai, B., and Springer, P.S. (2003). The Arabidopsis LATERAL ORGAN BOUNDARIES-domain gene ASYMMETRIC LEAVES2 functions in the repression of KNOX gene expression and in adaxial-abaxial patterning. Plant Cell **15,** 2241-2252.

Naito, T., Yamashino, T., Kiba, T., Koizumi, N., Kojima, M., Sakakibara, H., and Mizuno, T. (2007). A link between cytokinin and ASL9 (ASYMMETRIC LEAVES 2 LIKE 9) that belongs to the AS2/LOB (LATERAL ORGAN BOUNDARIES) family genes in Arabidopsis thaliana. Biosci Biotechnol Biochem **71,** 1269-1278.

Ori, N., Eshed, Y., Chuck, G., Bowman, J.L., and Hake, S. (2000). Mechanisms that control knox gene expression in the Arabidopsis shoot. Development **127,** 5523-5532.

Paponov, I.A., Teale, W.D., Trebar, M., Blilou, I., and Palme, K. (2005). The PIN auxin efflux facilitators: evolutionary and functional perspectives. Trends Plant Sci **10,** 170-177.

Phelps-Durr, T.L., Thomas, J., Vahab, P., and Timmermans, M.C. (2005). Maize rough sheath2 and its Arabidopsis orthologue ASYMMETRIC LEAVES1 interact with HIRA, a predicted histone chaperone, to maintain knox gene silencing and determinacy during organogenesis. Plant Cell **17,** 2886-2898.

Rast, M.I., and Simon, R. (2008). The meristem-to-organ boundary: more than an extremity of anything. Curr Opin Genet Dev **18,** 287-294.

Reinhardt, D., Pesce, E.R., Stieger, P., Mandel, T., Baltensperger, K., Bennett, M., Traas, J., Friml, J., and Kuhlemeier, C. (2003). Regulation of phyllotaxis by polar auxin transport. Nature **426,** 255-260.

Semiarti, E., Ueno, Y., Tsukaya, H., Iwakawa, H., Machida, C., and Machida, Y. (2001). The ASYMMETRIC LEAVES2 gene of Arabidopsis thaliana regulates formation of a symmetric lamina, establishment of venation and repression of meristem-related homeobox genes in leaves. Development **128,** 1771-1783.

Shuai, B., Reynaga-Pena, C.G., and Springer, P.S. (2002). The lateral organ boundaries gene defines a novel, plant-specific gene family. Plant Physiol **129,** 747-761.

Soyano, T., Thitamadee, S., Machida, Y., and Chua, N.H. (2008). ASYMMETRIC LEAVES2-LIKE19/LATERAL ORGAN BOUNDARIES DOMAIN30 and ASL20/LBD18 regulate tracheary element differentiation in Arabidopsis. Plant Cell **20,** 3359-3373.

Theissen, G., and Saedler, H. (2001). Plant biology. Floral quartets. Nature **409,** 469-471.

Truernit, E., Bauby, H., Dubreucq, B., Grandjean, O., Runions, J., Barthelemy, J., and Palauqui, J.C. (2008). High-resolution whole-mount imaging of three-dimensional tissue organization and gene expression enables the study of phloem development and structure in Arabidopsis. Plant Cell **20,** 1494-1503.

Tsiantis, M., Brown, M.l., Skibinski, G., and Langdale, J.A. (1999). Disruption of auxin transport is associated with aberrant leaf development in maize. Plant Physiol **121,** 1163-1168.

Ulmasov, T., Murfett, J., Hagen, G., and Guilfoyle, T.J. (1997). Aux/IAA proteins repress expression of reporter genes containing natural and highly active synthetic auxin response elements. Plant Cell **9,** 1963-1971.

Vernoux, T., Kronenberger, J., Grandjean, O., Laufs, P., and Traas, J. (2000). PIN-FORMED 1 regulates cell fate at the periphery of the shoot apical meristem. Development **127,** 5157-5165.

Vieten, A., Vanneste, S., Wisniewska, J., Benkova, E., Benjamins, R., Beeckman, T., Luschnig, C., and Friml, J. (2005). Functional redundancy of PIN proteins is accompanied by auxin-dependent cross-regulation of PIN expression. Development **132,** 4521-4531.

Williams, R.W. (1998). Plant homeobox genes: many functions stem from a common motif. Bioessays **20,** 280-282.

Xu, B., Li, Z., Zhu, Y., Wang, H., Ma, H., Dong, A., and Huang, H. (2008). Arabidopsis genes AS1, AS2, and JAG negatively regulate boundary-specifying genes to promote sepal and petal development. Plant Physiol **146,** 566-575.

Xu, L., Xu, Y., Dong, A., Sun, Y., Pi, L., Xu, Y., and Huang, H. (2003). Novel as1 and as2 defects in leaf adaxial-abaxial polarity reveal the requirement for ASYMMETRIC LEAVES1 and 2 and ERECTA functions in specifying leaf adaxial identity. Development **130,** 4097-4107.

Zazimalova, E., Krecek, P., Skupa, P., Hoyerova, K., and Petrasek, J. (2007). Polar transport of the plant hormone auxin - the role of PIN-FORMED (PIN) proteins. Cell Mol Life Sci **64,** 1621-1637.

Zgurski, J.M., Sharma, R., Bolokoski, D.A., and Schultz, E.A. (2005). Asymmetric auxin response precedes asymmetric growth and differentiation of asymmetric leaf1 and asymmetric leaf2 Arabidopsis leaves. Plant Cell **17,** 77-91.

Zhu, Y., Li, Z., Xu, B., Li, H., Wang, L., Dong, A., and Huang, H. (2008). Subcellular localizations of AS1 and AS2 suggest their common and distinct roles in plant development. J Integr Plant Biol **50,** 897-905.

5.1.7. Suplemental Data

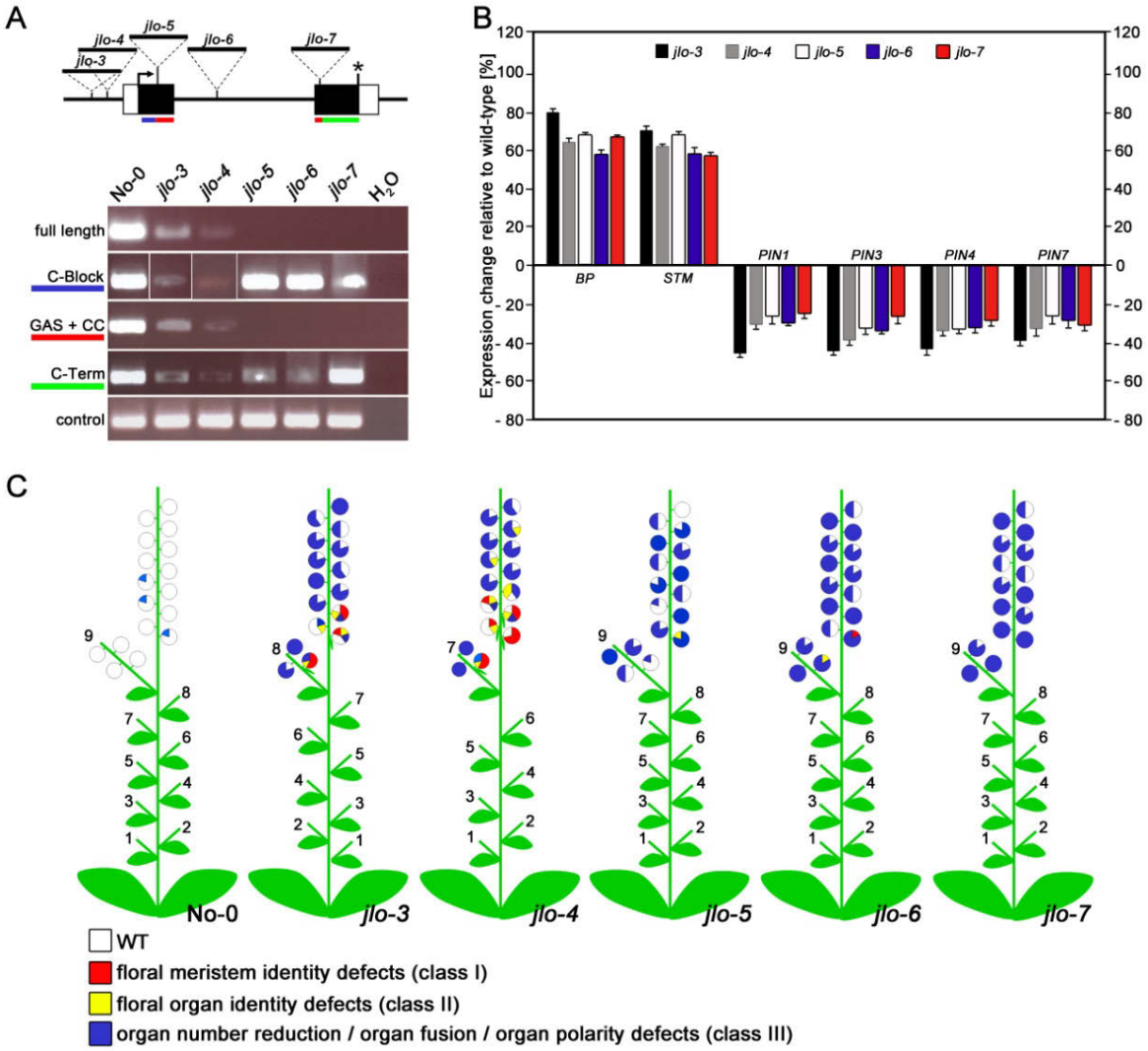

Suppl. Fig 1: Molecular and phenotypic analyses of the novel *jlo* alleles. (A) RT-PCR was performed with total RNA isolated from seedlings (5DAG) of the indicated genetic backgrounds to examine *JLO* transcript levels. Amplified transcripts (blue/red/green) and insertion positions are indicated in the gene model above. *jlo-3* and *jlo-4* seedlings show a reduction in *JLO* transcript level respectively. No full length transcript could be detected in homozygous *jlo-5* to *jlo-7* mutants but shortened transcripts 5' and 3' of the insertions. control: eIF4a. (B) qRT-PCR analysis of *BP, STM, PIN1, PIN3, PIN4* and *PIN7* transcript levels in homozygous *jlo-3* to *jlo-7* seedling (5DAG). *BP* and *STM* transcript levels are elevated while *PIN* gene expression is reduced. (C) Statistic analyses of floral phenotypes displayed by the different *jlo* alleles. A minimum of five plants were analyzed for each genetic background. The occurrence of each phenotypic class (I-III) within the first flower (circles) at main shoot and last side shoot is indicated as color code (white: wild-type flower; red: floral meristem identity defects (class I); yellow: floral organ identity defects (class II); blue: organ number, fusion, polarity defects (class III)). The average number of side shoots is show. Note that class I and class II phenotype were primarily found in the first flower of *jlo-3* and *jlo-4* mutants. These plants developed less side shoots than wild-type plants (No-0). Bars in (B) indicate standard errors (N ≥ 3).

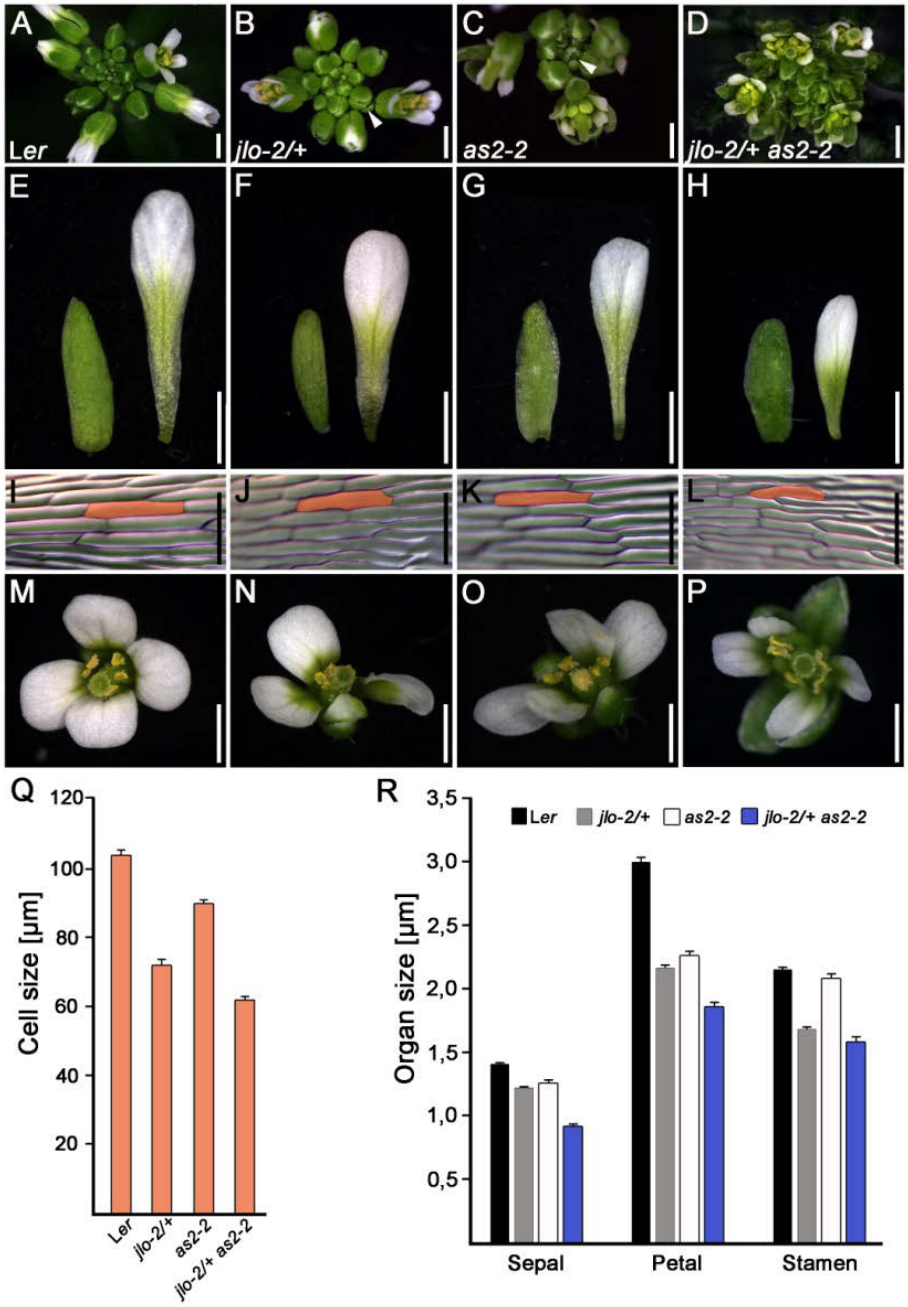

Suppl. Fig. 2: *jlo-2/+ as2-2* double mutant analysis. (A-D) Inforescences of wild-type L*er* (A); *jlo-2/+* (B); *as2-2* (C); *jlo-2/+ as2-2* (D) plants. Arrows indicate prematurely opened flowers. (E-H) Sepals and petals of L*er* (E); *jlo-2/+* (B); *as2-2* (G) and *jlo-2/+ as2-2* (D) flower. (I-L) Agarose prints were taken from the adaxial sepal surfaces to measure cell length (indicated in orange). Compared to L*er* (I) cell length is reduced in *jlo-2/+* (J) and *as2-2* (K) and further reduced in the double mutant (L). (M-P) Top view of flowers from L*er* (M); *jlo-2/+* (N); *as2-2* (O) and *jlo-2/+ as2-2* (P) plants. Mutants reveal defects in petal polarity and growth. (Q) Size of petal cells measured form agarose prints. Cell length is reduced in *jlo-2/+* and *as2-2* mutants and even more reduced in *jlo-2/+ as2-2* double mutants. (R) Sepal, petal and stamen size of L*er, jlo-2/+, as2-2* and *jlo-2/+ as2-2* flowers. Sepal and petal sizes are reduced in either single mutant and further reduced in the double mutant. Scale bars: (A-H; M-P): 1mm; (I-L): 50µm

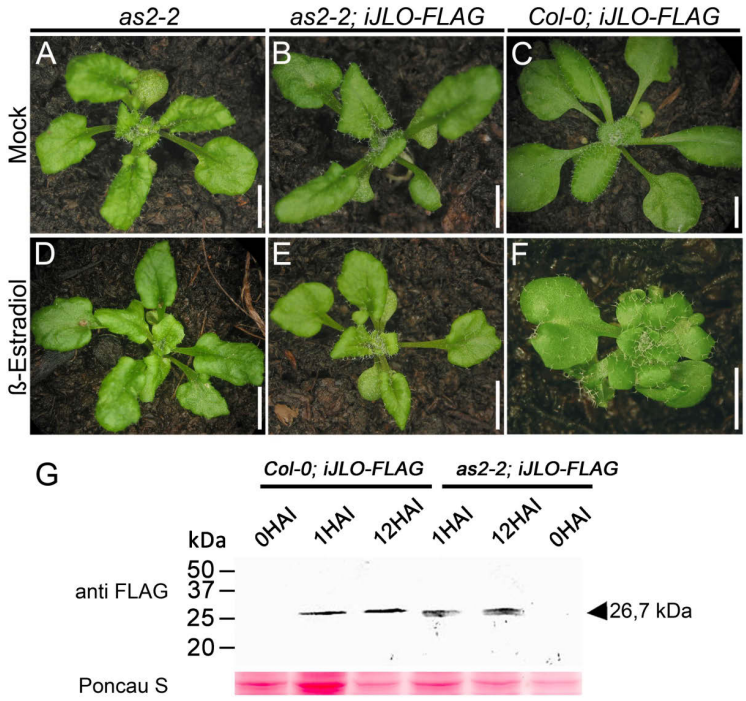

Suppl. Fig. 3: The *JLO* gain-of-function phenotype requires AS2 activity. (A-F) *as2-2* (A/D), *as2-2, iJLO-FLAG* (B/E) and *Col-0, iJLO-FLAG* (C/F) plants at 25DAG. (A-C) Untreated controls (D-F) ß-estradiol induced plants. JLO overexpression in WT (Col-0) background resulted in leaf lobing (F). Misexpression in *as2-2* mutant background did not alter the leaf morphology (E). (G) Western blot analysis with an anti-FLAG antibody to confirm the presence of the JLO-FLAG fusion protein (expected size 26.7 kDa), one hour or twelve hours after induction (HAI). Ponceau S stained protein bands of Rubisco are shown as loading control. Scale bars: 1cm

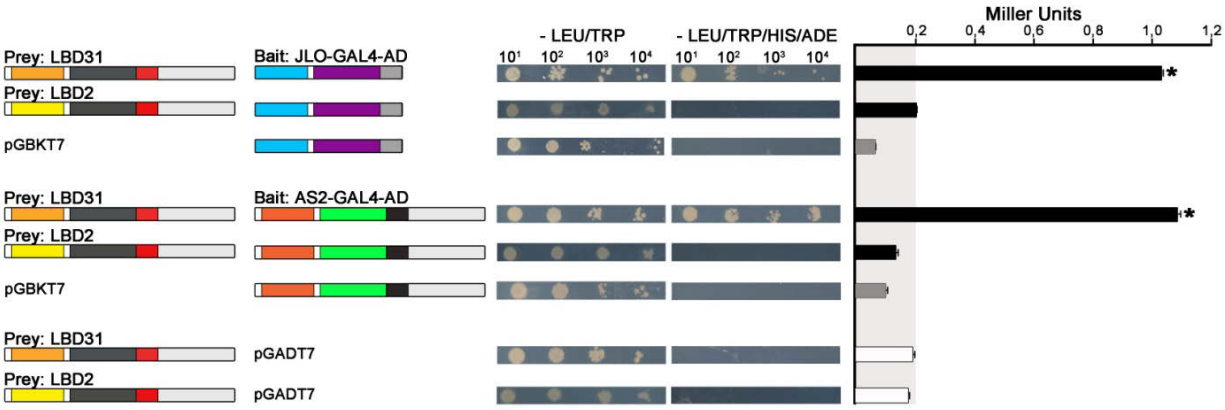

Suppl. Fig 4: Interaction of JLO and AS2 with LBD31 and LBD2. Matings with empty pGADT7 and pGBKT7 vectors were used to exclude autoactivation. Growth on nonselective media (-LEU/TRP) was used to confirm the presence of both plasmids. Full length AS2 and JLO LOB domain fused to the GAL4-AD were used for interaction studies. Full length LBD31 and LBD2 were fused to GAL4-BD. Matings revealed interaction between JLO and LBD31 as well as AS2 and LBD31 (growth on selective media -LEU/TRP/HIS/ADE). By contrast, no growth on selective media was observed with zygotes co-expressing JLO/LBD2 and AS2/LBD2. All yeast two hybrid results were verified via calculation of Miller Units in a liquid culture assay (black bars). Miller Units given by zygotes co-expressing fusion proteins and empty pGADT7 (white bars) or pGBKT7 vector (grey bars) were used to calculate the background (grey shadowed). Bars indicate standard errors. Student's t-test was used for statistic analysis (asterisk: significant difference to the background $p \geq 0.05$). Leu: Leucine; Trp: Tryptophan; His: Histidine; ADE: Adenine; C-BLOCK: blue (JLO); red (AS2); orange (LBD31); yellow (LBD2); GAS-BLOCK: lilac (JLO); green (AS2); grey (LBD31/LBD2); Coiled coil: grey (JLO); black (AS2); red (LBD31/LBD2).

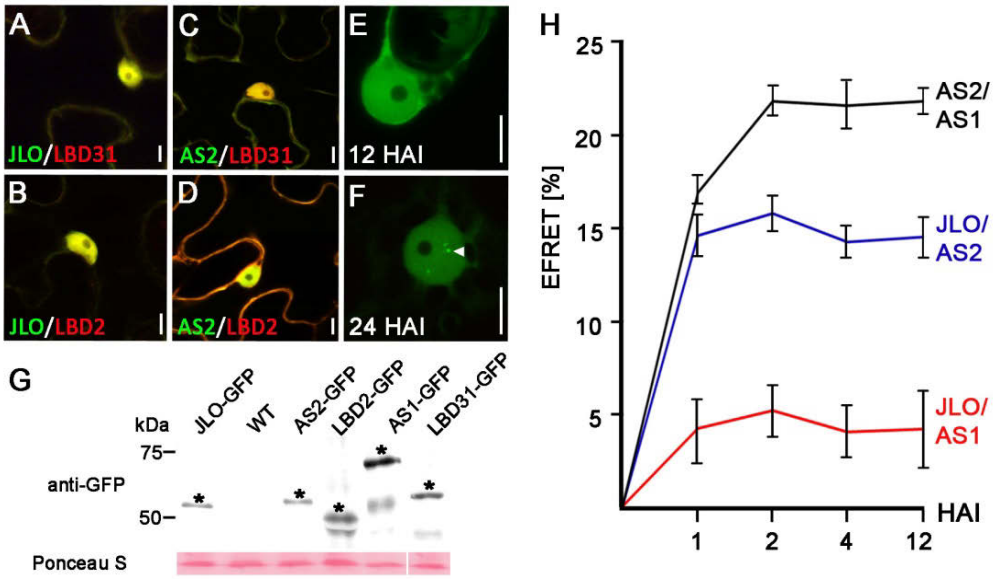

Suppl. Fig.5: Intracellular localizations of LBD31 and LBD2 and time course experiment. (A-D) Colocalization of the JLO, AS2, LBD31 and LBD2 fluorescence tagged fusion proteins in *N. benthamiana* epidermis cells. (E/F) Nuclear expression of JLO-GFP at 12HAI and 24HAI. Fluorescent aggregates (C, arrowhead) become visible after 24HAI. (G) Western blot analysis with an anti-GFP antibody. Protein bands at the expected size are marked with asterisks. Ponceau S stained Rubisco protein bands are shown as loading control. (H) E_{FRET} measured with a transient expression of FP-tagged protein in epidermis cells of *N. benthamiana* (N≥20 for each combination and time point). Measurements were performed at 1/2/4 and 12HAI with 20µM ß-estradiol to determine the effect of protein concentration on E_{FRET}. Scale bars: 10µm; Bars in (H) indicate standard error. kDa: kilo Dalton; HAI: hours after induction.

CHAPTER VI

CONCLUDING DISCUSSION

6. CONCLUDING DISCUSSION

The development of the body plan in plants or animals is controlled by large regulatory networks. These networks include a range of transcription factors that precisely coordinate the temporal and spatial developmental programs. The *LATERAL ORGAN BOUNDARY DOMAIN* (*LBD*) gene family encodes plant specific transcription factors, involved in such regulatory processes (Shuai et al., 2002; reviewed Majer et al., 2010). The *LBD* gene family thereby shares several characteristics with other large families of transcription factors.

6.1. LBD transcription factors contribute to complex regulatory networks

Phylogenic studies indicated that the high number of *LBD* genes in *Arabidopsis* (43 members; Shuai et al., 2002), and other species like rice (35 members; Yang et al., 2006) or maize (43 members; Schnable et al., 2009), derived from duplication events. Gene duplications serve as a mechanism to increase diversity at the molecular level (Ohno et al., 1968; Averof et al., 1995). The subsequent mutation of a duplicated locus is a primary contributor to evolve new developmental programs. By acquisition or deletion of regulatory elements, coding regions can be brought into a new regulatory context. This results in a modification of the spatial and temporal transcriptional profiles of duplicated genes. These changes in gene expression, rather than changes in the protein structure, are important to acquire novel gene functions (Mayer, 1996; reviewed in Reiser et al., 2000). Such duplication and diversification events are involved in the evolution of many plant and animal transcription factor families (Purugganan et al., 1995; Reiser et al., 2000; Holland et al., 1994). In line with this, *LBD* genes were found to be expressed in a variety of temporal- and tissue-specific patterns and published data implicated several family members in different developmental processes (Matsumura et al., 2009; Shuai et al., 2002; reviewed Majer et al., 2010).

Transcription factors often function in protein complexes which can involve related and unrelated proteins. Such activities were, among others, reported for MADS Box proteins in plants (Theissen et al., 2001; Honma et al., 2001) as well as for HOX Homedomain proteins in animals (Mann et al., 1998). These interactions are known to affect the activities of transcription factors as activators or repressors of different target genes. Based on my results and published data, LBD transcription factors act in a similar fashion (Husbands et al., 2007; Guo et al., 2008). I found that LBD proteins have the capacity to interact with other LBD proteins as JLO, AS2 and LBD31 can bind to each other *in vivo* (chapter 5.1.3.9). Similar results were obtained by S. Schmid who studied LBD interactions in various combinations (pers. communication). Furthermore, I found that JLO and AS2 form a trimeric complex with the MYB domain protein AS1 (chapter 5.1.3.7). Therefore, interactions between related and unrelated proteins in different tissues likely modulate the DNA-binding specificity and transcrip-

tional activity of LBD proteins. This leads to the hypothesis that LBD proteins undergo a wide range of combinatorial interactions which determines their effects on target gene expression.

This notion is consistent with the results obtained in this work. I found that JLO and AS2 jointly contribute to the regulation of *KNOX* and *PIN* gene expression. Both proteins act thereby in heteromeric, but also in homomeric complexes. My results also indicate that, depending composition, these complexes can trigger differential responses of target genes. This is demonstated by the observation that JLO homomers promote *PIN4* transcription, JLO/AS2 heteromers control normal *PIN4* levels, and AS2 homomers act to repress *PIN4* expression (discussed in chapter 5.1.4).

Shuttling of proteins between cell compartments is a common mechanism to regulate their activity. For example the phosphorylation status of the transcription factors BRI1 EMS SUPPRESSOR1 (BES1) and BRASSINAZOLE-RESISTANT 1 (BZR1), involved in brassinosteriod (BR) signal transduction, regulates their subcellular localization. BR signaling was shown to induce a nuclear localization by promoting dephosphorylation. In contrast, phosphorylation of BES1 and BZR1 results in binding of 14-3-3 proteins to these transcription factors and their cytoplasmic retention (Eckardt, 2007; Gampala et al., 2007). I found a predominant nuclear but also a cytoplasmic localization of fluorescent tagged JLO, AS2, LBD31 and LBD2 fusion proteins (chapter 5.1.3.8). Moreover, immunodetection experiments in *Arabidopsis* roots, using an antibody for specific detection of JLO, also showed this dual localization (chapter 4.1.5). Similar results were previously published for various other LBD proteins (Husbands et al., 2007; Iwakawa et al., 2002; Naito et al., 2007; Zhu et al., 2008). Therefore, these results could indicate a compartmentalization of LBD proteins into an active fraction in the nucleus and an inactive fraction in the cytoplasm. I could not identify a NLS (nuclear localization signal) or NES (nuclear export signal) signal by *in silico* studies of LBD proteins (http://smart.embl-heidelberg.de/). It therefore remains to be determined whether specific partners regulate LBD transcription factor activity by controlling their availability to the nuclear-import machinery.

Taken together, these observations suggest that *LBD* family members are involved in complex regulatory networks in *Arabidopsis*. This can include spatially and temporally restricted developmental roles, partially overlapping functions in tissues where related LBD genes are expressed together, combinatorial activities in protein complexes and, potentially, a regulation of LBD protein activity by dislocation between the nucleus and the cytoplasm.

6.2. Conclusions

How can these observations been associated with the results obtained by reverse genetic approaches? First of all, a functional characterization by phenotypic analysis of single knock-out mutants can be difficult. In contrast to *jlo* mutants, which reveal strong patterning defects (discussed in chapter 4.2), other *lbd* mutations only cause subtle morphological changes. This reflects regulatory roles in very specific developmental processes, as well as partially overlapping functions of LBD proteins. Without a clear expectation concerning the regulatory roles of the analyzed transcription factors, such mild phenotypic defects are easily overlooked. Such an approach can therefore provide information about the genuine gene activity but in most cases requires prior knowledge about gene expression domains (discussed in chapter 3.2).

It is also important to note that ectopic expression of *LBD* family members can cause (1) a misregulation of specific target genes, (2) a misexpression of genes which are normally regulated by other family members, and (3) a dimerization of LBD proteins in tissues where they usually not co-localize. Therefore, these overexpression experiments can generally uncover a spectrum of signal pathways in which LBD transcription factors are involved. Further experiments are then required to distinguish between the three alternatives mentioned above. The primary necessity will again be to elucidate the spatial and temporal expression pattern. This will provide first information about direct and indirect consequences of *LBD* overexpression and will help to narrow down the tissues in which *LBD* gain-of-function phenotypes should be further studied.

6.3. Perspectives

To date, a subset of *LBD* genes have been functionally characterized, whereas the roles of other family members remain to be determined. Therefore, a comprehensive analysis of *LBD* gene function in *Arabidopsis thaliana* will be a major task for the future. The aim will be to understand the complex regulatory networks in which large families of transcription factors, like the LBD family, are involved. A number of molecular and imaging methods can help to gain more insight into such regulatory interactions.

In the recent years, fluorescence measurements and analysis techniques have been strongly improved. These measurements possess a very high sensitivity and can be performed on single molecules. In this respect, the establishment of transgenic lines expressing fluorescent protein (FP) tagged LBD fusion proteins under control of their endogenous promoters will combine several advantages. First of all, this will provide information about spatial and temporal expression patterns as well as differential protein concentrations in *Arabidopsis.* This is possible because fluorescence intensity is linearly dependent on the number of fluorophores in a sample, thus allowing quantitative measurements. Moreover, co-expression of differentially labeled LBD fusion proteins will help to monitor overlapping expression do-

mains and will allow a spatial examination of specific LBD protein interactions. So far, all FRET based interaction studies were performed after induced overexpression of FP tagged LBD proteins (chapter 5.1.3.9). This method provides information about constitutive protein interactions but does not allow studying the dynamics of complex formations. Using the endogenous promoter, fluorescent intensity analyses and FRET interaction studies with endogenous protein concentrations can be performed. Such experiments could provide information about spatial and potentially environmental cues under which specific interactions predominately occur. Time-resolved fluorescence measurements and analysis techniques, like FCS and FLIM (reviewed in Liu et al., 2008), will also help to gain more insight into the dynamics of regulatory networks involving LBD proteins.

Other methods can help to learn more about the regulatory roles of transcription factors. Recent studies showed for example that a subpopulation of fluorescing cells can be protoplasted and sorted without significantly disturbing their transcriptional status (Birnbaum et al., 2003; Nawy et al., 2005). Such cell-sorting strategies (FACS) could be used to obtain the transcriptional profile of LBD protein expressing cells. A comparison between wild-type and LBD loss- or gain-of-function mutants should provide information about a set of potential target genes. This approach combined with subsequent chromatin immunoprecipitation (ChIP) experiments and qRT-PCR analyses will help to specifically isolate direct target genes. Furthermore, DNA isolated in ChIP experiments can also be used as a probe for whole genome microarrays. Such ChiP-on-ChiP analyses would not only allow to confirm (or exclude) potential target gene sequences but also to identify novel direct targets.

Taken together, several techniques are available which can help optimizing the functional characterizations of transcription factor families in the future. A combination of such strategies will probably lead to a better understanding of the molecular mechanisms that determine *Arabidopsis* development.

CHAPTER VII

SUMMARY

7. SUMMARY

The *LATERAL ORGAN BOUNDARY DOMAIN* (*LBD*) genes encode plant-specific DNA-binding transcription factors. In *A. thaliana*, the *LBD* gene family is composed of 43 members. During the last years substantial progress has been made in uncovering the regulatory roles of LBD transcription factors and the *LBD* family members have been implicated in a variety of developmental processes. In this study, reverse genetic approaches were carried out in order to learn more about *LBD* gene functions. A functional characterization by phenotypic analysis of *LBD* gain and loss-of-function mutants turned out to be difficult, as LBD proteins contribute to complex regulatory networks.

The results of this work show that the *LBD* family member *JAGGED LATERAL ORGANS* (*JLO*) is an important regulator of patterning processes in *Arabidopsis*. This is demonstrated by an aberrant embryonic development, defective lateral organ formation and separation, altered root architecture and a premature arrest of root and shoots meristem activity in *jlo* mutants. Some of these phenotypic aspects could be traced back to impaired auxin transport and signal transduction. Genetic studies, gene expression analyses and exogenous auxin treatment implicated a role for JLO in the transcriptional regulation of the auxin receptor TRANSPORT INHIBITOR RESPONSE 1 (TIR1). Reduced *TIR1* expression in *jlo* mutants causes a stabilization of the Aux/IAA protein BODENLOS (BDL). The failure to release the ARF transcription factor MONOPTEROS (MP) from BDL repression is partially the cause for a misexpression of several auxin regulated genes in *jlo* mutants. These genes comprise members of the *PINFORMED* (*PIN*) and *PLETHORA* (*PLT*) family as well as *AUXIN RESISTANT1* (*AUX1)* and *WUSCHEL-RELATED HOMEOBOX 5* (*WOX5*). Therefore, *JLO* can be considered to be a central regulator of auxin signaling and distribution during *Arabidopsis* development.

Furthermore, *JLO* was found to repress the expression of the class I *KNOX* genes *SHOOT MERISTEMLESS* (*STM*) and *BREVIPEDICELLUS* (*BP*) in lateral organs. Interaction studies and double mutant analyses provide evidence that JLO thereby acts in homomeric as well as in heteromeric complexes with ASYMMETRIC LEAVES 2 (AS2), another LBD protein. Moreover, AS2 can mediate an interaction between JLO and ASYMMETRIC LEAVES1 (AS1). This trimeric protein complex acts to promote organ development through restriction of *BP* expression from lateral organs.

Interestingly, JLO and AS2 also jointly contribute to the regulation of *PIN* genes in roots. Again, both proteins function in a heteromeric complex, but also independently from each other. This indicates that JLO and AS2 act in a combinatorial fashion. Both LBD proteins integrate the regulation of *KNOX* expression with the control of hormonal signaling. In further studies, LBD31 was identified to interact with JLO as well as with AS2. This result opens up the possibility for different or higher order LBD complexes in *Arabidopsis*.

7.1. ZUSAMMENFASSUNG

Die *LATERAL ORGAN BOUNDARY DOMAIN* (*LBD*) Gene kodieren pflanzenspezifische DNA-bindende Transkriptionsfaktoren. In *A. thaliana* besteht die *LBD* Genfamilie aus 43 Mitgliedern. In den letzten Jahren konnten große Fortschritte in der Aufdeckung der regulatorischen Funktionen von LBD Transkriptionsfaktoren verzeichnet werden und *LBD* Familienmitglieder wurden in eine Reihe verschiedenster Entwicklungsprozesse einbezogen. In dieser Studie wurde die Methode der reversen Genetik gewählt, um mehr Einblick in die *LBD* Genfunktionen in *Arabidopsis* zu erhalten. Eine funktionelle Charakterisierung durch die phänotypische Analysen von LBD Überexpressions,- und Funktionsverlustmutanten war dabei schwierig, da LBD Proteine in komplexen regulatorischen Netzwerken wirken.

Die Ergebnisse dieser Arbeit zeigen, dass das *LBD* Familienmitglied *JAGGED LATERAL ORGANS (JLO)* ein wichtiger Regulator von Musterbildungsprozessen in *Arabidopsis* ist. Dies zeigt sich in einer fehlerhaften Embryonalentwicklung, Defekten in der Bildung und Separierung lateraler Organe, einer veränderten Wurzelarchitektur, sowie einem vorzeitigen Arrest des Wurzel- und Sproßapikalmeristems. Einige dieser phänotypischen Aspekte konnten auf eine Störung der Auxinverteilung und Signaltransduktion zurückgeführt werden. Genetische Studien, Expressionsanalysen sowie externe Behandlung mit Auxin zeigten, dass JLO die Transkription des Auxinrezeptors TRANSPORT INHIBITOR RESPONSE 1 (TIR1) reguliert. Die reduzierte *TIR1* Expression in *jlo* Mutanten führt zu einer Stabilisierung des Aux/IAA Proteins BODENLOS (BDL). Dadurch wird die Funktion des Transkriptionsfaktors MONOPTEROS (MP) durchgehend von BDL inhibiert, was zum Teil der Grund für eine Fehlexpression verschiedener auxinregulierter Gene in *jlo* Mutanten ist. Diese Gene umfassen Mitglieder der *PINFORMED* (*PIN)* und *PLETHORA* (*PLT)* Familien sowie *AUXIN RESISTANT1* (*AUX1)* und *WUSCHEL-RELATED HOMEOBOX 5* (*WOX5)*. Daher kann *JLO* als ein zentraler Regulator der Auxin-Signaltransduktion und Verteilung in der Entwicklung von *Arabidopsis* betrachtet werden.

Desweiteren konnte gezeigt werden, dass *JLO* die Expression der Klasse I *KNOX* Gene *SHOOT MERISTEMLESS* (*STM*) und *BREVIPEDICELLUS* (*BP*) in lateralen Organen reprimiert. Interaktionsstudien und Doppelmutantenanalysen zeigten, dass JLO dabei in homomeren und heteromeren Proteinkomplexen mit ASYMMETRIC LEAVES 2 (AS2) agiert, einem weiteren LBD Protein. Ferner wurde gezeigt, dass AS2 eine Interaktion zwischen JLO und ASYMMETRIC LEAVES 1 (AS1) vermittelt. Dieser trimere Komplex begünstigt die Organentwicklung durch die Repression von *BP* in lateralen Organen.

Interessanterweise sind JLO und AS2 ebenfalls gemeinsam an der Regulation von *PIN* Genen in der Wurzel beteiligt. Auch hier wirken beide Proteine in einem Komplex, aber auch separat voneinander. Dies deutet daraufhin, dass JLO und AS2 in einer kombinatorischen Weise wirken. Beide LBD Proteine verbinden dabei die Regulation von *KNOX* Genexpressi-

on mit der Kontrolle von hormonellen Signalen. In weiteren Interaktionsstudien wurde LBD31 als ein Interaktionspartner von JLO, sowie von AS2 identifiziert. Dies eröffnet die Möglichkeit, dass verschiedene oder größere LBD Proteinkomplexe in *Arabidopsis* existieren.

CHAPTER VIII

LITERATURE

8. LITERATURE

Aida, M., and Tasaka, M. (2006). Genetic control of shoot organ boundaries. Curr Opin Plant Biol **9,** 72-77.

Aida, M., Ishida, T., and Tasaka, M. (1999). Shoot apical meristem and cotyledon formation during Arabidopsis embryogenesis: interaction among the CUP-SHAPED COTYLEDON and SHOOT MERISTEMLESS genes. Development **126,** 1563-1570.

Aida, M., Beis, D., Heidstra, R., Willemsen, V., Blilou, I., Galinha, C., Nussaume, L., Noh, Y.S., Amasino, R., and Scheres, B. (2004). The PLETHORA genes mediate patterning of the Arabidopsis root stem cell niche. Cell **119,** 109-120.

Albertazzi, L., Arosio, D., Marchetti, L., Ricci, F., and Beltram, F. (2009). Quantitative FRET analysis with the EGFP-mCherry fluorescent protein pair. Photochem Photobiol **85,** 287-297.

Ausubel, F.M. (1996). Current protocols in molecular biology. (New York: Wiley).

Averof, M., and Akam, M. (1995). Hox genes and the diversification of insect and crustacean body plans. Nature **376,** 420-423.

Belles-Boix, E., Hamant, O., Witiak, S.M., Morin, H., Traas, J., and Pautot, V. (2006). KNAT6: an Arabidopsis homeobox gene involved in meristem activity and organ separation. Plant Cell **18,** 1900-1907.

Benfey, P.N., and Scheres, B. (2000). Root development. Curr Biol **10,** R813-815.

Benkova, E., Michniewicz, M., Sauer, M., Teichmann, T., Seifertova, D., Jurgens, G., and Friml, J. (2003). Local, efflux-dependent auxin gradients as a common module for plant organ formation. Cell **115,** 591-602.

Bennett, M.J., Marchant, A., Green, H.G., May, S.T., Ward, S.P., Millner, P.A., Walker, A.R., Schulz, B., and Feldmann, K.A. (1996). Arabidopsis AUX1 gene: a permease-like regulator of root gravitropism. Science **273,** 948-950.

Birnbaum, K., Shasha, D.E., Wang, J.Y., Jung, J.W., Lambert, G.M., Galbraith, D.W., and Benfey, P.N. (2003). A gene expression map of the Arabidopsis root. Science **302,** 1956-1960.

Bleckmann, A., and Simon, R. (2009). Interdomain signaling in stem cell maintenance of plant shoot meristems. Mol Cells **27,** 615-620.

Bleckmann, A., Weidtkamp-Peters, S., Seidel, C.A., and Simon, R. (2010). Stem cell signaling in Arabidopsis requires CRN to localize CLV2 to the plasma membrane. Plant Physiol **152,** 166-176.

Blilou, I., Xu, J., Wildwater, M., Willemsen, V., Paponov, I., Friml, J., Heidstra, R., Aida, M., Palme, K., and Scheres, B. (2005). The PIN auxin efflux facilitator network controls growth and patterning in Arabidopsis roots. Nature **433,** 39-44.

Borghi, L., Bureau, M., and Simon, R. (2007). Arabidopsis JAGGED LATERAL ORGANS is expressed in boundaries and coordinates KNOX and PIN activity. Plant Cell **19,** 1795-1808.

Bortiri, E., Chuck, G., Vollbrecht, E., Rocheford, T., Martienssen, R., and Hake, S. (2006). ramosa2 encodes a LATERAL ORGAN BOUNDARY domain protein that determines the fate of stem cells in branch meristems of maize. Plant Cell **18,** 574-585.

Breuil-Broyer, S., Morel, P., de Almeida-Engler, J., Coustham, V., Negrutiu, I., and Trehin, C. (2004). High-resolution boundary analysis during Arabidopsis thaliana flower development. Plant J **38,** 182-192.

Brewer, P.B., Heisler, M.G., Hejatko, J., Friml, J., and Benkova, E. (2006). In situ hybridization for mRNA detection in Arabidopsis tissue sections. Nat Protoc **1,** 1462-1467.

Bureau, M., and Simon, R. (2008). JLO regulates embryo patterning and organ initiaion by controlling auxin transport. Plant Signaling and Behavior **3,** 1-3.

Bureau, M., Rast, M.I., Illmer, J., and Simon, R. (2010). JAGGED LATERAL ORGAN (JLO) controls auxin dependent patterning during development of the Arabidopsis embryo and root. Plant Mol Biol **74,** 479-491.

Byrne, M.E., Simorowski, J., and Martienssen, R.A. (2002). ASYMMETRIC LEAVES1 reveals knox gene redundancy in Arabidopsis. Development **129,** 1957-1965.

Byrne, M.E., Barley, R., Curtis, M., Arroyo, J.M., Dunham, M., Hudson, A., and Martienssen, R.A. (2000). Asymmetric leaves1 mediates leaf patterning and stem cell function in Arabidopsis. Nature **408,** 967-971.

Chalfun-Junior, A., Franken, J., Mes, J.J., Marsch-Martinez, N., Pereira, A., and Angenent, G.C. (2005). ASYMMETRIC LEAVES2-LIKE1 gene, a member of the AS2/LOB family, controls proximal-distal patterning in Arabidopsis petals. Plant Mol Biol **57,** 559-575.

Clough, S.J., and Bent, A.F. (1998). Floral dip: a simplified method for Agrobacterium-mediated transformation of Arabidopsis thaliana. Plant J **16,** 735-743.

Cui, H., Levesque, M.P., Vernoux, T., Jung, J.W., Paquette, A.J., Gallagher, K.L., Wang, J.Y., Blilou, I., Scheres, B., and Benfey, P.N. (2007). An evolutionarily conserved mechanism delimiting SHR movement defines a single layer of endodermis in plants. Science **316,** 421-425.

Curtis, M.D., and Grossniklaus, U. (2003). A gateway cloning vector set for high-throughput functional analysis of genes in planta. Plant Physiol **133,** 462-469.

Czechowski, T., Stitt, M., Altmann, T., Udvardi, M.K., and Scheible, W.R. (2005). Genome-wide identification and testing of superior reference genes for transcript normalization in Arabidopsis. Plant Physiol **139,** 5-17.

del Pozo, J.C., Dharmasiri, S., Hellmann, H., Walker, L., Gray, W.M., and Estelle, M. (2002). AXR1-ECR1-dependent conjugation of RUB1 to the Arabidopsis Cullin AtCUL1 is required for auxin response. Plant Cell **14,** 421-433.

Delaporta, S.L., and Wood, J. (1983). A plant DNA minipreparation. Version II. Plant Mol. Biol. Rep. **4,** 19-21.

Dharmasiri, N., and Estelle, M. (2004). Auxin signaling and regulated protein degradation. Trends Plant Sci **9,** 302-308.

Dharmasiri, N., Dharmasiri, S., and Estelle, M. (2005a). The F-box protein TIR1 is an auxin receptor. Nature **435,** 441-445.

Dharmasiri, N., Dharmasiri, S., Weijers, D., Lechner, E., Yamada, M., Hobbie, L., Ehrismann, J.S., Jurgens, G., and Estelle, M. (2005b). Plant development is regulated by a family of auxin receptor F box proteins. Dev Cell **9,** 109-119.

Di Laurenzio, L., Wysocka-Diller, J., Malamy, J.E., Pysh, L., Helariutta, Y., Freshour, G., Hahn, M.G., Feldmann, K.A., and Benfey, P.N. (1996). The SCARECROW gene regulates an asymmetric cell division that is essential for generating the radial organization of the Arabidopsis root. Cell **86,** 423-433.

Ding, Z., and Friml, J. (2010). Auxin regulates distal stem cell differentiation in Arabidopsis roots. Proc Natl Acad Sci U S A **107,** 12046-12051.

Dolan, L., Janmaat, K., Willemsen, V., Linstead, P., Poethig, S., Roberts, K., and Scheres, B. (1993). Cellular organisation of the Arabidopsis thaliana root. Development **119,** 71-84.

Eckardt, N.A. (2007). Brassinosteroid Signaling Involves theNucleocytoplasmic Shuttling Activity of BZR1. Plant Cell **19**.

Egea-Cortines, M., Saedler, H., and Sommer, H. (1999). Ternary complex formation between the MADS-box proteins SQUAMOSA, DEFICIENS and GLOBOSA is involved in the control of floral architecture in Antirrhinum majus. Embo J **18,** 5370-5379.

Evans, M.M. (2007). The indeterminate gametophyte1 gene of maize encodes a LOB domain protein required for embryo Sac and leaf development. Plant Cell **19,** 46-62.

Förster, T. (1948). Zwischenmolekulare Energiewanderung und Fluoreszenz. Annalen der Physik **437,** 55-75.

Friml, J., Vieten, A., Sauer, M., Weijers, D., Schwarz, H., Hamann, T., Offringa, R., and Jurgens, G. (2003). Efflux-dependent auxin gradients establish the apical-basal axis of Arabidopsis. Nature **426,** 147-153.

Gagne, J.M., Downes, B.P., Shiu, S.H., Durski, A.M., and Vierstra, R.D. (2002). The F-box subunit of the SCF E3 complex is encoded by a diverse superfamily of genes in Arabidopsis. Proc Natl Acad Sci U S A **99,** 11519-11524.

Galinha, C., Hofhuis, H., Luijten, M., Willemsen, V., Blilou, I., Heidstra, R., and Scheres, B. (2007). PLETHORA proteins as dose-dependent master regulators of Arabidopsis root development. Nature **449,** 1053-1057.

Galweiler, L., Guan, C., Muller, A., Wisman, E., Mendgen, K., Yephremov, A., and Palme, K. (1998). Regulation of polar auxin transport by AtPIN1 in Arabidopsis vascular tissue. Science **282,** 2226-2230.

Gampala, S.S., Kim, T.W., He, J.X., Tang, W., Deng, Z., Bai, M.Y., Guan, S., Lalonde, S., Sun, Y., Gendron, J.M., Chen, H., Shibagaki, N., Ferl, R.J., Ehrhardt, D., Chong, K., Burlingame, A.L., and Wang, Z.Y. (2007). An essential role for 14-3-3 proteins in brassinosteroid signal transduction in Arabidopsis. Dev Cell **13,** 177-189.

Gong, W., Shen, Y.P., Ma, L.G., Pan, Y., Du, Y.L., Wang, D.H., Yang, J.Y., Hu, L.D., Liu, X.F., Dong, C.X., Ma, L., Chen, Y.H., Yang, X.Y., Gao, Y., Zhu, D., Tan, X., Mu, J.Y., Zhang, D.B., Liu, Y.L., Dinesh-Kumar, S.P., Li, Y., Wang, X.P., Gu, H.Y., Qu, L.J., Bai, S.N., Lu, Y.T., Li, J.Y., Zhao, J.D., Zuo, J., Huang, H., Deng, X.W., and Zhu, Y.X. (2004). Genome-wide ORFeome cloning and analysis of Arabidopsis transcription factor genes. Plant Physiol **135,** 773-782.

Gray, W.M., Kepinski, S., Rouse, D., Leyser, O., and Estelle, M. (2001). Auxin regulates SCF(TIR1)-dependent degradation of AUX/IAA proteins. Nature **414,** 271-276.

Greenham, K., Santner, A., Castillejo, C., Mooney, S., Sairanen, I., Ljung, K., and Estelle, M. (2011). The AFB4 auxin receptor is a negative regulator of auxin signaling in seedlings. Curr Biol **21,** 520-525.

Guo, M., Thomas, J., Collins, G., and Timmermans, M.C. (2008). Direct repression of KNOX loci by the ASYMMETRIC LEAVES1 complex of Arabidopsis. Plant Cell **20,** 48-58.

Ha, C.M., Jun, J.H., Nam, H.G., and Fletcher, J.C. (2007). BLADE-ON-PETIOLE1 and 2 Control Arabidopsis Lateral Organ Fate through Regulation of LOB Domain and Adaxial-Abaxial Polarity Genes. Plant Cell **19,** 1809-1825.

Hamann, T., Mayer, U., and Jurgens, G. (1999). The auxin-insensitive bodenlos mutation affects primary root formation and apical-basal patterning in the Arabidopsis embryo. Development **126,** 1387-1395.

Hamann, T., Benkova, E., Baurle, I., Kientz, M., and Jurgens, G. (2002). The Arabidopsis BODENLOS gene encodes an auxin response protein inhibiting MONOPTEROS-mediated embryo patterning. Genes Dev **16,** 1610-1615.

Hardtke, C.S., and Berleth, T. (1998). The Arabidopsis gene MONOPTEROS encodes a transcription factor mediating embryo axis formation and vascular development. Embo J **17,** 1405-1411.

Hardtke, C.S., Ckurshumova, W., Vidaurre, D.P., Singh, S.A., Stamatiou, G., Tiwari, S.B., Hagen, G., Guilfoyle, T.J., and Berleth, T. (2004). Overlapping and non-redundant functions of the Arabidopsis auxin response factors MONOPTEROS and NONPHOTOTROPIC HYPOCOTYL 4. Development **131,** 1089-1100.

Harper, R.M., Stowe-Evans, E.L., Luesse, D.R., Muto, H., Tatematsu, K., Watahiki, M.K., Yamamoto, K., and Liscum, E. (2000). The NPH4 locus encodes the auxin response factor ARF7, a conditional regulator of differential growth in aerial Arabidopsis tissue. Plant Cell **12,** 757-770.

Hay, A., Barkoulas, M., and Tsiantis, M. (2006). ASYMMETRIC LEAVES1 and auxin activities converge to repress BREVIPEDICELLUS expression and promote leaf development in Arabidopsis. Development **133,** 3955-3961.

Heisler, M.G., Ohno, C., Das, P., Sieber, P., Reddy, G.V., Long, J.A., and Meyerowitz, E.M. (2005). Patterns of auxin transport and gene expression during primordium development revealed by live imaging of the Arabidopsis inflorescence meristem. Curr Biol **15,** 1899-1911.

Hejatko, J., Blilou, I., Brewer, P.B., Friml, J., Scheres, B., and Benkova, E. (2006). In situ hybridization technique for mRNA detection in whole mount Arabidopsis samples. Nat Protoc **1,** 1939-1946.

Helariutta, Y., Fukaki, H., Wysocka-Diller, J., Nakajima, K., Jung, J., Sena, G., Hauser, M.T., and Benfey, P.N. (2000). The SHORT-ROOT gene controls radial patterning of the Arabidopsis root through radial signaling. Cell **101,** 555-567.

Holland, P.W., Garcia-Fernandez, J., Williams, N.A., and Sidow, A. (1994). Gene duplications and the origins of vertebrate development. Dev Suppl, 125-133.

Honma, T., and Goto, K. (2001). Complexes of MADS-box proteins are sufficient to convert leaves into floral organs. Nature **409,** 525-529.

Husbands, A., Bell, E.M., Shuai, B., Smith, H.M., and Springer, P.S. (2007). LATERAL ORGAN BOUNDARIES defines a new family of DNA-binding transcription factors and can interact with specific bHLH proteins. Nucleic Acids Res **35,** 6663-6671.

Irish, V.F. (1991). Cell lineage in plant development. Curr Opin Genet Dev **1,** 169-173.

Iwakawa, H., Iwasaki, M., Kojima, S., Ueno, Y., Soma, T., Tanaka, H., Semiarti, E., Machida, Y., and Machida, C. (2007). Expression of the ASYMMETRIC LEAVES2 gene in the adaxial domain of Arabidopsis leaves represses cell proliferation in this domain and is critical for the development of properly expanded leaves. Plant J **51,** 173-184.

Iwakawa, H., Ueno, Y., Semiarti, E., Onouchi, H., Kojima, S., Tsukaya, H., Hasebe, M., Soma, T., Ikezaki, M., Machida, C., and Machida, Y. (2002). The ASYMMETRIC LEAVES2 gene of Arabidopsis thaliana, required for formation of a symmetric flat leaf lamina, encodes a member of a novel family of proteins characterized by cysteine repeats and a leucine zipper. Plant Cell Physiol **43,** 467-478.

Iyer-Pascuzzi, A.S., and Benfey, P.N. (2009). Transcriptional networks in root cell fate specification. Biochim Biophys Acta **1789,** 315-325.

Jun, J.H., Ha, C.M., and Fletcher, J.C. (2010). BLADE-ON-PETIOLE1 coordinates organ determinacy and axial polarity in arabidopsis by directly activating ASYMMETRIC LEAVES2. Plant Cell **22,** 62-76.

Kepinski, S., and Leyser, O. (2005). The Arabidopsis F-box protein TIR1 is an auxin receptor. Nature **435,** 446-451.

Koncz, C., Kreuzaler, F., Kalman, Z., and Schell, J. (1984). A simple method to transfer, integrate and study expression of foreign genes, such as chicken ovalbumin and alpha-actin in plant tumors. Embo J **3,** 1029-1037.

Koncz, C.a.S., Jeff. (1986). The promoter of T_L-DNA gene 5 controls the tissue-specific expression of chimaeric genes carried by a novel type of *Agrobacterium* binary vector. Mol Gen Genet**,** 383-396.

Kwiatkowska, D. (2004). Surface growth at the reproductive shoot apex of Arabidopsis thaliana pinformed 1 and wild type. J Exp Bot **55,** 1021-1032.

Kwiatkowska, D. (2006). Flower primordium formation at the Arabidopsis shoot apex: quantitative analysis of surface geometry and growth. J Exp Bot **57,** 571-580.

Lee, H.W., Kim, N.Y., Lee, D.J., and Kim, J. (2009). LBD18/ASL20 regulates lateral root formation in combination with LBD16/ASL18 downstream of ARF7 and ARF19 in Arabidopsis. Plant Physiol **151,** 1377-1389.

Leyser, H.M., Lincoln, C.A., Timpte, C., Lammer, D., Turner, J., and Estelle, M. (1993). Arabidopsis auxin-resistance gene AXR1 encodes a protein related to ubiquitin-activating enzyme E1. Nature **364,** 161-164.

Lin, W.C., Shuai, B., and Springer, P.S. (2003a). The Arabidopsis LATERAL ORGAN BOUNDARIES-domain gene ASYMMETRIC LEAVES2 functions in the repression of KNOX gene expression and in adaxial-abaxial patterning. Plant Cell **15,** 2241-2252.

Lin, W.C., Shuai, B., and Springer, P.S. (2003b). The Arabidopsis LATERAL ORGAN BOUNDARIES-domain gene ASYMMETRIC LEAVES2 functions in the repression of KNOX gene expression and in adaxial-abaxial patterning. Plant Cell **15,** 2241-2252.

Liscum, E., and Reed, J.W. (2002). Genetics of Aux/IAA and ARF action in plant growth and development. Plant Mol Biol **49,** 387-400.

Liu, H., Wang, S., Yu, X., Yu, J., He, X., Zhang, S., Shou, H., and Wu, P. (2005). ARL1, a LOB-domain protein required for adventitious root formation in rice. Plant J **43,** 47-56.

Liu, P., Ahmed, S., and Wohland, T. (2008). The F-techniques: advances in receptor protein studies. Trends Endocrinol Metab **19,** 181-190.

Majer, C., and Hochholdinger, F. (2010). Defining the boundaries: structure and function of LOB domain proteins. Trends Plant Sci **16,** 47-52.

Mangeon, A., Bell, E.M., Lin, W.C., Jablonska, B., and Springer, P.S. (2010). Misregulation of the LOB domain gene DDA1 suggests possible functions in auxin signalling and photomorphogenesis. J Exp Bot **62,** 221-233.

Mann, R.S., and Affolter, M. (1998). Hox proteins meet more partners. Curr Opin Genet Dev **8,** 423-429.

Marchant, A., Bhalerao, R., Casimiro, I., Eklof, J., Casero, P.J., Bennett, M., and Sandberg, G. (2002). AUX1 promotes lateral root formation by facilitating indole-3-acetic acid distribution between sink and source tissues in the Arabidopsis seedling. Plant Cell **14,** 589-597.

Matsumura, Y., Iwakawa, H., Machida, Y., and Machida, C. (2009). Characterization of genes in the ASYMMETRIC LEAVES2/LATERAL ORGAN BOUNDARIES (AS2/LOB) family in Arabidopsis thaliana, and functional and molecular comparisons between AS2 and other family members. Plant J **58,** 525-537.

Mattsson, J., Sung, Z.R., and Berleth, T. (1999). Responses of plant vascular systems to auxin transport inhibition. Development **126,** 2979-2991.

Mayer, A. (1996). The evolution of body plans: HOM/*hox* cluster evolution, model systems, and the importance of phylogeny. Oxford University Press**,** 99-113.

Moller, B., and Weijers, D. (2009). Auxin control of embryo patterning. Cold Spring Harb Perspect Biol **1,** a001545.

Muller, P.Y., Janovjak, H., Miserez, A.R., and Dobbie, Z. (2002). Processing of gene expression data generated by quantitative real-time RT-PCR. Biotechniques **32,** 1372-1374, 1376, 1378-1379.

Naito, T., Yamashino, T., Kiba, T., Koizumi, N., Kojima, M., Sakakibara, H., and Mizuno, T. (2007). A link between cytokinin and ASL9 (ASYMMETRIC LEAVES 2 LIKE 9) that belongs to the AS2/LOB (LATERAL ORGAN BOUNDARIES) family genes in Arabidopsis thaliana. Biosci Biotechnol Biochem **71,** 1269-1278.

Nawy, T., Lee, J.Y., Colinas, J., Wang, J.Y., Thongrod, S.C., Malamy, J.E., Birnbaum, K., and Benfey, P.N. (2005). Transcriptional profile of the Arabidopsis root quiescent center. Plant Cell **17,** 1908-1925.

Nemhauser, J.L., Mockler, T.C., and Chory, J. (2004). Interdependency of brassinosteroid and auxin signaling in Arabidopsis. PLoS Biol **2,** E258.

Oh, S.A., Park, K.S., Twell, D., and Park, S.K. (2010). The SIDECAR POLLEN gene encodes a microspore-specific LOB/AS2 domain protein required for the correct timing and orientation of asymmetric cell division. Plant J **64,** 839-850.

Ohno, S., Wolf, U., and Atkin, N.B. (1968). Evolution from fish to mammals by gene duplication. Hereditas **59,** 169-187.

Okushima, Y., Fukaki, H., Onoda, M., Theologis, A., and Tasaka, M. (2007). ARF7 and ARF19 regulate lateral root formation via direct activation of LBD/ASL genes in Arabidopsis. Plant Cell **19,** 118-130.

Okushima, Y., Overvoorde, P.J., Arima, K., Alonso, J.M., Chan, A., Chang, C., Ecker, J.R., Hughes, B., Lui, A., Nguyen, D., Onodera, C., Quach, H., Smith, A., Yu, G., and Theologis, A. (2005). Functional genomic analysis of the AUXIN RESPONSE FACTOR gene family members in Arabidopsis thaliana: unique and overlapping functions of ARF7 and ARF19. Plant Cell **17,** 444-463.

Ori, N., Eshed, Y., Chuck, G., Bowman, J.L., and Hake, S. (2000). Mechanisms that control knox gene expression in the Arabidopsis shoot. Development **127,** 5523-5532.

Paponov, I.A., Teale, W.D., Trebar, M., Blilou, I., and Palme, K. (2005). The PIN auxin efflux facilitators: evolutionary and functional perspectives. Trends Plant Sci **10,** 170-177.

Paponov, I.A., Paponov, M., Teale, W., Menges, M., Chakrabortee, S., Murray, J.A., and Palme, K. (2008). Comprehensive transcriptome analysis of auxin responses in Arabidopsis. Mol Plant **1,** 321-337.

Parry, G., Calderon-Villalobos, L.I., Prigge, M., Peret, B., Dharmasiri, S., Itoh, H., Lechner, E., Gray, W.M., Bennett, M., and Estelle, M. (2009). Complex regulation of the TIR1/AFB family of auxin receptors. Proc Natl Acad Sci U S A **106,** 22540-22545.

Phelps-Durr, T.L., Thomas, J., Vahab, P., and Timmermans, M.C. (2005). Maize rough sheath2 and its Arabidopsis orthologue ASYMMETRIC LEAVES1 interact with HIRA, a predicted histone chaperone, to maintain knox gene silencing and determinacy during organogenesis. Plant Cell **17,** 2886-2898.

Poethig, S. (1989). Genetic mosaics and cell lineage analysis in plants. Trends Genet **5,** 273-277.

Purugganan, M.D., Rounsley, S.D., Schmidt, R.J., and Yanofsky, M.F. (1995). Molecular evolution of flower development: diversification of the plant MADS-box regulatory gene family. Genetics **140,** 345-356.

Ramos, J.A., Zenser, N., Leyser, O., and Callis, J. (2001). Rapid degradation of auxin/indoleacetic acid proteins requires conserved amino acids of domain II and is proteasome dependent. Plant Cell **13,** 2349-2360.

Rast, M.I., and Simon, R. (2008). The meristem-to-organ boundary: more than an extremity of anything. Curr Opin Genet Dev **18,** 287-294.

Reinhardt, D., Pesce, E.R., Stieger, P., Mandel, T., Baltensperger, K., Bennett, M., Traas, J., Friml, J., and Kuhlemeier, C. (2003). Regulation of phyllotaxis by polar auxin transport. Nature **426,** 255-260.

Reiser, L., Sanchez-Baracaldo, P., and Hake, S. (2000). Knots in the family tree: evolutionary relationships and functions of knox homeobox genes. Plant Mol Biol **42,** 151-166.

Ruegger, M., Dewey, E., Gray, W.M., Hobbie, L., Turner, J., and Estelle, M. (1998). The TIR1 protein of Arabidopsis functions in auxin response and is related to human SKP2 and yeast grr1p. Genes Dev **12,** 198-207.

Sabatini, S., Heidstra, R., Wildwater, M., and Scheres, B. (2003). SCARECROW is involved in positioning the stem cell niche in the Arabidopsis root meristem. Genes Dev **17,** 354-358.

Sarkar, A.K., Luijten, M., Miyashima, S., Lenhard, M., Hashimoto, T., Nakajima, K., Scheres, B., Heidstra, R., and Laux, T. (2007). Conserved factors regulate signalling in Arabidopsis thaliana shoot and root stem cell organizers. Nature **446,** 811-814.

Scheres, B., Wolkenfelt, H., Willemsen, V., Terlouw, M., Lawson, E., Dean, C., and and Weisbeek, P. (1994). Embryonic origin of the Arabidopsis primary root and root meristem initials. Development **120,** 2475-2487.

Schlereth, A., Moller, B., Liu, W., Kientz, M., Flipse, J., Rademacher, E.H., Schmid, M., Jurgens, G., and Weijers, D. (2010). MONOPTEROS controls embryonic root initiation by regulating a mobile transcription factor. Nature **464,** 913-916.

Schnable, P.S., Ware, D., Fulton, R.S., Stein, J.C., Wei, F., Pasternak, S., Liang, C., Zhang, J., Fulton, L., Graves, T.A., Minx, P., Reily, A.D., Courtney, L., Kruchowski, S.S., Tomlinson, C., Strong, C., Delehaunty, K., Fronick, C., Courtney, B., Rock, S.M., Belter, E., Du, F., Kim, K., Abbott, R.M., Cotton, M., Levy, A., Marchetto, P., Ochoa, K., Jackson, S.M., Gillam, B., Chen, W., Yan, L., Higginbotham, J., Cardenas, M., Waligorski, J., Applebaum, E., Phelps, L., Falcone, J., Kanchi, K., Thane, T., Scimone, A., Thane, N., Henke, J., Wang, T., Ruppert, J., Shah, N., Rotter, K., Hodges, J., Ingenthron, E., Cordes, M., Kohlberg, S., Sgro, J., Delgado, B., Mead, K., Chinwalla, A., Leonard, S., Crouse, K., Collura, K., Kudrna, D., Currie, J., He, R., Angelova, A., Rajasekar, S., Mueller, T., Lomeli, R., Scara, G., Ko, A., Delaney, K., Wissotski, M., Lopez, G., Campos, D., Braidotti, M., Ashley, E., Golser, W., Kim, H., Lee, S., Lin, J., Dujmic, Z., Kim, W., Talag, J., Zuccolo, A., Fan, C., Sebastian, A., Kramer, M., Spiegel, L., Nascimento, L., Zutavern, T., Miller, B., Ambroise, C., Muller, S., Spooner, W., Narechania, A., Ren, L., Wei, S., Kumari, S., Faga, B., Levy, M.J., McMahan, L., Van Buren, P., Vaughn, M.W., Ying, K., Yeh, C.T., Emrich, S.J., Jia, Y., Kalyanaraman, A., Hsia, A.P., Barbazuk, W.B., Baucom, R.S., Brutnell, T.P., Carpita, N.C., Chaparro, C., Chia, J.M., Deragon, J.M., Estill, J.C., Fu, Y., Jeddeloh, J.A., Han, Y., Lee, H., Li, P., Lisch, D.R., Liu, S., Liu, Z., Nagel, D.H., McCann, M.C., SanMiguel, P., Myers, A.M., Nettleton, D., Nguyen, J., Penning, B.W., Ponnala, L., Schneider, K.L., Schwartz, D.C., Sharma, A., Soderlund, C., Springer, N.M., Sun, Q., Wang, H., Waterman, M., Westerman, R., Wolfgruber, T.K., Yang, L., Yu, Y., Zhang, L., Zhou, S., Zhu, Q., Bennetzen, J.L., Dawe, R.K., Jiang, J., Jiang, N., Presting, G.G., Wessler, S.R., Aluru, S., Martienssen, R.A., Clifton, S.W., McCombie, W.R., Wing, R.A., and Wilson, R.K. (2009). The B73 maize genome: complexity, diversity, and dynamics. Science **326,** 1112-1115.

Schwechheimer, C., Serino, G., and Deng, X.W. (2002). Multiple ubiquitin ligase-mediated processes require COP9 signalosome and AXR1 function. Plant Cell **14,** 2553-2563.

Semiarti, E., Ueno, Y., Tsukaya, H., Iwakawa, H., Machida, C., and Machida, Y. (2001). The ASYMMETRIC LEAVES2 gene of Arabidopsis thaliana regulates formation of a symmetric lamina,

establishment of venation and repression of meristem-related homeobox genes in leaves. Development **128,** 1771-1783.

Shuai, B., Reynaga-Pena, C.G., and Springer, P.S. (2002). The lateral organ boundaries gene defines a novel, plant-specific gene family. Plant Physiol **129,** 747-761.

Soyano, T., Thitamadee, S., Machida, Y., and Chua, N.H. (2008). ASYMMETRIC LEAVES2-LIKE19/LATERAL ORGAN BOUNDARIES DOMAIN30 and ASL20/LBD18 regulate tracheary element differentiation in Arabidopsis. Plant Cell **20,** 3359-3373.

Stahl, Y., Wink, R.H., Ingram, G.C., and Simon, R. (2009). A signaling module controlling the stem cell niche in Arabidopsis root meristems. Curr Biol **19,** 909-914.

Steeves, R.A. (1989). Clinical considerations in the use of external microwaves for local hyperthermia. Radiol Clin North Am **27,** 519-524.

Steeves, T.A., and Sussex, I.M. (1989). Pattern in plant development. Cambridge University Press.

Szemenyei, H., Hannon, M., and Long, J.A. (2008). TOPLESS mediates auxin-dependent transcriptional repression during Arabidopsis embryogenesis. Science **319,** 1384-1386.

Tan, X., Calderon-Villalobos, L.I., Sharon, M., Zheng, C., Robinson, C.V., Estelle, M., and Zheng, N. (2007). Mechanism of auxin perception by the TIR1 ubiquitin ligase. Nature **446,** 640-645.

Terpstra, I., and Heidstra, R. (2009). Stem cells: The root of all cells. Semin Cell Dev Biol **20,** 1089-1096.

Theissen, G., and Saedler, H. (2001). Plant biology. Floral quartets. Nature **409,** 469-471.

Tiwari, S.B., Hagen, G., and Guilfoyle, T. (2003). The roles of auxin response factor domains in auxin-responsive transcription. Plant Cell **15,** 533-543.

Tiwari, S.B., Hagen, G., and Guilfoyle, T.J. (2004). Aux/IAA proteins contain a potent transcriptional repression domain. Plant Cell **16,** 533-543.

Tromas, A., and Perrot-Rechenmann, C. (2010). Recent progress in auxin biology. C R Biol **333,** 297-306.

Tromas, A., Braun, N., Muller, P., Khodus, T., Paponov, I.A., Palme, K., Ljung, K., Lee, J.Y., Benfey, P., Murray, J.A., Scheres, B., and Perrot-Rechenmann, C. (2009). The AUXIN BINDING PROTEIN 1 is required for differential auxin responses mediating root growth. PLoS One **4,** e6648.

Truernit, E., Bauby, H., Dubreucq, B., Grandjean, O., Runions, J., Barthelemy, J., and Palauqui, J.C. (2008). High-resolution whole-mount imaging of three-dimensional tissue organization and gene expression enables the study of phloem development and structure in Arabidopsis. Plant Cell **20,** 1494-1503.

Tsiantis, M., Brown, M.l., Skibinski, G., and Langdale, J.A. (1999). Disruption of auxin transport is associated with aberrant leaf development in maize. Plant Physiol **121,** 1163-1168.

Ulmasov, T., Hagen, G., and Guilfoyle, T.J. (1999). Dimerization and DNA binding of auxin response factors. Plant J **19,** 309-319.

Ulmasov, T., Murfett, J., Hagen, G., and Guilfoyle, T.J. (1997). Aux/IAA proteins repress expression of reporter genes containing natural and highly active synthetic auxin response elements. Plant Cell **9,** 1963-1971.

Vanneste, S., and Friml, J. (2009). Auxin: a trigger for change in plant development. Cell **136,** 1005-1016.

Vaughn, J.G. (1952). Structure of the angiosperm apex. Nature **169,** 468-459.

Vernoux, T., Kronenberger, J., Grandjean, O., Laufs, P., and Traas, J. (2000). PIN-FORMED 1 regulates cell fate at the periphery of the shoot apical meristem. Development **127,** 5157-5165.

Vieten, A., Vanneste, S., Wisniewska, J., Benkova, E., Benjamins, R., Beeckman, T., Luschnig, C., and Friml, J. (2005). Functional redundancy of PIN proteins is accompanied by auxin-dependent cross-regulation of PIN expression. Development **132,** 4521-4531.

Voinnet, O., Rivas, S., Mestre, P., and Baulcombe, D. (2003). An enhanced transient expression system in plants based on suppression of gene silencing by the p19 protein of tomato bushy stunt virus. Plant J **33,** 949-956.

Weijers, D., and Jurgens, G. (2004). Funneling auxin action: specificity in signal transduction. Curr Opin Plant Biol **7,** 687-693.

Weijers, D., and Jurgens, G. (2005a). Auxin and embryo axis formation: the ends in sight? Curr Opin Plant Biol **8,** 32-37.

Weijers, D., Schlereth, A., Ehrismann, J.S., Schwank, G., Kientz, M., and Jurgens, G. (2006). Auxin triggers transient local signaling for cell specification in Arabidopsis embryogenesis. Dev Cell **10,** 265-270.

Weijers, D., Benkova, E., Jager, K.E., Schlereth, A., Hamann, T., Kientz, M., Wilmoth, J.C., Reed, J.W., and Jurgens, G. (2005b). Developmental specificity of auxin response by pairs of ARF and Aux/IAA transcriptional regulators. Embo J **24,** 1874-1885.

Williams, R.W. (1998). Plant homeobox genes: many functions stem from a common motif. Bioessays **20,** 280-282.

Wisniewska, J., Xu, J., Seifertova, D., Brewer, P.B., Ruzicka, K., Blilou, I., Rouquie, D., Benkova, E., Scheres, B., and Friml, J. (2006). Polar PIN localization directs auxin flow in plants. Science **312,** 883.

Xu, B., Li, Z., Zhu, Y., Wang, H., Ma, H., Dong, A., and Huang, H. (2008). Arabidopsis genes AS1, AS2, and JAG negatively regulate boundary-specifying genes to promote sepal and petal development. Plant Physiol **146,** 566-575.

Xu, L., Xu, Y., Dong, A., Sun, Y., Pi, L., Xu, Y., and Huang, H. (2003). Novel as1 and as2 defects in leaf adaxial-abaxial polarity reveal the requirement for ASYMMETRIC LEAVES1 and 2 and ERECTA functions in specifying leaf adaxial identity. Development **130,** 4097-4107.

Yang, Y., Yu, X., and Wu, P. (2006). Comparison and evolution analysis of two rice subspecies LATERAL ORGAN BOUNDARIES domain gene family and their evolutionary characterization from Arabidopsis. Mol Phylogenet Evol **39,** 248-262.

Zazimalova, E., Krecek, P., Skupa, P., Hoyerova, K., and Petrasek, J. (2007). Polar transport of the plant hormone auxin - the role of PIN-FORMED (PIN) proteins. Cell Mol Life Sci **64,** 1621-1637.

Zgurski, J.M., Sharma, R., Bolokoski, D.A., and Schultz, E.A. (2005). Asymmetric auxin response precedes asymmetric growth and differentiation of asymmetric leaf1 and asymmetric leaf2 Arabidopsis leaves. Plant Cell **17,** 77-91.

Zhu, Y., Li, Z., Xu, B., Li, H., Wang, L., Dong, A., and Huang, H. (2008). Subcellular localizations of AS1 and AS2 suggest their common and distinct roles in plant development. J Integr Plant Biol **50,** 897-905.

Zuo, J., Niu, Q.W., and Chua, N.H. (2000). Technical advance: An estrogen receptor-based transactivator XVE mediates highly inducible gene expression in transgenic plants. Plant J **24,** 265-273.

CHAPTER IX

APPENDIX

9. APPENDIX

9.1. Abbreviations

AA	Amino acid	LB	Luria Bertoni broth
A. thaliana	*Arabidopsis thaliana*	M	molar
ATP	Adenosin-triphospate	mg	milligram
bp	base pair	min	minute
cDNA	copy DNA	ml	millilitre
Col-0	Ecotype Columbia	mM	milli molar
Da	Dalton	MNE	mean normalized expression
DAI	days after induction	mRNA	messenger RNA
DAG	days after germination	MW	molecular weight
DTT	Dithiothreitol	ng	nanogram
dH2O	destilled water	nm	nanometer
DEPC	Diethylpyrocarbonat	nmol	nanomolar
DNA	Deoxyribonucleic acid	No-0	Ecotype Nossen
dsDNA	double stranded DNA	NPA	*N*-1-Naphthylphthalamic Acid
dNTP	Desoxyribonucleoside 5"- triphos-phate	ODx nm	optical density
DMSO	Dimethylsulfoxid	PAGE	Polyacrylamid gelectrophoreses
E. coli	*Escherichia coli*	PCR	Polymerase chain reaction
EDTA	Ethylendiamine tetraacidic acid	pg	picogram
Fig.	Figure	PVDF	Polyvinylidenfluoride
FP	Fluorescent protein	Rif	Rifampicin
FRET	Fluorescence resonance energy transfer	RNA	Ribonucleic acid
GAL4-AD	GAL4 activation domain	RT	room temperature
GAL4-BD	GAL4 DNA binding domain	RT	reverse transcriptase
Gent	Gentamycin	qRT-PCR	quantitative Real Time-PCR
GFP	Green fluorescing protein	SDS	Sodiumdodecylsulfate
h	hour	Spec	Spectinomycin
HAI	hour after induction	Tab.	Table
HRP	Horse raddish peroxidase	*Taq*	*Thermus aquaticus*
Hyg	Hygromycin	v/v	volume per volume
IAA	indole-3-acetic acid (IAA)	w/v	weight per volume
Kan	Kanamycin	WT	wild type
kb	kilobase pair	µg	micro gramm
kDa	Kilo Dalton	µl	micro litre
L*er*	Ecotype Landsberg *erecta*	2,4-D	2,4-Dichlorophenoxyacetic acid
L	litre		

9.2. List of figures

9.3. List of tables

CHAPTER I:
Rast et al., 2008

CHAPTER II:

CHAPTER II:

CHAPTER IV:
Bureau et al., 2010

9.4. Plasmid maps

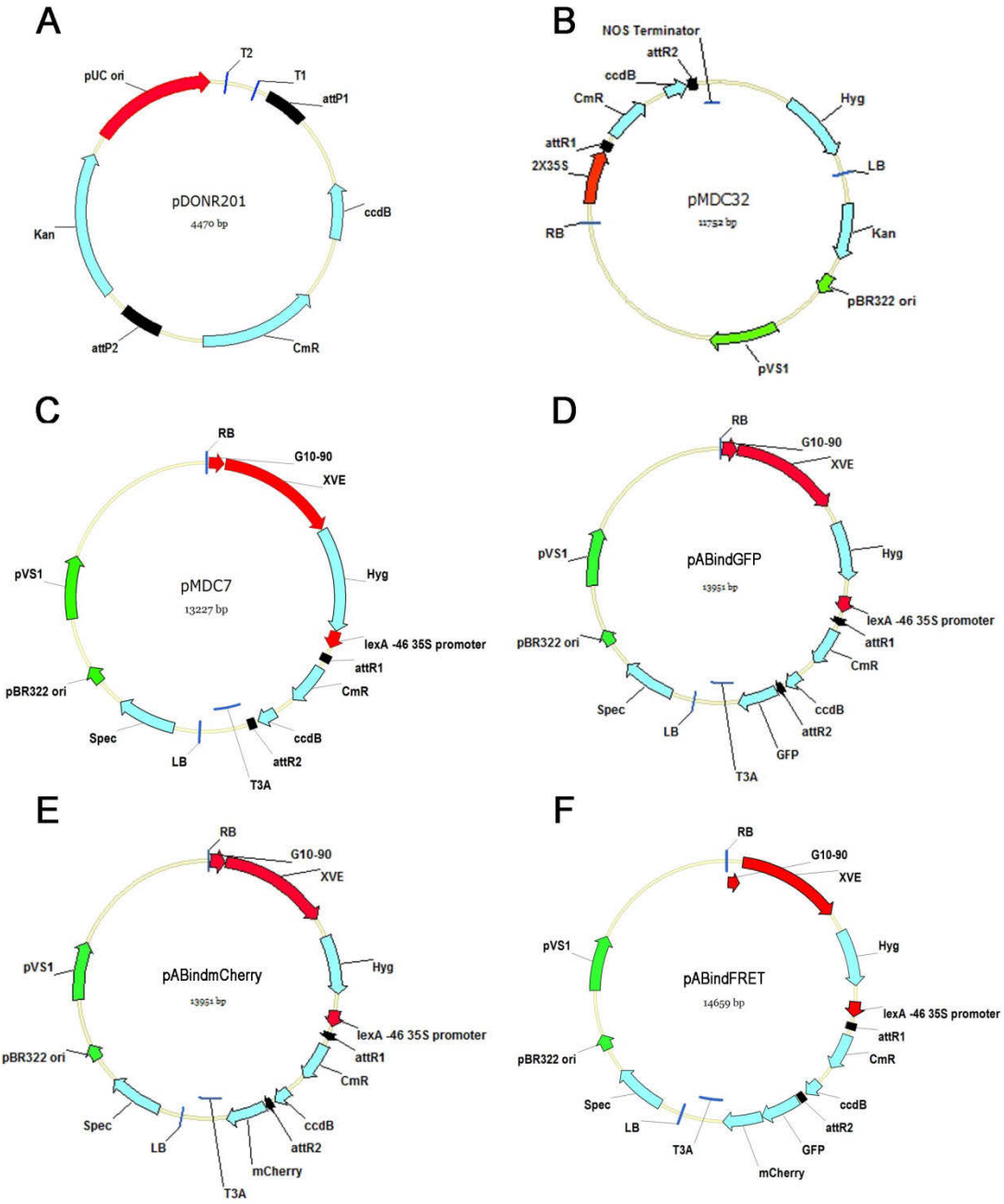

Fig. 9.1: Gateway compatible vectors used in this work. (A) The vector pDONR201 was used as entry clone: blue arrows: CDS of the selection markers, red arrow: replication origin in *E.coli*, black boxes: recombination sites attB1/2. (B-F) Used destination vectors: (B) The pMDC32 vector was used for constitutive LBD misexpression; a (C) The pMDC7 vector was used for ß-estradiol inducible misexpression; (D-F) pABindGFP; pABindmCherry and pABindFRET vectors were used for inducible production of fluorescent tagged proteins. blue arrows: CDS of the selection marker and fluorescent proteins; green arrows: origin of replication (pVS1: *E.coli*; pBR322: A. tumefacience); black boxes: recombination sites attR1/2; red arrows: promoter. Kan: kanamycin resistance gene; CmR: chloramphenicol resistance gene; ccdB: toxin that inhibits DNA amplification in most *E. coli* strains; Spec: Spectinomycin resistance; LB: left border; RB: right border

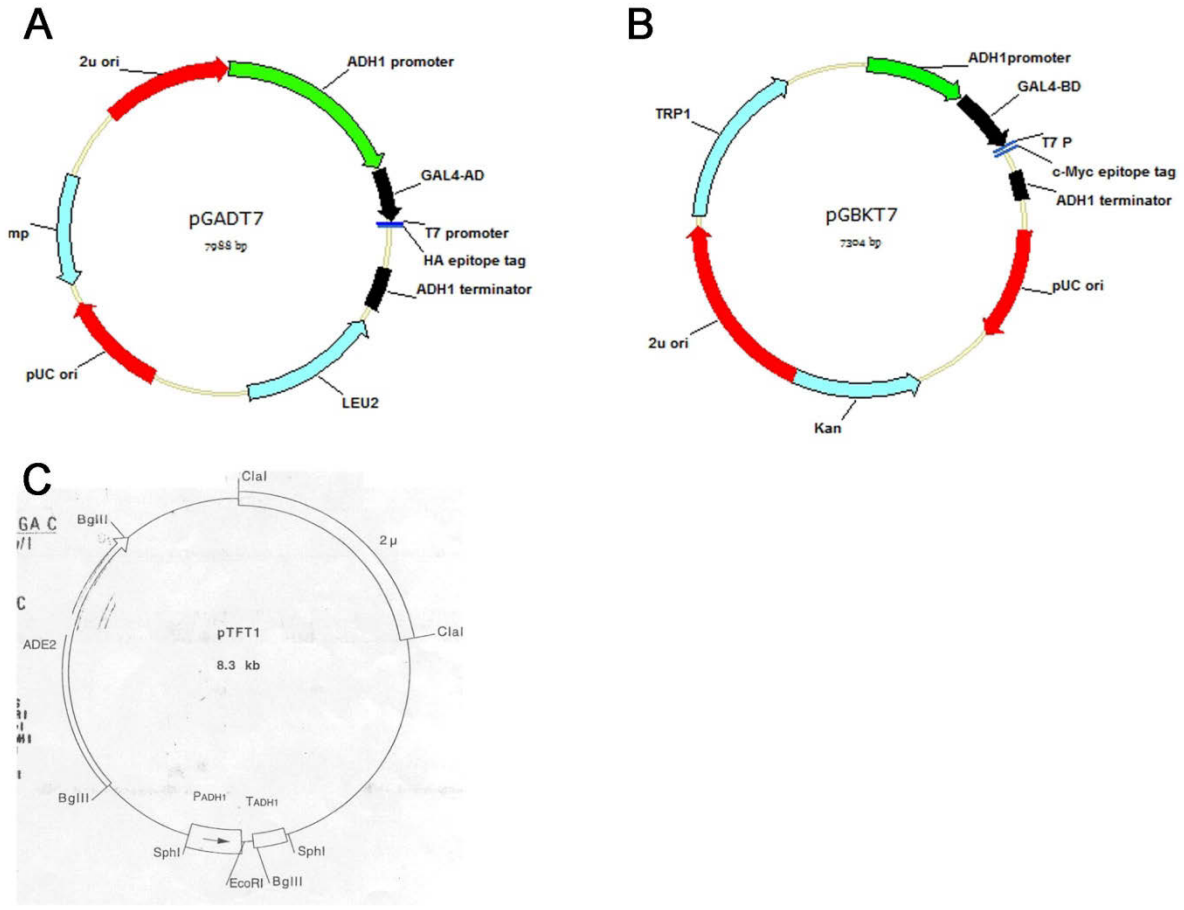

Fig. 9.2: Basic plasmids for Yeast interaction studies. (A) The pGADT7 vector was used to express proteins fused to amino acids 768–881 of the GAL4 activation domain (GAL-AD; black arrow): blue arrows: CDS of the selection markers (*E. coli*: Ampicilin (Amp); yeast: Leucin (LEU2)); red arrows: origin of replication (*E. coli*: pUC ori; yeast: 2u ori); green arrow: ADH1promoter for constitutive expression in yeast; black box: ADH1 terminator; blue line: T7 promoter and HA epitope tag for western blot analyses. (B) The pGBKT7 vector was used to expresses proteins fused to amino acids 1–147 of the GAL4 DNA binding domain (GAL-BD, black arrow): blue arrows: CDS of the selection marker (*E. coli:* Kanamycin (Kan); yeast: Leucin (TRP1)); red arrows: origin of replication (*E. coli*: pUC ori; yeast: 2u ori); green arrow: ADH1promoter for constitutive expression in yeast; black box: ADH1 terminator; blue line: T7 promoter and c-Myc epitope tag for western blot analyses. (C) The pTFT1 vector was used for yeast three hybrid interaction analyses. Origin of replication in yeast: 2u ori; PADH1: promoter; TADH1: terminator; Selection marker in yeast: ADE2.

EIDESSTATTLICHE ERKLÄRUNG

Eidesstattliche Erklärung zur Dissertation
mit dem Titel:

„Studies on the role of the *Arabidopsis thaliana* *LATERAL ORGAN BOUNDARY DOMAIN* (*LBD*) gene family"

Hiermit erkläre ich, dass ich diese Dissertation selbstständig verfasst und keine anderen als die angegebenen Hilfsmittel genutzt habe. Alle wörtlich oder inhaltlich übernommenen Stellen habe ich als solche gekennzeichnet.

Ich versichere außerdem, dass ich die beigefügte Dissertation nur in diesem und keinem anderen Promotionsverfahren eingereicht habe und dass diesem Promotionsverfahren keine gescheiterten Promotionsverfahren vorausgegangen sind.

Ort, Datum

Unterschrift

ACKNOWLEDGEMENTS

Mein Dank gilt besonders meinem Doktorvater Prof. Dr. Rüdiger Simon, der es mir ermöglicht hat an diesem Projekt zu arbeiten. Danke für die andauernde Hilfsbereitschaft, Unterstützung und die ständige Bereitschaft zur Diskussion die wesentlich zum Gelingen dieser Arbeit beigetragen hat.

Bedanken möchte ich mich auch bei Dr. Daniel Schubert für die hilfreichen Diskussionen und die Bereitschaft zur Übernahme des Zweitgutachtens.

Meiner Mutter gilt besonderer Dank, da ohne sie ein Studium und eine Doktorarbeit nicht möglich gewesen wären. Meiner Schwester Nicole danke ich dass sie in jeder Lebenslage an meiner Seite ist. Danke dass ich mich immer auf euch beide verlassen kann!

Ein herzliches Dankeschön geht an meine Laborkollegen, die mich in der ganzen Zeit unterstützt haben und mit denen ich viele schöne Momente teilen durfte. Liebe Andrea, Marc Yvonne, Renè, Helge, Cornelia, Carin und Silke vielen Dank für die gute Arbeitsatmosphäre und vielen lustigen Momente. Ihr alle habt es ermöglicht, dass ich mich als „Simpson“ sehr wohl gefühlt habe. Auch den jüngeren Mitgliedern der Arbeitsgruppe, Adrian, Julia und Stefan gilt mein Dank. Desweiteren möchte ich mich bei Dr. Marina Bureau bedanken die Düsseldorf viel zu früh verlassen musste. Vielen Dank für die freundschaftliche Zusammenarbeit bei gemeinsamen Projekten.

Liebe Andrea und Nici euch beiden möchte ich ganz besonderes danken. Wir haben zusammen unsere Doktorarbeit begonnen und viele schöne aber auch gelegentlich harte Stunden geteilt. Ich bin sehr glücklich solche Arbeitskollegen und Freunde gefunden zu haben und möchte euch nicht mehr missen!

Ein riesiges Dankeschön geht natürlich auch an alle „ Schuberts“, insbesondere Marcel, Mareike und Daniel auf deren Hilfe ich immer zählen konnte.

Abschließend danke ich allen die freundlicherweise Teile meiner Arbeit Korrektur lasen, insbesondere Marc für sein Bemühen mein Englisch zu verbessern.